Elemental Identification and Radiological Characterization of Core and Surface Samples for Environmental Assessment in Gas Field Regions of Bangladesh

by

Mahbuba Begum

A thesis submitted in partial fulfillment of the requirements for the degree of Doctor of Philosophy (Ph.D.) in the

Department of Electrical and Electronic Engineering, University of Dhaka
Dhaka, Bangladesh
Registration no: 100/2021-22 (new); 152/2016-17 (old)

Declaration

I hereby declare that the research work presented in this thesis entitled 'Elemental identification and radiological characterization of core and surface samples for environmental assessment in gas field regions of Bangladesh' is the result of my investigation which have been carried out by me under the supervision of Dr. Syed Mohammod Hossain, Chief Scientific Officer and Director, Planning and Development Division under Bangladesh Atomic Energy Commission, and Dr. S. M. Mostafa Al Mamun, Professor, Department of Electrical and Electronic Engineering, University of Dhaka. The results quoted from other work have been properly referred to. I further declare that this thesis has not been submitted for the award of any degree to this university or any other university or institution inside the country or abroad.

Mahbuba Begum

Department of Electrical and Electronic Engineering
University of Dhaka

Joint-Supervisor
Dr. Syed Mohammod Hossain
Chief Scientific Officer & Director
Planning and Development Division
Bangladesh Atomic Energy Commission

Supervisor
Dr. S. M. Mostafa Al Mamun
Professor, Department of Electrical and Electronic Engineering,
University of Dhaka

Certificate of Approval

This is to certify that Ms. Mahbuba Begum, Ph.D. scholar, Department of Electrical and Electronic Engineering, University of Dhaka has carried out research work under our supervision and guidance in the above mentioned department. The result of research work has been submitted by Ms. Mahbuba Begum in this thesis entitled 'Elemental identification and radiological characterization of core and surface samples for environmental assessment in gas field regions of Bangladesh' for the degree of Doctor of Philosophy.

Ms. Mahbuba Begum has fulfilled all the requirements under the PhD Regulations of the University of Dhaka and meets acceptable presentation standards. To the best of our knowledge, this thesis as a whole or any part thereof has not been submitted to any other University or Institution for any other degree or diploma.

Joint-Supervisor
Dr. Syed Mohammod Hossain
Chief Scientific Officer & Director
Planning and Development Division
Bangladesh Atomic Energy Commission

Supervisor
Dr. S. M. Mostafa Al Mamun
Professor, Department of Electrical and Electronic Engineering,
University of Dhaka

Acknowledgements

The author is delighted to express her heartiest gratitude to her supervisors Dr. Syed Mohammod Hossain, Chief Scientific Officer (CSO) & Director, Planning and Development Division, Bangladesh Atomic Energy Commission (BAEC) and Dr. S. M. Mostafa Al Mamun, Professor, Department of Electrical and Electronic Engineering (EEE), University of Dhaka, respectively; under their continuous guidance, direction and supervision, the enriched end of research has become possible.

The author gratefully acknowledges Bangabandhu Fellowship Trust under Ministry of Science and Technology, Government of the People's Republic of Bangladesh, for this PhD research funding.

The author acknowledges with sincerest thankfulness to Dr. Rahat Khan, Principal Scientific Officer (PSO); Reactor and Neutron Physics Division (RNPD), INST under BAEC for his great cooperation during laboratory works and valuable suggestions.

It is my pleasure to have many fruitful discussions with Dr. Zahid Hassan Mahmood, Professor, Department of Electrical and Electronic Engineering, University of Dhaka, which have stimulated my research activities.

I am grateful to Dr. Kamrun Naher, Head & CSO, RNPD, Institute of Nuclear Science and Technology (INST) under BAEC, for her invaluable advice and support during laboratory works for conducting the INAA and radioactivity measurement using HPGe detector.

I also would like to acknowledge Dr. Md. Amirul Islam, CSO and Ms. Umma Tamim, SSO for their support during conducting the experiment. The author is also expressing sincere gratitude to the technical personnel who were associated with this study of Reactor and Neutron Physics Division (RNPD) in Institute of Nuclear Science and Technology (INST); under Bangladesh Atomic Energy Commission (BAEC). The author would like to acknowledge to the technical personnel associated with this study, who involved in the TRIGA Mark II research reactor operation at the Center for Research Reactor in Atomic Energy Research Astablishment, Savar.

Author is grateful to Dr. Bilkis Ara Begum, Director & CSO and from Health Physics Division (HPD) Ms. Syeda Ferdous Mahal, Ex-Head & CSO and Ms. Selina Yeasmin, Head & CSO of Atomic Energy Centre, Dhaka (AECD) under BAEC, for their kind support during study period.

Author is deeply thankful to the Bangladesh Oil, Gas & Mineral Corporation (PetroBangla) and Bangladesh Petroleum Exploration and Production Company Ltd. (BAPEX) and for kindly providing information and core samples. Author is thankful to Dr. Sheikh Manjura Hoque, Head & CSO of Materials Science Division (MSD) and Dr. Shamshad Begum Quraishi, Head & CSO & Dr. Yeasmin Nahar Jolly, CSO of Chemistry Division (CE) of AECD under BAEC, for their generous support during laboratory works.

I gladly want to acknowledge Mr. Jamiul Kabir, PSO; Engr. Shirin Akhter, PE and the technical personnel who were associated of CD, AECD for their support in conducting the ED-XRF experiment. I delightedly want to acknowledge Ms. Arijun Nahar, SSO and Nazmunnahar Begum, JEO of MSD, AECD for their support in conducting SEM, EDX and XRD experiments.

The greatest pleasure to me is to express my gratitude to my parents who always have been with me as precious guides. Finally, the author would like to thank her husband, Shah Md. Serajus Salekin, for his invaluable support and ideas along with his assistance in last phase of this work. The author is grateful to her family members, friends and colleagues for their co-operation during the doctoral studies.

Scientific publications

1. "Potential redistributions of NORMs in and around a Gas-field: Radiological risks assessment".
Mahbuba Begum, Rahat Khan, Syed Mohammod Hossain and S. M. Mostafa Al Mamun.

Springer Journal of Radioanalytical and Nuclear Chemistry, (2021).

https://doi.org/10.1007/s10967-021-08107-x

2. "Geochemical characterization of Miocene core sediments from Shahbazpur gas-wells (Bangladesh) in terms of elemental abundances by Instrumental Neutron Activation Analysis".
Begum, M., Khan, R., Roy, D.K., Habib, M.A., Rashid, M.B., Naher, K., Islam, M.A., Tamim, U., Das, S.C., Mamun, S.M.M.A., Hossain, S.M..

Springer Journal of Radioanalytical and Nuclear Chemistry, (2021).

https://doi.org/10.1007/s10967-021-07770-4

Paper published in the Conference Proceeding

1. **Paper ID: 6156:** "Experimental study using XRD and SEM of geological materials of potential petroleum bearing formation of Bangladesh".
M. Begum, S. M. Hossain, M. Rajib, A. N. Airin, S. M. Hoque, M. S. Hossain, M. M. Hoque, Zahid Hasan Mahmood. **International Conference on Material Science and Semiconductor Devices**, 7th - 8th September 2018, University of Dhaka, Bangladesh, page. 137-138.

***Dedicated** to my respected parents, teachers of every institution of my life, both for moral and educational lessons and to my beloved children, namely Afia Mubashira and Mohammad Zaiyan.*

Index

Abstract

In the oil and gas production industries all over the world, produced water contain the largest portion of wastes and the second largest portion of wastes is drilling waste, both of which are dumped into the evaporation pond and so the pond is assumed to be the main deposit of higher level of toxic element wastes and naturally occurring radioactive materials (NORMs). In Bangladesh, this contaminated water mostly in rainy season, over-flooded and spread to the nearby environment and resulting soil contamination. The yearly produced water deposition of Shabazpur gas field, Saldanadi gas field and Fenchuganj gas field are 27,53,244 L, 2,26,499 L and 28,13,944 L respectively, along with producing more scale and sludge.

Metal concentrations above threshold levels affect the microbiological balance of soils and can reduce their fertility where most vital soil pollutants are heavy metals owing to carcinogenic, hazardous, and non-degradable properties The hydrocarbon extraction industries are the source of heavy metals like arsenic, barium, cadmium, chromium, iron, lead, mercury, nickel, vanadium, and zinc which are introduced chiefly through the disposal of produced water and drilling muds where arsenic, cadmium, chromium, lead, and mercury have comparatively higher degree of toxicity. Again, radiation can produce fetus abnormality, sterility, erythema, leukemia, epilation, genetic diseases and cancer in the blood-forming tissue, skin, bone, lung, thyroid and so on. So environmental assessment both for radioactivity and toxic elements concentration have been analyzed for Shahbazpur gas field, Saldanadi gas field and Fenchuganj gas field of Bangladesh in this study.

Newly developed integrated in-site hydrocarbon and uranium recovery technology with very low grades of uranium ore deposits and also Th and many other valuable minerals recovery technology is economically feasible. So, core samples from gas reservoir wells of different depth from 1279m to 4091m of these three gas fields have been analyzed for elemental identification with concentrations and radioactivity levels, which can reflect information of the sedimentary formation at greater depth of gas reservoir zone and could be used as baseline data for mentioned technology in near future. Neutron Activation Analysis (NAA) method has been used to represent a set of high-quality elemental data for the core sediments of gas reservoir zone along with rare earth elements (REE) and trace elements more precisely for baseline data and to study the possible elemental contamination from gas reservoir wells to the surface environment due to gas abstraction activity. Elemental abundance analysis of gas field environmental samples for toxic waste elements identification have been done using energy dispersive X-ray fluorescence (EDXRF) method with inter-comparison among NAA and EDXRF methods.

In the Shahbazpur gas field, Saldanadi gas field and Fenchuganj gas field environmental soil and sediment samples, the mean concentration of Pb are found to be 70.5 ppm (range in ppm: 7.27 – 113), 493 ppm (range in ppm: 85.5 – 1675) and 107 ppm (range in ppm: 101 - 114) respectively in this study, where the concentration of Pb of upper continental crust (UCC) and world soil median values are 17 ppm and 35 ppm respectively. In the Saldanadi gas field, highest concentration detected for the Pb in the sample is from north side of the waste pumped evaporation pond where, used up batteries of car and other heavy vehicles of this gas field also

have been dumped from which very high Pb and Sr concentration can be occurred compared to other environmental soil samples of these gas field areas. The average concentration of As are 26.6 ppm (range in ppm: 9.83 - 43.9), 33.8 ppm (range in ppm: 29.2 - 37.6) and 32.4 ppm (range in ppm: <MDL - 42.6) respectively in the Shahbazpur gas field, Saldanadi gas field and Fenchuganj gas field environmental soil and sediment samples, where the concentration of As of upper continental crust (UCC) and world soil median values are 4.8 ppm and 6 ppm respectively. So, the average concentration of both Pb and As in soil samples of these three gas fields are significantly higher than corresponding UCC and world soil median values. According to all three environmental indicators, namely geo-accumulation index (I_{geo}), contamination factor (CF) and enrichment factors (EF) of average elements abundances values of the three gas fields, environmental samples are contaminated mostly by As, Pb and Ti which can be due to anthropogenic incorporation for gas abstraction activities. Core samples data reveal moderate enrichment of the values of As and Cs relative to UCC of all three gas fields. So, there is a possibility of environmental soil and sediment samples to be contaminated by As and Cs from gas-abstraction activities of these three gas fields. The X-Ray diffraction (XRD) analytical technique is used for chemical composition information of all core samples and some core samples have been analyzed using energy dispersive X-ray (EDX) analysis to get an idea about the elemental abundance concentration. Arsenic exposure affects all organ systems including the cardiovascular, dermatologic, nervous, hepatobiliary, renal, gastrointestinal, and respiratory systems with significantly higher mortality rates for cancers of the bladder, kidney, skin, and liver. In the human body, the greatest percentage of lead is taken into the kidney, then liver and the other soft tissues such as heart and brain and skeleton, again lead absorbed by the pregnant mother is readily transferred to the developing fetus.

^{232}Th and ^{40}K radioactivity concentration ranges of this study are significantly higher than other soil samples of the oil and gas production facilities in different countries of the world which may be due to geological formation variation as explained in one of this thesis research papers "Geochemical characterization of Miocene core sediments from Shahbazpur gas-wells (Bangladesh) in terms of elemental abundances by instrumental neutron activation analysis". All seven radiological hazard indices namely, radium equivalent activity, gamma representative level, external absorbed dose rate, annual effective dose rate, external hazard index, internal hazard index and excess lifetime cancer risk of core samples of all three gas fields are significantly higher than the corresponding recommended values. On the other hand, environmental surface soil and sediment samples in and around the gas-fields have significantly lower radioactivity levels compare to those in core samples of these gas fields but hazard indices, like gamma representative level index, external absorbed dose rate and excess lifetime cancer risk of most of the surface samples are around the corresponding recommended values.

Day by day the waste increases in gas production field. So, this is high time to be aware of preventing more contamination and taking necessary action against contamination from both radiological and chemically toxic elements. Furthermore, there are many fruit trees and leafy vegetables with in the boundary of the gas field areas where comparatively higher toxic elemental concentration and radioactivity concentration levels along with excess values of some radiological hazard indices and environmental contamination indices than corresponding

recommended values have been found in soil samples. Moreover, abundant grass grows in the areas of high radioactivity and toxic elemental abundance, which are collected by the local inhabitants for their domestic animals. Thus, by consuming fruits, vegetables, milk and meats can indirectly be exposed to the radiation and toxic metals/metalloids, that may develop into cancer and other diseases.

Environmental assessment for the elemental contents and radiological hazard indices suggesst considerable risks and invoke that environmental samples in and around the gas-field should be monitored routinely as the soil and sediment samples can be contaminated more by toxic elements like, Pb, As etc. and NORMs originated from gas-abstraction activities. Outcomes of this study can help the policy-makers to take necessary actions and adopt required regulations to avoid toxic elements and radiation hazards from the studied site as well as the other sites around the globe having identical category.

List of Abbreviation

AEv - Ambient Environment
Avg. - Average
BoS – Bottom Sediment
CF - Contamination Factor
CRec – Corresponding Recommended
CWA – Corresponding World Average
D – Absorbed Dose Rate
EA - Elemental Abundances
EC- Environmental Contamination
EF - Enrichment Factor
E_{ff} - Annual Effective Dose Rate
ES- Environmental Samples
ELCR - Excess Lifetime Cancer Risk
Fench - Fenchuganj
FGF - Fenchuganj Gas Field
GAA – Gas Abstraction Activities
GFA – Gas Field Area
GFEv – Gas Field Environmental
G&O – Gas and Oil
GRW – Gas Reservoir Well
GWC - Gas Well Core
HEI - Hydrocarbon Exploration Industry
HPP - Hydrocarbon Production Process
HPI - Hydrocarbon Production Industry
HM&M - Heavy Metals and Metalloids
H_{ex} - External Hazard Index
H_{in} - Internal Hazard Index
HEA - Hydrocarbon Extraction Activities
IAGB – In and Around Gas-Field Boundary
I_{geo} - Geoaccumulation Index
ISHURT - In-Site/Situ Hydrocarbon and Uranium Recovery Technology
I_{γ} - Gamma Representative Level Index
MB – Mud and Brine
Max. – Maximum
Min. - Minimum
M&M - Metals and Metalloids
NAA-Neutron Activation Analysis
NR – Natural Radionuclide
NR3 – Three Natural Radionuclides: ^{226}Ra, ^{232}Th and ^{40}K
Sbz - Shahbazpur
PW – Produced Water
PF - Production Facilities/Fields
RHI – Radiation/Radiological Hazard Index/ Indices
R&C – Radiologically and Chemically
Ra_{eq} - Radium Equivalent Activity
RC – Radioactivity Concentration
RM- Radioactive Materials
RR - Radiological Risks
RPSL – Reference Point of Sample Location
Salda - Saldanai
S&S - Soil and Sediment
SGF - Saldanadi Gas Field
SubS - Subsurface Soil
SurS - Surface Soil
GF - Gas Field
Sc-Sl – Scale and Sludge
UCC - Upper Continental Crust
WDEvp Pond - Waste Deposited Evaporation Pond

Chapter-1
Introduction

1 General Introduction

Over the past two decades, greater consideration has been paid to hazard assessment of environmental contamination (EC) owing to rising requirements of the population, the expansion of variety of industrial processes, such as minerals exploration, production of gas and oil (G&O) which concentrate naturally occurring radioactive materials (NORM) and chemical toxins including heavy metals and metalloids (HM&M) [1.1, 1.2]. Previous studies demonstrated that the industrial wastes from coal, G&O exploration industry has been enhanced the level of radiologically and chemically (R&C) hazardous elements in the adjacent environment which can ultimately cause health threats to the workers and local inhabitants [1.3-1.5]. In Bangladesh, still now total 27 gas fields (GF) are acting the dynamic role as chief energy source [1.3, 1.7]. According to International Energy Agency, above 70% of the worldwide energy demands are presently met through G&O [1.3, 1.6].

The largest portion of wastes in G&O production industries, is acknowledged as produced water (PW) which keeps higher level of NORMs [1.3, 1.8-1.10]. PW can be characterized as inorganic and organic compounds along with dispersed and dissolved oils, scale products, waxes, radionuclides, HM&M, dissolved gases, salts, formation solids, treating chemicals, dissolved oxygen and microorganisms [1.11-1.12]. Fasihi et al., assessed the EC status of Tehran, where high concentration of petroleum compounds and HM&M were found in air and soil samples of that area and was reported as harmful for human health. The physical and chemical characteristics of PW can be varied broadly on chemical formation in the reservoir of the G&O phases, the geologic age, depth and the hydrocarbon bearing formation geochemistry, also to the added production chemicals, [1.13]. The yearly PW discharge of Sbz GF is 27,53,244 L, SGF is 2,26,499 L and FGF is 28,13,944 L, with more Sc-Sl (scale & sludge). [1.14].

The second chief volume waste is the drilling waste produced by the HEI (hydrocarbon exploration industries) [1.15] The HEI are the source of HM&M which are principally introduced through the dumping of PW and drilling muds [1.16]. All waste of drilling like mud and brine (MB) and PW are disposed into the WDEvp pond of the hydrocarbon PF (production field) and so the pond is assumed to be the chief source of NORMs and toxic element wastes [1.3]. When this contaminated water, mostly in rainy season, over-flooded and spread to the nearby ponds and mainly to the nearby soil, resulting EC (environmental contamination) to the local pedosphere.

1.1 Environmental Elemental Identification of Gas and Oil (G&O) Production Fields (PF)

EC is very prominent in point source zones, like mining, different metal-based industrial processes [1.1, 1.3-1.4]. Above threshold levels of metal concentrations can reduce soils fertility through disturbing microbiological balance. The most vital soil pollutants are HM&M, organic matters and acid precipitation, where owing to carcinogenic, hazardous, and non-degradable properties, HM&M possess considerable attention [1.4]. Due to the presence of HM&M in trace concentrations from ppb to less than 10 ppm range in several environmental mediums, they are

also characterized as trace elements. Assuming toxicity and heaviness are correlated, very low level of HM&M, like arsenic can persuade harm of exposure [1.2].

As extremely significant source of soil HM&M contaminants, the G&O PF is considered as one of the contaminating industries despite its importance [1.6]. Anthropological activity can increase HM&M concentrations of soil and bioaccumulation of hazardous HM&M through biota have adverse effects on the ecosystems [1.5]. In this way, EC by hazardous HM&M of terrestrial ecosystems of hydrocarbon producing countries have become common issue [1.8].

In onshore hydrocarbon drilling events, the drilling mud and brine (MB) have been dumped in the on-site reserve pits or directly into the WDEvp Pond. PW are dumped into the WDEvp Pond after has been processed through different layers of stone and sands of skimming pit in onshore G&O production industry rather than reinject basically for the gas production fields. The hydrocarbon extraction industries are the source of HM&M like arsenic (As), lead (Pb), mercury (Hg), barium (Ba), cadmium (Cd), chromium (Cr), iron (Fe), nickel (Ni), vanadium (V), and zinc (Zn) which are chiefly occurred through the dumping of PW and drilling MB [1.9, 1.18]. Higher concentration of HM&M can arise in the environment through metal evaporation from water bodies to surface soil (SurS), leaching of HM&M to groundwater, through metal erosion, geological deposition and soil weathering. PW from G&O exploration activity contains HM&M for examples lead and mercury, with metalloids like arsenic, at different concentrations according to the duration of the hydrocarbon production and reservoir formation geology [1.11, 1.17]. Nazarpour et al. studied HM&M in the G&O field SurS for assessment of EC level and the possible ecological risk, where they noticed notable quantity of contamination in all metals, except V [1.18].

1.1.1 Effects of Hazardous Metals on Human Health

Toxic elements with both bio-accumulative and persistent nature are more dangerous [1.19]. Arsenic (As), mercury (Hg), chromium (Cr), lead (Pb) and cadmium (Cd) are the priority metals based on health concern due to high grade of toxicity, though toxicity depends on route and dose of exposure, nutritional status, age and gender of exposed individuals etc. [1.20]. Metal ions are able to interact with DNA and nuclear proteins of cells causing DNA injury or damage and can progress to carcinogenesis. According to US EPA and IARC (international agency for research on cancer), metals are either recognized or possible human carcinogens, can be classified based on study between exposure and humans' cancer occurrence [1.20].

HM&M, like cadmium, lead and mercury are nephrotoxic [1.21]. In toxicity, the chemical form is vital of the HM&M. [1.22]. Several million people of different countries namely Bangladesh, India, Mexico, Taiwan, Chile and Uruguay are chronically exposed to arsenic through highly contaminated arsenic baring groundwater [1.23]. The severity of adverse effects of arsenic on health is dependent on time, dose and the chemical form and significantly higher mortality rates in arsenic polluted areas have been found due to cancers in bladder, liver, kidney and skin [1.24-

1.25]. Again, the chief percentage of Pb in the human body is collected into the kidney, then liver, skeleton heart and brain, though, the most defenseless Pb poisoning target is the nervous system. [1.28]. Lead poisoning to the pregnant women is of great concern and to the pediatric health problem is common nowadays in United States [1.20, 1.29-1.30]. The early lead effect symptoms to the central nervous system are headache, loss of memory, irritability and dullness [1.27-1.28].

1.2 Radiological Characterization

1.2.1 Natural Sources of Radiation

Since earth's origin, natural radionuclides (NR) be in the earth's crust and all living beings are exposed to natural radiation chiefly due to the radioactivity concentration (RC) of primordial NR with longer half-lives and surviving since their creation, they are ^{232}Th, ^{238}U and their product of decay, with ^{40}K are existing in the crust of earth [1.31-1.32]. Again, the cosmic radiation originates from outer space and contributes expressively in high elevation areas and also with latitude [1.31, 1.33-1.34]. There are limited areas of high background radiation in the world because of the local geochemical and geological properties, such as selected areas of India, China and Brazil [1.31-1.32, 1.36]. Overall population generally receive E_{ff} (annual effective dose rate) mostly from the natural background radiation which contributes about 80% [1.31-1.32, 1.35].

1.2.2 Radiological Characterization of Hydrocarbon Production Areas

Different industrial processes containing the NR at higher RC are denoted to as naturally occurring radioactive materials (NORMs), such as minerals exploration, G&O production can put varying amounts of additional load of NORMs in the AEv (ambient environment) [1.38]. In this way, human health risk can be associated from contaminated environment by uncontrolled and higher levels of NORMs of generated wastes release of several industrial processes [1.38 - 1.40].

Lacking has been found in the NORMs deposit characterization of onshore gas and oil abstraction industry though much studies already been done on offshore global hydrocarbon production sites. NORMs in the hydrocarbon production industry have become a global issue. As by-product wastes, worldwide many G&O abstraction fields thought to be accumulated with NORMs at elevated concentrations within more than 40,000 hydrocarbon abstraction fields [1.37].

1.2.3 Origin of Radioactivity in Gas and Oil (G&O) Production Fields (PF)

Radioactivity occurs in the environment naturally but can be accumulated as a result of industrial activities, for example, greater than the background radioactivity level has been observed in the G&O recovery waste [1.43]. According to Begum M. et al., through HPP (hydrocarbon production process), NORM associated with G&O and the RC levels can be exceeded the surface background, where Sc-Sl (scale and sludge) either gather with alkaline earth metals' silicate, carbonate or sulphate and precipitated in storage tank, pipe lines or else flow through PW and can differ

markedly from one PF to another depending on several issues like geological formation, operational condition etc. [1.8-1.9, 1.44 -1.46, 1.48].

The radioactivity of G&O production waste stream depends on chemical composition of formation fluid and concentration of subsurface (SubS) radionuclides; again extraction, treatment process, and the duration of production changes pressure, temperature also changes NORMs concentration [1.41]. ^{226}Ra, the primary radioisotope of concern from hydrocarbon abstraction wastes, has a wide range from undetectable to 1000 $kBqkg^{-1}$ [1.42] and in another scientific research of similar industrial wastes, ^{226}Ra activity concentration was found up to 15 $MBqkg^{-1}$; hence monitoring of hydrocarbon PF for environmental RC level is burning necessity today [1.8, 1.44].

According to Begum M. et al., ^{226}Ra in the waste-stream connected to ^{226}Ra in SubS formation, PW chemistry, the volume of formed wastes and treatment procedures and mean RC of NR in discharged PW to the environment is assessed world-wide as 10 $Bq.l^{-1}$ [1.38, 1.44, 1.49]. In G&O abstraction industries, huge volume of radioactive waste dumping is the principal problem, where the main portion of wastes is assessed as PW with higher RC of NORM [1.8-1.10, 1.44, 1.50].

1.2.4 Radiation Effects on Health

The radiation effects are typically classified as: i) stochastic effects and ii) tissue reactions; where stochastic effects can create solid cancer and leukemia and tissue reactions or non-stochastic effects can create fetus abnormality, epilation, sterility, ARS (acute radiation syndrome) such as cardiovascular wound, BM (bone marrow) wound [1.52]. Radiation induced cancers may mature after many years of radiation dose received and radiation can create cancer in the lung, bone, thyroid, skin, blood-forming tissue, etc. of a human being [1.51]. Effects above threshold i.e. the severity of the damage rises with dose are identified as non-stochastic effects or tissue reactions. Stochastic effects are those that occur in a statistical manner and there is no harmless dose, i.e. no threshold dose present. Stochastic effect classified as: i) somatic effect and ii) genetic effect, where first type happens in somatic cells and can be cancerous and second type happens in the germinal tissue cells and can do genetic disorders in the offspring and significant concerning fact is that the exposure severity is not related to the radiation dose [1.53].

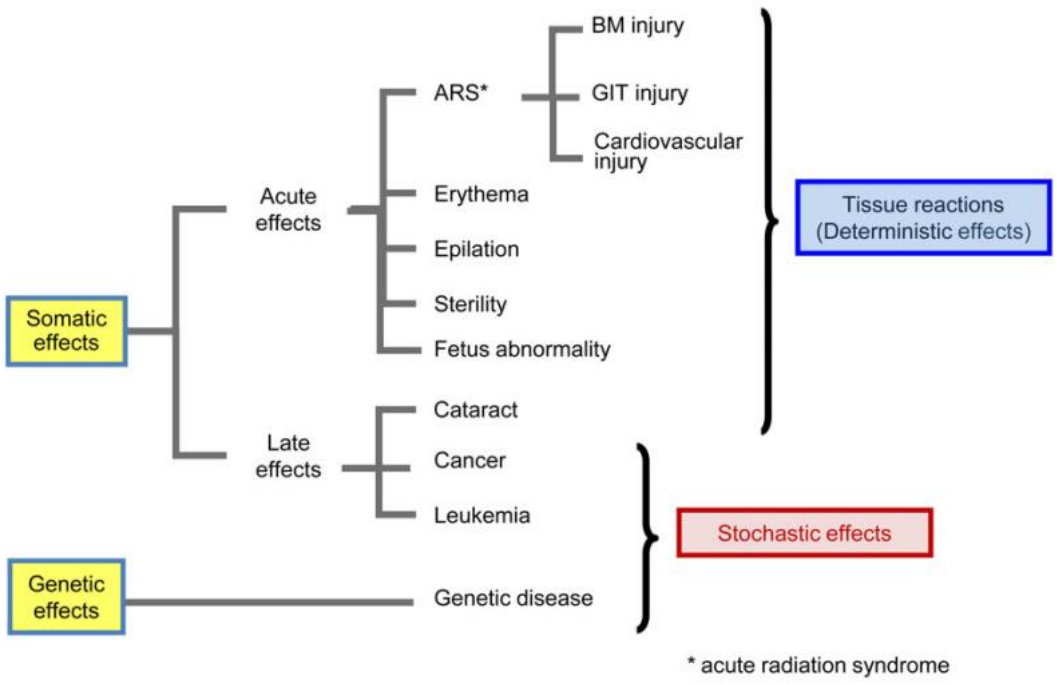

Fig. 1. Human effects of radiation [1.52]

1.3 Gas and Oil (G&O) Field Environmental Hazard Management

Many research works through drilling cutting, well logging data and coring samples analysis established that, higher levels of U, Th and other different valuable metals are available in the same hydrocarbons bearing zone of geological-formation [1.54-1.57]. Newly developed integrated in-site hydrocarbon and uranium recovery technology (ISHURT) is economically feasible with very low grades of uranium ore deposits as low as 0.002 % rather than dispose U, Th and many other valuable minerals as wastes directly into the environment which is the severe cause of EC and harmful for human health, upcoming generations also [1.56-1.57]. Again, thorium separation is easier than uranium [1.56]. This is an excellent solution for eliminating the huge volume of daily produced wastes with less environmental footprints and pollutions, where the implementation of this ISHURT with HPI (hydrocarbon production industry) will take some time as more researches are needed. It will be vast price saving as investigation, abstraction and production procedure and other auxiliary rich G&O PF are present and will be used for extracting U, Th, G&O and other important metals with separation facility only to be attached [1.56].

1.4 Motivation

As mentioned above, in the G&O production industry, PW bare the largest portion of wastes and the second largest portion is drilling waste which are deposited into the WDEvp pond and so the pond is the chief source of higher level of NORM and toxic element wastes. When this

contaminated water mostly in rainy season, over-flooded and spread to the nearby ponds and mainly to the nearby environment, resulting soil contamination to the local pedosphere. The yearly PW deposition of Sbz GF is 27,53,244 L, SGF is 2,26,499 L and FGF is 28,13,944 L with producing additional Sc-Sl [1.14].

Metal ions interact with DNA and nuclear proteins of cell causing conformational changes or damage of DNA that may cause carcinogenesis or apoptosis. Again, radiation can produce fetus abnormality, sterility, erythema, leukemia, epilation, genetic diseases and cancer in the bone, lung, thyroid, blood-forming tissue, skin and so on [1.51-1.52]. So environmental assessment both for radioactivity and toxic elements concentration are essential for different GF of Bangladesh.

As mentioned above, newly developed integrated in-site hydrocarbon and uranium recovery technology with very low grades of uranium ore deposits, and also Th and many other valuable minerals recovery technology is economically feasible. So, GWC (gas well core) samples of different depth should be analyzed for elemental identification and RC levels, which can also present data of the deeper sedimentary formation and could be used as baseline data for mentioned technology in near future.

Still now, published base line data are not available about environmental RC level and hazardous metals assessment of GF of Bangladesh.

1.5 Objective of this study

Elemental identification and radiological characterization of both (a) gas field environmental samples and (b) core samples of gas reservoir wells of different depth from 1279m to 4091m of three GF namely Sbz GF, SGF and FGF of Bangladesh have been conducted for environmental assessment.

1. Neutron Activation Analysis (NAA) method for high-quality elemental data analysis of GWC samples of gas reservoir zone with REE and trace elements more exactly,

(a) to collect information about the concentration of EA of gas reservoir zone and in the sedimentary formation at greater depth and
(b) to study the possible elemental contamination from gas reservoir wells to the surface environment due to gas abstraction activity

2. EA analysis of GFEv samples for toxic waste elements identification using energy dispersive X-ray fluorescence (EDXRF) method with inter-comparison among NAA and EDXRF methods.

3. Measurement of three environmental indicators for assessing elemental contents of both (a) GFEv samples and (b) core samples of gas reservoir wells of different depth.

4. The X-Ray diffraction (XRD) analytical technique is used for chemical composition information of all core samples along with some core samples have been analyzed using energy dispersive X-ray (EDX) analysis to get an idea about the EA concentration.

5. Radioactivity level measurement of both (a) GFEv samples and (b) GWC samples of gas reservoir wells of different depth from 1279m to 4091m of three GF,

a) to study the possible NORM redistributions from gas reservoir wells (GRW) to the surface environment in and around GF

b) which can present data of RC levels in the deeper sedimentary formation zones and

c) to evaluate associated radiological-risks (RR).

Chapter-2

Explanation with Literature Review

2.1 Geology about Hydrocarbon

Organic matter trapped in sedimentary rock through thermal cracking in subsurface geological formations produces hydrocarbons identified as source rocks which convert organic matter, kerogen into gas and oil (G&O) after maturity. Porous sedimentary rock holds water, G&O that can be covered by impenetrable rock called cap rock together consist the hydrocarbon reservoir as shown in Fig. 2.1. By pressure hydrocarbons move upward direction or sideways through insignificant cracks and faults within carrier rock as G&O are lighter than water. Example of vital source rocks are coal, shales, carbonates etc. [2.1].

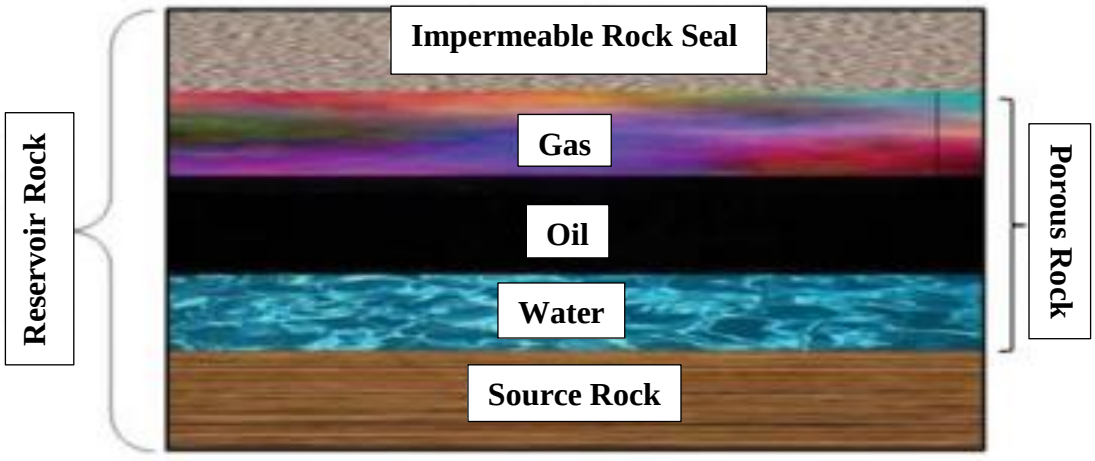

Figure 2.1. Hydrocarbon geology with typical reservoir, adopted from ref. [2.2].

2.2 Onshore Hydrocarbon Industry

In onshore hydrocarbon drilling events, the drilling fluid are being dumped in the on-site reserve pits. Production wastes like produced water are dumped into the evaporation pond after has been processed through different layers of stone and sands of skimming pit in onshore G&O production industry rather than reinject basically for the gas production fields. The influences on the environment can be predicted by measuring the solubilities of the metals and also NORM in the pit and the migration of the hazardous ions [2.3]. When this contaminated water, mostly in rainy season spread to the nearby environment, resulting soil contamination.

2.3 Produced Water (PW)

When the ‘formation water’ of the G&O reservoir transported to the exterior with hydrocarbon production then this water is termed as PW. These waters (formation and produced) can mobilize

the more soluble NORMs and metals in the AEv. The main waste product in the G&O extraction process is PW [2.3]. High salt content is the primary cause of toxicity of produced water [2.3]. The concentration of different metals and also NORMs in PW depends on geology of the formation of reservoir along with the G&O production field age [2.4].

2.3.1 Chemical Composition of Produced Water (PW)

The properties of PW differ broadly dependent on the geochemistry, geologic age, depth, chemical composition of hydrocarbon bearing zone. The elements like arsenic, antimony, silver and molybdenum have extreme geochemical mobility [2.3]. PW from G&O abstraction activity bears HM&M like Pb, As and Hg of different concentrations depending on the age of the hydrocarbon production well and reservoir formation geology [2.4-2.5].

2.4 Drilling Mud

A number of M&M, including Ba, As, Cd, Pb, Cr and Zn are contained in drilling mud where the sorts of M&M compounds and concentrations differ broadly among different sorts of mud [2.3]. Compounds like As, Pb and Cd are not added certainly to the drilling fluids, but they can arise as trace contaminants from different materials used in the 'G&O reservoir well' drilling process such as pipe dope or from the formation [2.3]. To avoid the drill pipe threads damage, the pipe dope is used to create drill string structure which usually has high concentrations of lead, copper and zinc [2.3]. Generally to weight the fluids in drilling muds, barium is used as the most prevalent metal in barite or barium sulfate.

2.5 Waste Deposited Evaporation (WDEvp) Pond of Gas Field of Bangladesh

All wastes of drilling and production of the GF are discarded to their WDEvp pond and so the pond is assumed to be the key source of technologically enhanced NORMs and toxic element wastes. The chief threat from HM&M in petroleum industry is from their migration from waste disposal to groundwater and surface water of dissolved metals and the passage of vapors and particles through the atmosphere [3]. All wastes of drilling like MB and PW like produced water of the GF are deposited into their WDEvp pond in Bangladesh and so the WDEvp pond is assumed to be the main deposit of technologically enhanced NORMs and toxic element wastes.

Figure 2.2: Pictures of WDEvp Pond Site of SBZ GF, Bangladesh.

2.6 Heavy Metals and Metalloids (HM&M)

The most vital soil contaminants are HM&M, organic matters and acid precipitation, where HM&M have involved significant consideration due to their toxic, non-degradable and cancer-causing effects [2.6]. Now HM&M is defined as "naturally occurring metals having atomic number greater than 20 and an elemental density greater than 5 $g \cdot cm^{-3}$" [2.7]. HM&M are also measured as trace elements due to their existence in trace levels in several environmental mediums from ppb to less than 10 ppm range [2.8]. With the assumption that toxicity and heaviness are interconnected, HM&M, like As are capable of persuade toxicity at slight exposure level [2.9].

Having existence of highly significant source of soil HM&M contaminants, the G&O industry is measured as one of the contaminating industries despite its importance [2.10]. The presence of HM&M in the environment are through natural and anthropological mechanisms where, human activity can increase the amount of HM&M in the environment. All HM&M are hazardous above normal concentration levels to the soil and bioaccumulation of HM&M in biota can have adverse impacts on the humans through the ecosystems [2.11-2.12].

2.7 Essential and Nonessential Metals

Deficiency or excess of an essential HM&M can generates abnormal conditions and leads to diseases, where different HM&M are essential for different creatures like, microorganisms, plants, animals, and interactions of different organisms with HM&M are very complex [2.13]. Nonessential HM&M like, Cd, Pb, As, Hg etc. are poisonous to humans, plants and animals at very low levels of concentration and essential HM&M are poisonous beyond threshold concentrations of trace amounts, where essentiality level is very narrow for some elements [2.14].

2.7.1 Environmentally Most Hazardous HM&M

In the environmental context, the most toxic HM&M are Pb, As, Cr, Ni, Hg, Cu, Cd and Zn, where, upon duration and dose of exposure, the toxicity of biota are dependent [2.15].

2.7.2 Sources of HM&M in the Environment

Sources of HM&M in the environment may be natural or geogenic and anthropogenic, where natural sources of HM&M are weathering, volcanic eruptions and anthropogenic sources of HM&M are naturally occurring elements and found in the earth's crust. are industrialization and urbanization like mining, smelting operations, domestic use, agricultural use, industrial production, industrial use of metallic compounds [2.16 - 2.17]. Different industrial sources of metals are processing in refineries, petroleum industry, textiles, microelectronics, paper-processing plants and wood preservation [2.18-2.19].

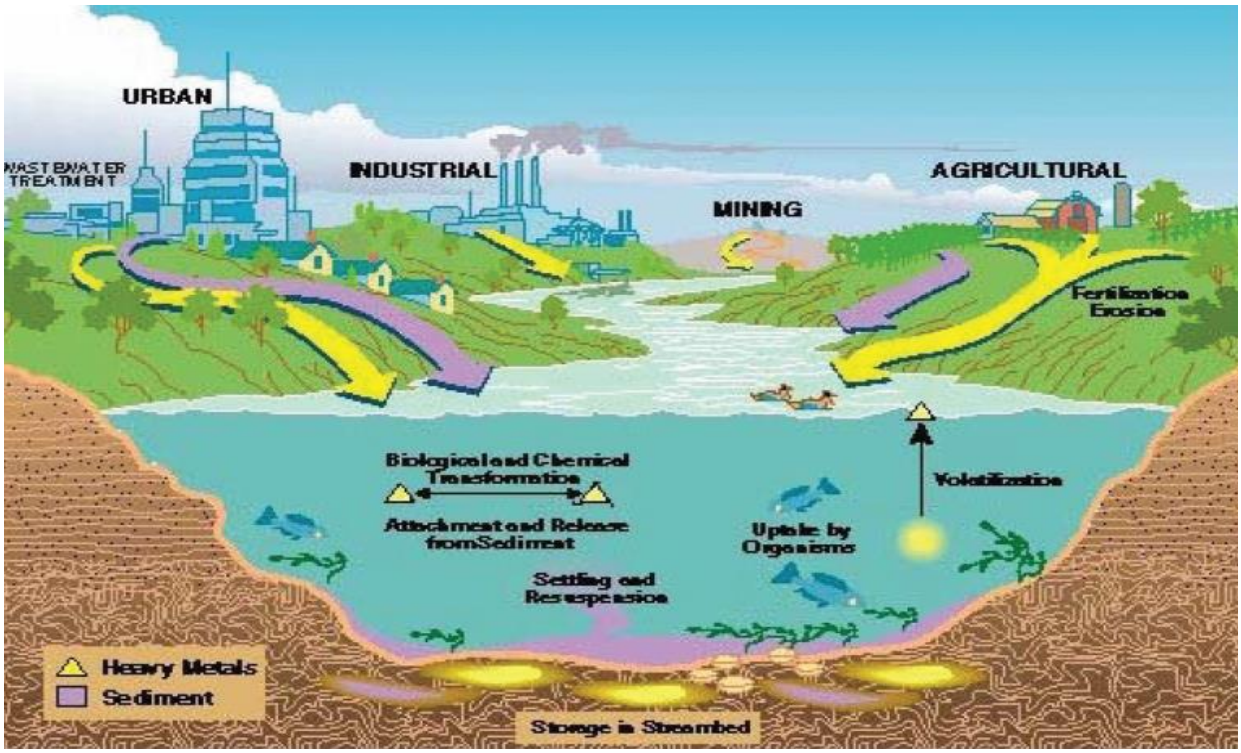

Figure 2.3: Sources and sinks of heavy metals [2.20]

HM&M causes global EC in both nautical and terrestrial ecologies because of their perseverance, bioaccumulation, and poisonousness behaviors. Environmentally related most harmful HM&M like Cr, Ni, As, Cd, Pb, Hg through marine and terrestrial food chains do harms for biota and human health [2.21].

2.8 Human Exposure to Heavy Metals and Metalloids (HM&M)

In this research work, according to all three environmental indicators of Avg. EA values studied of the three GF, ES are contaminated mostly by toxic HM&M, like, As and Pb, the health hazards of which are explained briefly as bellows:

2.8.1 Arsenic (As)

In different countries, such as, Bangladesh, Taiwan, India, Uruguay, Mexico and Chile, more than some million population are chronically exposed to As, which affects almost all organic systems [2.22]. Various As contaminated areas have pointedly greater death rates due to cancers of kidney, skin, and liver, where the time and dose dependent severity is also related to the chemical form of As [2.23-2.24].

Figure 2.4: Arsenic keratosis, so called [2.37, 2.39]

Figure 2.5: Skin lesions due to arsenicosis by drinking-water contamination of As in Bangladesh [2.37, 2.40]

2.8.2 Lead (Pb)

In the human body, most of Pb affecting the kidney, then nervous system, heart, brain, liver etc. [2.25-2.26]. Now Pb toxicity is usual health problem for children and pregnant women are of distinct anxiety due to Pb poisoning in United States [2.27-2.33]. Pb can mimic the activities of Ca within mineral of skeleton [2.27]. Research indicates that Pb is actually cancer-causing, which induce gene mutations and sister chromatid exchanges [2.34-2.36].

2.9 The Biological Effects of Radiation

The biological effects of radiation may be broadly classified into two categories,

i) Stochastic effects and ii) Tissue reactions or, Non-stochastic effects, which have been explained in chapter-1.

2.9.1 Acute and Chronic Exposure

There are two types of radiation exposure of concern: (1) high dose accidental radiation exposure of short time duration termed as acute exposure, which can produce health hazards within short duration after exposure (2) low level of radiation exposure of long-term due to insufficient protective measures termed as chronic/continuous exposure, where health hazards results from overexposure can be apparent after many years.

2.9.2 Somatic Effects

In this effect, the harms appear in the exposed person himself. Such damage will occur in parts of the body which receive radiation directly but may subsequently spread elsewhere if, for example, blood-forming tissue is affected [2.34].

2.9.3 Hereditary Effects or Genetic Effects

This effect results from the damage to the germ cells and appear only in the progenies of the radiation exposed person. Hereditary effects do not become apparent until subsequent generations are born [2.34].

2.10 Literature Review

M.R. Ghorbani et al. (2020), assessed Ahvaz oil field surface soil (66 soil samples) to study the possible health hazard from HM&M exposure. Using ICP-OES, Avg. levels of HM&M concentrations were measured 5.9, 67.4, 0.4, 7.1, 36.5, 41.2, 39.8, 31.5, and 77.6 mg/kg, for As, Pb, Cd, Co, Cr, Cu, Ni, V, and Zn respectively, where. Levels of V, Co, and Cr were much greater than corresponding reference-points, though they were noticed from natural sources. Again, As, Pb, Cd, Cu, Ni and Zn with suggestively higher EF were noticed from manmade sources like drilling mud and petroleum seepage [2.38].

According to A. R. Karbassi et al. (2015), contaminants from soil of G&O exploitation and extraction (Huge oil fields of Ahvaz, Iran) were measured as serious human health hazards and required to control toxins (mostly HM&M) dispersion from origin, where concentration of eight HM&M were determined [2.41].

According to Hossein D. Atoufi and David J. Lampert (2020), increased G&O PF is a EC subject of the United States, where potential EC connected to PW managing, with long-term sediment contamination by toxic composites like, HM&M, salts, NORM and different organic compounds. Procedures of reduction EC from sediments are surface covering, phytoremediation and. bioremediation [2.42].

Junhui Li et al. (2009), studied HM&M accumulation in agricultural 70 SurS (0–20 cm depth) samples near petrochemical area, Guangzhou, China. Analyzed concentrations of Zn, Cu, Pb, Cd and As did not surpass the corresponding Max. permissible levels of agricultural soil in China, excluding Hg only. With greater distance from the petrochemical complex boundary, lower effect of release in air of HM&M and their accumulation on soil observed. Concentrations of HM&M reduced with soil depth, which reveals, these HM&M mostly from anthropogenic origin. Necessary actions to avoid more HM&M pollution of soils to avoid health affect through cultivated foodstuffs [2.43].

Sheldon Landsberger et al., (2012) examined HM&M levels in NORM by NAA where very high levels of radionuclides: ^{226}Ra, ^{228}Ra and ^{210}Pb along with HM&M like Ba and Sr were found. Sheldon Landsberger et al., (2013) studied TENORM samples from G&O exploration, where elevated amounts of Ca, Sr and Ba were observed by using NAA.

E.I. Obiajunwa et al. (2002), examined 14 elements using EDXRF method to determine HM&M concentrations in S&S and solid wastes like, Sc-Sl samples around crude-oil PF, of Niger Delta,

Nigeria. Very elevated EF were found for Sr, Pb, Ba, Fe and Zr in each and every samples. Again very elevated EF were found for K, Mn and Ca in Sc-Sl waste samples. To reduce the EC waste disposal monitoring is essential as, significant HM&M pollution might be associated with crude-oil PF [2.44].

Ware, Katherine Daniels (1993), investigated the EC through HM&M by the petroleum industry (HEI and HPP) as they can impact the health. They found minor portion of HM&M contributed by petroleum industry compared to natural and other different industrial causes of HM&M presence to the environment. So, bioavailability are much low of HM&M presented by the petroleum industry into the environment and HM&M. impact could be reduced by reprocessing, appropriate waste handling like, reprocessing of preserved PW, drilling MB chemicals and oily wastes [2.3].

P.B. Tchounwou et al. (2012) explained that, various factors dependent HM&M toxicity subject to exposure dose, chemical forms, exposed persons age, heredities and nutritional status. Most health hazardous with high grade toxicity HM&M are As, Pb, Hg, Cd and Cr, which can damage even, multiple organs at low exposure level and called as human carcinogens [2.45].

According to H. Ali et al. (2019), owing to toxicity, bio accumulative and environmental perseverance nature, HM&M are recognized as ecological pollutants and food chain contaminant accordingly. Most hazardous HM&M for EC are Pb, Hg, Cd, Cr, Ni, Cu, Zn and As where these HM&M transfer to food chains through water and terrestrial zones have negative impacts to human health and also for wildlife. To monitor the of potentially hazardous HM&M concentrations in various environmental samples and resident biota samples are of necessity today, to minimize HM&M impact on health and environment [2.21].

Navani (2020) stated that, many research works through drilling cutting, well logging data and coring samples analysis established that, higher levels of U, Th and other different valuable metals are available in the same hydrocarbons bearing zone of geological-formation [2.46-2.47]. Newly developed integrated in-site hydrocarbon and uranium recovery technology is economically feasible with very low grades of uranium ore deposits as low as 0.002 % rather than dispose U, Th and many other valuable minerals as wastes directly into the environment which is the severe cause of EC and harmful for human health, upcoming generations also. Again, thorium separation is easier than uranium. This is an excellent solution for eliminating the huge volume of daily produced wastes with less environmental footprints and pollutions, where the implementation of this newly invented technique with HPI (hydrocarbon production industry) will take some time as more researches are needed. It will be vast price saving as investigation, abstraction and production procedure and other auxiliary rich G&O PF are present and will be used for extracting U, Th, G&O and other important metals with separation facility only to be attached [2.48]

El Afifi and Awwad (2005) studied nuclear RM in wastes produced from G&O industry chiefly contain ^{238}U, ^{235}U and ^{232}Th series and minerals with elements like, Al, Na, Fe, Mg, Ca, Sr, Si, Ba along with trace elements like, HM&M as Mn, Cu, Fe, Zn and Pb, where concentrations of these

mentioned radioactive and chemical elements in PW are proportional to the amount of generated PW [2.50-2.51]. Spectral γ-logs in the G&O industry determined increased thorium (Th) readings generally indicate heavy minerals occurrence in deposits and high uranium (U) readings indicate organic matter existence [2.48-2.49]

According to J. Garner (2017), mainstream of NORM wastes in G&O industry is much lower than nuclear industry i.e. alike intermediate level of nuclear waste, but carefully handling and dumping are required to decrease exposure. Radioactive Sc-Sl accumulation in pipes and containers in G&O production equipment required maintenance to clean them, where occupational radiation exposure occurs [2.52].

Al-Saleh and Al-Harshan in 2008, analyzed 27 Riyadh Refinery petroleum samples: 14 products and 13 wastes (3 scales, 10 sludges) samples by γ-spectrometry system. The RC of ^{238}U, ^{232}Th, ^{226}Ra and ^{40}K of all samples had higher values for sludge than scale samples. The determined D for some sludges were upper than CRec dose level so these samples could present significant waste burden. Also the samples were examined by XRF method where Mg, Al, Fe, Ca, Si and S had been observed in each and every samples. [2.53]

According to Hajer Hrichi et al. (2013), observed uncontrolled TENORM wastes release of HPI are of countless worry for the uncontrolled health impacts.In this study, 14 product samples, 12 waste samples and 3 surrounding environmental samples of Tunisian Refinery area and 2 onshore HPI were analized by γ-spectrometry method.The measured NR3 for all the Tunisian Refinery STIR have showed riskless for radiological aspect to employees and environment. But onshore two production oilfields could be recommended for safe use due to all RHI of some scale samples of this study [2.54].

According to T. L. Tasker, (2019), accurate and precise analyses of PW and Sc-Sl of G&O PF are essential for monitoring EC through tracing possible G&O PF polluted zones. Often below 7 out of 15 laboratories were able to detect with nearly 40% accurateness of trace HM&M concentrations like, Cu, Cr, Ni, Zn, As and Pb. Despite Max. laboratories used ICP-MS with poor detection abilities for trace elements analyses and huge factors of dilution of sample preparation [2.55].

Amin Taheri et al. (2019), studied health threats and EC for RC of the south pars GFA, Iran by analyzing total 17 soil, water and sludge samples. RC of 13% samples have great danger and 27% of samples are of intermediate risk levels have found for environmental assessment. The health threat assessment showed that 3% of activities have high health risk and 24% of the tasks contain intermediate risk. They suggest to consider personal protective equipment, engineering controls, administrative controls, altering the system of execution activities and by means of the appropriate disposal procedures to reduce the risk for these purposes [2.56].

Amin in 2016 using NaI gamma spectrometer investigated the NORM concentration in the ZB-269 samples of oil well drilling mud of different geological formations: from depth range: (140–150) m to 2764.5 m of Az Zubair oil field, Basra, Iraq. Avg. RC of NR3 were (614.5, 233.0 and

6201.4) Bq.kg^{-1} respectively which were greater than recommended values for ^{238}U, ^{232}Th and ^{40}K. According to Amin (2016) the RC were depth independent and influenced by the lithological variations of the oil well [2.57].

Maria et al. (2004), studied the RC in directly collected Sc-Sl samples of PETROBRAS units, Brazil using γ-spectrometry system with HPGe detector. RC of sludge from 2 distinct containers samples were (1399 and 742.6) kBq.kg^{-1} for ^{226}Ra and ^{228}Ra respectively. For ^{226}Ra and ^{228}Ra, RC of scale sample from PW pipeline internal surface were (629.7 and 403) kBq.kg^{-1} respectively. So, to avoid EC and to decrease radiation exposure of maintenance workers, special attentions have to be given during cleaning processes [2.58].

E.O. Agbalagba et al. (2012), analyzed NR3 in G&O field environmental samples of Delta state by γ-spectroscopy method, where Avg. RC of ^{226}Ra, ^{232}Th and ^{40}K were found 41, 30 and 413 Bq.kg^{-1} respectively and Max. RC were found 94, 48 and 712 Bq.kg^{-1} respectively. The Avg. RHI, for Ra_{eq}, I_{γ}, D, E_{ff}, H_{ex} and H_{in} were found 99 Bq.kg^{-1}, 0.8, 55 hGyh^{-1}, 0.07 mSvy^{-1}, 0.3 and 0.4 respectively, where corresponding dose rate related with every factors were much lower from permitted border [2.59].

D.O. Kpeglo et al. (2016), characterized PW from 2 offshore oil PF of Ghana by α-spectrometry, ICP-MS and γ-spectrometry, where the Max. RC of ^{226}Ra, ^{228}Ra and ^{224}Ra NORM components were 22.3, 35.5 and 7.0 Bq.L^{-1} respectively. Avg. RC of ^{226}Ra and ^{228}Ra of this 2 oil PF surpassed Derived Release Limit (DRL) of liquid discharges. In both oil PF, relationship of radium isotopes with different physio-chemical constraints were found decent. Avg. RC of PW from Salt pond oil field was found nearly five times greater than Avg. RC of Jubilee oil field, which may be due to the geological formation of reservoir rocks and/or due to the maturity of Salt pond field is higher in comparison to Jubilee field. Radium RC of PW from oil PF of Ghana are comparatively higher than oil PF of different countries [2.60].

CAPP (2000) report explained about NORM and its occurrence in G&O PF. Health threats from NORM contamination and the way of minimizing NORM hazards through monitoring and following proper working guidelines of management of contaminated wasters were also explained in this report [2.61].

M. Omar et al. (2004), studied RC of radium of 470 different waste samples of G&O industries by γ-spectrometry system, where the Max. Avg. RC of ^{226}Ra and ^{228}Ra were found 114,300 and 130,120 Bq.kg^{-1} respectively determined in scale samples. About 75% of Sc-Sl waste samples were within the standard range in soils for radium RC in Malaysia with Max. Avg. radium RC of sludge samples was 560 Bq.kg^{-1}. RC analysis of waste samples are required before treatment and dumping to clarify about TENORM waste. So, management of Sc-Sl contamination have to be maintained according to TENORM handling protection procedures [2.62].

IAEA (2003) report No. 34, title is: "radiation protection and the management of radioactive waste in the G&O industry". NORM in G&O PF explanation, like kinds of isotopes originated, about

EC during decommissioning and other different related matters, had been discussed in this IAEA report. This is a nice guideline for studying about NORM of G&O PF. ICRP (1996) suggested that radiation protection system: “principles of optimization, justification and limitation” – have to be maintained for occupational-workers for NORM-exposures, if Avg. annual doses greater than 1 mSv. These recommendations were accepted by IAEA in 1996 [2.63-2.64].

Chapter 3

Different Analytical Techniques for Elemental Identification

3.1 Neutron Activation Analysis (NAA) Technique for Elemental Identification

Nuclear reaction based NAA is a method of great efficiency for the precise measurement of approximately 26 to 29 major, minor and trace EA in ppb-ppm range of different samples like, environmental, geological, biological etc. NAA along with gamma spectrometry is termed as activation spectrometry [3.1].

3.1.1 Basic Principle of NAA

In the following diagram of basic principles of NAA process, a bombarding neutron is absorbed by an atomic nucleus after (n, γ) nuclear reaction and a compound nucleus is formed which is highly excited and unstable. And immediately emits gamma (γ) ray, named as prompt gamma ray. As still it is in excited state, so after certain time (different for different nucleus) the excited nucleus releases a β particle and a γ-ray, at that time the γ-ray is detected by HPGe detector (not presented here). Here for an example Arsenic is presented as an target element.

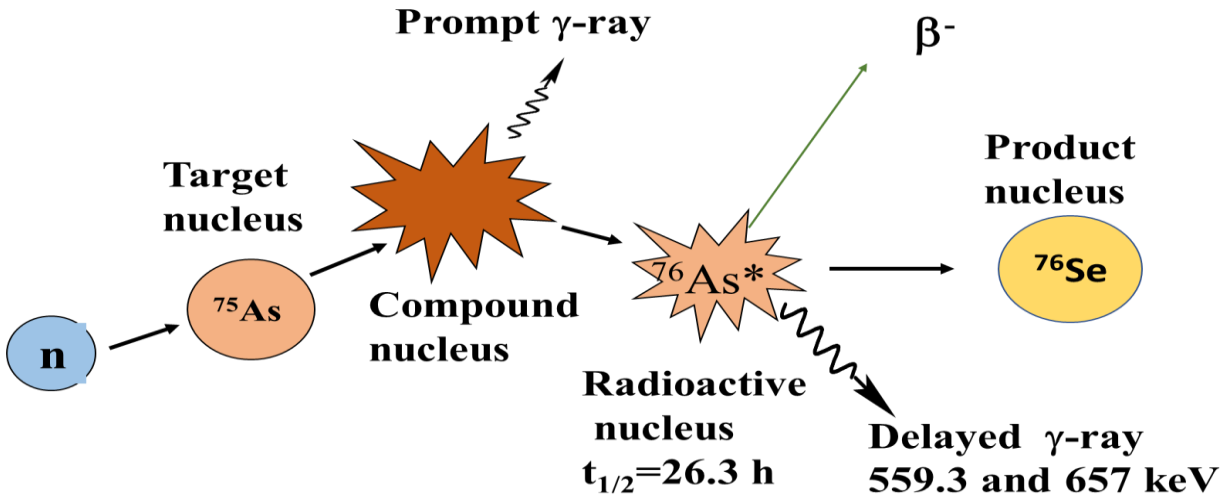

Figure 3.1: Procedure of neutron capture through the target nucleus and the release of γ-rays.

Actually in NAA, the EA to be measured in a sample are changed to radioactive by exposing the sample with neutrons. The rate at which the gamma-rays are emitted from an element is directly proportional to its concentrations.

3.2 Method of Quantifying an Element via NAA

1. The EA be measured in a sample are changed to radioactive by exposing the sample with neutrons (mostly thermal).
2. The radionuclides formed (represented by half-lives) emit their characteristic radiation(s) like, γ-rays.
3. The emitted γ-rays are then determined.
4. Measurement of γ-rays of a particular energy delivers the parent element's concentration.

3.3 Advantages and Applications of the Neutron Activation Analysis Method

1. **Multi-elemental analysis capability:** One run can analyze 30+ elements simultaneously.
2. **Nondestructive easy sample preparation:** No sample digestion, extraction, volume loss or dilution required. Integrity of the sample is not changed by sample preparation**.**
3. **High precision:** Often better than 2% relative standard deviation.
4. **Wide applicability:** Applicable in almost every field of interest e.g.- geology and geochemistry, pharmaceuticals, semiconductor, environmental, forensic, archeological, Biomedicine etc.
5. **Matrix independent:** Comparative independence from matrix and interfering effects.
6. **High sensitivity:** NAA bids superior sensitivities than other procedures, of the order ppb or better.
7. **Reference method:** As NAA method is categorized as accurate and reliable. NAA method is used like adjudicator technique when other procedures produced confusing outcomes and when new methods being invented.

3.4 Classification of Neutron Activation Analysis

There are several procedures of NAA, which are as follows:

- INAA (Instrumental NAA): If NAA is carried out directly of irradiated samples, then it is called INAA.
- RNAA (Radiochemical NAA): Sometimes chemical separation is needed for irradiated samples to concentrate the interested radioisotope or to eliminate interfering species, then this method is termed as RNAA.
- PGNAA (Prompt γ-ray NAA): Prompt γ-ray have to be measured during irradiation using gamma spectrometry system by online measurement. Prompt γ-ray is measured for very short half-life and light element for which Prompt gamma-ray measurement is sensitive. On-line measurement, non destructive, sensitive for light elements H, B, C, N, P, S, etc.

- FNAA (Fast NAA): Nondestructive, poor sensitivity, applicable for O, N, F, Mg, Al, Si, P.
- ENAA (Epithermal NAA): For ENAA, epithermal neutron flux is used for sample irradiation.

3.5 Principles of Neutron Activation with Neutrons

The elements to be determined in a sample are made radioactive by irradiating the sample with neutrons and the radionuclide formed (characterized by their half-lives) give of their characteristic radiation such as gamma rays, which are then identified and measured. All material in this section have been adapted from "Activation Spectrometry in Chemical Analysis" by Susan J. Parry [3.1].

There are two main methods for Neutron Activation Analysis (NAA), those are as follows:

- Absolute Neutron Activation Analysis Approach
- Comparative Neutron Activation Analysis Approach

3.5.1 Absolute Neutron Activation Analysis Approach

Eq. 3.1 is the basic equation for NAA. When the half-life of the radionuclide is short it may also be required to correct by the factor for deterioration during the time (t_c) of counting also.

$$A = N\phi\sigma(1-e^{-\lambda t_i}).e^{-\lambda t_d}.\frac{1-e^{-\lambda t_c}}{\lambda t_c} \quad \ldots \quad \ldots \quad \ldots \quad 3.1$$

For γ-spectrometry, Activity, $A = \frac{\frac{c}{t_c}}{\varepsilon \cdot I_\gamma}$

Where, c/t_c = count/counting time i.e. disintegration/sec. (dps)

ε = the counting efficiency and I_γ = the γ-ray intensity

In Eq. 3.1:

ϕ = the neutron flux, in neutrons m^{-2} s^{-1}

σ = the cross section, in m^2

$\left(1-e^{-\lambda t_i}\right)$ = Irradiation factor

$e^{-\lambda t_d}$ = Decay factor

$\frac{1-e^{-\lambda t_c}}{\lambda t_c}$ = Counting factor

No. of target radionuclides in atoms, N $= \frac{N_{av} \times w \times \theta}{A_{wt}}$

Here, N_{av} = Avogadro's number

w = mass of the target element

θ = isotopic abundance

A_{wt} = Atomic weight

By taking w, i.e. mass of the element to the left side of the Eq. 3.1 and activity, A to the right side then It can be possible to calculate the concentration of the element i.e. mass of the elemental abundance (EA) in a sample, if all the factors on the right side of the equation are known or can be calculated. This is called absolute method and It is very difficult to evaluate all the parameters precisely.

3.5.2 Comparative Neutron Activation Analysis Approach

In the comparative NAA method (using a standard), an element in a sample and a known amount of the same element as a standard are irradiated together and both sample and standard are counted under exactly the same conditions by the same radiation detector. Then divide this Eq. 3.1 by the same equation for standard which eliminates most of the parameters of irradiation and detection and thus the Eq. 3.1 reduced to a simple form, as shown in Eq. 3.2 below:

$$\frac{\text{Weight of element" Z" in sample}}{\text{Weight of element" Z" in standard}} = \frac{\text{Activity (Az) in sample} \times \left(e^{\lambda td}\right)sam}{\text{Activity (Az) in standard} \times \left(e^{\lambda td}\right)std} \quad \ldots \quad \ldots \quad \ldots \quad 3.2$$

So, Comparative method approach is the most simple and accurate way of measuring the concentration of an element. Therefore, by knowing the decay corrected activities of the element in sample and standard, and mass of the element in standard, the mass of the element in the sample,

3.6 Why do Neutrons Widely Used for Nuclear Analysis?

- Neutrons have greater range of penetration into target materials
- Neutrons have large reaction cross section
- Neutrons have high available fluxes

3.7 Prerequisite for NAA

The fundamental requirements to carry out NAA analysis are:

- Neutron source that is preferably a nuclear research reactor.
- Suitable instrumentation for measuring γ-rays that is HPGe detector along with γ-spectrometry system.
- Thorough information of the reactions of neutrons interactions with target nuclei.
- For comparative technique (used in this study), a standard sample is used which removes any ambiguity in the parameters Φ, σ, decay scheme, λ and detection efficiency [3.3].
- Software for gamma-ray spectrum acquisition, peak analysis and concentration calculation

3.7.1 Neutron Source in this Study: Research Reactor

Fig. 3.2 presents 3MW TRIGA Mark-II Research Reactor under Bangladesh Atomic Energy Commission (BAEC), which have been used in this work for irradiation. A partial view of the 3 MW TRIGA MARK- II research reactors is shown in Fig. 3.2.. The characteristic of this reactor is clear from the name "TRIGA" which is a combination of the words Training, Research, Isotope production and name of the manufacturing company GA (General Atomic Company, USA). TRIGA: T-Training, R-Research, I-Isotope production, G-General, A-Atomics.

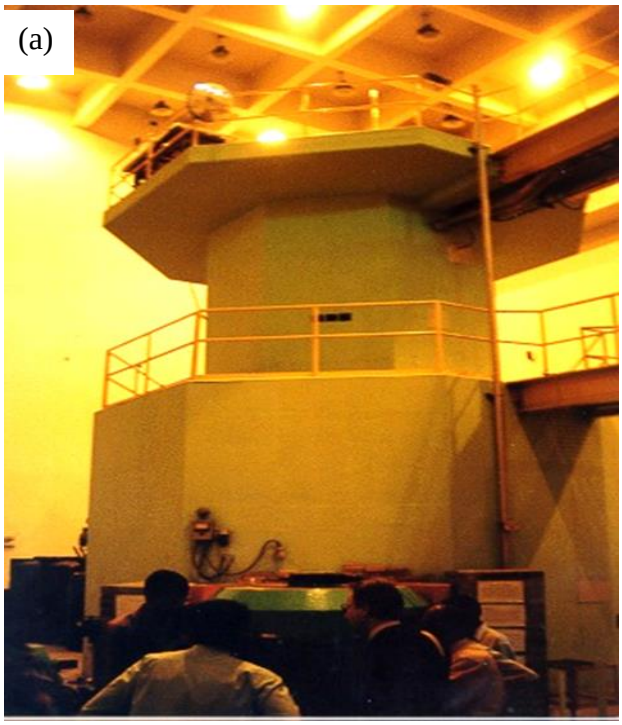

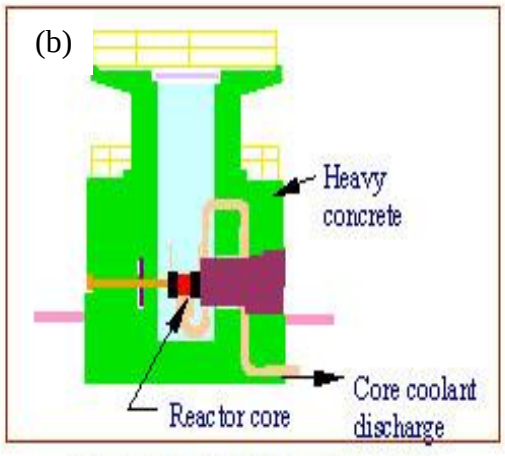

Figure 3.2 : (a) BAEC 3MW Research Reactor .

(b) Sectional Sight of the Reactor [3.3]

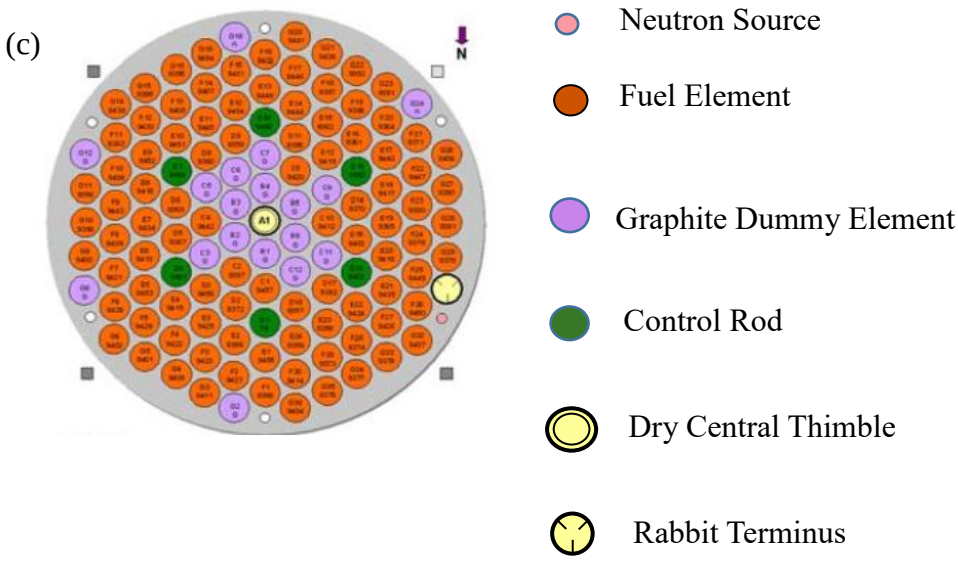

Figure 3.2: (c) Core Configuration of the TRIGA Reactor [3.3]

There are different channel in reactor for sample irradiation. In this study rabbit channel is used for irradiation. Short irradiation has been done individually for each samples encapsulated separately in a rabbit irradiation tube. Long irradiation has been done with all samples and reference materials together. Short irradiation required to measure these elements as their half-lives are short. For an example, half-life of Al is 2.25 min. Long irradiation required to measure these elements as their half-life are Long. For an example, half-life of Co is 5.27 yr.

3.7.2 Another Requirement for NAA

Another requirement for NAA is suitable instrumentation for detecting gamma rays that is High Purity Germanium (HPGe) detector along with gamma spectrometry system. High Purity Germanium (HPGe) detector along with gamma spectrometry system is required both for NAA technique and radioactivity concentration measurement. In this study both techniques have been used for elemental identification and radiological characterization respectively. Gamma Spectrometry Method has been described in the next chapter i.e. in chapter 4.

3.8 The Energy Dispersive X-ray Fluorescence (EDXRF) Analytical Technique for Elemental Identification

When a target is bombarded with photons or particles there may be an interaction with the atomic-shell electrons. The electrons may be ejected and X rays promptly emitted in there arrangement of the electrons in the shells. The energies of these X rays are characteristic for each element and in particular the K and sometimes also the L X rays can be effectively used for analytical purposes. The energy-dispersive X-ray fluorescence (EDXRF) or simply XRF and particle-induced X-ray emission (PIXE) techniques are of primary interest because in both cases semiconductor detectors, mainly Si(Li) detectors, are used as X-ray spectrometers. XRF has the longer tradition and wider application and is well established all over the world [3.4], but the community of PIXE users is comparatively smaller.

In the XRF method the sample atoms are excited by photons originating either from a radioactive source or from an X-ray generator tube. The best for the energy of the exciting radiation is slightly above the K edge (or L edge) of the element to be detected, because the K-shell ionization cross section for a given element strongly decreases with increasing energy above this edge. Frequently used radionuclides in excitation sources are ^{57}Co (Mn K X rays at 6 keV), ^{109}Cd (Ag K X rays at 22 keV), and ^{241}Am (Y rays at 60 keV).

In contrast to the monoenergetic radiation of these and other radioactive sources, the electron bremsstrahlung of an X-ray tube is continuous. Its shape depends on the high voltage and the atomic number of the anode material. Superimposed on the continuum are characteristic X rays

induced by electron and bremsstrahlung excitation in the anode. By inserting filters between tube and sample, by varying the voltage and anode material and by introducing secondary targets, the spectrum of emitted photons can be tailored to the specific analytical problem.

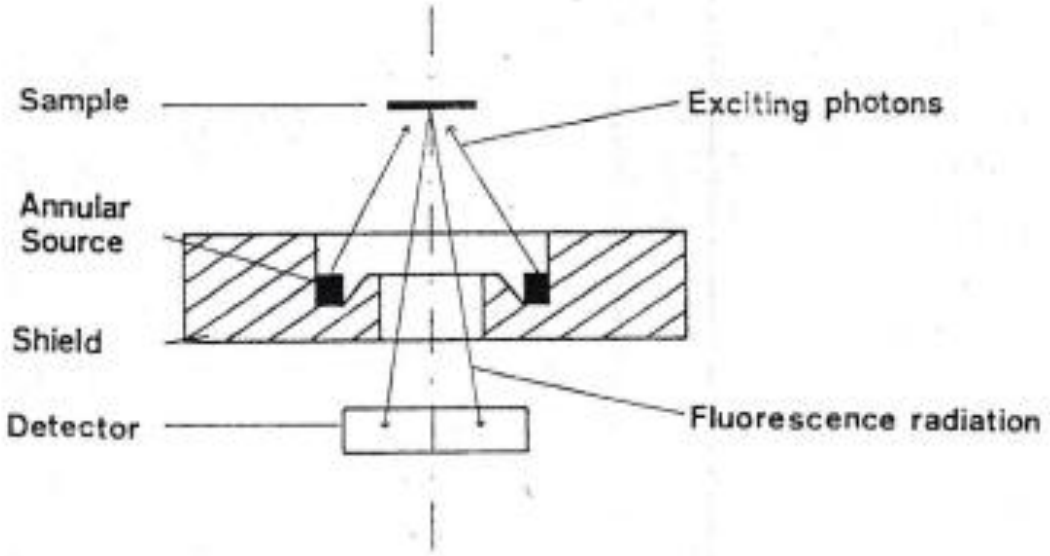

Figure 3.3 : Array with annular radioactive source for the production of X-ray-fluorescence radiation (XRF) [3.5].

A typical measuring geometry in an XRF analysis with a radioactive source as the photon emitter is shown in Fig. 3.3. The detector is mounted at a sufficiently large angle to the direction of the exciting photons so that it can be effectively shielded against the direct source radiation and the secondary radiation induced in assembly components other than the sample.

For sufficiently thin sample layers, in which both the attenuation and the energy loss of the exciting charged particles are negligible, the yield of K-X-ray fluorescence radiation, I_{XK}, can be calculated according to

$I_{XK} = I_0 \sigma_k \omega_k . (m_a/M).N_A$ …… …….. …….. 3.3

I_0 =photon or charged-particle flux imposing on the sample (in s^{-1}),

σ_k =K-shell ionization cross section (in cm^2),

ω_k= K-shell fluorescence yield,

m_a =area-related mass of target element (in g cm^{-2}),

M =molar mass of target element (in $g.mol^{-1}$), and

N_A =Avogadro constant (in mol^{-1}).

The expected full-energy-peak count rate in the Si(Li) spectrometer is

$n = I_{XK}.\ \varepsilon/C$ …… …….. …… 3.4

where ε is the full-energy-peak efficiency and C is a correction factor which accounts for self attenuation of the fluorescence radiation in the target, pile-up losses and any other measurement corrections. Combining eqs. (3.3) and (3.4) we get

$$m_a = \frac{nCM}{I_0\ \sigma_k \omega_k \varepsilon N_A} \quad \text{…….. …… …….. 3.5}$$

The above assumption that the attenuation or energy loss of the exciting photons or charged particles in the sample is negligible is usually not fulfilled, and a further correction factor on the right side of eq. (3.5) has to be added. A compromise aiming at high fluorescence-radiation yield and moderate attenuation or energy loss is frequently chosen. The calculation of m_a according to eq. (3.5) is further complicated by a possible excitation of sample atoms by secondary radiation produced in the sample. Fluorescence radiation from the sample matrix atoms or electrons can give rise to additional excitation. These matrix effects can be very complex and quite significant.

Although many efforts have been made to calculate all effects influencing the fluorescence-radiation yield and to develop appropriate computer codes for the application of this "fundamental-parameter" or "absolute" method, relative methods based on the use of standard reference materials (SRM) are frequently preferred. In the ideal case when the standard and the sample contain the same element and have the same matrix and thickness, the task reduces to measure the peak count rates. In multielement analyses appropriate standards of all elements may not be available. But, since M, σ_k, ω_k, ε and the attenuation of the fluorescence radiation in the matrix are continuous functions of the atomic number Z, if jumps due to K or L edges do not occur, the sensitivity of an XRF setup for any Z in the interval covered by the standard elements can be interpolated.

For crowded spectra as they occur in multielement analyses the spectrum-component analysis method, it is necessary either to establish a library with measured response functions for each element or to rely on a calculational model for the spectral shape. For a specific element i this function, $F_i(E)$, can be approximately described by the sum of several Gaussian functions for each of the j individual characteristic X-ray lines (e.g., K_α, $K_{\beta 1}$, $K_{\beta 2}$, L_α, ...) and the affecting escape peaks, that is

$$F_i(E) = \sum_j a_{ij} [G(E, E_{ij}) + r_{ij}.G(E, E_{ij} - E_{esc})].\ \varepsilon_{ij} \quad \text{..... ..... 3.6}$$

with

E = energy corresponding to the channel number in the spectrum,

E_{ij} = energy of X ray j of element i,

E_{esc} =- Si K_α energy (1.74 keV),

a_{ij} =fractional intensities of X rays j for element i ($\sum_j a_{i\,j}$ =1),

r_{ij} =ratio of escape-peak area to full-energy-peak area (N_e/N in fig. 4.11),

G(E, E_{ij}) =normalized Gaussian function ($\int_0^\infty G(E, E_{ij})\, dE = 1$) with the parameters E_{ij} and w_{ij} (=FWHM), and

ε_{ij} =full-energy-peak efficiency for photons with energy E_{ij}

The Gaussian function may be supplemented by an asymmetry term to account for the low-energy tailing. The energies E_{ij} and the relative intensities a_{ij} possible can be taken from data tables, and the energy dependence of possible asymmetry parameters, The FWHM, r_{ij} and ε_{ij} can be represented by functions with parameters determined experimentally or from a model.

Thus F_i (E) completely describes the shape of the pulse-height spectrum produced by X rays of element i, at least under ideal conditions (i.e., no X-ray attenuation in the matrix, no Compton interactions in the detector, etc.). The remaining task in a multielement analysis is then to fit the sum Σ_i b_i F_i (E) to the measured spectrum by the linear least-squares method. For each element i we have only the one free parameter b_i for its relative abundance.

EDXRF technique consist of Si(Li) detector (Canberra, Model SL 80175) with a Cd-109 radioisotope annular source etc., is available in the Chemistry Division, Atomic Energy Centre, Dhaka.

3.9 The X-Ray diffraction (XRD) Analytical Technique for Chemical Composition Information

X-ray powder diffraction (XRD) is a rapid analytical method primarily selected for crystalline material phase identification and thereby can reveal chemical composition information. The incident rays interaction with the sample produce constructive interference and diffracted ray when Bragg's Law ($n\lambda=2d \sin\theta$) conditions have been satisfied. This law relates the electromagnetic radiation wavelength to the diffraction angle and lattice spacing in a sample of crystalline structure. These diffracted X-rays are then detected, treated and counted.

In this study, the possible mineralogical composition of the samples have been investigated by using PHILIPS PW3040 X'pert PRO X-Ray Diffractometer (XRD) as XRD is a basic tool in the mineralogical analysis. All the data of the samples have been analyzed using computer software "X' PERT HIGHSCORE''. For diffraction applications, only short wavelength (here λ=0.15418nm) of X-rays are used as comparable to the size of atoms. The diffractometer geometry is such that, when the sample rotates the X-rays beam at an angle θ, then diffracted X-rays will rotate at an angle of 2θ. In this study, 2θ scan has been taken from 03° to 75° to find possible fundamental peaks of the sample.

Moreover, some samples of this study have been analyzed using Energy Dispersive X-ray Analysis (EDX) to investigate the chemical identification of elements and their concentration. In EDX, producing X-rays of characteristic wavelength by means of knocking out electrons from atoms by electrons.

Figure 3.4: Philips X'pert PRO X-Ray Diffractometer (PW3040) at materials science division of Bangladesh Atomic Energy Commission.

3.10 Environmental Indicators for Assessing the Elemental Abundances (EA)

3.10.1 Base-line Data for EA

Base-line data selection is important to assess the S&S samples' EA in terms of EC indices like geo-accumulation index (I_{geo}), contamination factor (CF) and enrichment factor (EF). In this study, the EA of upper continental crust [3.6] has been selected as the base-line data.

3.10.2 Enrichment Factor (EF) of Elemental Abundances (EA)

EF is casted widely to distinguish manmade and natural sources of M&M [3.7 – 3.8]. Fe has been used in this study to calculate EF as Fe naturally has almost uniform concentrations and also displays alike to many trace elements' geochemistry [3.9 – 3.11]. EF is measured by the equation below:

$$\mathrm{EF} = \frac{(\mathrm{M/Fe})_{\mathrm{Sample}}}{(\mathrm{M/Fe})_{\mathrm{Background}}} \quad \ldots\ldots \quad \ldots\ldots\ldots \quad \ldots\ldots\ldots \quad 3.7$$

Here, M represents metal. EF above 1.0 represents that the element is from manmade source. EF values 1.5 to 3; 3 to 5; 5 to 10 and above 10 are the indication of minor, moderate, severe and very severe alteration, respectively [3.12].

3.10.3 Geo-Accumulation Index (I_{geo}) of Elements

Depending on the choice of base-line data i.e. background levels, I_{geo} values exhibit huge variations. In this work, upper continental crust's (UCC) EA according to [2] have been selected as the base-line data to calculate I_{geo}. The concentration comparison is the alternative of polluted and unpolluted sediments which are mineralogically and texturally comparable, [3.13].

I_{geo} is well-defined by the equation below [3.12]:

$$I_{geo} = \log_2\left(\frac{Cz}{1.5\ X\ B_z}\right) \quad \ldots\ldots \quad \ldots\ldots\ldots \quad \ldots\ldots\ldots \quad 3.8$$

Where, Cz is the z metal concentration, Bz is the z metal geochemical background concentration. Factor 1.5 is the background correction matrix. I_{geo} consists of 7 grades: [3.15].

1. $I_{geo} \leq 0$ grade represents almost uncontaminated
2. $0 < I_{geo} < 1$ grade represents uncontaminated to moderately contaminated
3. $1 < I_{geo} < 2$ grade represents moderately contaminated
4. $2 < I_{geo} < 3$ grade represents moderately to heavily contaminated
5. $3 < I_{geo} < 4$ grade represents heavily contaminated
6. $4 < I_{geo} < 5$; grade represents heavily to extremely contaminated
7. $5 < I_{geo}$. grade represents heavily to extremely contaminated, which is open grade and can be hundredfold higherr than background [3.16].

3.10.4 Contamination Factor (CF) of Individual Elements

CF is calculated of the specific HM&M for a specific sampling site and is calculated by the equation below [3.17].

$$CF = \frac{(MC)_{Sample}}{(MC)_{Background}} \quad \ldots\ldots\ldots \quad \ldots\ldots\ldots \quad \ldots\ldots\ldots \quad 3.9$$

Here, MC = Metal Concentration. CF is helpful for the detection of contamination status of metals [3.18]. CF values of EC for S&S samples are characterized as low: CF < 1; moderate CF: 1 to 3; considerable CF: 3 to 6 and high: CF > 6 [3.19].

Chapter 4

Analytical Technique for Radiological Characterization: Gamma Spectrometry System

4.1 Radionuclide Detection System of Radioactive Samples

A number of analysis techniques exists which are able to determine the activity level of specific radionuclide content in different types of samples. For all types of samples, the gamma spectrometry system is usually the most effective technique to study gamma emitting radio nuclides. The two most important and available gamma spectrometry system with detectors are sodium iodide crystal detector (NaI) and liquid nitrogen cooled high purity germanium detector (HPGe). These methods are highly appropriate for accurate multi-nuclide analysis for environmental materials without any chemical separation, which is costly and time consuming, so extensively used by laboratories for analyzing gamma radioactivity. Due to excellent resolution compared to NaI crystal, HPGe detector has become chief tool for the analysis of RM.

4.2 Specification of HPGe Detector

In this study, for natural radioactivity measurement, a p-type co-axial High Purity Germanium (HPGe) detector (CANBERRA: Model GC-4019; serial no. 07089419) with 40% efficiency relative to a NaI(Tl) detector has been used. The effective volume of the detector is 93 cm^3 and energy resolution of the detector has been found to be 1.8keV at 1332 keV energy peak of ^{60}Co γ-ray line and the detector was coupled to a Multichannel Analyzer (MCA) with 16k channel.
The spectra acquisitions of a sample have been studied by using the spectra analyzing software MAESTRO-32 (ORTEC) and Genie-2000 (Canberra), and by using the software Hypermet PC version 5.12, the gamma peak analysis has been done.

4.3 Gamma Ray Spectrometry System Setup

For gamma-ray counting, HPGe detector coupled with digital γ-spectrometer has been used.

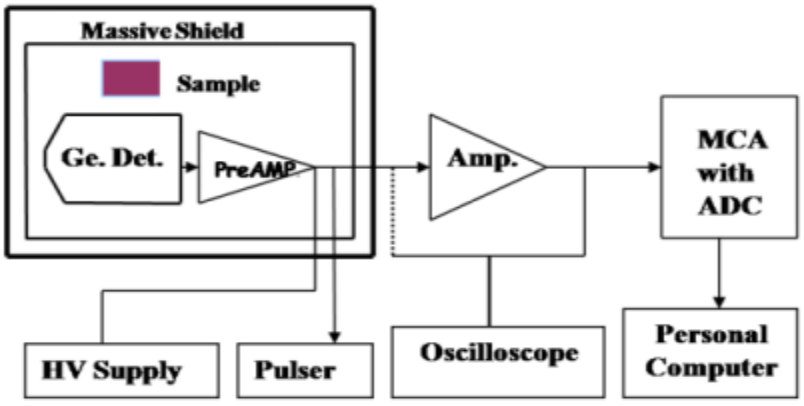

Figure 4.1: Electronic block diagram of high resolution γ-spectrometry system [4.1].

This Figure shows a schematic for the procedures that arise during γ-spectrometry using HPGe detector. Subsequently the detector, the processing includes preamplifier, amplifier and MCA to create a spectrum.

4.4 High Purity Germanium (HPGe) Detector

As γ-rays are uncharged their detection depends on the transmission of their energy to electrons within a detector material. HPGe detector is one sort of semiconductor detector. Semiconductor detector produces available free charge carriers that can be used for detection and measurement of incident different radiations. [4.2].

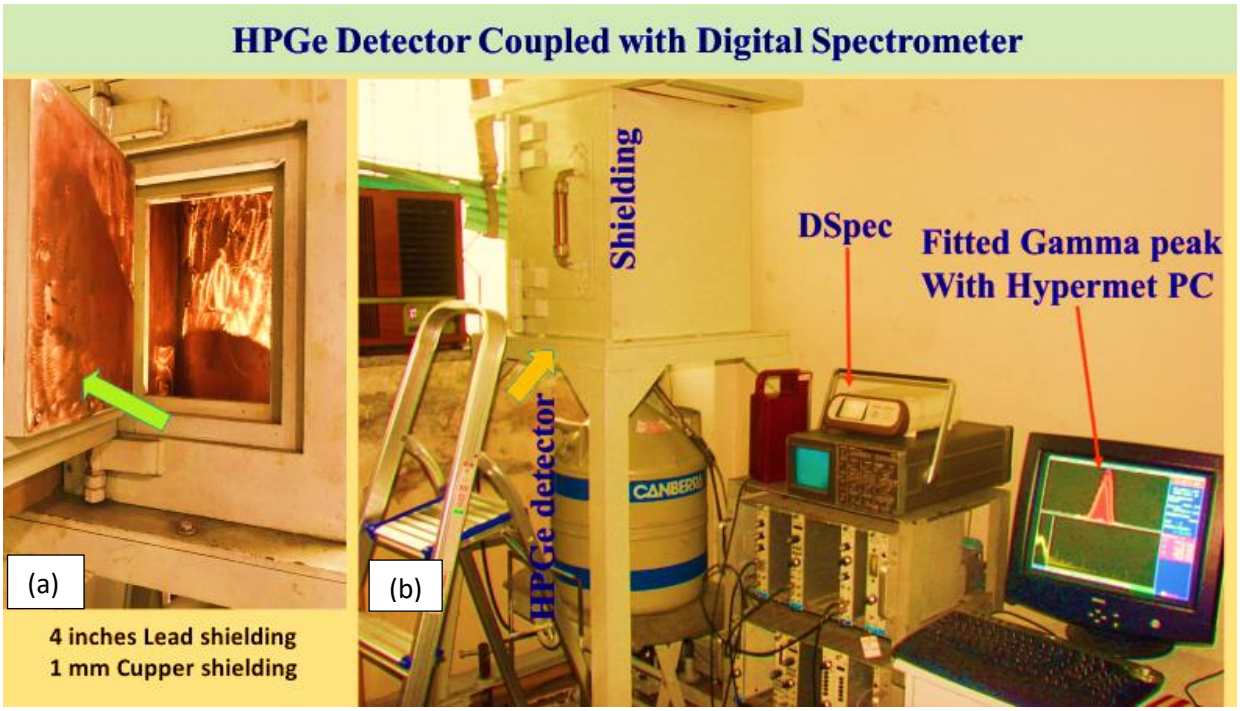

Figure 4.2: HPGe Detector Coupled with Digital Spectrometer at Reactor and Neutron Physics Division, Institute of Nuclear Science and Technology, Savar under BAEC.

4.4.1 Shielding Arrangement

According to Fig. 4.2 (a) detector is inside the Shielding. Around the detector, shielding is used to protect background radiation. Here four (4) inches thick heavy lead shielding with 1 mm thin cupper shielding have been used, where low energy lead (Pb) X-ray noise created inside the

detector being absorbed within the cupper lining. Shielding arrangement picture of the HPGe detector has been presented in Fig. 3.2.2 (a). For the construction of radiation shields, Lead shielding is the most widely used material because of its high density (11.4 gm/cc).

4.5 Gamma-ray Interactions with Matter

In this study, we use one sort of semiconductor detector which is HPGe detector for uncharged γ-ray detection, in which there are three focal mechanisms of energy dependent interaction of photon with the matter: 1) low energy dominant, photoelectric effect 2) important mid-energy range dominated Compton scattering and 3) only high energy range occurred pair production. When high-energy γ-ray photon passing through the semiconductor detector ionizes the atoms and creating electron-hole pairs, where the electrons and holes move to the electrodes under the effect of electric field and then produce a pulse which can be determined in the outer circuit. Full-energy peak above 150 keV, multiple Compton-photoelectric actions are the most dominant contributors. For γ-ray energies above 1.022 MeV, there is a probability of electron-positron pair production.

4.6 Secular equilibrium

When the half-life of the parent is very long compared to the half-life of the progeny, i.e. $t_{1/2}$ parent >> $t_{1/2}$ daughter, then the equilibrium state is mentioned as secular equilibrium.

As $t \rightarrow \infty$, so the secular equilibrium equation tends to:

$$\lambda_2 N_2 = \lambda_1 N_1 \quad \ldots \quad \ldots \quad \ldots \quad 4.1$$

According to the radioactive decay definition:

$$A_2 = A_1 \quad \ldots \quad \ldots \quad \ldots \quad 4.2$$

So, when the radioactivity of one radionuclide is determined in a decay chain, then it is assumed that the same radioactivity will be found to other radionuclides of that chain for secular equilibrium state.

4.7 Basic Equation for Radioactivity Concentration (RC)

The RC or the specific radioactivity is the radioactivity per unit mass of the sample. The basic equation for RC is as follows:

$$A = N/(P_\gamma \times \varepsilon \times W) \quad \ldots \quad \ldots \quad \ldots \quad 4.3$$

Here 'A' represents the RC which we would like to measure.

N = Net counts per second/net cps = (Sample cps) – (Background cps)

P_γ = Gamma intensity

ε = Detection efficiency

W = Sample weight (kg)

We get gamma-peak count at different energies when analyzing unknown sample using gamma spectrometry and when dividing by total counting time, we get 'count per second (cps)'. By deducting background cps from sample cps, we get net cps. Where for background count monitor of NORMs around, a blank sealed vessel of same geometry like the samples carrier and same way has been counted. We have to measure detection efficiency, it will be explained in next chapter. And we get gamma intensity correspond to each energy from literature data. Sample weight is measured in kilogram.

The γ-ray lines of ^{214}Pb (295.21 keV, 351.93 keV and 1120.29 keV) and ^{214}Bi (609.32 keV) have been used to measure the RC of ^{226}Ra. The RC of ^{232}Th was determined by the γ-ray lines of ^{208}Tl (510.77 and 583.19) keV, ^{212}Pb (238.63 keV) and ^{228}Ac (911.204 keV). The radio-activities of ^{40}K and any anthropogenic ^{137}Cs have been measured directly by their specific 1460.8 keV and 661.6 keV single γ-ray lines respectively. These have been measured using above mentioned Eq. 4.3.

4.8 Radiological Hazard Indices Explanation

Radiological hazard indices (RHI) are calculated using formulas and their recommended values are incorporated according to their adverse effect radiological on human being or environment. The following RHI are calculated to assess whether the annual dose exceed 1mSv/y because of the additional external γ-radiation. On the other hand, world Avg. value depends on radioactivity levels of different areas of the world and does not depend on radiological hazed risk assessment. Though with increasing radioactivity level, the values of RHI also increase but RHI values have their specific threshold values beyond which is hazardous for human being and environment. And world Avg. value has no threshold value, depends only on different areas of the world. This threshold of value is called recommended value within which is acceptable range i.e not harmful. Moreover these recommended valves are specified by different world wide famous organizers like IAEA, UNSCEAR etc.

4.8.1 Radium Equivalent Activity (Ra_{eq}) and γ-representative Level Index (I_γ)

A common RHI is presented through a single quantity for the RR associated with the materials containing NR3, defined as Ra_{eq} and is measured predicting that 10, 7, and 130 $Bq.kg^{-1}$ of ^{226}Ra, ^{232}Th and ^{40}K respectively produce the same γ-dose rate as the equation stated below [4.3 -4.4]:

$$Ra_{eq} = A_{Ra} + 1.43\ A_{Th} + 0.077\ A_K \quad ... \quad ... \quad ... \quad 4.4$$

Here A_{Ra}, A_{Th} and A_K (in $Bq.kg^{-1}$) are the RC of ^{226}Ra, ^{232}Th and ^{40}K respectively and Ra_{eq} level have to be less than 370 $Bq.kg^{-1}$ for natural soil.

I_γ is applied for the assessment of γ-radiation in the soil occurred with NR, which is measured as equation shown below [4.1, 4.3];

$$I_\gamma = A_{Ra}/150 + A_{Th}/100 + A_K/1500 \leq 1 \quad \ldots \quad \ldots \quad 4.5$$

where CRec level is 1 for I_γ, which corresponds to $E_{ff} \leq 1$ mSv.

4.8.2 External Absorbed Dose Rate and Annual Effective Dose Rate

Absorbed dose rates (D) for the uniformly distributed naturally occurring radionuclides caused by the γ-radiation at 1m above the ground level in the air have been calculated as follows according to the guidelines provided by UNSCEAR (2000) [4.5]:

$$D\ (nGyh^{-1}) = 0.462\ A_{Ra} + 0.621\ A_{Th} + 0.0417\ A_K \quad ... \quad ... \quad 4.6$$

D-value due to γ-radiation from ^{226}Ra, ^{232}Th and ^{40}K have been converted to annual effective dose (E) by the following equation [4.5]:

$$E\ (mSv\ yr^{-1}) = D\ (nGyh^{-1}) \times 8760\ h\ yr^{-1} \times O \times C \quad \ldots \quad \ldots \quad 4.7$$

Here C (in mSv/nGy) is the absorbed to effective dose conversion coefficient which is 0.7 Sv/Gy and O is the occupancy factor of 0.2 for the outdoor exposure [4.5].

4.8.3 External and Internal Hazard Indices

The external hazard index (H_{ex}) reflecting the external exposure is calculated by the following equation [4.3,4.5]:

$$H_{ex} = A_{Ra}/370 + A_{Th}/239 + A_K/4810 \leq 1 \quad \ldots \quad \ldots \quad 4.8$$

On the other hand, the internal hazard index (H_{in}) is characterized in such a way to lessen the maximum permissible abundances of ^{226}Ra to half the values appropriate for the external exposure alone which reflects the internal exposure to radon (^{222}Rn: gaseous short-lived decay product of ^{226}Ra) along with the contributions of other NORMs and their progenies due to their adverse effects on the respiratory organs. H_{in} can be defined as [4.3, 4.5]:

$$H_{in} = A_{Ra}/185 + A_{Th}/259 + A_K/4810 \leq 1 \quad \ldots \quad \ldots \quad 4.9$$

In calculating the both indices (H_{ex} and H_{in}) the normalizing factors have the same unit as that of activity

4.8.4 Excess Lifetime Cancer Risk (ELCR)

ELCR is caused by the E_{ff} for external exposure is determined as bellows [4.1, 4.6]:

$$ELCR = E_{ff} \times ALT \times RF \quad \ldots \quad \ldots \quad \ldots \quad 4.10$$

Where, ALT is Avg. life time (assumed 70 years) and RF is risk factor.

Chapter-5

Materials and Methods

5.1 Sample collection and processing

Total fortytwo samples have been collected for elemental identification and radiological characterization of gas well core (GWC) and surface samples for environmental assessment in GF regions of Bangladesh, where twenty environmental S&S samples and twentytwo GWC samples of gas reservoir wells (GRW) from three different GF, namely Sbz GF, SGF and FGF.

Table 5.1: List of the Gas Field environmental ((GFEv) soil and sediment (S&S) samples of Shahbazpur (Sbz) gas field (GF) with ancillary information.

Sample ID	Sample Description (depth)	Location Description	Distance from reference point/ Other information
EB-1	Sediment[a]	Reference point[b]	0.0
EB-2.1	Surface soil (0 - 6")	Near pond[c]	40 m
EB-2.2	Soil sample (6"- 8")	Near pond[c]	40 m
EB-3.1	Surface soil (0 - 6")	Bank of pond[c]	43 m
EB-3.2	Soil sample (6"- 8")	Bank of pond[c]	43 m
EB-4.1	Surface soil (0 - 6")	Near the south side of pond[c]	52 m
EB-4.2	Soil sample (6"- 8")	Near the south side of pond[c]	52 m
EB-5	Sediment[a]	At the south-west side of pond[d]	61 m
EB-6	Sediment[a]	At the north-east side of pond[d] (chemical wastes dumping zone)	60 m
EB-7	Surface soil (0 - 6")	Outside gas field boundary	Bank of local cannel
EB-8	Surface soil (0 - 6")	Outside gas field boundary	Near the local cannel

[a]Sediment sample from the bottom of the Waste Deposited Evaporation Pond (WDEvp Pond); [b]Reference point of the sample location assumed as the WDEvp Pond north-west corner where produced water falls; [c]The fresh water pond; [d]The WDEvp Pond.

The longitude and latitude of GRW-2 & 4 of Sbz GF of Bangladesh are 90°45'07.01" E; 22°28'13.74" N and 90°45'19.626" E; 22°27'52.095" N respectively with Sbz structural location lies in the southern part of the central deep Bengal basin in the Hatia trough.

Figure 5.1: Sbz GF area along with sampling locations.

A total of eleven samples have been collected from Sbz GF environment, where 3 surface-soil (SurS) (0 - 6"), 3 sub-surface-soil (SubS) (6"- 8"), 3 bottom sediment of WDEvp pond and 2 SurS samples from nearby local canal outside the GF boundary were included. The canal is connected with the GF drainage. The WDEvp pond corner where PW fall (sample ID: MB-1) is considered as the reference point of the sample location. Fig. 5.1 presents the different locations of the Sbz GF of Bangladesh and presents the different areas of sampling locations.

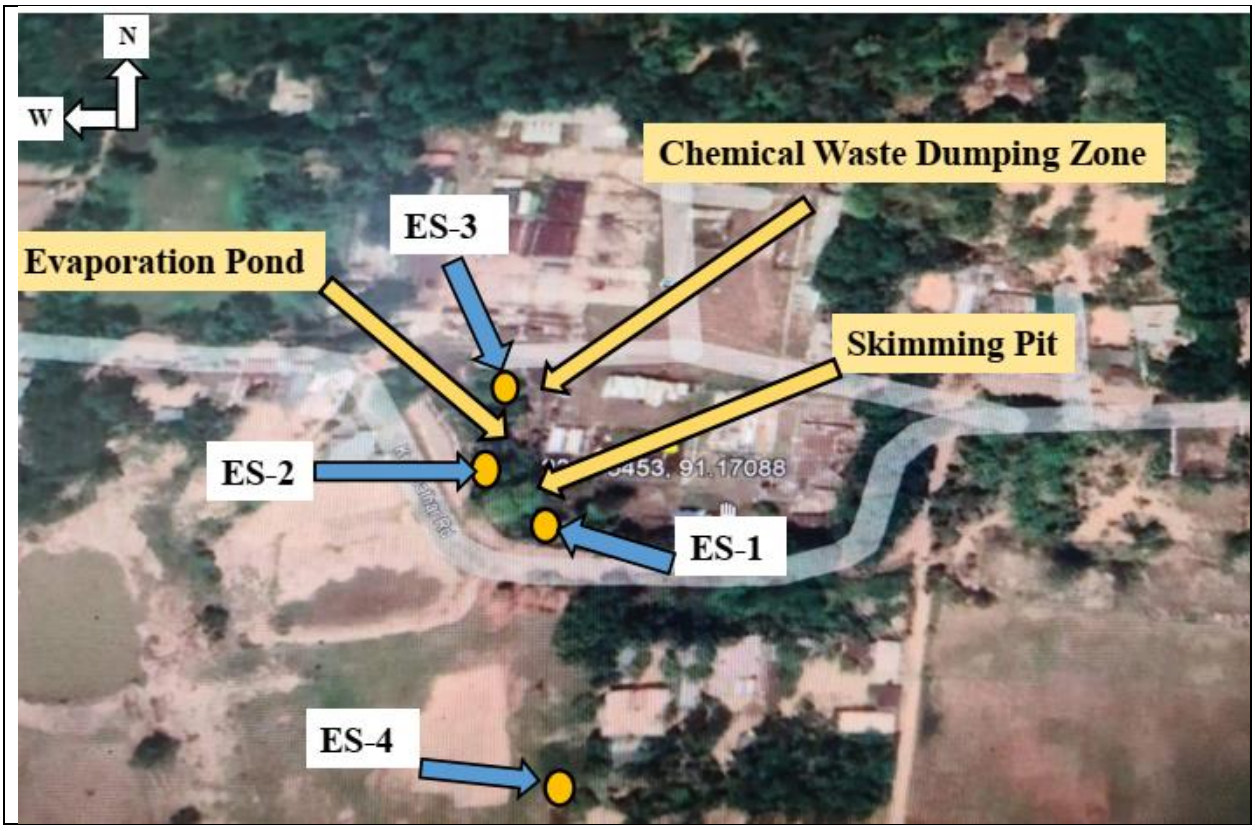

Figure 5.2: SGF area along with sampling locations

The longitude and latitude of GRW-1 of SGF of Bangladesh are 91°10'19.73"E and 22°40'29.73"N respectively. Again the longitude and latitude of GRW-2 of FGF of Bangladesh are 91°57'23"E and 24°36'46"N respectively. Description of the nine GFEv S&S samples of SGF and FGF have been presented in table-5.2. Fig. 5.2 and Fig. 5.3 present the different locations of the SGF and FGF of Bangladesh and present the different areas of sampling locations.

Table 5.2: List of the GFEv S&S samples of SGF and FGF with ancillary information.

Sample ID	Field Name	Sample Location Description	Sample Description (Depth in inches)	Sampling Location
ES-1	Saldanadi	Skimming pit area	SurS (0 - 6")	23.675453 N 91.170885 E
ES-2		North-East corner of pond	SurS (0 - 6")	23.676311 N 91.170065 E
ES-3		South-West corner of pond	SurS (0 - 6")	23.675823 N 91.169342 E
ES-4		Field location area	SurS (0 - 6")	23.674338 N 91.170523 E
EF-1	Fenchuganj	Skimming pit area	SurS (0 - 6")	Field Location 24.6162 N 91.9529 E
EF-2		Bottom of the pond	Sediment	
EF-3		Pond side area-1	SurS (0 - 6")	
EF-4		Pond side area-2	SurS (0 - 6")	
EF-5		Out side of gas field & plant area.	SurS (0 - 6")	

Surface Soil (SurS)

Seven GWC samples of two different GRW from various depths of the boreholes of Sbz GF, seven GWC samples of SGF and eight GWC samples of FGF of Bangladesh have been collected from Chittagong regional office store of Bangladesh Petroleum Exploration and Production Company Ltd. (BAPEX). Description of the GWC samples of these three different GF have been presented in table-5.3. After collection, the samples are arranged according to different depths and wells. The samples are numbered and coded for better identification and then the samples have been dried properly. All the GWC samples have been ground and homogenized by agate mortar where harder samples have been crushed firstly by using special type hand mortar which is made of hardened alloy of steel.

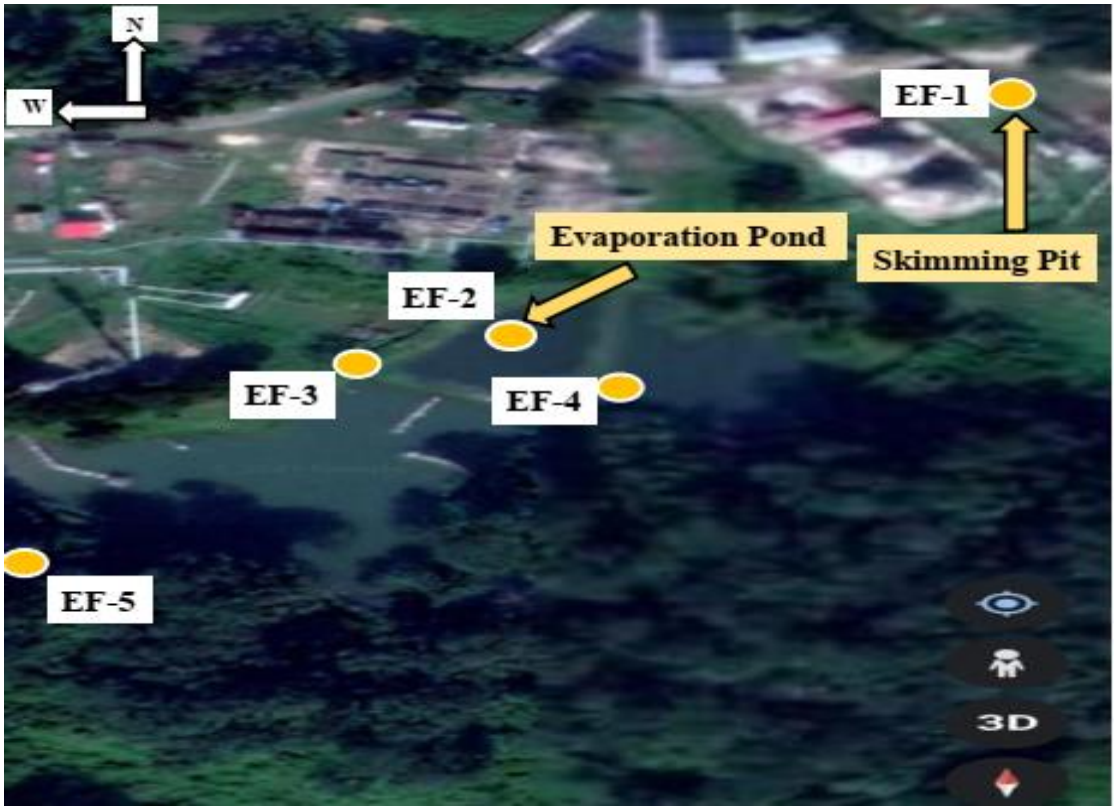

Figure 5.3: FGF area along with sampling locations

Sediment samples have been collected from the WDEvp pond of GF by using acrylic pipe with height 2 m and diameter 4 cm. By screwing at ~15cm depth, the pipe was injected through the sediment and then the upper opening side of that pipe was blocked with rubber-cork. The pipe was then taken out slowly by unscrewing, and a sample remover made of rubber with another pipe of smaller diameter than that acrylic pipe was casted for removing the samples from horizontally placed pipe after take out the cork [5.1]. To collect the individual sample, separate hand gloves have been used for avoiding cross-contamination. Additionally, sample collecting equipment were washed (by normal water followed by distilled water) properly between every sub-sequent sampling. The samples have been marked distinctly by giving the identification (ID) number properly.

Table 5.3: Description of the core samples of three different GF.

Field No.	Field Name	Well No.	Core No.	Sample ID	Depth (m)	Lithology
1.	Shahbazpur (Sbz) gas field (GF)	2	C-1	CB-1.1	2591-91.8	Shale
			C-1	CB-1.2	2591.8 -92	Shale
			C-1	CB-1.3	2592-93	Shale
			C-2	CB-1.4	3263-64	Shale
		4	C-1	CB-2.1	2929-30	Sand
			C-2	CB-2.2	3420-21	Sand
			C-3	CB-2.3	3698-99	Shale
2.	Saldanadi (SGF)	1	C-1	CS-1	1279-80	Shale
			C-2	CS-2	1570-71	Shale
			C-3	CS-3	1774-75	Shale
			C-4	CS-4	2096-97	Shale
			C-5	CS-5	2311-12	Fine Sand
			C-5	CS-6	2313-14	Fine Sand
			C-5	CS-7	2316-17	Shale
3.	Fenchuganj (FGF)	2	C-4	CF-1	2194-95	Shale
			C-7	CF-2	3141-42	Shale
			C-8	CF-3	3259-60	Shale
			C-8	CF-4	3263-64	Shale
			C-8	CF-5	3267-68	Shale
			C-10	CF-6	3624-25	Sand
			C-11	CF-7	3770-71	Shale
			C-12	CF-8	4090-91	Shale

About 1.0–1.5 kg top-soil or sediment samples had been collected from each sampling locations, and then allowed to dry in electric-oven at 60°C to have constant weight. From the dried S&S samples, botanical debris and stones have been separated. Samples are then ground by agate mortar to obtain homogenized powder form.

Figure 5.4: Sediment sample collection process from the WDEvp Pond of GF by using acrylic pipe.

5.2 Geological Background

The North West – South East trending oval shaped Sbz structure lies in the Hatia trough of Bengal Foredeep. Sbz structure is parallel to the Kutubdia structure and this structure is relatively 69.4 m higher than the Kutubdia structure. The longitude and latitude of Sbz gas well-2 is 90°45'07.01" and 22°28'13.74" and gas well-4 is 90°45'19.626" and22°27'52.095", respectively. Drill hole SB-2 and SB-4 is situated in the southern part of the central deep basin in the Hatia trough. Structurally the Hatia trough is categorized by NNW-SSE trending anticline structure [5.2].

Lithologic Column of Different Well

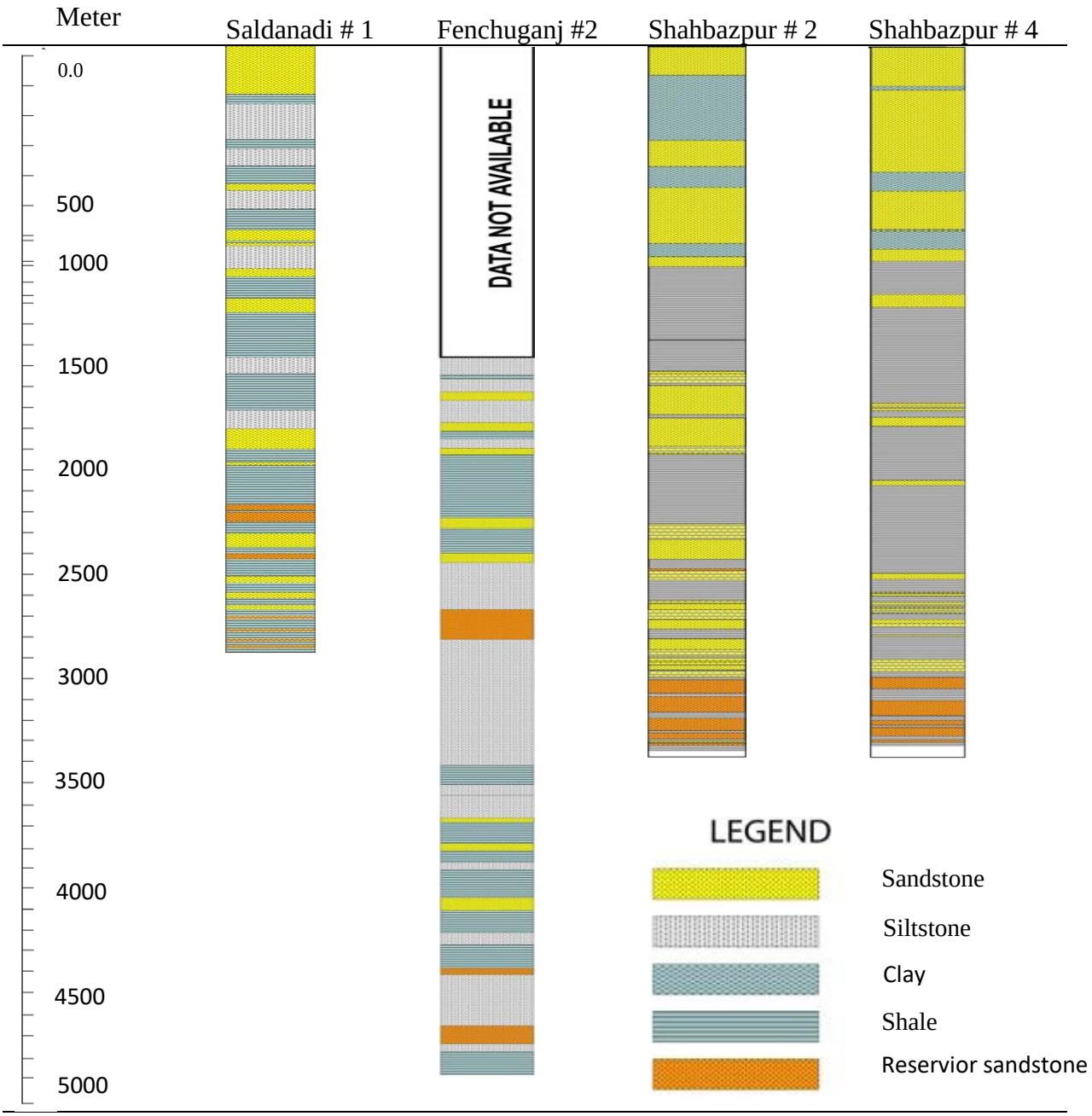

Figure 5.5: Stratigraphy and lithology of the SGF well#1, FGF well#2 and SBZ GF well#2 and# 4; i.e. all wells information of this study [5.3 - 5.6].

Detailed account of the stratigraphy and lithology of the SGF well#1, FGF well#2 and Sbz GF well#2 & 4; i.e. all wells information of this study have been presented in Fig. 5.5 [5.3 – 5.6]. The core samples of Sbz GF collected from Surma group formation of Miocene age from 25 to 5 million years ago of Deltaic shallow marine environment. The Surma Group sediment in drilled

Well#2 & 4 of Sbz GF mainly consist of shale and sandstone with occasional interbedded siltstone and claystone. Some massive- bedded sandstone layers are also present in the sedimentary sequence. In all wells of all three GF of this study, above twothousand meter depth i.e. the lower parts of GRW are composed of reservoir sandstone. These sandstones are intercalated by shale and siltstone, according to Fig. 5.5.

5.3 Sample preparation for elemental identification

Sample preparation of this study for elemental identification by INAA, EDXRF and XRD methods have been shown in Fig, (a), (b) and (c) respectively.

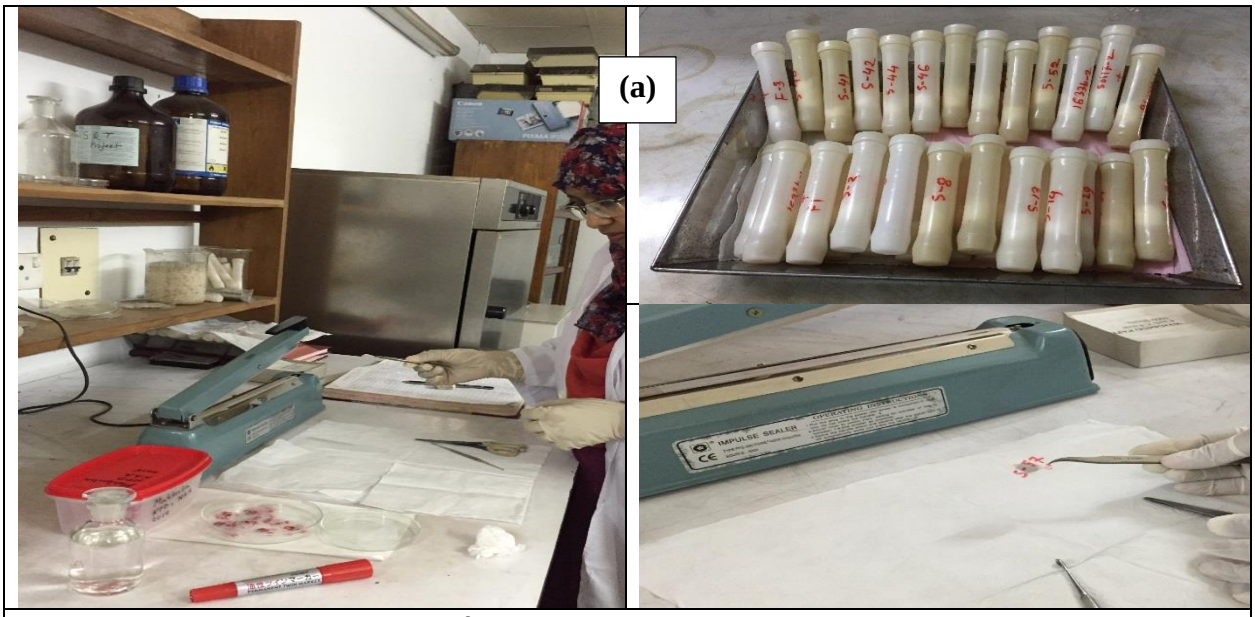

Figure 5.6(a): Sample preparation for instrumental neutron activation analysis (INAA)

Figure 5.6(b): Sample preparation for EDXRF

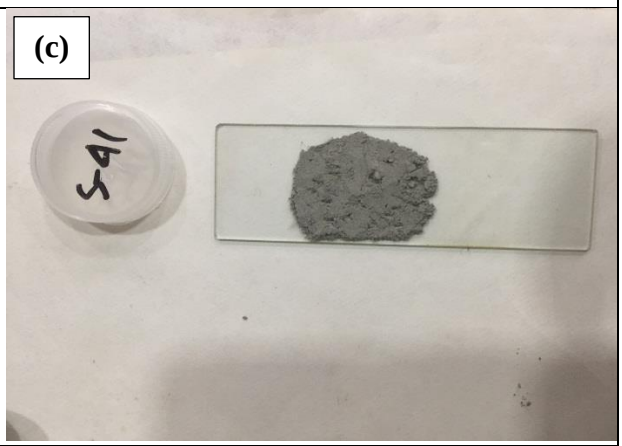

Figure 5.6(c): Sample preparation for XRD

5.3.1 Sample preparation for instrumental neutron activation analysis

Approximately 50 mg of each powdered samples were weighed in polyethylene bags (1×1 cm), heat-sealed and double packed for avoiding potential contaminations. Standard reference material NIST-1633b (coal fly ash) and reference material IAEA-Soil-7 (soil) were used in this study for relative standardization approach. NIST-1633b was used as the standard (multi-element comparator) while IAEA-Soil-7 was used as the control sample for ensuring the data quality. Along with the studied samples, comparator and control samples, Al and Si reagents (Spex, USA) and IRMM-530RA Al-0.1% Au (0.1 mm foil) were used for correcting the spectral interference and monitoring the neutron flux, respectively [5.7].

5.3.1.1 Sample irradiation

At the 3 MW TRIGA Mark–II research reactor at Institute of Nuclear Science and Technology (INST), Savar under Bangladesh Atomic Energy Commission (BAEC), two irradiation schemes have been performed for this study using pneumatic transfer (rabbit) system. Short irradiation has been performed separately for each sample (encapsulated separately in a rabbit irradiation tube) with the thermal neutron flux of 5.28×10^{12} n.cm^{-2}.s^{-1} for 60 s at 250 kW and long irradiation has been performed simultaneously with all the samples and standards with the thermal neutron flux of 2.11×10^{13} n.cm^{-2}.s^{-1} for 8 min at 2 MW [5.2]. Blank sample has been irradiated under identical conditions and corrections have been made accordingly. To determine the neutron flux gradient within the sample stack, three IRMM-530RA Al-0.1 % Au (0.1 mm foil) monitor foils have been irradiated by placing them at the bottom, middle and top of the sample stack for the long irradiation scheme whereas for the short irradiation scheme Al-Au-foils were irradiated sequentially after certain interval.

5.3.1.2 Gamma-ray counting

After irradiation, gamma-ray counting has been performed with a high purity germanium (HPGe) detector [CANBERRA, 25% efficiency relative to a NaI(Tl) detector and 1.8 keV resolution at 1332.5 keV of ^{60}Co] coupled with a digital gamma spectrometer (ORTEC, DSPEC Jr™). For short irradiated samples, first counting has been performed for 300 s after a decay time of about 300 s and second counting for 600 s after a decay time of 2–3 hr. For long irradiation, first counting has been performed for 30 min after a decay time of 2 days, second counting has been performed for 2 hr after a decay time of 10-15 days. Short-lived and long-lived radionuclides have been determined from the short and long irradiation separately [5.2].

5.3.2 Basic protective measures for radiation safety

When handling radioactive sample, we should maintain three basic protective measures for radiation safety. These are minimize time, maximize distance and use shielding.

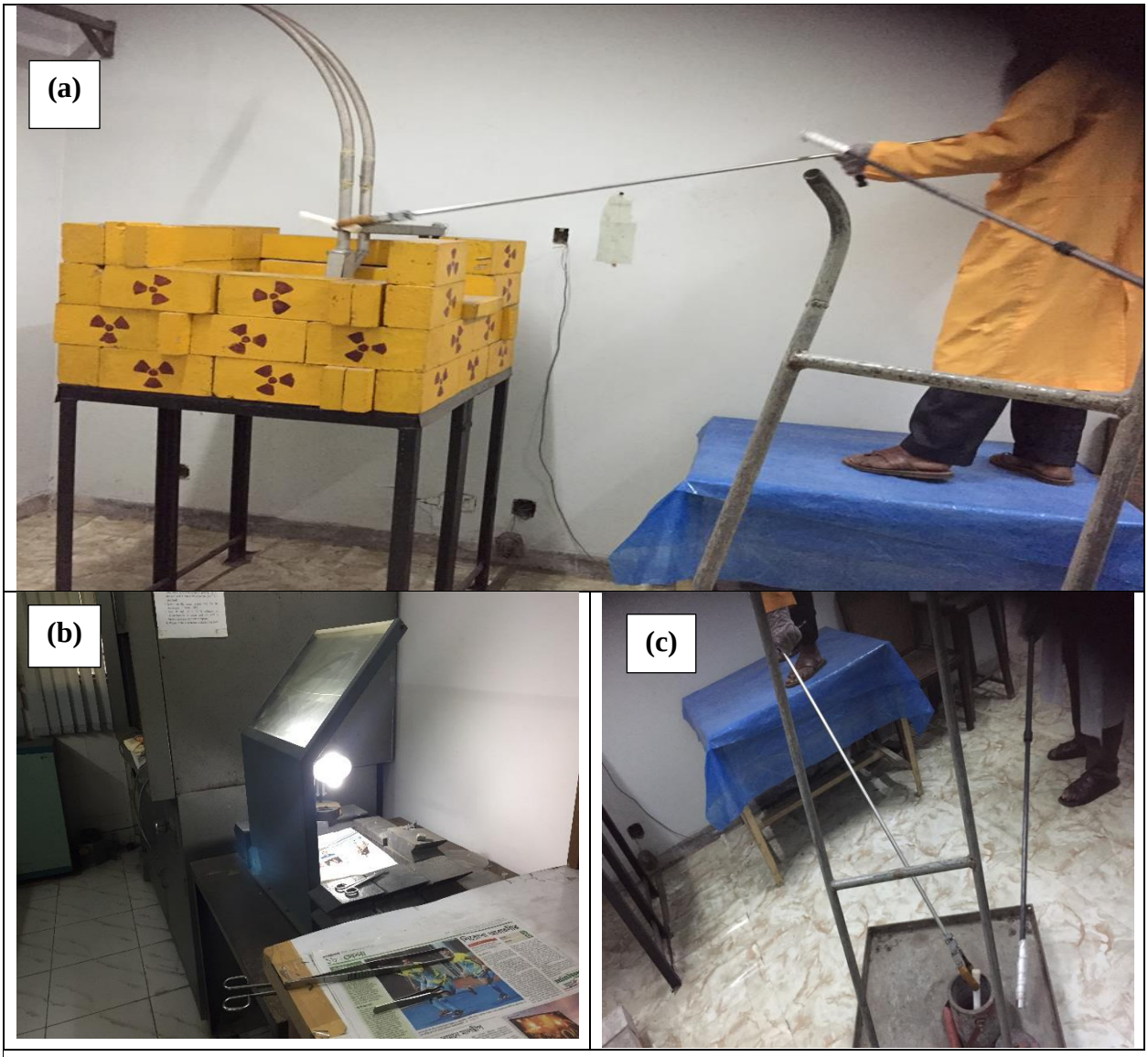

Figure 5.7: Rabbit system room (a) & (c) and sample preparation laboratory (b) sites respectively,

Fig. 5.7(a) and 5.7(c) present sites of rabbit system room and Fig. 5.7(b) presents site of sample preparation laboratory. According to Fig. 5.7(b), radioactive sample after irradiation prepared for analysis within lead shielding. Also radioactive sample is kept in shielded pot according to Fig. 5.7(c).

For handaling sample from rabbit system, long tong is used to maintain distance from radiation according to Fig. 5.7(a). Again to spend less time in radiation area shifting duty is maintained. According to Fig. 5.7(c), irradiated sample is carried by trolley for maintaining distance from the sample as well as spending less time with it. In these ways, three basic protective measures for radiation safety i.e. minimize time, maximize distance and use shielding have been maintained when handling radioactive sample of this study. As the guiding principle of radiation safety is "ALARA" which stands for "as low as reasonably achievable". According to the principle, even if it is a small dose, if receiving that dose has no direct advantage, we should try to avoid it.

5.3.3 Spectrum acquisition, data calculation and reliability

The data acquisition has been performed using the software Genie-2000 (Canberra) and MAESTRO-32 (ORTEC) and the gamma peak analysis has been executed using the software Hypermet PC version 5.12. To identify the radionuclide in gamma spectra, more than one photo peaks have been evaluated in the available cases. The accuracy and reproducibility of our analytical data have been ensured by the repeated analysis (n=3) of certified reference sample, IAEA-Soil-7 (data available in next chapter). Within the range of analytical uncertainties analytical results of the elemental contents in the reference material (IAEA-Soil-7) are consistent to those of the certificate values provided by IAEA.

5.4 Materials and Method for Radiological Characterization

5.4.1 Sample Preparation

Each dried power sample has been shifted to each cylindrical plastic container with net sample weight around 200g. All the sample-filled plastic containers then wrapped with thick vinyl-tape air-tightly around the sealed cap and stored with proper identification number, for at least 4 weeks. This is an essential approach to ensure the measurement of radon gas and its progenies in samples by enabling the secular equilibrium of ^{226}Ra in the ^{238}U series and ^{228}Ra in the ^{232}Th series with their daughter products [5.1].

5.4.2. Sample Analysis

Total fortytwo (42) samples have been analyzed for natural radioactivity measurement by using a p-type co-axial High Purity Germanium (HPGe) detector (CANBERRA: Model GC-4019; serial no. 07089419) with 40% efficiency relative to a NaI(Tl) detector. The effective volume of the detector is 93 cm3 and energy resolution of the detector has been found to be 1.8 keV at 1332 keV energy peak of ^{60}Co γ-ray line and the detector was coupled to a Multichannel Analyzer (MCA) with 16k channel. An empty sealed container with the same geometry as the samples and same manner was counted to monitor the background levels of NORMs around the detector and used to

obtain the net-peak area of γ-spectra of measured isotopes. The spectra acquisitions of a sample have been studied by using the spectra analyzing software MAESTRO-32 (ORTEC) and Genie-2000 (Canberra), and by using the software Hypermet PC version 5.12, the gamma peak analysis has been done. The efficiency of the detector for different natural radionuclides have been estimated by using homogeneously assimilated standard solutions of ^{226}Ra into inactive media, Al_2O_3 as standard solid sample [5.1]. The geometry of the samples and the standard maintained same and the counting time for all the sample were around 20,000 seconds. Energy calibration of the HPGe-detector has been done by ^{60}Co and ^{137}Cs point-sources. Data quality was ensured by the triplicate measurements of two reference materials (IAEA-RM-375 and IAEA-RM-Soil-6) with identical experimental set-up (data available in next chapter).

5.5 Efficiency Curve Construction

For actual radioactivity calculation, efficiency parameter is essential. The table- shows the data for efficiency curve construction for this study. Here for standard source, Ra-226 standard solution mixed homozeniously in Aluminum oxide powder has been used to maintain the comparable density with soil sample. Here eight energies of Radium-226 have been used for construction of efficiency curve. Radium emits these energies where corresponding gamma intensity has been found from literature. Here counting time was 58260 seconds. For efficiency calculation, this equation has been used:

$$\varepsilon = \frac{N}{I_\gamma \times A}; \qquad \text{Where} \quad A = A_o \times e^{-\lambda \Delta t} \qquad \ldots \quad \ldots \quad \ldots\ldots \quad 5.1$$

Here, A is current radioactivity, A_o is initial activity, N is net count per second (net cps), λ is the decay constant, and Δt is the decay time.

For constructing this graph in fig. , only radium standard is used but using this constructed graph, we will be able to measure the efficiency of any radionuclide's energy, like any radionuclide from Thorium series or K etc.

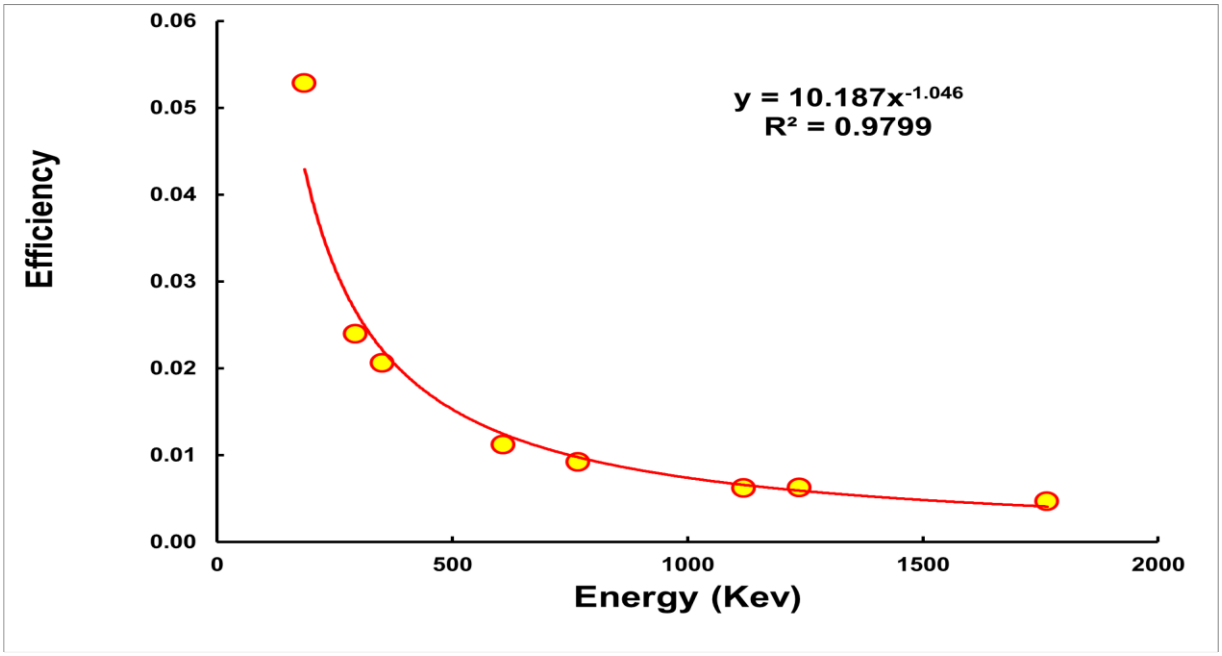

Figure 5.8 : Constructed efficiency curve of this study.

In this study, the efficiency of the detector for different NR have been estimated by using homogeneously assimilated standard solutions of ^{226}Ra into inactive media, Al_2O_3 as standard solid sample [5.1, 5.8].

5.6 Energy calibration

Before starting any measurement, an energy calibration was made, by determining the spectrum of a known standard point source and comparing the determined peak positions with the known energies and for any change corrected accordingly. To cover the full energy range we measured energies of at least two standard point sources like Co and Cs.

Table 5.4 : Data for efficiency curve construction of this study.

Energy (Kev)	Intensity of gamma ray (Iγ)	Standard Ra-226 Source in Aluminum oxide					Background					Net CPS	±	Efficiency	±
		Total Counts	±	Time (sec)	Counts per sec (CPS)	±	Total Counts	±	Time (sec)	Counts per sec (CPS)	±				
186.21	0.04	49739	249	58260	0.854	0.004	363	38.84	20022	0.018	0.002	0.836	0.005	0.0528	0.0003
295.21	0.19	106790	320		1.833	0.005	692	62		0.035	0.003	1.798	0.006	0.023924	8E-05
351.91	0.36	174558	349		2.996	0.006	1364	44		0.068	0.002	2.928	0.006	0.020557	4E-05
609.31	0.47	125686	377		2.157	0.006	1490	51		0.074	0.003	2.083	0.007	0.011201	4E-05
768.34	0.05	11058	221		0.190	0.004	157	13.35		0.008	0.001	0.182	0.004	0.009198	0.0002
1120.27	0.17	26260	131		0.451	0.002	674	36		0.034	0.002	0.417	0.003	0.006201	4E-05
1238.00	0.06	9250	83		0.159	0.001	206	11.54		0.010	0.001	0.148	0.002	0.006255	6E-05
1764.00	0.17	19871	99		0.341	0.002	548	18.08		0.027	0.001	0.314	0.002	0.004664	3E-05

5.7 Detection limit (DL)

Detection limit refers to the ability of an analytical procedure to determine Min. amounts of radioactivity in a sample reliably.

For elemental identification, the detection limit represents the ability to determine the Min. amounts of an element reliably.

The detection limit is calculated based on three-sigma (3σ) criteria. In this study, 3σ value is also used for DL calculation, where σ is the square root of the background counts under the photo peak of interest.

For calculating detection limit in gamma-ray spectrometry, Currie's formula is also used, which is shown here.

$$DL = 2.71+4.65\sqrt{B} \quad \ldots \quad \ldots \quad \ldots \quad 5.2$$

Where, B is the background counts of the photo peak of interest.

Chapter-6:

Quality Assurance or Quality Control

6.1 Precision and Accuracy

A simple but well depicted explanation of accuracy and precision is shown in the following figure:

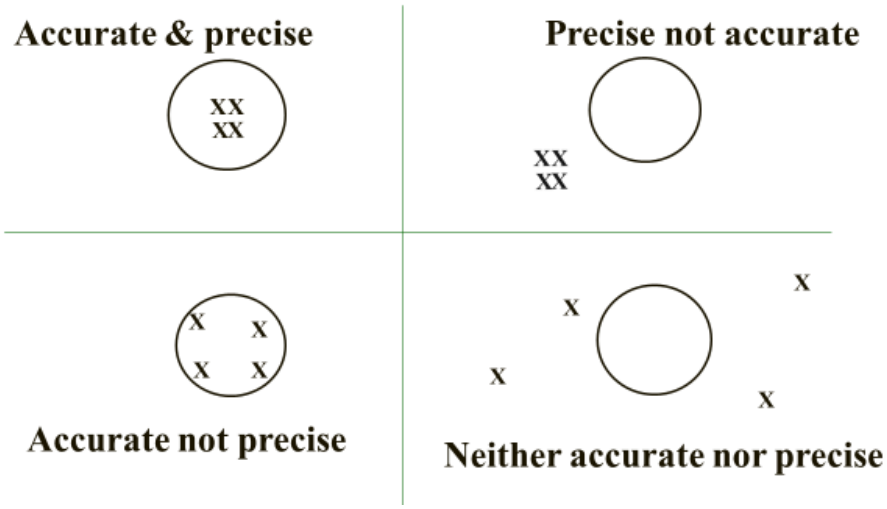

Figure 6.1: Explanation of accuracy and precision [6.1]

6.2 Quality Assurance for Elemental Identification by INAA

Standard reference material NIST-1633b (SRM: coal-fly-ash) and two reference materials (RMs): IAEA-SL-1 and IAEA-Soil-7 (soil) were used for relative standardization approach in this work. Each of the standards were prepared as the alike technique and same geometry as samples where standards and samples were irradiated simultaneously. Here NIST-1633b has been used as the standard (multi-elemental comparator) while Soil-7 and SL-1 were used as control samples for ensuring the data quality.

Accuracy and reproducibility of analytical data have been performed by triplicate analysis of IAEA standard sample namely, Soil-7.

The Table-6.1 presents the EA of standard sample, IAEA standard sample -Soil-7 of this study in repeated analysis of three times, with certificate values along with the analytical parameters. Half-life of measured radionuclides are shown here as short or long irradiation system required, depends on half -life of the elements.

Table 6.1: Elemental abundances in repeated analysis (n=3) of IAEA-Soil-7 of this study, certificate values along with the analytical parameters.

		This study (n=3)										Certificate value			DL	QL	Measured	Half
		(1)	±	(2)	±	(3)	±	Mean	SD	RSD	Certificate	Min.	Max.	[3σ]	[10σ]	radionuclide	life
Na	[%]	0.21	0.01	0.23	0.01	0.22	0.01	0.22	0.01	5.27	0.24	0.23	0.25	0.001	0.004	^{24}Na	15.02h
Al	[%]	5.04	0.06	4.84	0.04	4.94	0.03	4.94	0.10	1.95	4.70	4.40	5.10	0.004	0.013	^{28}Al	2.25m
K	[%]	1.16	0.08	1.25	0.09	1.21	0.08	1.21	0.04	3.72	1.21	1.13	1.27	0.03	0.11	^{42}K	12.36h
Sc	[µg/g]	8.23	0.07	8.19	0.07	8.37	0.07	8.26	0.09	1.13	8.30	6.90	9.00	0.02	0.06	^{46}Sc	83.83d
Ti	[%]	0.42	0.03	0.33	0.01	0.30	0.02	0.35	0.06	17.1	0.30	0.26	0.37	0.03	0.09	^{51}Ti	5.76m
V	[µg/g]	78.1	3.90	66.4	2.64	75.8	2.64	73.4	6.19	8.44	66.0	59.0	73.0	1.1	3.8	^{52}V	3.76m
Cr	[µg/g]	63.9	1.53	56.7	1.43	65.4	1.55	62.0	4.68	7.55	60.0	49.0	74.0	1.0	3.3	^{51}Cr	27.7d
Mn	[µg/g]	624	8.07	613	8.31	626	57.0	621	7.17	1.15	631	604	650	0.5	1.6	^{56}Mn	2.58h
Fe	[%]	2.45	0.05	2.54	0.05	2.63	0.04	2.54	0.09	3.71	2.57	2.52	2.63	0.01	0.03	^{59}Fe	44.50d
Co	[µg/g]	7.99	0.34	8.93	0.35	9.83	0.36	8.92	0.92	10.3	8.90	8.40	10.1	0.1	0.4	^{60}Co	5.27y
Zn	[µg/g]	94.5	5.70	94.7	5.56	96.2	5.56	95.1	0.94	0.99	104	101	113	3.2	10.5	^{65}Zn	244.1d
Rb	[µg/g]	54.3	2.77	56.8	3.05	51.6	2.84	54.3	2.61	4.81	51.0	47.0	56.0	2.6	8.7	^{86}Rb	18.66d
Cs	[µg/g]	4.93	0.16	5.58	0.17	5.52	0.16	5.34	0.36	6.68	5.40	4.90	6.40	0.1	0.33	^{134}Cs	2.062y
Ba	[µg/g]	158	10.5	162	12.3	191	10.3	170	18.0	10.6	159	131	196	32	108	^{131}Ba	11.8d
La	[µg/g]	28.2	2.53	28.1	3.22	29.8	0.34	28.7	0.97	3.39	28.0	27.0	29.0	0.2	0.8	^{140}La	1.68d
Ce	[µg/g]	53.2	0.81	69.3	1.15	52.8	0.94	58.4	9.40	16.1	61.0	50.0	63.0	0.8	2.6	^{141}Ce	32.51d
Sm	[µg/g]	5.34	0.21	4.64	0.24	5.76	0.02	5.25	0.57	10.8	5.10	4.80	5.50	0.04	0.13	^{153}Sm	1.94d
Eu	[µg/g]	1.06	0.03	0.81	0.02	1.20	0.03	1.03	0.20	19.1	1.00	0.90	1.30	0.03	0.1	^{152}Eu	13.33y
Dy	[µg/g]	4.39	0.18	3.93	0.20	3.71	0.15	4.01	0.35	8.77	3.90	3.20	5.30	0.09	0.3	^{165}Dy	2.33h
Yb	[µg/g]	2.30	0.07	2.37	0.11	2.39	0.14	2.35	0.05	2.09	2.40	1.90	2.60	0.3	0.8	^{169}Yb	32.02d
Hf	[µg/g]	4.85	0.15	4.63	0.15	4.68	0.11	4.72	0.11	2.43	5.10	4.80	5.50	0.1	0.33	^{181}Hf	42.39d
Ta	[µg/g]	1.21	0.10	0.66	0.07	0.86	0.08	0.91	0.28	30.9	0.80	0.60	1.00	0.05	0.17	^{182}Ta	115d
Th	[µg/g]	7.31	0.12	7.31	0.12	8.32	0.13	7.64	0.58	7.61	8.20	6.50	8.70	0.07	0.22	^{233}Pa	27d
U	[µg/g]	2.36	0.09	2.23	0.07	2.44	0.05	2.35	0.11	4.63	2.60	2.20	3.30	0.1	0.33	^{239}Np	2.35d

DL: Detection Limit; QL: Quantification Limit; Half-lives in minutes (m), hours (h), days (d) and years (y).

Summary from the Table-6.1 is as follows:

- As measured values are very close to certificate values so accuracy is good.
- Detection limit is very low compared to measured values which flourish the accuracy.
- Mean value is consistent with certified value.
- Precision or reproducibility that is relative standard deviation of this study for all EA in Soil-7 are within 10 %, except for Ti (titanium), Ce, Eu and Ta. (Ta-Tantalum).

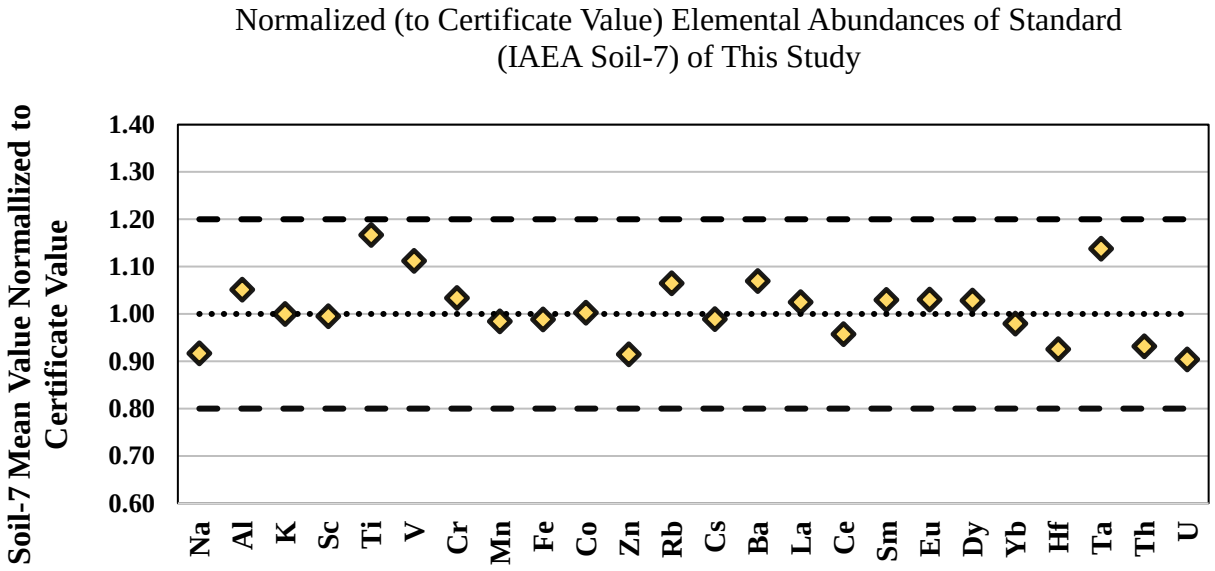

Figure 6.2: Normalized elemental abundances of Standard "IAEA Soil-7" by certificate value.

Further graphical representation has been done in Fig.6.2, where normalized to certified value, the mean value of EA of standard (IAEA Soil-7) of this study is shown. In this study, measured values of EA of the standard are consistent with certified values and have deviations less than 20%. So, accuracy is good.

As, both accuracy and reproducibility are good, so a set of high quality precise elemental data for the core sediments in this study can be expected.

6.3 Quality Assurance for Elemental Identification by EDXRF Concentration Calibration

This section information has been provided from EDXRF analysis laboratory under chemistry division of AECD under BAEC.

A direct comparison method based on EDXRF technique has been used for EA measurement [6.2-6.3] in soil sample to avoid any matrix effect. Three soil standards (IAEA Soil-7, Montana-1/2710a, Montana-2/2711a) were used for calibration curves construction for carrying out

elemental analysis of soil. Accuracy and reproducibility of analytical data have been performed by triplicate analysis of IAEA standard sample namely, Montana-1. According to Table 6.2, variation of the certified and measured values were found in acceptable range of error [6.2].

Table 6.2: Comparison between Laboratory Results and the Certified Values of Standard Reference Materials (mg kg^{-1}) [6.2].

Elements	**Soil (Montana- 1)**		
	Results Obtained	Certified Values	Error (%)
K	21113	21700	2.71
Ca	9136	9640	5.23
Mn	2128	2140	0.56
Fe	39685	43200	8.14
Ni	8.67	8.0	-8.38
Cu	3409	3420	0.32
Zn	4179	4180	0.02
As	1441	1540	6.43
Se	1.2	1.0	-20.0
Pb	5382	5520	2.5

6.4 Quality Assurance for Radiological Characterization by HPGe Gamma Spectrometry System

Accuracy and reproducibility of analytical data were performed by triplicate analysis of RC of both standard samples IAEA-RM-375 (soil) and IAEA-RM-Soil-6 (soil) for this study and compared with the certificate values.

Table 6.3: Descriptive statistics of radioactivity concentrations in repeated analyses (n = 3) of IAEA-RM-375 (soil) and IAEA-RM-Soil-6 (soil) of this study along with the certificate values and detection limits.

Radio-nuclide	Unit	IAEA-RM-375 (soil)						IAEA-RM-Soil-6						Detection Limits
		This work			Certificate			This work			Certificate			
		Mean (n=3)	SD (1σ)	RSD (%)	Value	Min.	Max.	Mean (n=3)	SD (1σ)	RSD (%)	Value	Min.	Max.	
^{226}Ra	Bq.kg^{-1}	18.5	1.6	8.6	20	18	22	85.2	5.6	6.6	79.9	69.6	93.4	0.5
^{232}Th	Bq.kg^{-1}	19.8	1.9	9.6	20.5	19.2	21.9							0.5
^{40}K	Bq.kg^{-1}	428	35	8.2	424	417	432							20

IAEA-RM-375: Certificate values are taken from IAEA reference sheet issued on January, 2000.

IAEA-RM-Soil-6: Certificate values are taken from IAEA reference sheet issued on April, 1984. (pCi.kg^{-1} is converted to Bq.kg^{-1} as 1 Pico-curie = 0.037 Becquerel)

Table-6.3 presents the descriptive statistics of RC in repeated analysis (n = 3) of two IAEA standard samples of this study along with the certificate values. Certificate values for IAEA-RM-375 have been taken from IAEA reference sheet issued on January, 2000 and certificate values for IAEA-RM-Soil-6 have been taken from IAEA reference sheet issued on April, 1984 respectively. Summary from the Table-6.3 is as follows:

- Mean values for RC of all natural radionuclides (^{226}Ra, ^{232}Th and ^{40}K) are consistent with corresponding certified values.
- Detection limit is very low compared to measured values which flourish the accuracy.
- Precision or reproducibility (RSDs in %) of this study for RC of all natural radionuclides (^{226}Ra, ^{232}Th and ^{40}K) in IAEA-RM-375 (soil) and IAEA-RM-Soil-6 (soil)are within 10 %.

As both accuracy and reproducibility are good, so high-quality precise data of RC in this study can be expected.

It is known that proper documentation is the main criteria of quality assurance.

Chapter-7

Results and Discussion on Elemental Identification

7.1.1 Elemental Abundances of Environmental Samples of Shahbazpur (Sbz) Gas Field

A total of 15 elemental (K, Ca, Ti, Cr, Mn, Fe, Ni, Cu, Zn, As, Rb, Sr, Y, Zr and Pb) abundances in environmental sediment and soil (S&S) samples of Shahbazpur (Sbz) gas field (GF), Bangladesh have been determined by EDXRF which have been tabulated in Table 7.1. Max. values, Min. values, Avg. abundances, median value, RSD and SD along with the relative literature data of respective elements are also shown in Table 7.1.

Comparatively higher contamination could be found in the samples of waste deposited evaporation (WDEvp) pond bottom sediments, especially in the north-east side of WDEvp pond (sample ID: EB-6), where also brine and mud (MB) chemicals be dumped and comparatively lower contamination could be found in soil samples away from WDEvp pond area, had been predicted before the research result obtained.

For radioactivity concentration (RC), after investigation the results have been found inverted i.e., lowest RC level and all seven radiation hazard indices (RHI) values obtained in sample EB-6 i.e. chemical WDEvp pond corner. MB chemicals could dilute radioactive materials (RM) in the WDEvp pond. And highest values of all RHI obtained in sample EB-3.1, which is distant location from WDEvp pond. At the time of maintenance work, the natural gas production equipments are cleaned using high-speed jet water, by which RM may be washed away from sludge-scale and spread to nearby areas through the drain on the way to WDEvp pond. The higher radioactivity areas could be the result of NORMs' spreading by over flooded mostly in rainy season.

But for metal and metalloid (M&M) concentration, interestingly the result has been found exactly right i.e. for Ca, Ti, Mn and Sr EA have been found highest in sample MB-6 compared to other environmental samples of Sbz GF area of this study. Again lowest EA have been found for Cr, Fe, Rb, Y and Zr this specific sample. There may have possibility of Ti-rich HM&M abundances such as rutile in this gas well core (GWC) samples and sediment samples can be polluted from GAA by anthropogenic incorporation. Geochemical data for sediments could be affected by constant sum effect, because in a dataset, changes may occur in relative EA when concentration of one element changes, which may be an evidence of here mentioned situation [7.1].

Table 7.1: Elemental abundances (EA) of Shahbazpur (Sbz) gas field (GF) in environmental S&S samples.

Ele-ment	Unit	EB-1	±	EB-2.1	±	EB-2.2	±	EB-3.1	±	EB-3.2	±	EB-4.1	±	EB-4.2	±
K	[%]	0.91	0.06	0.95	0.06	0.91	0.06	0.43	0.03	0.57	0.04	0.84	0.05	0.27	0.02
Ca	[%]	3.34	0.46	3.74	0.51	4.73	0.65	2.06	0.28	2.22	0.30	3.72	0.51	2.52	0.34
Ti	[%]	0.46	0.02	0.57	0.02	0.39	0.01	0.59	0.02	0.27	0.01	0.47	0.02	0.50	0.02
Mn	[µg/g]	544	32.1	732	43.2	653	38.5	299	17.6	503	29.7	601	35.5	615	36.3
Fe	[%]	3.93	0.18	4.48	0.21	4.16	0.20	4.76	0.22	4.74	0.22	4.74	0.22	4.76	0.22
Ni	[µg/g]	70.5	6.20	75.5	6.64	98.4	8.66	27.2	2.40	50.1	4.41	70.5	6.20	31.9	2.80
Zn	[µg/g]	117	8.92	79.8	6.10	116	8.88	64.0	4.90	129	9.89	121	9.27	102	7.79
As	[µg/g]	33.2	1.59	31.8	1.52	35.6	1.70	12.1	0.58	18.4	0.88	33.2	1.59	10.7	0.51
Rb	[µg/g]	115	10.1	107	9.40	94.6	8.29	116	10.18	100	8.78	109	9.61	119	10.44
Sr	[µg/g]	158	22.1	121	16.9	152	21.3	130	18.2	137	19.1	122	17.1	161	22.5
Y	[µg/g]	39.4	4.27	51.7	5.61	47.8	5.18	30.4	3.30	41.4	4.49	37.5	4.07	51.1	5.54
Zr	[µg/g]	300	69.6	351	81.4	322	74.6	256	59.4	248	57.5	297	68.9	281	65.2
Pb	[µg/g]	87.1	10.3	86.8	10.2	97.1	11.4	7.27	0.86	59.4	6.99	96.3	11.3	35.1	4.14

Continued

Table 7.1: Elemental abundances (EA) of Sbz GF in environmental S&S samples. **(**Continued**)**

Ele-ment	Unit	EB-5	±	EB-6	±	EB-7	±	EB-8	±	Mean	SD	RSD	Median	Max.	Min.	UCC[a]	World Soil Median[b]	Shale[b]
K	[%]	1.05	0.07	1.17	0.08	0.87	0.06	1.25	0.08	0.84	0.30	36.1	0.91	1.25	0.27	2.32	1.4	2.45
Ca	[%]	3.68	0.50	5.03	0.69	4.03	0.55	1.69	0.23	3.34	1.09	32.8	3.68	5.03	1.69	2.6	1.5	1.6
Ti	[%]	0.52	0.02	3.44	0.12	0.50	0.02	0.51	0.02	0.74	0.90	121	0.50	3.44	0.27	0.38	0.5	0.46
Mn	[µg/g]	568	33.5	844	49.8	618	36.5	639	37.7	601	136	22.7	615	844	299	775	1000	850
Fe	[%]	4.42	0.21	1.52	0.07	2.88	0.14	5.14	0.24	4.14	1.06	25.5	4.48	5.14	1.52	3.92	4	4.8
Ni	[µg/g]	102	8.95	83.5	7.35	74.6	6.56	24.5	2.16	64.4	27.3	42.4	70.5	102	24.5	47	-	68
Zn	[µg/g]	80.0	6.12	104	7.97	97.0	7.42	112	8.53	102	20.2	19.8	104	129	64.0	67	90	120
As	[µg/g]	31.9	1.53	31.9	1.53	43.9	2.10	9.83	0.47	26.6	11.7	43.9	31.9	43.9	9.83	4.8	6	13
Rb	[µg/g]	94.3	8.26	29.1	2.55	54.9	4.81	118	10.4	96.3	28.9	30.0	107	119	29.1	84	150	160
Sr	[µg/g]	135	18.9	391	54.7	156	21.9	118	16.6	162	77.5	47.9	137	391	118	320	250	300
Y	[µg/g]	31.7	3.44	24.3	2.63	34.3	3.72	37.5	4.07	38.8	8.73	22.5	37.5	51.7	24.3	21	40	41
Zr	[µg/g]	238	55.3	112	26.1	260	60.3	268	62.1	267	61.2	23.0	268	351	112	193	400	160
Pb	[µg/g]	87.1	10.3	82.5	9.71	113	13.3	22.9	2.70	70.5	34.4	48.8	86.8	113	7.27	17	35	23

[a] [2]; [b] [3]

7.1.2 Environmental Contamination (EC) Indices of Shahbazpur (Sbz) Gas Field in Sediment and Soil (S&S) Samples

Base-line data selection is important to assess the S&S samples' EA in terms of EC indices like geoaccumulation index (I_{geo}), contamination factor (CF) and enrichment factor (EF). In this study, the EA of upper continental crust (UCC: [7.2]) has been selected as the base-line data.

7.1.2.1 Enrichment Factor (EF) of Elemental Abundances (EA) of Sbz Gas Field (GF) Environmental Samples (ES)

EF is casted widely to distinguish manmade and natural sources of M&M [7.4 – 7.5]. Fe has been used in this study to calculate EF as Fe naturally has almost uniform concentrations and also displays alike to many trace elements' geochemistry [7.6 - 7.8].

To study the anthropogenic nature and mobilization of EA with the crustal origin, EF in specific S&S samples for each element has been calculated and are graphically presented in Fig. 7.1.

In the environmental sediment sample EB-6, collected from the north-east side of WDEvp pond where MB chemicals are dumped, significantly EF of most of the M&M have been found compared to other environmental S&S samples of Sbz GF area of this research work.

The EF values of the As ranges from 1.56 to 17.12 with the highest EF value is detected for the As is 17.12 in sample EB-6. Similar trend is obtained for Pb (EF range: 1.03 to 12.48) and Ti (EF range: 1.02 to 23.31) with the highest EF values for both Pb and Ti are detected in sample EB-6 which are 12.48 and 23.31 respectively. Within eleven ES, the EF values of As and Pb in seven samples revealed that the S&S samples have been around severely enriched with these M&M. Comparatively lower EF values of EA in soil samples have been found which are far away from produced WDEvp Pond. And lowest EF values of both As and Pb are found in sample EB-8, which has been collected from outside the IAGB and comparatively high land as base-line data. Again second highest EF values of both As and Pb are found in sample EB-7, which has been collected from outside the IAGB but connected through GF drainage system. All these evidences reveal that these elements are from the anthropogenic origin.

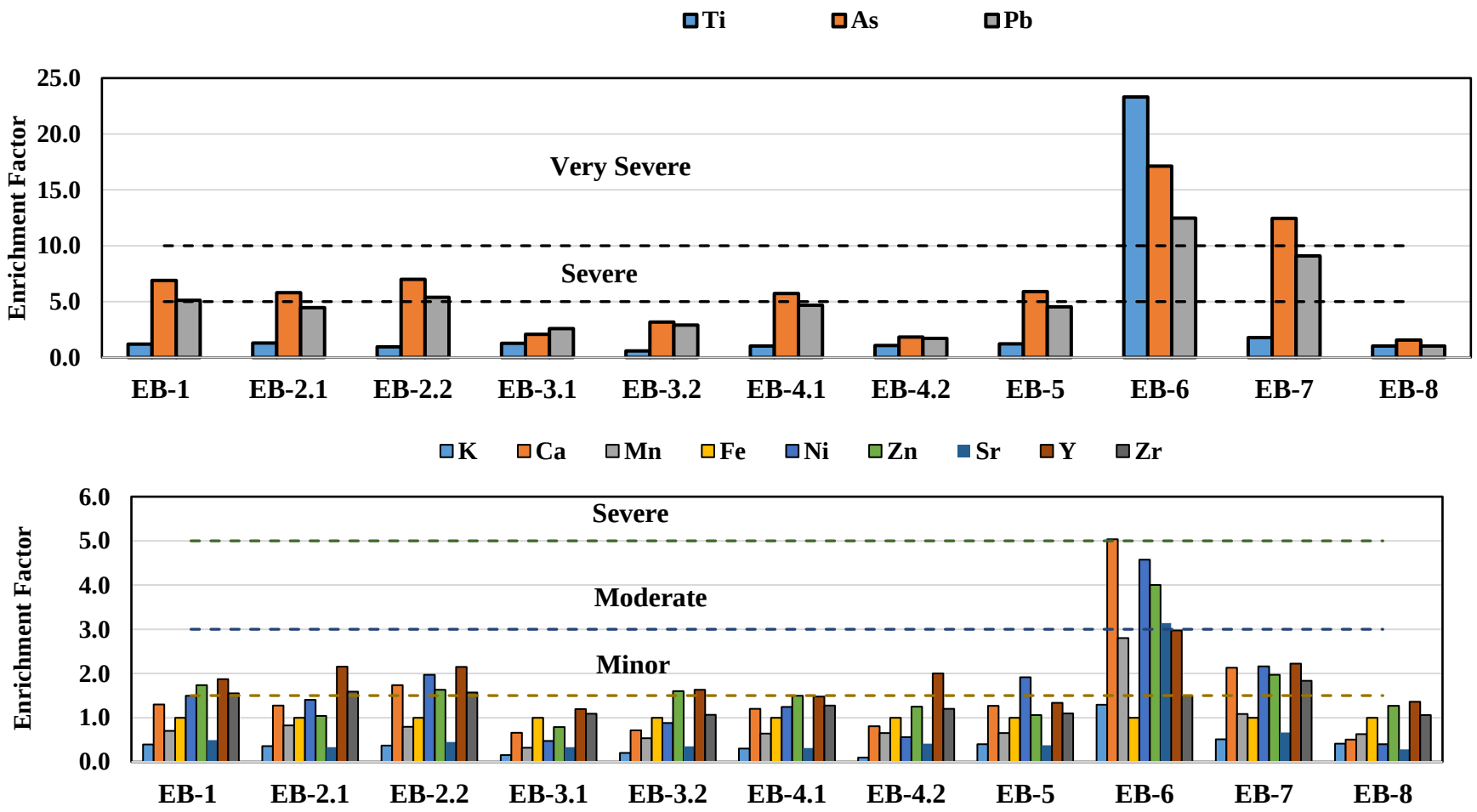

Figure 7.1: Plotted EF relative to UCC and Fe in the S&S samples of the individual elements of Sbz GF.

7.1.2.2 I_{geo} of Elements of Sbz Gas Field (GF) Environmental Samples (ES)

Depending on the choice of base-line data i.e. background levels, I_{geo} values exhibite huge variations. In this work, upper continental crust's (UCC) EA according to [7.2] have been selected as the base-line data to calculate I_{geo}. The concentration comparison is the alternative of polluted and unpolluted sediments which are mineralogically and texturally comparable, [7.9].

The graphical representation of geo-accumulation index (I_{geo}) of EA of Sbz GF environmental S&S samples have been shown in Fig. 7.2.

Based on [7.10] classification, graphical representation of I_{geo} presented in Fig. 7.2 revealed moderately contaminated by Pb in all S&S samples of Sbz GF area except two samples. Among these two samples, one is SubS of 6″ to 8″ depth and another sample has been collected as background data of sample ID: EB-8. The I_{geo} value for sample EB-8 is -0.154, which indicates that no contamination present in this sample. Again according to Müller's [7.10] classification revealed moderate to heavily contaminated by As in seven S&S samples out of eleven samples of this GF area. Also in this case, the I_{geo} value for sample EB-8 is lowest and value is 0.449. Highest I_{geo} value of both As and Pb are found in sample EB-7, which has been collected from outside the IAGB but connected through GF drainage system. In the sample EB-6, collected from the north-east side of WDEvp pond where MB chemicals are dumped, extremely higher compared to all other environmental S&S samples of Sbz GF area has been found for I_{geo} value of Ti which is 2.6. All the mentioned evidence reveal that these elements are from the anthropogenic origin.

Along with these elements, in some ES, the I_{geo} values for Ca, Ni, Zn and Y are higher than zero i.e., these elements are more probably to be from the manmade origin rather than a natural crustal source.

The negative I_{geo} values for K, Mn, Fe and Sr in all the samples revealed that in the S&S samples of the investigated locations are lower than their respective natural background values and thus, indicates no contamination present of these elements.

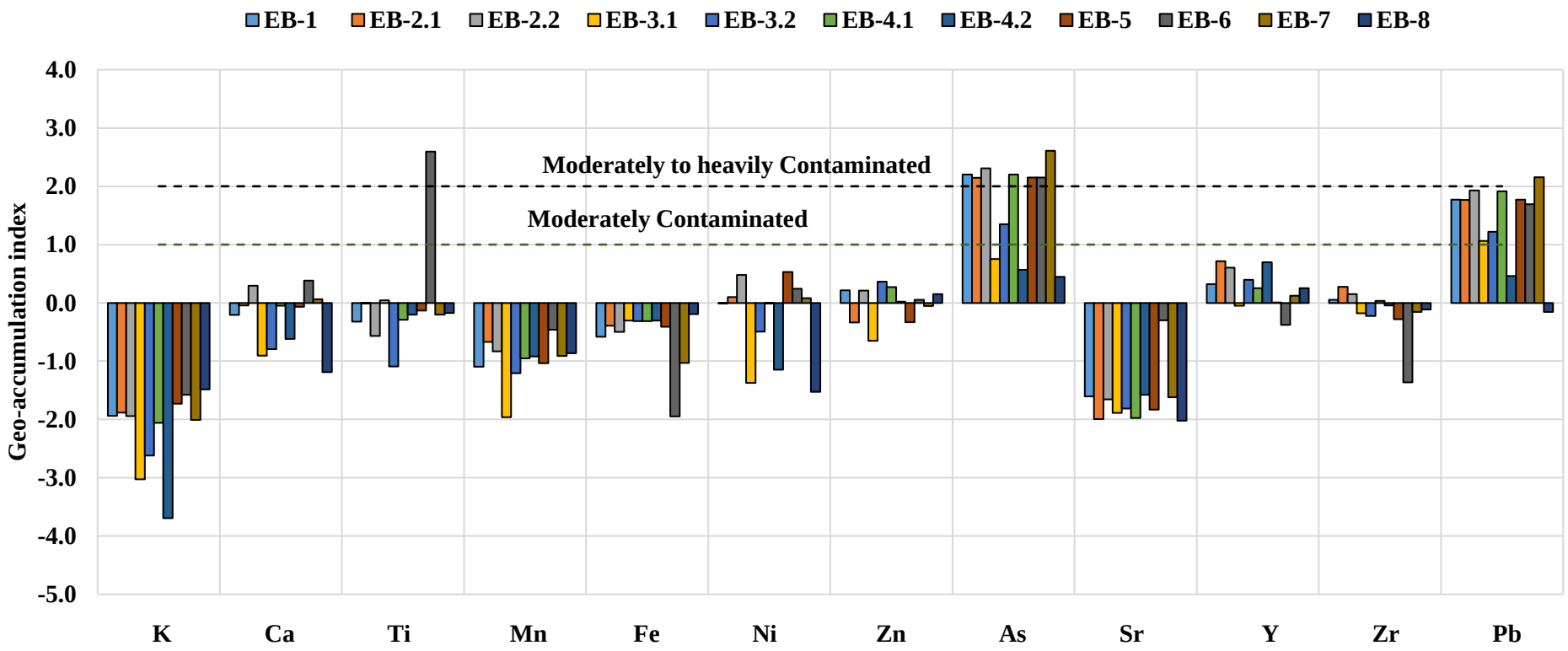

Figure 7.2: Geo-accumulation Index (I_{geo}) of elements of Sbz GF S&S samples.

7.1.2.3 Contamination Factor of Elements of Sbz Gas Field Environmental Samples

The contamination factor (CF) is helpful for the detection of contamination status of metals [7.11]. CF values of EC for S&S samples are characterized as low: CF < 1; moderate CF: 1 to 3; considerable CF: 3 to 6 and high: CF > 6 [7.12].

The graphical representation of CF of EA of Sbz GF environmental S&S samples have been shown in Fig. 7.3.

Both for As and Pb, CF values are found high i.e. CF > 6 in two samples namely EB-6 and EB-7. Here the environmental sediment sample EB-6 has been collected from the north-east side of WDEvp pond where MB chemicals are dumped of Sbz GF. Again sample EB-7 has been collected from outside the GF boundary but connected through GF drainage system. Within eleven EF, the CF values of As in seven samples revealed that the S&S samples have been highly contaminated with As metalloid. Similar trend is observed for Pb, the CF values of Pb in eleven samples revealed that the S&S samples have been considerably contaminated to around high level by Pb. Comparatively lower CF values of EA in soil samples have been found which are far away from produced WDEvp Pond. And lowest CF values of both As and Pb are found in sample EB-8, which has been collected from outside the IAGB and comparatively high land region as base-line data. All these evidences reveal that contamination by these elements are from the anthropogenic origin.

Along with these elements, the CF values for Ca, Ni, Zn, Y and Zr are much higher than one i.e., these elements are more probably to be from the manmade origin rather than a natural crustal source.

Wastes like Sc-Sl from the GAA can also enhance the contamination of M&M in the AEv. Within which some sampling locations IAGB (like sample ID: EB-2.1, EB-2.2 and EB-4.1) are at the fresh water pond's bank and nearby various fruit trees. At the time of maintenance work, the natural gas production equipments are cleaned using high-speed jet water, by which M&M may be washed away from Sc-Sl and contamination spread to nearby areas through the drain on the way to WDEvp pond. Comparatively higher concentrated M&M areas could be the result of contaminated M&M by overflowing of skimming pit and WDEvp pond mostly in rainy season.

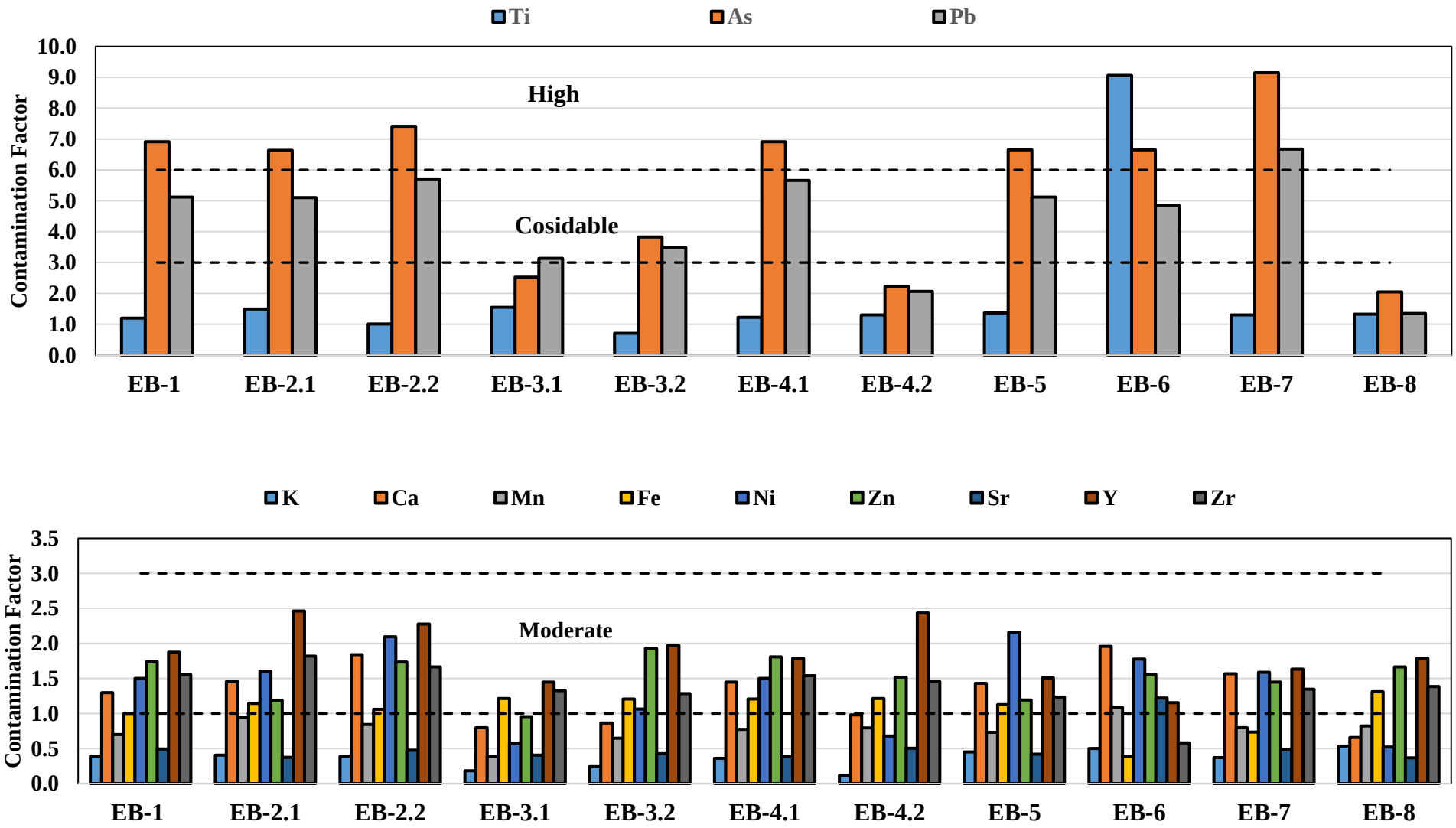

Figure 7.3: Contamination factor (CF) of elements of Sbz GF soil and sediment (S&S) samples

7.2.1 Elemental Abundances (EA) of Environmental Samples (ES) from Saldanadi Gas Field (SGF)

A total of 13 elemental (K, Ca, Ti, Mn, Fe, Ni, Zn, As, Rb, Sr, Y, Zr and Pb) abundances in environmental soil SGF, Bangladesh have been determined by EDXRF which have been tabulated in Table 7.2. Max. values, Min. values, mean abundances, median value, RSD and SD along with the relative literature data of respective elements are also shown in Table 7.2.

In SGF, comparatively lower RC level and all seven RHI values obtained interestingly in the sample namely ES-3 where concentration for Sr and Pb EA have been found higher compared to other ES.

M&M in chemicaly contaminated areas could dilute RM in the WDEvp pond.

Table 7.2: Elemental abundances in environmental soil samples of Saldanadi gas field (SGF).

Ele-ment	Unit	ES-1	±	ES-2	±	ES-3	±	ES-4	±	Mean	SD	RSD	Median	Max.	Min.	UCC[a]	World Soil Median[b]	Shale[b]
K	[%]	0.91	0.06	0.78	0.05	0.54	0.03	0.91	0.06	0.79	0.18	22.4	0.84	0.91	0.54	2.32	1.4	2.45
Ca	[%]	3.10	0.42	3.10	0.42	1.28	0.18	3.84	0.53	2.83	1.09	38.5	3.10	3.84	1.28	2.6	1.5	1.6
Ti	[%]	0.45	0.02	0.58	0.02	1.94	0.07	0.42	0.01	0.85	0.73	86.7	0.51	1.94	0.42	0.38	0.5	0.46
Mn	[µg/g]	676	39.9	591	34.9	221	13.0	582	34.3	517	202	39.0	586	676	221	775	1000	850
Fe	[%]	3.54	0.17	5.81	0.27	2.98	0.14	4.24	0.20	4.14	1.22	29.5	3.89	5.81	2.98	3.92	4	4.8
Ni	[µg/g]	59.5	5.23	67.5	5.94	28.3	2.49	67.5	5.94	55.7	18.7	33.5	63.5	67.5	28.3	47	-	68
Zn	[µg/g]	103	7.87	147	11.2	89.8	6.87	103	7.89	111	24.9	22.5	103	147	89.8	67	90	120
As	[µg/g]	31.8	1.52	37.6	1.80	29.2	1.40	36.5	1.74	33.8	3.94	11.7	34.1	37.6	29.2	4.8	6	13
Rb	[µg/g]	75.1	13.5	104	18.7	44.5	8.02	102	18.4	81.4	27.9	34.3	88.8	104	44.5	84	150	160
Sr	[µg/g]	116	16.2	178	24.9	760	106	100	14.0	289	316	109	147	760	100	320	250	300
Y	[µg/g]	30.6	3.31	61.2	6.63	46.4	5.03	40.2	4.35	44.6	12.8	28.8	43.3	61.2	30.6	21	40	41
Zr	[µg/g]	274	63.7	195	45.3	112	26.0	339	78.6	230	98.1	42.6	235	339	112	193	400	160
Pb	[µg/g]	85.5	10.1	108	12.7	1675	197	105	12.3	493	788	160	106	1675	85.5	17	35	23

[a] [2]; [b] [3]

7.2.2 Environmental Contamination (EC) Indices of Soil Samples from Saldanadi Gas Field (SGF)

7.2.2.1 Enrichment Factor (EF) of Elemental Abundances (EA) of SGF Environmental Samples (ES)

To distinguish anthropogenic and natural sources of M&M using EF, Fe has been selected as Fe naturally has almost uniform concentrations.

EF in specific soil samples for each element has been measured and are graphically presented in Fig. 7.4.

In the SurS sample ES-3, collected from the north side of WDEvp pond where both PW and chemical wastes are disposed, significantly higher EF of Pb, Y, Sr and Zn have been found compared to other environmental soil samples of SGF area.

The EF values of the Pb ranges from 4.3 to 129.5 where the both lowest and highest EF values are detected for the Pb are from WDEvp pond corners samples namely ES-2 and ES-3 which have been collected from south and north sides of that WDEvp pond respectively. In sample location ES-3 i.e. north side of WDEvp pond, used up batteries of car and other heavy vehicles of this GF have been dumped from which very severe Pb enrichment can be occurred compared to other environmental soil samples of SGF area of this study.

Similar trend is obtained for As (EF range: 5.3 to 8) and Ti (EF range: 1.0 to 7) with the highest EF values for both As and Ti are detected in sample ES-3 which are 8 and 7 respectively. In all four ES, the EF values (within 5 to 10) of As revealed that the soil samples have been severely enriched with this M&M.

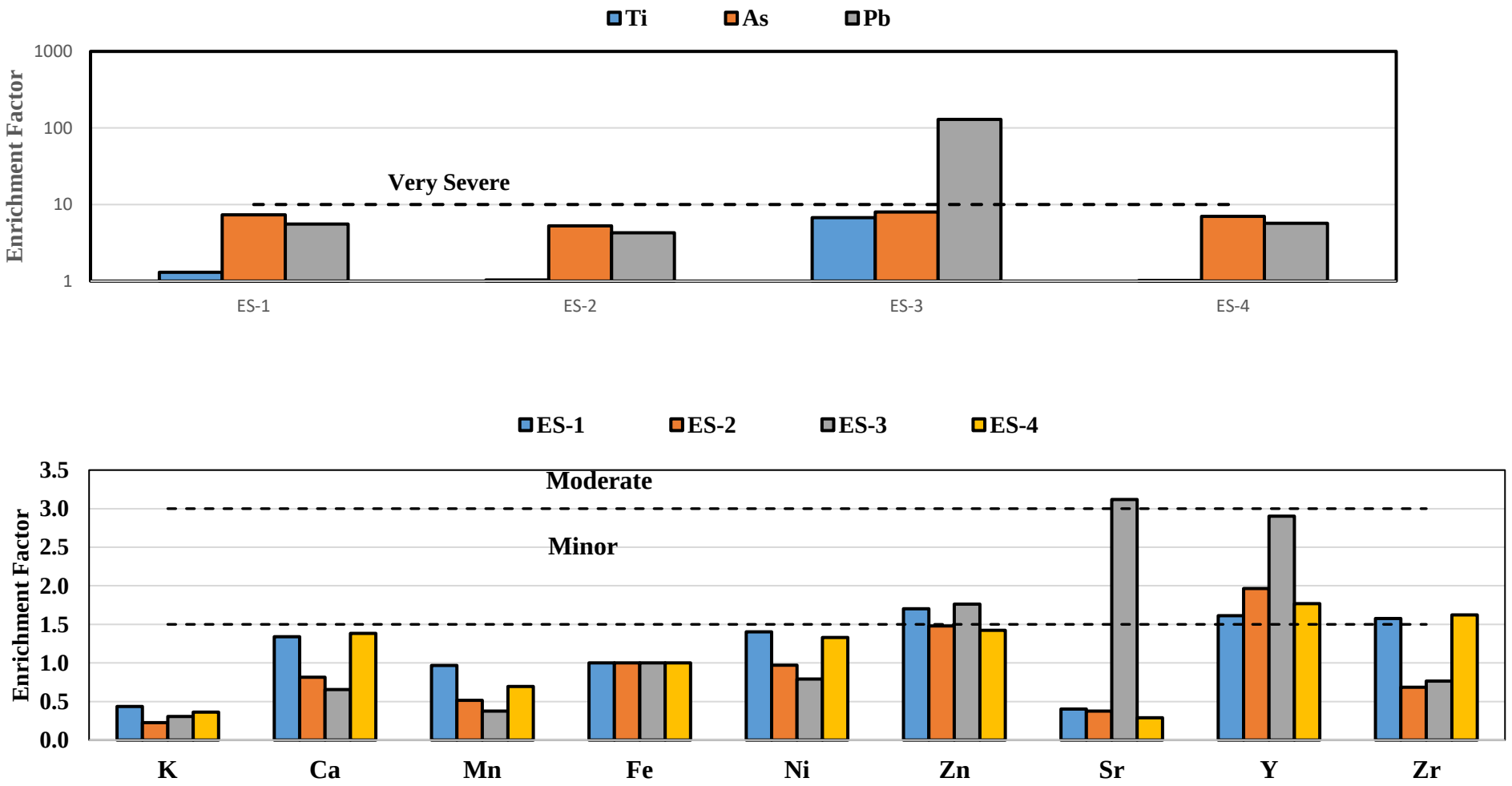

Figure 7.4: Plotted EF comparative to UCC and Fe in the soil samples of the individual elements of SGF.

7.2.2.2 I_{geo} of Elements of SGF Environmental Samples (ES)

Here, EA of UCC (upper continental crust) have been nominated as the base-line data to assess I_{geo}. The graphical representation of geo-accumulation index (I_{geo}) of EA of SGF environmental soil samples have been shown in Fig. 7.5.

According to Fig. 7.5, all soil samples of SGF area are moderately to heavily contaminated by As. All soil samples of this GF area have been moderately and moderately to heavily contaminated by Pb except highest value of Igeo for Pb which is 6.04 in sample ES-3 i.e. extremely contaminated. All the evidences make known that these elements are from the anthropogenic origin.

Along with these elements, in some ES, the I_{geo} values for Ti, Zn, Sr and Y are higher than zero i.e., these elements are more probably to be from the manmade origin rather than a natural crustal source.

The negative I_{geo} values for K, Ca, Mn, Fe and Ni in all the samples revealed that in the soil samples of the research site is lower than their respective natural background values and thus, indicates no contamination present of these elements.

Highest value of I_{geo} for Pb detected in sample namely ES-3 which has been collected from north side of the WDEvp pond. In sample location ES-3 used up batteries of cars and other heavy vehicles of this GF have been dumped from which extremely Pb contamination can be occurred compared to other environmental soil samples of SGF area of this study. For accuracy the sample ES-3 has been analyzed several times of same pellet and different pellet of same location sample.

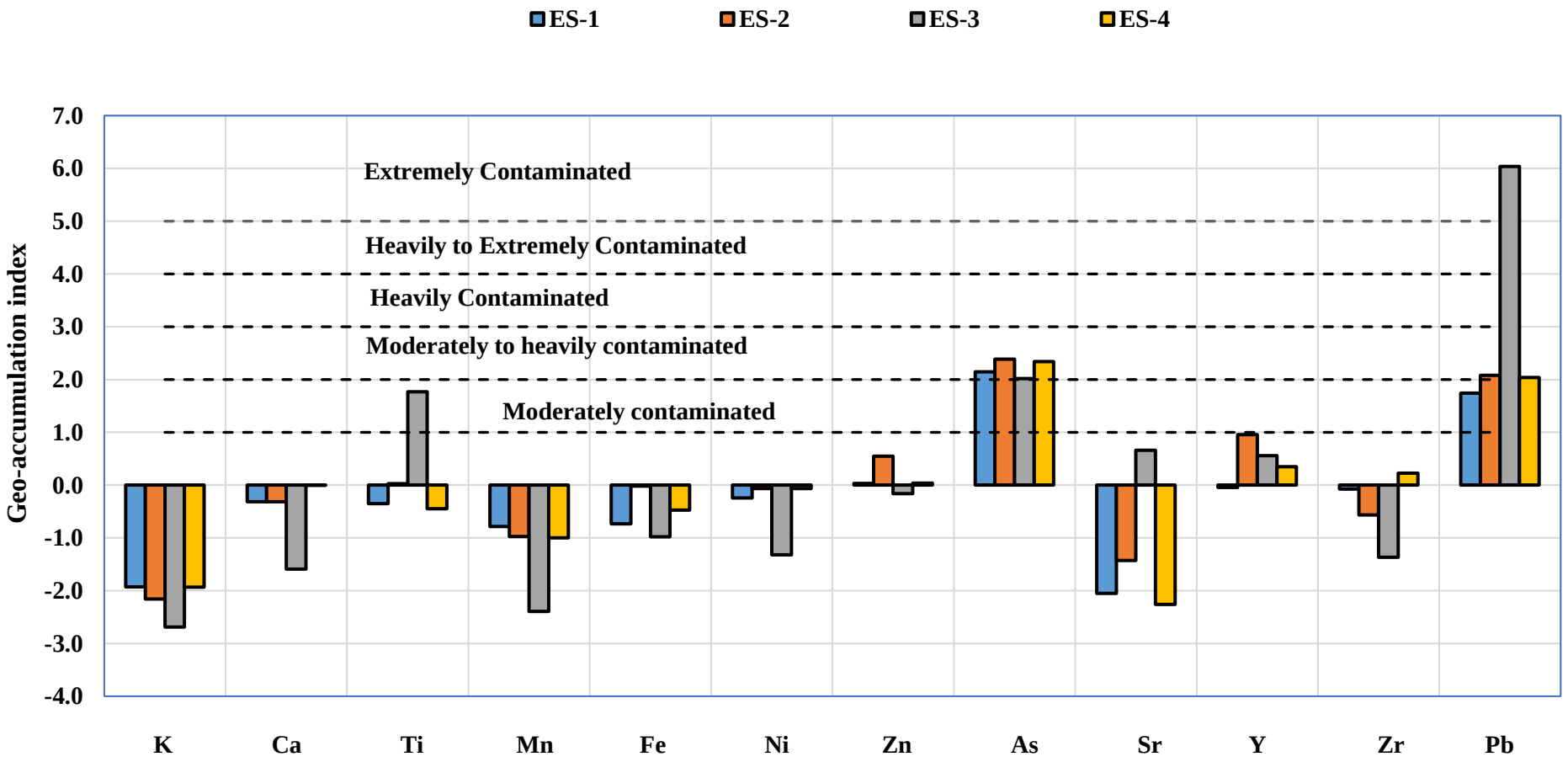

Figure 7.5: I_{geo} of elements of SGF soil samples.

7.2.2.3 Contamination Factor (CF) of Elements of SGF Environmental Samples (ES)

CF of elements of SGF soil samples have been shown graphicaly in Fig. 7.6, where CF= 98.6 for Pb in sample ES-3 is not presented, as using logarithmic scale could interrupt other CF of EA data presentation.

The CF is helpful for the detection of contamination status of metals [7.13]. CF values of environmental pollution for S&S samples are characterized as low: CF < 1; moderate CF: 1 to 3; considerable CF: 3 to 6 and high: CF > 6 [7.12].

Both for As and Pb, CF values are found high i.e. CF > 6 in all samples (except ES-1 for Pb CF=5.03). Highest value of CF for Pb detected in sample namely ES-3 which has been collected from north side of the WDEvp Pond. In sample location ES-3 used up batteries of cars and other heavy vehicles of this GF have been dumped from which extremely Pb contamination can be occurred compared to other environmental soil samples of SGF area of this study. For accuracy the sample ES-3 has been analyzed several times of same pellet and different pellet of same location sample. This evidence discloses that contamination by As and Pb are from the anthropogenic origin.

Along with these elements, the CF values for Ca, Ni, Zn, Y and Zr are much higher than one i.e., these elements are more probably to be from the manmade origin rather than a natural crustal source.

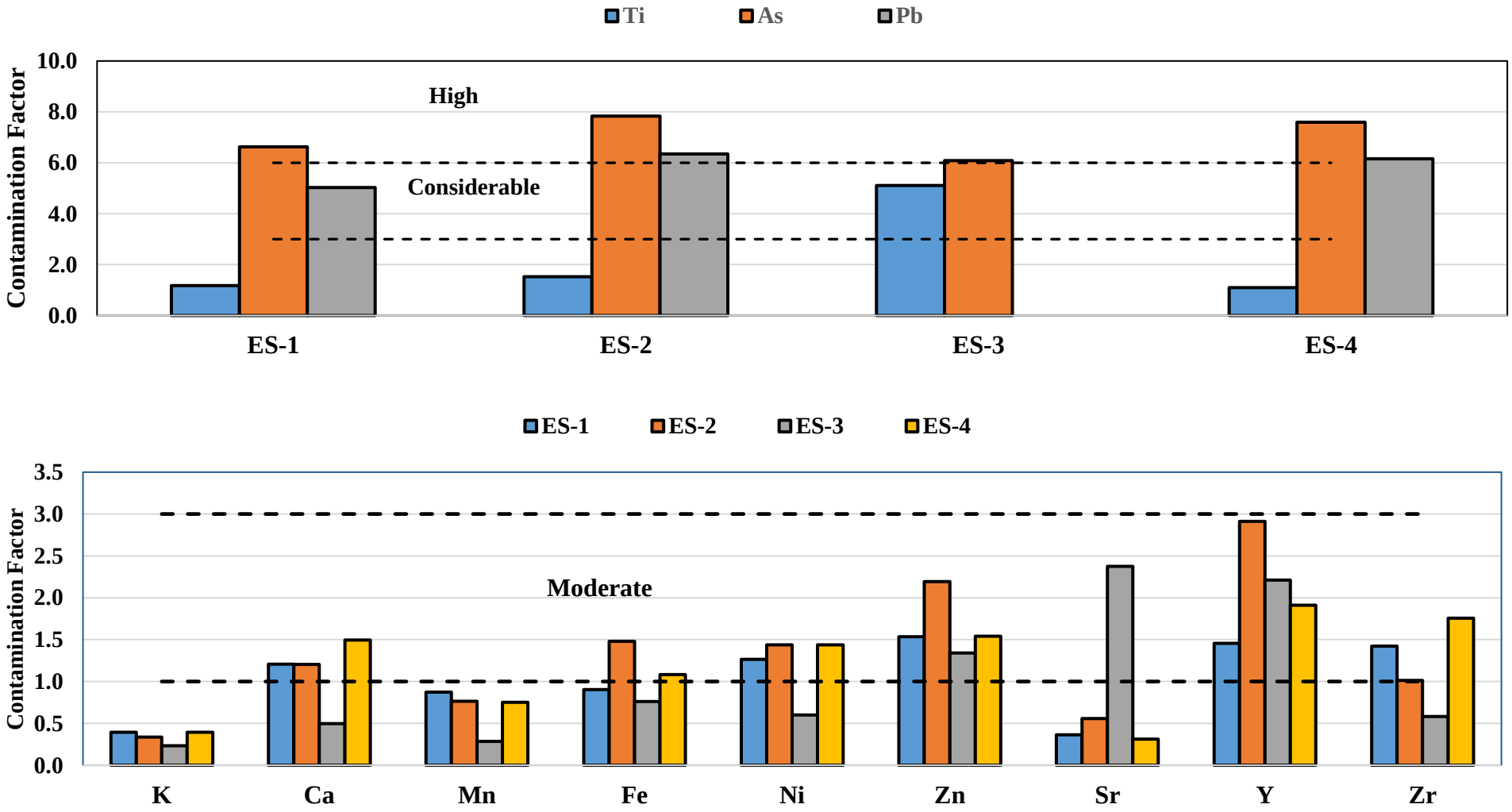

Figure 7.6: CF of elements of SGF soil samples. [N.B.: CF= 98.6 for Pb in sample ES-3 which is not shown in this graph, otherwise using logarithmic scale could interrupt other CF of elemental abundances data presentation.]

7.3.1 Elemental Abundances (EA) of Environmental Samples (ES) of Fenchuganj Gas Field (FGF)

A total of 13 elemental (K, Ca, Ti, Mn, Fe, Ni, Zn, As, Rb, Sr, Y, Zr and Pb) abundances in environmental S&S samples of FGF, Bangladesh have been determined by EDXRF which have been tabulated in Table 7.3. Max. values, Min. values, Avg. abundances, median value, RSD and SD along with the relative literature data of respective elements are also shown in Table 7.3.

Lowest RC level and all seven RHI values obtained in sample EF-4 i.e. WDEvp pond side area-2 of FGF. Highest values of all seven RHI obtained in sample EF-5, which location is selected as base-line data from outside the GF and plant area of this FGF. Interestingly the result has been found for M&M concentration exactly opposite from RC i.e. for Ca, Ti, Mn, As, Sr and Pb EA have been found highest in sample EF-4 compared to other ES of the GF area of this study. And lowest values of most of the EA have been found in sample EF-5 compared to other ES of FGF.

Table 7.3: Elemental abundances (EA) in environmental S&S samples of FGF.

Ele-ment	Unit	EF-1	±	EF-2	±	EF-3	±	EF-4	±	EF-5	±	Mean	SD	RSD	Median	Max.	Min.	UCC[a]	World Soil Median[b]	Shale[b]
K	[%]	1.09	0.07	1.59	0.10	1.40	0.09	0.00	0.00	1.33	0.09	1.08	0.63	58.3	1.33	1.59	0.00	2.32	1.4	2.45
Ca	[%]	4.32	0.59	6.82	0.93	0.00	0.00	8.36	1.14	3.70	0.51	4.64	3.21	69.1	4.32	8.36	0.00	2.6	1.5	1.6
Ti	[%]	3.25	0.11	7.98	0.27	6.34	0.21	10.7	0.36	0.00	0.00	5.64	4.14	73.4	6.34	10.7	0.00	0.38	0.5	0.46
Mn	[µg/g]	867	51.2	2139	126	1353	79.8	2186	129	695	41.0	1448	696	48.0	1353	2186	695	775	1000	850
Fe	[%]	2.54	0.12	2.97	0.14	3.55	0.17	1.34	0.06	6.29	0.30	3.34	1.84	55.1	2.97	6.29	1.34	3.92	4	4.8
Ni	[µg/g]	85.6	7.53	101	8.86	0.00	0.00	0.00	0.00	79.4	6.99	53.1	49.1	92.4	79.4	101	0.00	47	-	68
Zn	[µg/g]	199	15.3	249	19.0	248	19.0	234	17.9	260	19.9	238	23.4	9.84	248	260	199	67	90	120
As	[µg/g]	40.4	1.93	41.1	1.96	<MDL	0.00	42.6	2.04	38.0	1.81	32.4	18.2	56.1	40.4	42.6	<MDL	4.8	6	13
Rb	[µg/g]	57.4	5.02	25.1	2.20	34.0	2.98	31.6	2.77	145	12.8	58.8	50.1	85.3	34.0	145	25.1	84	150	160
Sr	[µg/g]	1104	155	980	137	1503	210	2062	289	84.8	11.9	1147	729	63.5	1104	2062	84.8	320	250	300
Y	[µg/g]	30.8	3.34	0.00	0.00	29.7	3.22	32.4	3.51	60.2	6.52	30.6	21.3	69.6	30.8	60.2	0.00	21	40	41
Zr	[µg/g]	238	55.2	104.6	24.3	137	31.7	88.7	20.6	221	51.2	158	67.8	43.0	137	238	88.7	193	400	160
Pb	[µg/g]	114	13.4	105.6	12.4	105	12.4	111	13.0	101	11.8	107	5.24	4.89	106	114	101	17	35	23

[a] [2]; [b] [3].

7.3.2 Environmental Contamination (EC) Indices of S&S Samples from Fenchuganj Gas Field (FGF)

Base-line data selection is essential to assess the S&S samples' EA in terms of EC indices like geoaccumulation index (I_{geo}), contamination factor (CF) and enrichment factor (EF). In this research work, the EA of UCC (upper continental crust) [7.2] has been selected as the base-line data.

7.3.2.1 Enrichment Factor (EF) of Elemental Abundances (EA) of FGF Environmental Samples (ES)

To study the anthropogenic nature and mobilization of EA with the crustal origin, EF in specific S&S samples for each element has been measured and are graphically presented in Fig. 7.7. EF value is 82.2 for Ti in sample EF-4 which is not shown in this graph, otherwise using logarithmic scale could interrupt other EA data presentation.

EF is casted widely to distinguish manmade and natural sources of M&M [7.4 - 7.5]. Fe has been used in this study to calculate EF as Fe naturally has almost uniform concentrations and also displays alike to many trace elements' geochemistry [7.6-7.8].

In the GF environmental soil sample EF-4 i.e. WDEvp pond side area-2 of FGF, significantly higher EF of most of the M&M have been found compared to other environmental S&S samples of this GF area of this research work. Interestingly for EF of Ca, Ti, Mn, Zn, As, Sr, Y and Pb EA have been found highest in sample EF-4 compared to other ES of this GF area. And lowest values of EF for most of the EA have been found in sample EF-5, which location is selected as base-line data from outside the GF and plant area of this FGF compared to other samples.

The EF values of the Ti ranges from 0.0 to 82.2 with the highest EF value is detected for the Ti is 82.2 in sample EF-4. The EF values of the As ranges from 0.0 to 26 with the highest EF value is detected for the As is 26 in same sample EF-4. Similar trend is obtained for Pb (EF range: 3.7 to 19) and Sr (EF range: 0.17 to 18.9) with the highest EF values for both Pb and Ti are detected in sample EF-4 which are 19 and 18.9 respectively. Within five ES, the EF values of Ti, As and Pb in four samples revealed that the S&S samples have been severely enriched with these M&M (except As in sample EF-3) excluding sample EF-5, which location is selected as base-line data from outside the GF and plant area of this FGF. All these evidences disclose that these elements are from the anthropogenic origin.

Along with these elements, the CF values for Ca, Mn, Ni, Zn, Sr and Y are pointedly higher than one i.e., these elements are more probably to be from the manmade origin rather than a natural crustal source. Comparatively higher concentrated M&M areas could be the result of contaminated M&M by overflowing of skimming pit and WDEvp pond mostly in rainy season. At the time of maintenance work, the natural gas production equipments are cleaned using high-speed jet water, by which M&M may be washed away from Sc-Sl and contamination spread to nearby areas through the drain on the way to WDEvp pond.

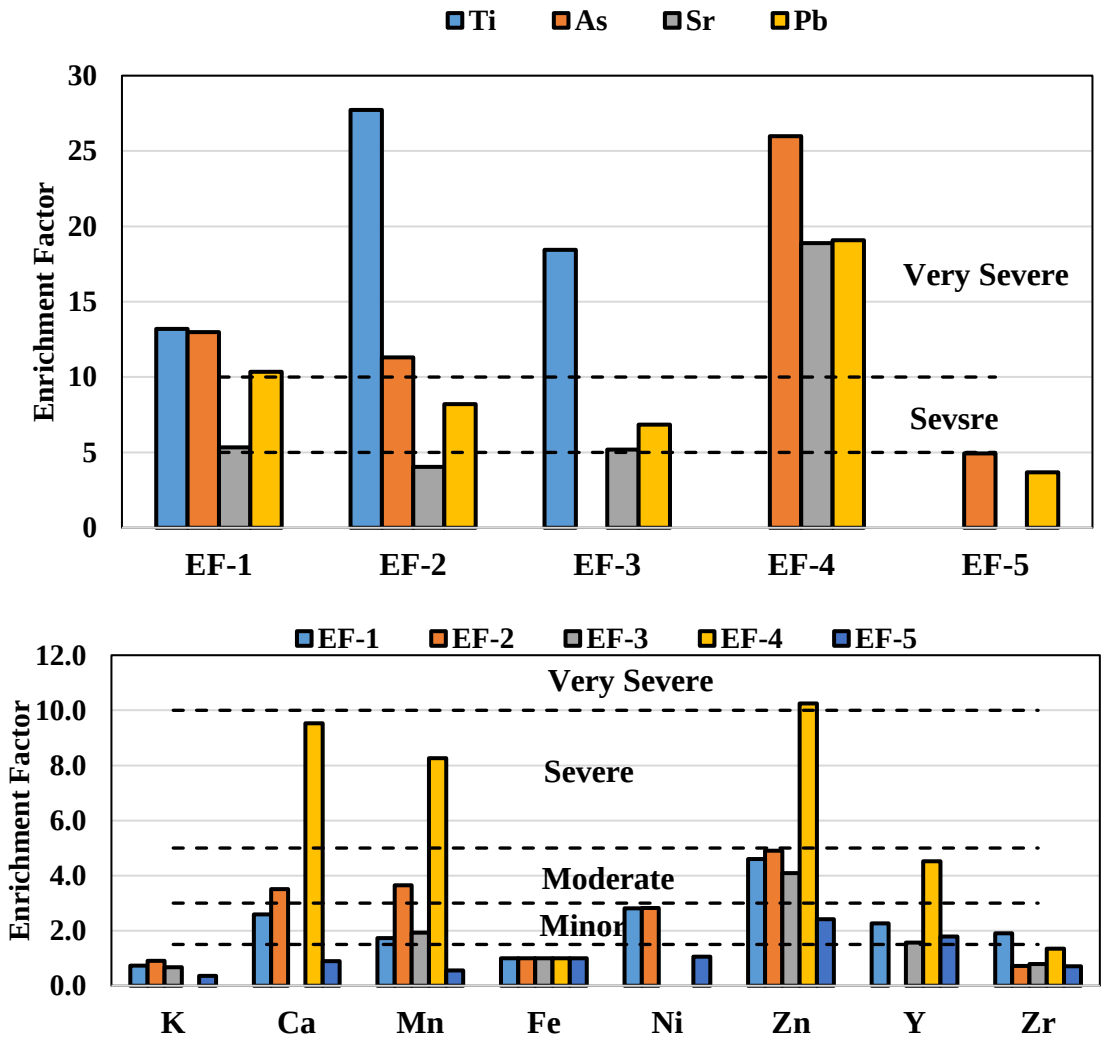

Figure 7.7: Plotted EF comparative to UCC and Fe in the S&S samples of the individual elements of FGF. [N.B.: EF= 82.2 for Ti in sample EF-4 which is not shown in this graph, otherwise using logarithmic scale could interrupt other EA data presentation.]

7.3.2.2 I_{geo} of Elements of FGF Environmental Samples (ES)

The graphical representation of I_{geo} of EA of FGF environmental S&S samples have been shown in Fig. 7.8. In this research work, EA of UCC (upper continental crust) have been selected as the base-line data to estimate I_{geo} [7.2].

I_{geo} values of samples of the GF area are ranged from 2.51 to 4.22 with Max. value is heavy to extremely contaminated by Ti. Graphical representation of I_{geo} shown in Fig. 7.8 revealed moderate to heavily contaminated by As and Pb in all S&S samples of FGF area. Figure also shows moderately contamination of Zn and Sr in most of the samples of GF area. All these indications reveal that these elements are from the anthropogenic origin.

The negative I_{geo} values for K, Fe and Zr in all the samples (except Fe in sample EF-5 i.e. background sample) discovered that in the S&S samples of the research site is lower than their respective natural background values and thus, indicates no contamination present of these elements.

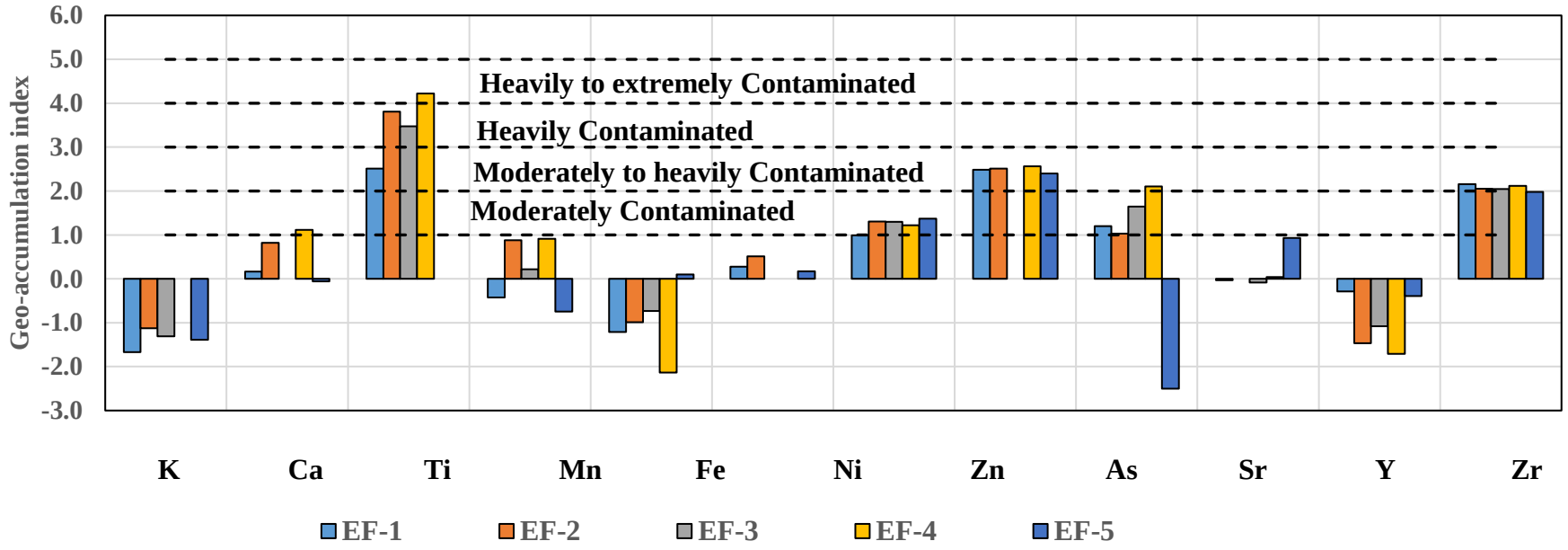

Figure 7.8: I_{geo} of elements of FGF S&S samples.

7.3.2.3 Contamination Factor (CF) of Elements of FGF Environmental Samples (ES)

The graphical representation of CF of EA of FGF environmental S&S samples have been shown in Fig. 7.9.

For Ti, As and Pb, CF values are found high i.e. CF > 6 in all samples (except Ti in sample EF-5 i.e. background sample and As<MDL in EF-3) of FGF. This evidence discloses that contamination by these elements are from the anthropogenic origin.

Along with these elements, the CF values for Ca, Mn, Ni, Zn, Sr and Y are pointedly higher than one i.e., these elements are more probably to be from the manmade origin rather than a natural crustal source. At the time of maintenance work, the natural gas production equipments are cleaned using high-speed jet water, by which M&M may be washed away from Sc-Sl and contamination spread to nearby areas through the drain on the way to WDEvp pond. Comparatively higher concentrated M&M areas could be the result of contaminated M&M by overflowing of skimming pit and WDEvp pond mostly in rainy season.

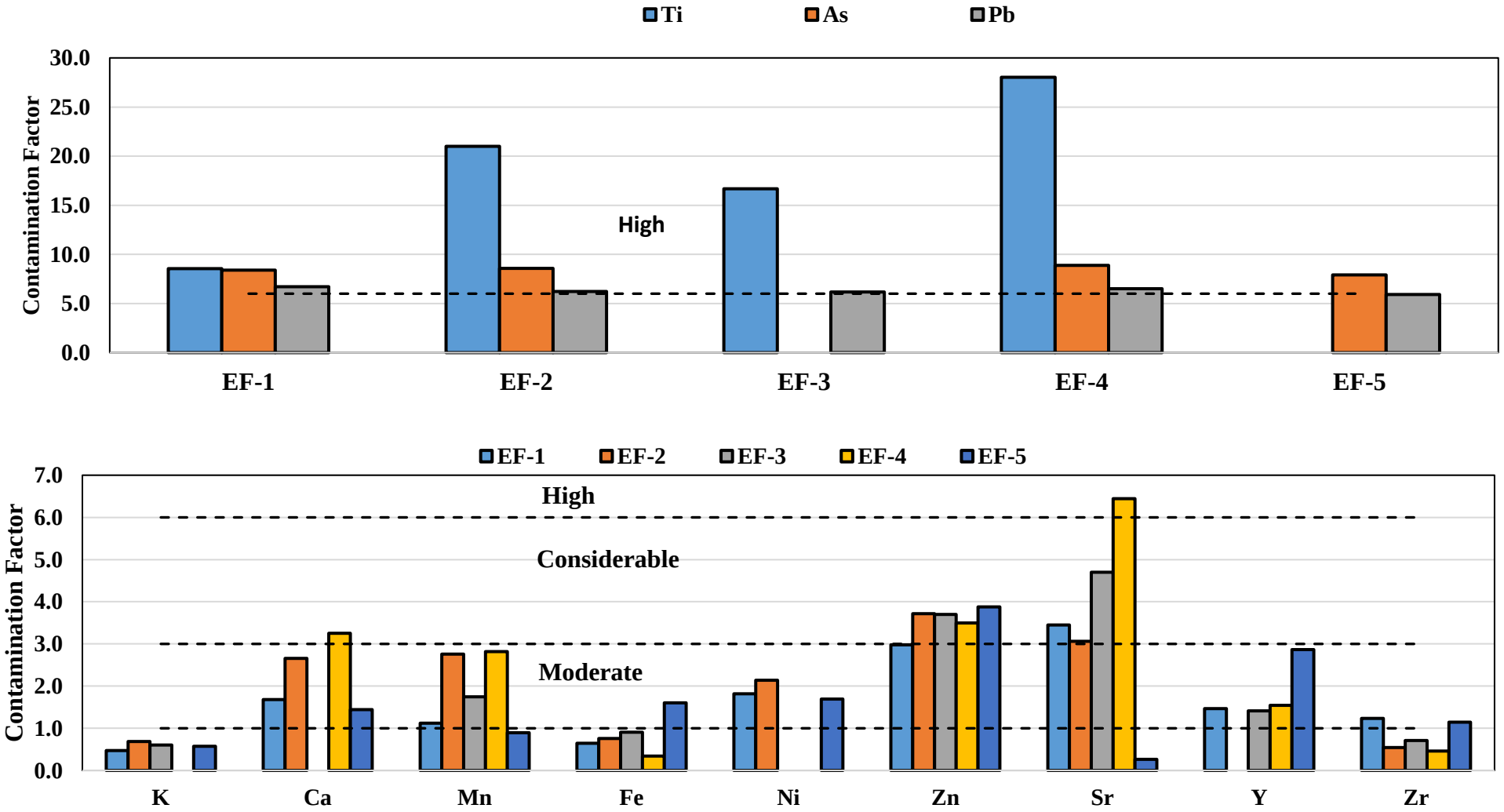

Figure 7.9: CF of elements of FGF S&S samples.

7.4 Inter-Comparison of the Three Gas Fields (GF) Environmental Contamination (EC) Indices

7.4.1 Inter-Comparison of Enrichment Factor (EF) of Elements of the Three GF Samples

Graphical presentation of inter-comparison of enrichment factor (EF) of EA of the three GF environmental samples are shown in Fig. 7.10.

EF comparative to UCC and Fe in the S&S samples of the individual elements are plotted of the three GF where very high value, EF=129.5 of Pb in soil sample ES-3 of SGF not included here.

For almost all EF of EA of the Avg. value of FGF are significantly higher compared to other two GF. According to EF of almost all EA Avg. values, SGF is in second position and Sbz GF in last position. According to the duration of production of researved gas, just opposite serial is observed i.e. highest duration observed for FGF and lowest duration observed for Sbz GF which can be an evedance for enrichment variation of anthropogenic incorporation due to GAA.

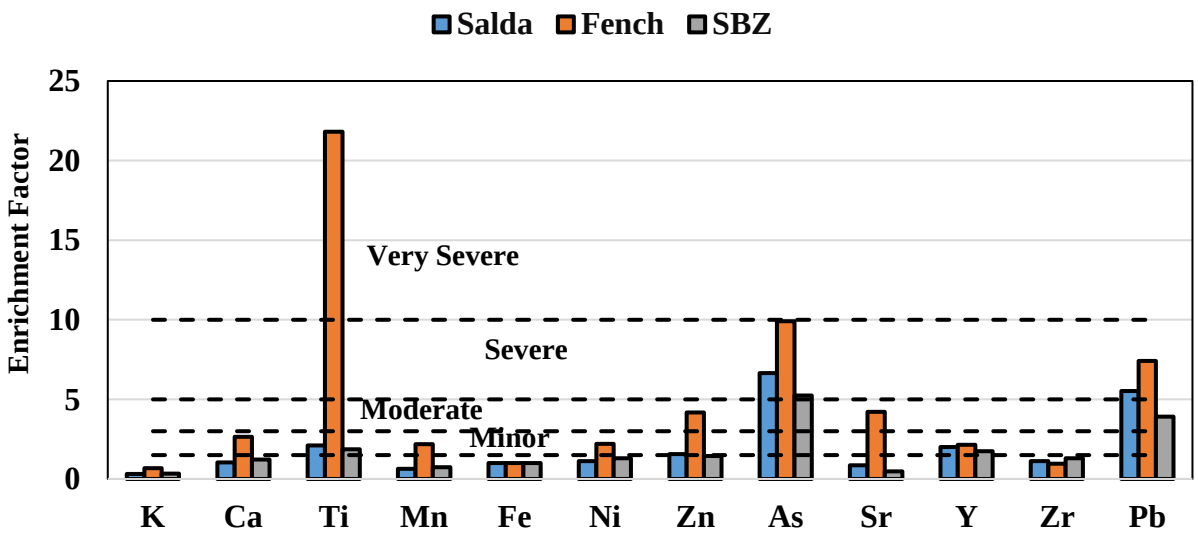

Figure 7.10: Plotted EF comparative to UCC and Fe in the S&S samples of the individual elements of three GF. [Very high value of Pb in soil sample (ES-3) of SGF not included here]

7.4.2 Inter-Comparison of I_{geo} of Elements of the Three GF Samples

Similar trend is obtained for I_{geo} of EA Avg. values of the three GF samples with some exceptions of FGF samples.

According to I_{geo} of EA Avg. values of the three GF ES are contaminated mostly by As, Pb and Ti which can be due to anthropogenic integration for GAA.

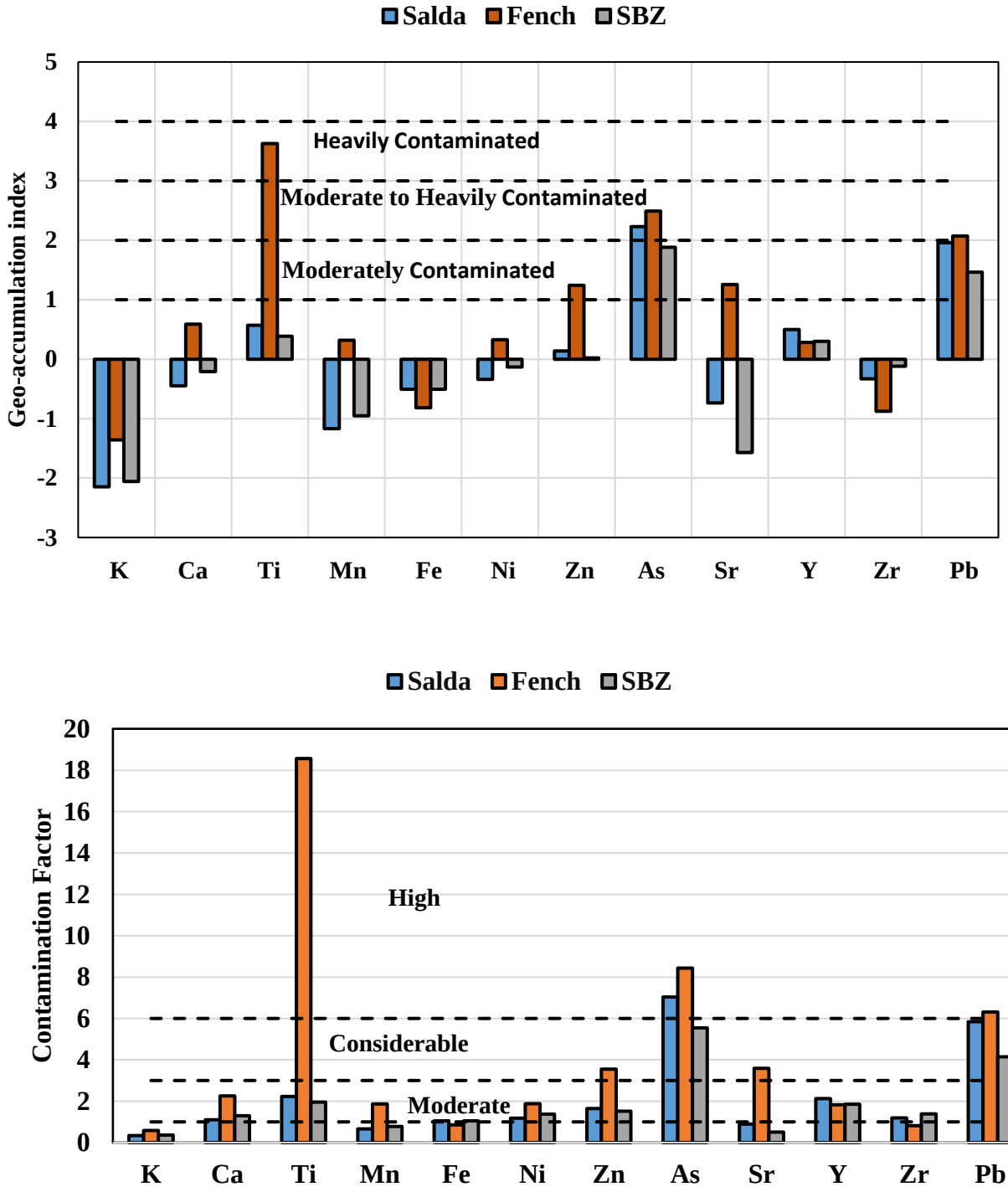

Figure 7.12: CF of elements of the three GF S&S samples**.** [Very high value of Pb in soil sample (ES-3) of SGF not included here].

7.5.1 EF of EA of Gas Well Core (GWC) Samples Analysis of FGF and Sbz Gas Field (GF) by ED-XRF

Eleven GWC samples of FGF and Sbz GF have been analysed by ED-XRF and EF of EA of "GWC samples" are graphicaly shown in Fig. 7.13.

The EF of As and Pb EA in all core samples revealed that the "GWC samples" have been within moderately enriched to severely enriched with these M&M except sample CB_x-1.2. Similar trend is obtained for both the GF core samples.

Almost all GWC samples show considerable enrichment of As and Pb EA which reveals that ES can be contaminated by As, Pb and other toxic M&M originated from GAA to the surrounding environment of GF.

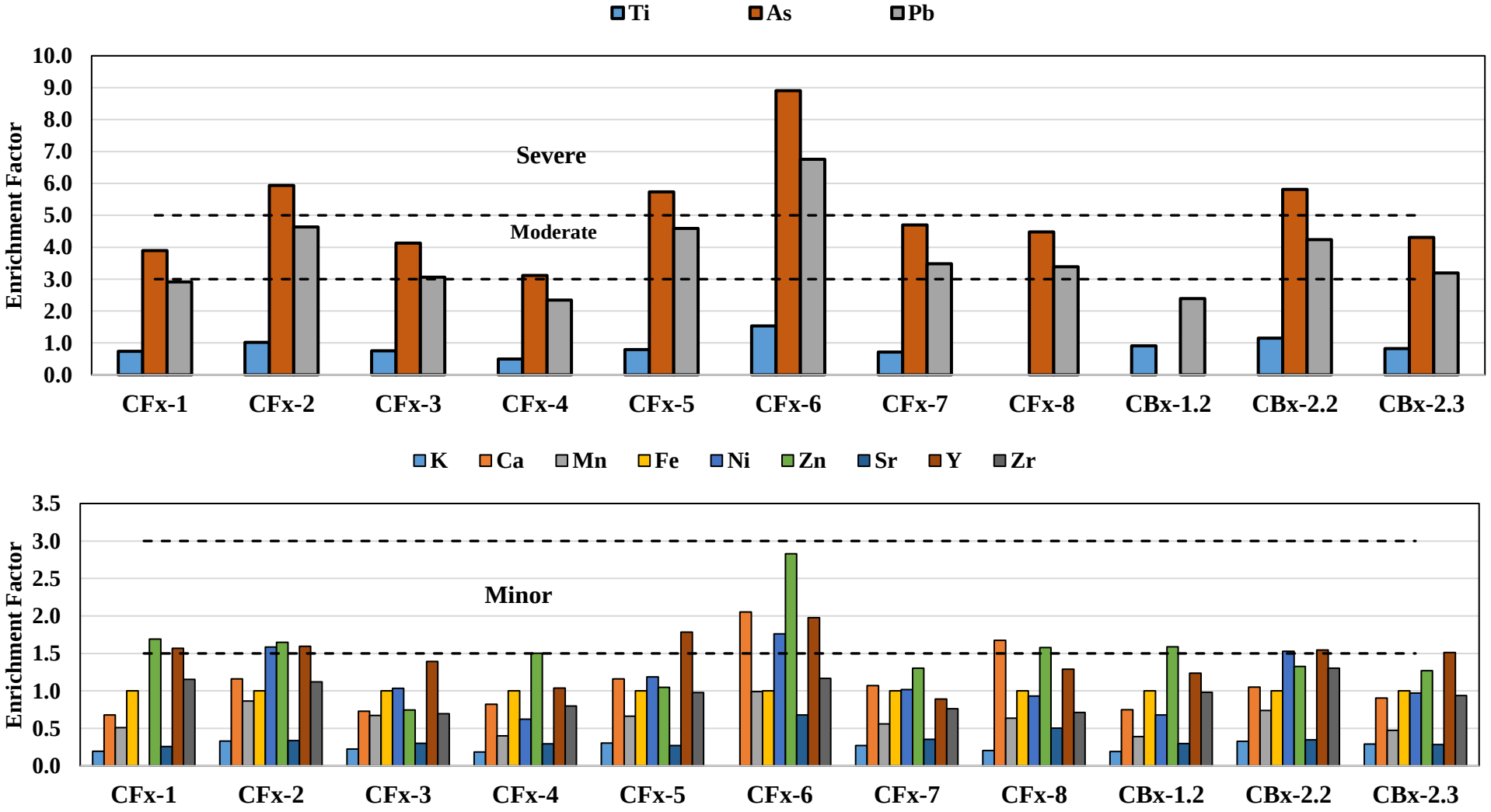

Figure 7.13: EF of core samples' EA analysis of FGF and Sbz GF by ED-XRF

7.5.2 I_{geo} of EA of GWC Samples Analysis of FGF and Sbz GF by ED-XRF

Graphical representation of I_{geo} shown in Fig. 7.14 revealed moderate to heavy geo-accumulation of As and almost moderate to heavy geo-accumulation of Pb in all "GWC samples" of FGF and Sbz GF.

The negative I_{geo} values for K, Ca, Ti, Mn, Sr and Zr in almost all the samples (except sample CB_x-1.2) discovered that in the S&S samples of the research work site is lower than their respective natural background values. Similar trend is obtained for both the GWC samples.

Geochemical data of sediments could be affected by constant sum effect, because in a dataset, changes may occur in relative abundant elements when concentration of one element changes [7.1], which situation is clearly observed in exception sample CB_x-1.2.

7.5.3 Normalized to UCC of EA of Core Samples Analysis of FGF and Sbz Gas Field by ED-XRF

According to Fig. 7.15 for As and Pb values normalized to UCC are found high i.e. CF > 6 or almost high in all samples (except for As in sample CB_x-1.2) of the two GWC samples. As graphical presentation, the situation of exception sample CB_x-1.2 where other EA normalized to UCC are comparatively higher can be explained as geochemical data of sediments could be affected by constant sum effect, because in a dataset, changes may occur in relative abundant elements when concentration of one element changes [7.1].

Almost all GWC samples show considerable enrichment of As and Pb EA normalized to UCC which reveals that ES can be contaminated by As, Pb and other toxic M&M originated from GAA to adjacent areas of the GF.

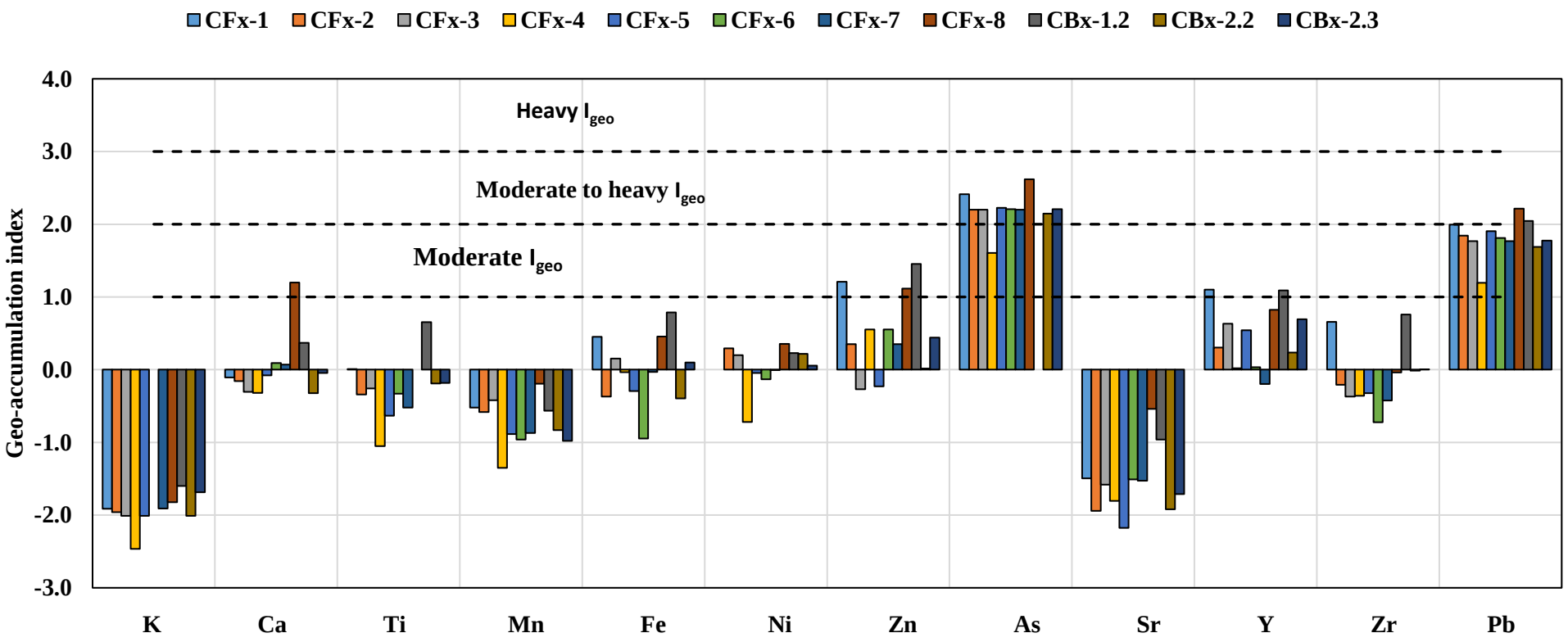

Figure 7.14: I_{geo} of EA of GWC samples analysis of FGF and Sbz GF by ED-XRF

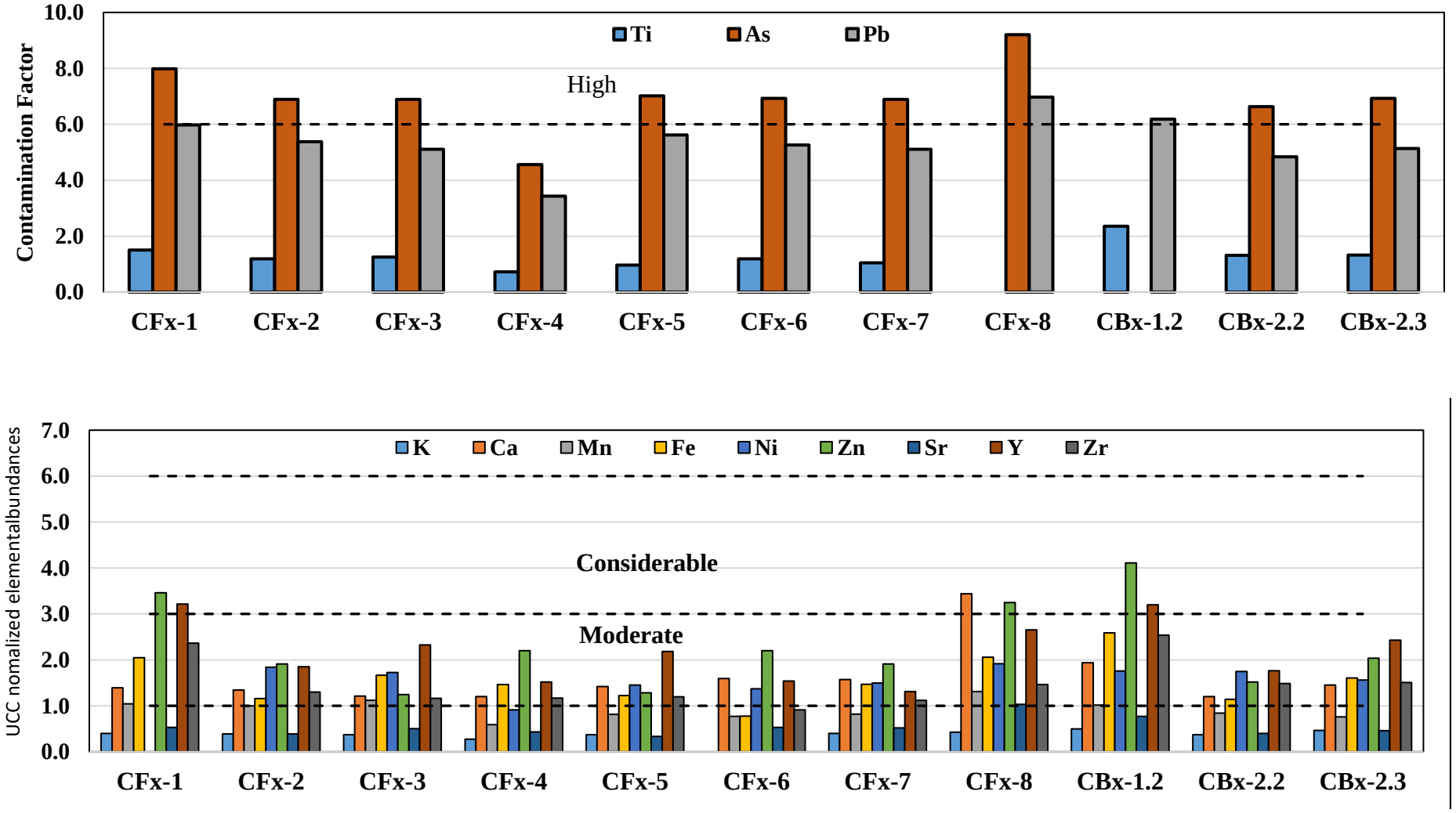

Figure 7.15: UCC normalized EA of GWC samples of FGF and Sbz GF.

Table 7.4: EA in environmental S&S samples of Sbz gas field (GF) by ED-XRF using two pellets of each sample for comparison.

Sample ID	K	Ca	Ti	Mn	Fe	Ni	Zn	As	Rb	Sr	Y	Zr	Pb
	[%]	[%]	[%]	[µg/g]	[%]	[µg/g]	[µg/g]	[µg/g]	[µg/g]	[µg/g]	[µg/g]	[µg/g]	[µg/g]
EB-1	0.91	3.34	0.46	544	3.93	70	117	33	115	158	39	300	87
EB-1 a	0.90	3.34	0.51	644	3.53	64	145	32	103	130	34	230	96
EB-2.1	0.95	3.74	0.57	732	4.48	75	80	32	107	121	52	351	87
EB-2.1 a	0.89	3.21	0.58	543	4.40	70	86	36	98	142	48	310	100
EB-2.2	0.91	4.73	0.39	653	4.16	98	116	36	95	152	48	322	97
EB-2.2 a	0.83	4.46	0.41	645	3.71	76	78	31	71	130	25	236	82
EB-3.1	0.43	2.06	0.59	299	4.76	27	64	12	116	130	30	256	53
EB-3.1 a	0.50	2.59	0.52	338	5.38	24	122	11	120	131	56	283	25
EB-3.2	0.57	2.22	0.27	503	4.74	50	129	18	100	137	41	248	59
EB-3.2 a	0.87	3.21	0.37	519	4.76	67	112	33	114	128	44	276	91
EB-4.1	0.84	3.72	0.47	601	4.74	70	121	33	110	122	38	297	96
EB-4.1 a	0.87	3.46	0.41	669	5.10	100	80	43	135	150	37	275	129

According to Table 7.4, elemental abundances in environmental S&S samples of Sbz GF have been studied by ED-XRF using two pellets of each sample for comparison, where for all the elements results of two pellets of each sample are comparable with each other.

Table 7.5: EA of all GWC samples of FGF and some of Sbz GF have been shown by two methods INAA and ED-XRF for intercomparison.

Gas Field	Sample ID	K	Ca	Ti	Mn	Fe	Zn	As	Rb
		[%]	[%]	[%]	[µg/g]	[%]	[µg/g]	[µg/g]	[µg/g]
Fenchuganj	CF_X-1	0.92	3.58	0.57	810	8.03	232	38	123
	CF-1	2.13	<MDL	0.47	495	3.99	88	6	138
	CF_X-2	0.89	3.45	0.45	776	4.55	128	33	101
	CF-2	2.29	<MDL	0.45	477	3.84	67	7	163
	CF_X-3	0.86	3.12	0.48	868	6.54	83	33	119
	CF-3	2.34	<MDL	0.57	565	4.91	97	14	164
	CF_X-4	0.63	3.09	0.28	456	5.74	147	22	124
	CF-4	2.35	2.23	0.60	423	4.88	69	11	146
	CF_X-5	0.86	3.65	0.37	629	4.80	86	34	95
	CF-5	2.19	3.30	0.54	432	4.45	76	9	162
	CF_X-6	<MDL	4.10	0.45	598	3.05	147	33	50
	CF-6	1.39	<MDL	0.23	427	2.55	47	2	58
	CF_X-7	0.93	4.04	0.40	636	5.75	128	33	97
	CF-7	2.13	<MDL	0.49	514	4.87	103	10	155
	CF_X-8	0.98	8.84	<MDL	1016	8.06	218	44	122
	CF-8	1.96	1.55	0.43	937	3.63	46	12	117
Shahbazpur	CB_X-1.2	1.15	4.98	0.90	786	10.14	276	<MDL	184
	CB-1.2	2.81	<MDL	0.43	563	4.75	115	<MDL	165
	CB_X-2.2	0.86	3.08	0.50	653	4.48	102	32	84
	CB-2.2	2.68	<MDL	0.53	469	3.95	104	<MDL	148
	CB_X-2.3	1.08	3.74	0.50	590	6.30	137	33	134
	CB-2.3	3.31	<MDL	0.62	413	5.24	140	<MDL	199

In Table 7.5, EA of all GWC samples of FGF and some of Sbz GF have been shown by two methods namely INAA and ED-XRF for intercomparison. Here CF_x and CB_x sample ID have been used for ED-XRF analysis method and for INAA analysis method CF and CB have been used for samples of FGF and Sbz GF respectively. For large portion of samples, EA data are comparable for both methods with some errors, where INAA method is used as standard method. NAA method is used like adjudicator technique when other procedures produced confusing outcomes and when new methods being invented as per NAA method is characterized as accurate and reliable.

7.6 Elemental Abundances (EA) of Gas Well Core (GWC) Samples of Three Gas Fields by NAA

INAA method have been used to determine a set of high-quality elemental data of petroleum reservoir formation zone which could serve as baseline data for newly developed integrated in-site G&O and uranium recovery technology and to do geochemical interpretation of gas reservoir zone. With high precision and high sensitivity as INAA method offers high quality data so precious and not easily available drilling GWC samples of gas reservoir zone have been analyzed by INAA method.

7.6.1 Elemental Abundances of Core Samples for SBZ Gas Field

A total of 25 major, trace and REE EA (Na, Al, K, Sc, Ti, V, Cr, Mn, Fe, Co, Zn, As, Rb, Cs, Ba, La, Ce, Sm, Eu, Dy, Yb, Hf, Ta, Th and U) in seven GWC samples from two GRW of Sbz GF, Bangladesh were determined by INAA which have been presented in Table 7.6. Max. values, Min. values, mean abundances (n=11), median value, relative standard deviations (RSD) and standard deviations (SD) along with the relative literature data of corresponding elements are also shown in Table 7.6.

Table 7.6: EA in GWC samples of gas-reservior well (GRW) of Sbz gas field (GF) by NAA

Ele-ment	Unit	CB-1.1	±	CB-1.2	±	CB-1.3	±	CB-1.4	±	CB-2.1	±	CB-2.2	±
Na	%	1.10	0.01	1.10	0.01	1.14	0.01	0.97	0.01	1.39	0.01	1.16	0.01
Al	%	9.79	0.06	9.53	0.06	9.29	0.07	11.0	0.07	6.59	0.05	8.68	0.06
K	%	2.79	0.07	2.81	0.08	2.61	0.07	3.42	0.09	2.18	0.06	2.68	0.07
Sc	µg/g	16.2	0.11	17.0	0.12	15.0	0.11	20.7	0.13	9.40	0.08	14.0	0.11
Ti	%	0.50	0.03	0.43	0.03	0.43	0.03	0.49	0.03	0.38	0.03	0.53	0.04
V	µg/g	136	4.72	146	5.10	130	4.80	161	5.34	65.3	3.02	111	4.29
Cr	µg/g	100	2.02	137	2.62	98.9	2.09	136	2.55	56.4	1.38	89.4	1.97
Mn	µg/g	646	8.73	563	7.85	517	112	692	9.32	378	5.38	469	101
Fe	%	4.70	0.06	4.75	0.06	4.25	0.05	5.61	0.06	3.11	0.04	3.95	0.05
Co	µg/g	19.6	0.56	20.0	0.60	18.2	0.56	27.2	0.71	12.4	0.42	16.5	0.53
Zn	µg/g	127	6.38	115	6.34	88.7	5.28	101	5.68	59.8	3.97	104	5.92
As	µg/g	7.73	0.26	7.40	0.27	8.89	0.30	14.2	0.37	0.00	0.00	10.4	0.32
Rb	µg/g	157	5.82	165	6.27	149	5.80	209	7.36	98.0	4.05	148	5.77
Cs	µg/g	10.6	0.27	10.9	0.29	10.0	0.27	18.4	0.43	4.75	0.16	8.97	0.25
Ba	µg/g	1553	48.6	1847	57.5	565	23.3	734	27.4	393	16.7	557	23.0
La	µg/g	48.0	0.91	48.5	0.98	45.4	0.93	49.1	0.96	25.5	0.61	46.9	0.95
Ce	µg/g	88.6	1.27	92.8	1.38	81.3	1.26	98.8	1.40	51.4	0.89	93.1	1.38
Sm	µg/g	8.04	0.07	8.42	0.08	7.60	0.07	8.68	0.08	4.58	0.05	8.18	0.08
Eu	µg/g	1.68	0.11	1.83	0.13	1.46	0.11	1.87	0.12	1.15	0.09	1.91	0.13
Dy	µg/g	6.18	0.09	6.10	0.10	5.81	2.76	6.43	0.10	3.94	0.07	6.22	2.96
Yb	µg/g	3.31	0.15	2.91	0.14	2.62	0.13	2.70	0.13	2.16	0.11	2.54	0.13
Hf	µg/g	5.13	0.17	6.33	0.21	5.87	0.20	5.32	0.18	3.72	0.14	7.14	0.23
Ta	µg/g	1.46	0.12	1.74	0.14	1.33	0.11	1.44	0.12	0.72	0.07	1.24	0.11
Th	µg/g	21.0	0.24	20.59	0.25	17.0	0.22	22.2	0.26	11.6	0.16	18.2	0.23
U	µg/g	3.56	0.14	3.25	0.14	2.88	0.13	3.50	0.14	1.76	0.09	2.77	0.13

Continued

Table 7.6: EA in GWC samples of Sbz gas field (GF), Bangladesh.(cont.)

Ele-ment	Unit	CB-2.3	±	Mean	SD	RSD	Median	Max.	Min.	UCC[a]	World Soil Median[b]	Shale[b]
Na	%	1.22	0.01	1.15	0.13	11.2	1.14	1.39	0.97	2.43	0.5	0.6
Al	%	9.66	0.06	9.23	1.36	14.8	9.53	11.04	6.59	8.15	7.1	8.8
K	%	3.31	0.08	2.83	0.42	14.9	2.79	3.42	2.18	2.32	1.4	2.45
Sc	µg/g	17.3	0.12	15.6	3.47	22.2	16.2	20.7	9.40	14	7	13
Ti	%	0.62	0.04	0.48	0.08	15.9	0.49	0.62	0.38	0.38	0.5	0.46
V	µg/g	141	4.52	127	31.4	24.7	136	162	65.3	97	90	130
Cr	µg/g	102	2.13	103	27.8	27.0	100	137	56.4	92	70	90
Mn	µg/g	413	5.91	525	116	22.2	517	692	378	775	1000	850
Fe	%	5.24	0.06	4.52	0.83	18.5	4.70	5.61	3.11	3.92	4	4.8
Co	µg/g	22.7	0.65	19.5	4.68	24.0	19.6	27.2	12.4	17.3	8	19
Zn	µg/g	140	7.18	105	26.3	25.0	104	140	59.8	67	90	120
As	µg/g	20.7	0.45	11.6	5.11	44.2	9.67	20.7	0.00	4.8	6	13
Rb	µg/g	199	7.17	161	36.7	22.8	157	209	98.0	84	150	160
Cs	µg/g	13.0	0.33	11.0	4.15	37.8	10.6	18.4	4.75	4.9	4	5.5
Ba	µg/g	636	25.0	898	564	62.8	636	1846	393	624	500	550
La	µg/g	52.5	1.01	45.1	8.93	19.8	48.0	52.5	25.5	31	40	49
Ce	µg/g	84.2	1.28	84.3	15.7	18.6	88.6	98.8	51.4	63	50	96
Sm	µg/g	8.69	0.08	7.74	1.45	18.7	8.18	8.69	4.58	4.7	4.5	7
Eu	µg/g	1.73	0.12	1.66	0.27	16.3	1.73	1.91	1.15	1	1	1.2
Dy	µg/g	5.87	0.09	5.79	0.84	14.6	6.10	6.43	3.94	3.9	5	5.8
Yb	µg/g	3.33	0.16	2.80	0.42	15.1	2.70	3.33	2.16	2	3	3.9
Hf	µg/g	7.55	0.24	5.86	1.30	22.2	5.87	7.55	3.72	5.3	6	2.8
Ta	µg/g	1.69	0.14	1.38	0.34	24.7	1.44	1.74	0.72	0.9	2	2
Th	µg/g	21.8	0.26	18.9	3.75	19.8	20.6	22.2	11.6	10.5	9	12
U	µg/g	3.58	0.15	3.04	0.65	21.5	3.25	3.58	1.76	2.7	2	3.7

[a] [2]; [b] [3].

7.6.2 EF Assessment of Elements of Gas Well Core Samples (GWC) of Sbz Gas Field

Base-line data selection is important to assess the EA of GWC samples (shale and sand) by different indices like I_{geo}, CF and EF. In this research work, the EA of UCC [7.2] has been selected as the base-line data. has been used in this study to calculate EF as Fe naturally has almost uniform concentrations and also displays alike to many trace elements' geochemistry [7.6-7.8].

To study the mobilization of EA with the crustal origin, EF in specific GWC samples for each element has been measured and are graphically presented in Fig. 7.16.

The EF values of the As ranges from <MDL to 3.22 i.e. the highest enrichment of As is moderate in GWC samples of Sbz GF. In this GF ES, EF values of the As are also severely enriched. So, there is a possibility of environmental S&S samples contamination by As from GAA.

Similar trend is obtained for Cs (EF range: 1.22 to 2.62), Eu (EF range: 1.30 to 1.89) and Th (EF range: 1.39 to 1.72), which elements are minorly enriched in drilling GWC samples of GRW. Also rare earth lanthanide metals like La, Ce, Sm, Dy and Yb show enrichment.

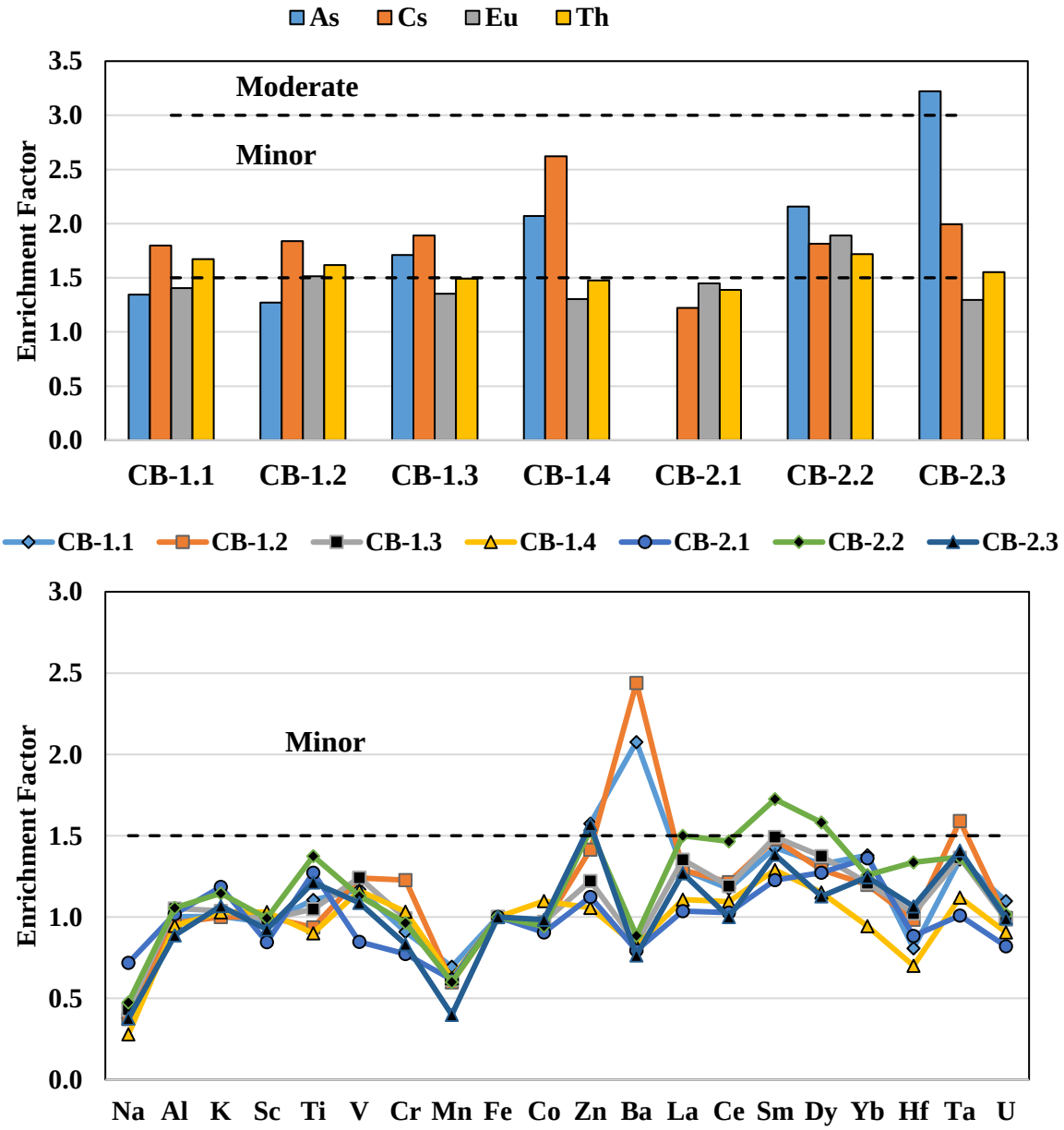

Figure 7.16: Plotted EF comparative to UCC and Fe of the different elements in the GWC samples of Sbz GF.

7.6.3 I_{geo} Assessment of Elements of Gas Well Core (GWC) Samples of Sbz Gas Field (GF)

Depending on the choice of base-line data i.e. background levels, I_{geo} values exhibite huge variations. In this work, EA of UCC according to [7.2] have been nominated as the base-line data to measure I_{geo}. The alternative is to compare concentrations GWC samples of GRW which is mineralogically and texturally comparable [7.9].

The graphical representation of geo-accumulation index (I_{geo}) of EA of Sbz GF GWC samples have been shown in Fig. 7.17.

Based on [7.10] classification, graphical representation of I_{geo} shown in Fig. 7.17 revealed moderate geo-accumulation of As and Cs in core samples of Sbz GF.

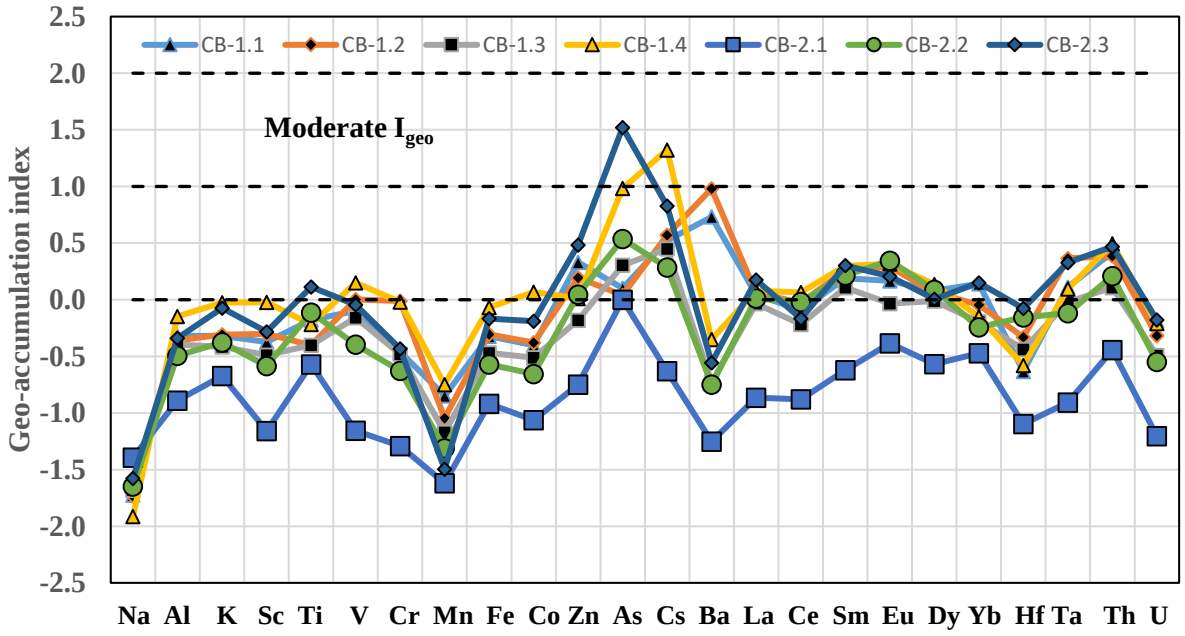

Figure 7.17: I_{geo} of EA of Sbz GF GWC samples.

The Max. I_{geo} value of As is 1.52 i.e. the highest geo-accumulation of As is moderate in GWC samples of Sbz GF. In this GF environmental samples, I_{geo} values present moderate to heavy geo-accumulation of As. So, there is a possibility of environmental S&S samples to be polluted by As from GAA.

Similar trend is obtained for Cs (Max. I_{geo} value: 1.32), Eu (Max. I_{geo} value: 0.35) and Th (Max. I_{geo} value: 0.49), which elements are also geo-accumulated in drilling GWC samples of GRW. According to Fig. 7.17, comparatively lower values of almost all elemental I_{geo} are found in core sample ID: CB-2.1, where also radioactivity level of ^{40}K is found lowest. In core sample namely CB-2.1, EA of As is also below detection level i.e. <MDL.

7.6.4 EA Normalized to UCC of GWC Samples of Sbz GF

The graphical representation of EA normalized to UCC of GWC samples of Sbz GF have been shown in Figure 7.18.

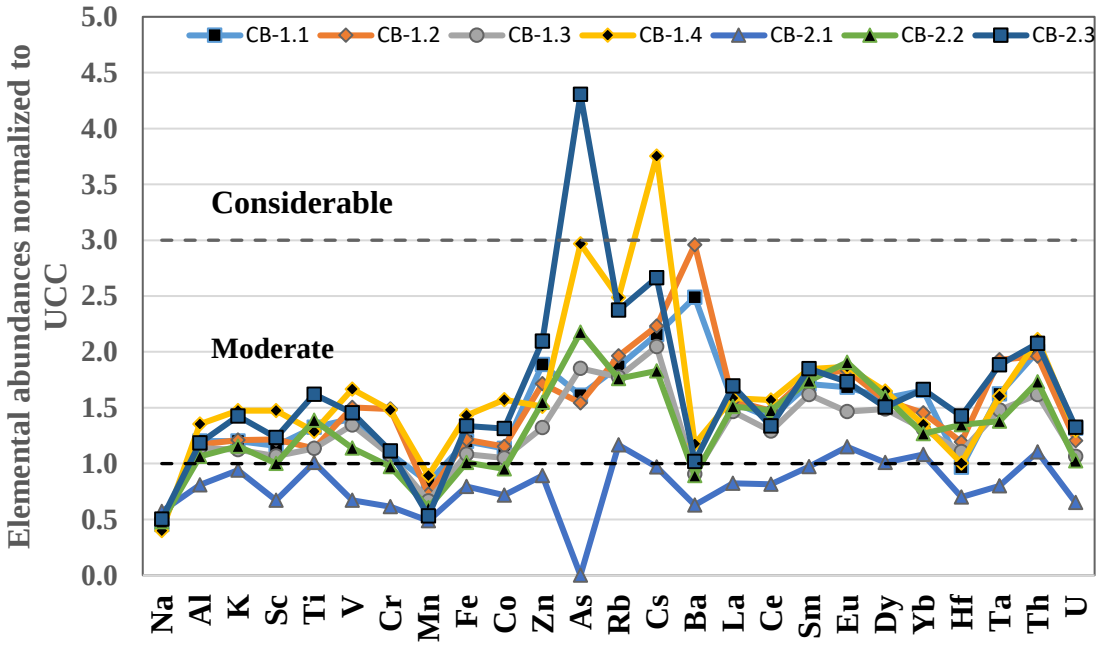

Figure 7.18: Normalized to UCC, EA of GWC samples of two different wells from Sbz GF.

Graphical presentation of normalized data of GWC samples reveal considerable enrichment of Max. value of As and Cs compare to UCC, where Max. values are 4.31 and 3.75 respectively. So, there is a possibility of environmental S&S samples to be polluted by As and Cs from GAA.

EA of all core samples are moderately enriched compare to UCC except EA of Na and Mn and also except for sample ID CB-2.1. According to Fig. 7.18, comparatively lower values of almost all elemental normalized data are found in GWC sample ID: CB-2.1, where also radioactivity level of ^{40}K is found lowest. In core sample namely CB-2.1, EA of As is also below detection level i.e. <MDL.

7.7.1 EA of GWC Samples for SGF

A total of 25 major, trace and REE EA (Na, Al, K, Sc, Ti, V, Cr, Mn, Fe, Co, Zn, As, Rb, Cs, Ba, La, Ce, Sm, Eu, Dy, Yb, Hf, Ta, Th and U) in seven GWC samples from GRW-1 of SGF, Bangladesh were determined by INAA which have been presented in Table 7,7. Max. values, Min. values, mean abundances (n=11), median value, relative standard deviations (RSD) and standard deviations (SD) along with the relative literature data of corresponding elements are also shown in Table 7.7.

Table 7.7: EA in GWC samples of gas-reservior well (GRW) of SGF.

Ele-ment	Unit	CS-1	±	CS-2	±	CS-3	±	CS-4	±	CS-5	±	CS-6	±
Na	%	1.03	0.01	0.99	0.01	1.08	0.01	0.98	0.01	1.12	0.01	1.01	0.01
Al	%	9.44	0.06	10.13	0.08	9.97	0.06	10.0	0.06	8.27	0.05	8.01	0.05
K	%	2.38	0.10	2.96	0.11	2.34	0.09	2.56	0.10	2.14	0.09	1.83	0.08
Sc	µg/g	14.0	0.11	17.22	0.12	14.1	0.10	14.4	0.11	11.51	0.09	11.35	0.09
Ti	%	0.43	0.03	0.62	0.03	0.41	0.03	0.46	0.03	0.43	0.03	0.54	0.03
V	µg/g	126.1	4.64	135	4.81	128	4.38	131.8	4.46	99.5	3.49	109	4.02
Cr	µg/g	97.8	2.19	115	2.32	96.1	2.00	98.8	2.07	99.1	2.02	79.0	1.82
Mn	µg/g	873	11.7	763	10.3	547	7.52	900	11.9	473	6.63	750	10.1
Fe	%	4.03	0.05	4.63	0.06	3.97	0.05	4.02	0.05	3.86	0.05	4.71	0.06
Co	µg/g	17.7	0.55	19.4	0.58	16.0	0.49	16.2	0.51	15.0	0.47	25.9	0.68
Zn	µg/g	113	6.24	103	5.80	91.2	5.18	95.2	5.41	81.1	4.76	90.1	5.17
As	µg/g	9.30	0.44	10.5	0.50	5.26	0.25	11.2	0.53	24.1	1.15	5.32	0.25
Rb	µg/g	148	6.10	173	6.51	151	5.75	151.1	5.82	115	4.68	116	4.92
Cs	µg/g	9.04	0.25	12.5	0.32	9.94	0.26	9.47	0.25	5.73	0.18	7.65	0.22
Ba	µg/g	480	23.3	483	21.3	429	19.1	444	19.9	397	18.1	372	18.6
La	µg/g	44.6	1.06	48.7	1.09	44.4	0.99	46.9	1.05	41.8	0.95	33.2	0.85
Ce	µg/g	86.6	1.37	96.6	1.41	88.8	1.29	92	1.35	81.8	1.22	63.5	1.08
Sm	µg/g	7.57	0.08	8.29	0.08	7.66	0.08	7.75	0.08	6.98	0.07	5.97	0.07
Eu	µg/g	1.79	0.12	1.65	0.12	1.51	0.11	1.80	0.12	1.38	0.10	1.48	0.10
Dy	µg/g	6.63	0.11	6.17	0.10	7.13	0.10	7.21	0.11	6.12	0.09	5.93	0.10
Yb	µg/g	2.25	0.13	3.26	0.15	3.01	0.14	3.09	0.15	2.72	0.13	2.86	0.14
Hf	µg/g	6.51	0.22	5.93	0.20	8.47	0.26	5.94	0.20	8.74	0.26	5.76	0.19
Ta	µg/g	1.25	0.11	1.47	0.12	1.47	0.12	1.13	0.10	1.36	0.11	0.88	0.08
Th	µg/g	17.4	0.23	20.0	0.25	18.4	0.23	19.5	0.24	20.2	0.24	13.0	0.18
U	µg/g	2.32	0.13	3.17	0.15	2.75	0.13	2.27	0.12	2.32	0.12	1.47	0.09

Continued

Table 7.7: EA in GWC samples of GRW of SGF. (cont.)

Ele-ment	Unit	CS-7	±	Mean (n=8)	SD (1σ)	RSD (%)	Median	Max.	Min.	UCC[a]	World Soil Median[b]	Shale[b]
Na	%	1.21	0.01	1.06	0.08	7.66	1.03	1.21	0.98	2.43	0.5	0.6
Al	%	10.46	0.06	9.47	0.96	10.1	9.97	10.5	8.01	8.15	7.1	8.8
K	%	2.40	0.10	2.37	0.35	14.7	2.38	2.96	1.83	2.32	1.4	2.45
Sc	µg/g	15.30	0.11	14.0	2.06	14.7	14.1	17.2	11.4	14	7	13
Ti	%	0.48	0.03	0.48	0.07	15.3	0.46	0.62	0.41	0.38	0.5	0.46
V	µg/g	145	4.9	125	15.6	12.5	128	145	99.5	97	90	130
Cr	µg/g	111	2.35	99.5	11.6	11.6	98.8	115	79.0	92	70	90
Mn	µg/g	520	7.37	690	175	25.3	750	900	473	775	1000	850
Fe	%	4.49	0.06	4.25	0.35	8.30	4.03	4.71	3.86	3.92	4	4.8
Co	µg/g	16.1	0.52	18.1	3.73	20.6	16.2	25.9	15.0	17.3	8	19
Zn	µg/g	89.4	5.35	94.7	10.3	10.9	91.2	113	81.1	67	90	120
As	µg/g	8.45	0.40	10.6	6.39	60.4	9.30	24.1	5.26	4.8	6	13
Rb	µg/g	136	5.68	141	20.8	14.7	148	173	115	84	150	160
Cs	µg/g	8.29	0.24	8.94	2.09	23.3	9.04	12.5	5.73	4.9	4	5.5
Ba	µg/g	408	20.5	431	41.6	9.67	429	483	372	624	500	550
La	µg/g	47.9	1.10	43.9	5.29	12.0	44.6	48.7	33.2	31	40	49
Ce	µg/g	89.4	1.39	85.6	10.7	12.5	88.8	96.6	63.5	63	50	96
Sm	µg/g	7.95	0.08	7.45	0.76	10.3	7.66	8.29	5.97	4.7	4.5	7
Eu	µg/g	1.76	0.12	1.62	0.17	10.3	1.65	1.80	1.38	1	1	1.2
Dy	µg/g	7.83	0.12	6.72	0.70	10.4	6.63	7.83	5.93	3.9	5	5.8
Yb	µg/g	3.80	0.18	3.00	0.48	16.0	3.01	3.80	2.25	2	3	3.9
Hf	µg/g	6.67	0.22	6.86	1.24	18.0	6.51	8.74	5.76	5.3	6	2.8
Ta	µg/g	1.45	0.12	1.29	0.22	17.2	1.36	1.47	0.88	0.9	2	2
Th	µg/g	18.3	0.24	18.1	2.45	13.6	18.4	20.2	13.0	10.5	9	12
U	µg/g	2.63	0.14	2.42	0.53	21.7	2.32	3.17	1.47	2.7	2	3.7

[a] [2]; [b] [3].

7.7.2 EF of Elemental Abundances (EA) of GWC Samples of SGF

Base-line data selection is important to assess the EA of GWC samples (shale and sand) using different indices like I_{geo} and EF. In this work, the EA of UCC [7.2] has been selected as the base-line data. Fe has been used in this study to calculate EF as Fe naturally has almost uniform concentrations and also displays alike to many trace elements' geochemistry [7.6-7.8].

To study the mobilization (due to weathering and depositional environmental condition at different stages) of EF with the crustal origin, EF for each EA in different GWC samples have been measured and are graphically presented in Fig, 7.19.

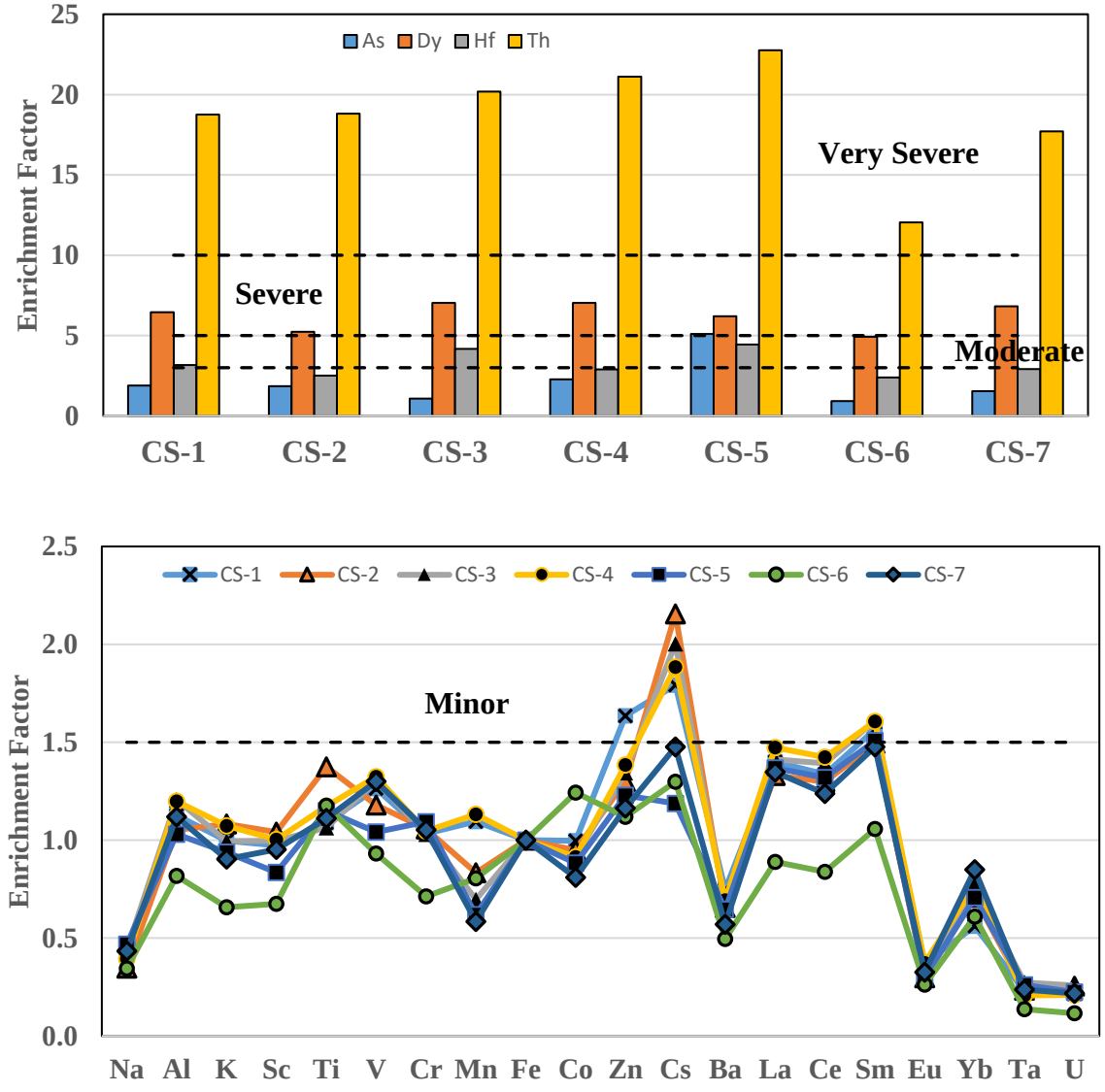

Figure 7.19: Plotted EF comparative to UCC and Fe of the individual EA in the GWC samples of SGF.

The EF values of the Th ranges from 12.05 to 22.76 i.e. enrichments of Th are very severe in all the GWC samples of SGF. The enrichments of the Dy and Hf are ranged from 4.93 to 7.04 and 2.40 to 4.44 respectively i.e. Max. EF values are severe and moderate respectively in the GWC samples of SGF. The EF values of the As ranges from 1.0 to 5.1 i.e. the highest enrichment of As is just severe in GWC samples of this GF. In this GF ES, EF values of the As are also severely enriched. So, there is a possibility of environmental S&S samples to be polluted more by As from GAA.

Similar trend is obtained for Cs (EF range: 1.2 to 2.2) which is minorly enriched in drilling core samples of GRW. Also rare earth lanthanide metals like La, Ce and Sm and also Al, Ti and V show enrichment.

According to Fig. 7.19, comparatively lower values of most of the elemental EF values are found in GWC sample ID: CS-6, where also RC levels of NR3 are found lowest. In this GWC

sample namely CS-6, elemental EF value of As is also found lowest but elemental EF value of Co is found highest in this sample relative to other GWC samples of SGF.

7.7.3 I_{geo} of EA of GWC Samples of SGF

Depending on the choice of base-line data i.e. background levels, I_{geo} values exhibite huge variations. In this work, EA of UCC according to [7.2] have been selected as the base-line data to calculate I_{geo}. The alternative is to compare concentrations GWC samples of GRW which is mineralogically and texturally comparable, [7.9].

The graphical representation of I_{geo} of EA of SGF GWC samples have been shown in Fig. 7.20.

Based on [7.10] classification, graphical representation of I_{geo} shown in Fig. 7.20 revealed Max. geo-accumulation of As is moderate, where I_{geo}=1.74 within GWC samples of SGF. In this GF ES, I_{geo} values present moderate to heavy geo-accumulation of As. So, there is a possibility of environmental S&S samples to be polluted more by As from GAA. The Max. I_{geo} value of Cs is 0.76 in GWC samples.

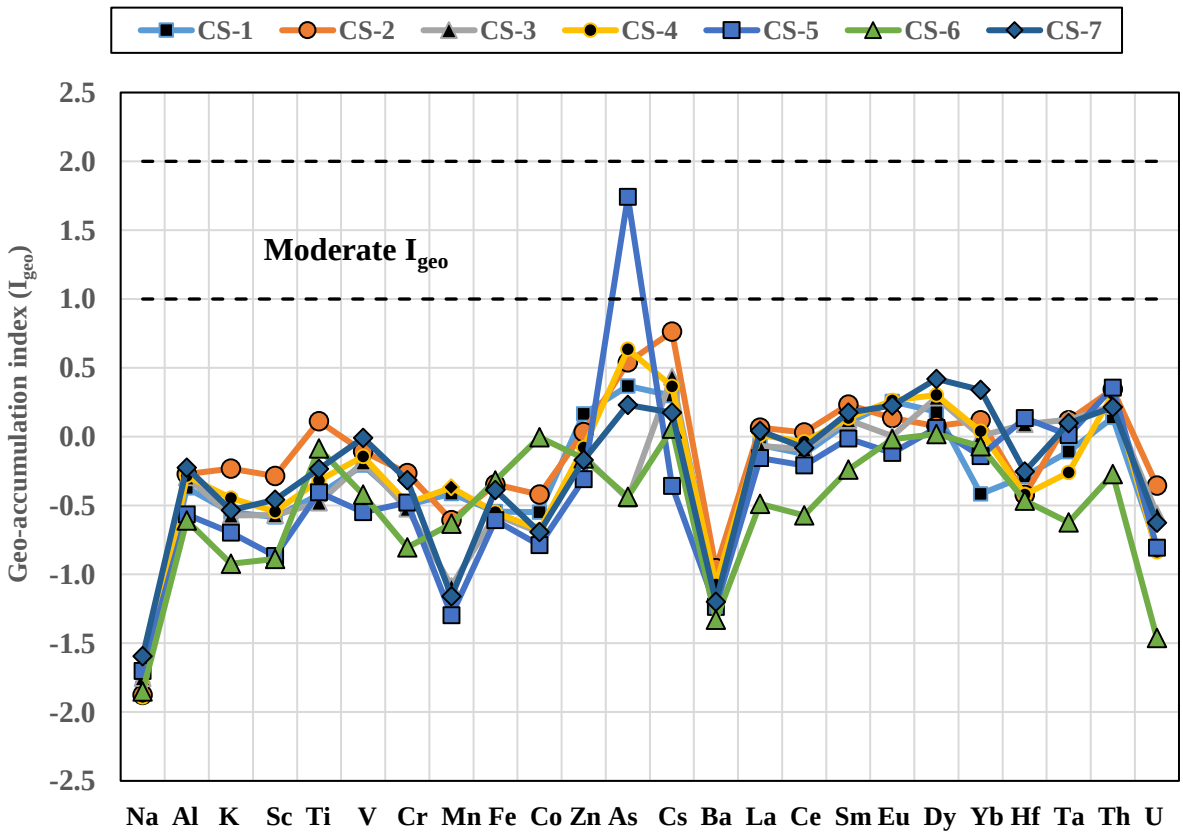

Figure 7.20: I_{geo} of EA of Sbz GF GWC samples.

7.7.4 EA Normalized to UCC of GWC Samples of SGF

The graphical representation of EA normalized to UCC of GWC samples of SGF have been shown in Fig. 7.21.

Graphical presentation of normalized data of GWC samples reveal considerable enrichment of Max. value of As relative to UCC, where Max. value is 5.02. So, there is a possibility of environmental S&S samples to be polluted by As from GAA.

EA of all GWC samples are moderately enriched compare to UCC except Na, Mn and Ba.

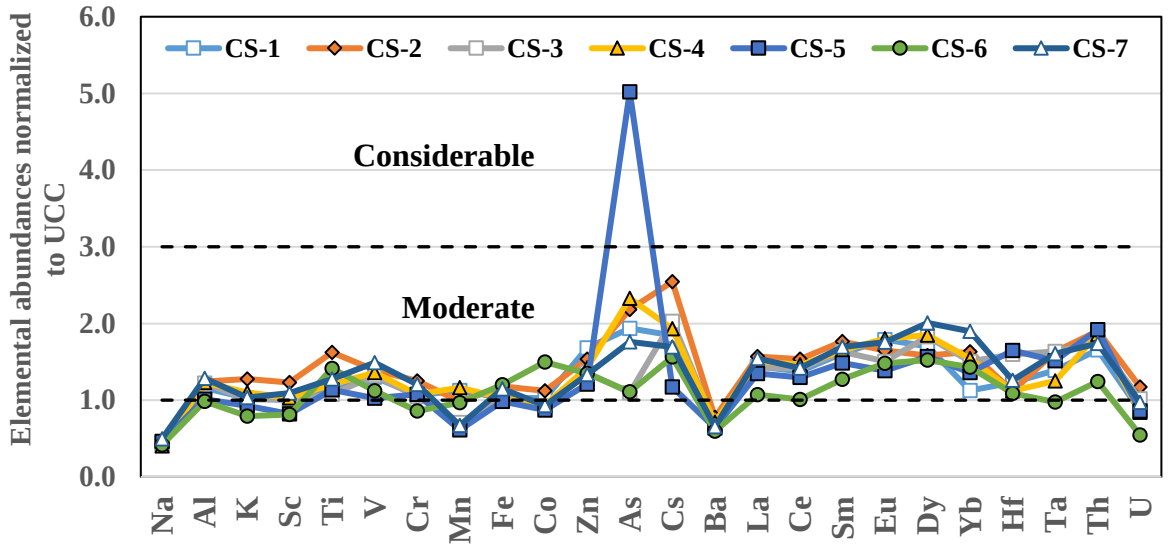

Figure 7.21: Normalized to UCC, EA of GWC samples of SGF.

7.8.1 EA of GWC Samples for FGF

A total of 29 major, trace and REE elemental (Na, Al, K, Ca, Sc, Ti, V, Cr, Mn, Fe, Co, Zn, Ga, As, Rb, Sb, Cs, Ba, La, Ce, Sm, Eu, Dy, Yb, Hf, Ta, W, Th and U) abundances in eight GWC samples from GRW-2 of FGF, Bangladesh were determined by INAA which have been presented in Table 7.8. Max. values, Min. values, Avg. abundances, median value, RSD and SD along with the relative literature data of corresponding elements are also shown in Table 7.8.

Table 7.8: EA in GWC Samples of FGF, Bangladesh.

Ele-ment	Unit	CF-1	±	CF-2	±	CF-3	±	CF-4	±	CF-5	±	CF-6	±
Na	%	1.11	0.00	1.00	0.00	1.05	0.00	0.90	0.00	0.99	0.00	1.31	0.00
Al	%	7.15	0.05	7.91	0.05	9.43	0.06	8.57	0.06	7.93	0.05	5.30	0.04
K	%	2.13	0.11	2.29	0.11	2.34	0.11	2.35	0.12	2.19	0.11	1.39	0.08
Ca	%	0.00	0.00	0.00	0.00	0.00	0.00	2.23	0.43	3.30	0.57	0.00	0.00
Sc	µg/g	13.8	0.13	14.5	0.15	18.3	0.18	17.9	0.21	16.5	0.17	8.51	0.13
Ti	%	0.47	0.03	0.45	0.03	0.57	0.03	0.60	0.04	0.54	0.03	0.23	0.02
V	µg/g	87.2	3.24	98.0	3.68	144	4.33	109	3.88	119	3.90	55.7	2.54
Cr	µg/g	102	3.05	119	3.95	136	4.47	133	4.97	114	4.01	53.4	2.72
Mn	µg/g	495	13.8	477	13.5	565	15.5	423	12.3	432	12.3	427	12.3
Fe	%	3.99	0.07	3.84	0.08	4.91	0.09	4.88	0.10	4.45	0.09	2.55	0.07
Co	µg/g	14.6	0.51	14.6	0.61	19.5	0.75	17.2	0.80	16.4	0.68	9.32	0.52
Zn	µg/g	88.0	6.08	67.2	6.15	97.0	7.95	68.9	7.47	75.8	6.91	47.2	5.58
Ga	µg/g	25.6	0.86	29.8	0.97	39.1	1.08	34.0	1.08	36.0	1.06	20.3	0.79
As	µg/g	5.73	0.13	6.86	0.15	13.8	0.20	11.3	0.20	9.18	0.17	1.70	0.07
Rb	µg/g	138	8.38	163	10.7	164	11.2	146	11.4	162	11.1	58.4	6.09
Sb	µg/g	0.44	0.02	0.48	0.02	0.40	0.02	0.65	0.03	0.61	0.02	0.13	0.01
Cs	µg/g	7.42	0.24	8.76	0.31	12.7	0.41	11.7	0.44	10.9	0.38	2.45	0.16
Ba	µg/g	447	38.1	679	58.8	483	48.7	509	56.4	499	49.9	624	59.9
La	µg/g	45.6	0.50	43.9	0.50	46.4	0.49	48.3	0.53	47.3	0.50	30.8	0.39
Ce	µg/g	85.0	1.72	75.0	1.89	76.5	2.00	86.2	2.44	89.2	2.20	52.7	1.70
Sm	µg/g	7.59	0.03	6.68	0.03	7.81	0.03	6.88	0.03	6.97	0.03	4.45	0.02
Eu	µg/g	1.52	0.12	1.24	0.13	1.79	0.16	1.23	0.15	1.48	0.15	0.95	0.12
Dy	µg/g	5.92	0.21	5.13	0.19	5.86	0.21	5.07	0.20	4.74	0.19	3.10	0.15
Yb	µg/g	2.66	0.12	3.02	0.15	2.54	0.15	2.59	0.17	2.34	0.14	1.35	0.11
Hf	µg/g	7.81	0.31	7.00	0.32	4.52	0.25	5.05	0.31	5.45	0.29	3.57	0.23
Ta	µg/g	1.78	0.15	0.00	0.00	1.29	0.15	0.00	0.00	1.39	0.16	0.00	0.00
W	µg/g	2.57	0.15	2.60	0.15	2.87	0.16	2.47	0.15	2.57	0.15	0.00	0.00
Th	µg/g	15.7	0.28	16.1	0.34	16.0	0.35	19.2	0.44	16.2	0.35	9.02	0.26
U	µg/g	2.46	0.09	2.31	0.09	2.93	0.10	3.88	0.13	2.88	0.10	1.32	0.07

Continued

Table 7.8: EA in GWC Samples of FGF, Bangladesh (cont.)

Element	Unit	CF-7	±	CF-8	±	Mean (n=8)	SD (1σ)	RSD (%)	Median	Max	Min	UCC[a]	World Soil Median[b]	Shale[b]
Na	%	0.99	0.02	1.06	0.00	1.05	0.12	11.4	1.03	1.31	0.90	2.43	0.5	0.6
Al	%	9.25	0.06	7.51	0.05	7.88	1.31	16.7	7.92	9.43	5.30	8.15	7.1	8.8
K	%	2.13	0.11	1.96	0.10	2.10	0.31	14.9	2.16	2.35	1.39	2.32	1.4	2.45
Ca	%	0.00	0.00	1.55	0.33	0.88	1.31	148	0.00	3.30	0.00	2.6	1.5	1.6
Sc	µg/g	18.2	0.18	13.0	0.16	15.1	3.37	22.3	15.5	18.3	8.51	14	7	13
Ti	%	0.49	0.03	0.43	0.03	0.47	0.12	24.5	0.48	0.60	0.23	0.38	0.5	0.46
V	µg/g	127	4.12	83.9	3.42	103	27.8	27.0	104	144	55.7	97	90	130
Cr	µg/g	136	4.56	84.6	3.46	110	29.1	26.5	116	136	53.4	92	70	90
Mn	µg/g	514	14.4	937	24.8	534	170	31.9	486	937	423	775	1000	850
Fe	%	4.87	0.09	3.63	0.08	4.14	0.82	19.8	4.22	4.91	2.55	3.92	4	4.8
Co	µg/g	19.1	0.72	13.4	0.63	15.5	3.31	21.4	15.5	19.5	9.32	17.3	8	19
Zn	µg/g	103	8.11	46.5	5.00	74.2	21.1	28.5	72.4	103	46.5	67	90	120
Ga	µg/g	36.8	1.08	23.5	0.88	30.6	6.89	22.5	31.9	39.1	20.3	17.5	20	23
As	µg/g	10.3	0.17	12.1	0.20	8.87	3.92	44.2	9.74	13.8	1.70	4.8	6	13
Rb	µg/g	155	11.1	117	9.14	138	35.9	26.0	151	164	58.4	84	150	160
Sb	µg/g	0.41	0.02	0.60	0.02	0.46	0.17	35.8	0.46	0.65	0.13	0.4	1	1.5
Cs	µg/g	10.8	0.37	7.49	0.30	9.04	3.29	36.4	9.80	12.7	2.45	4.9	4	5.5
Ba	µg/g	681	64.9	232	14.4	519	147	28.4	504	681	232	624	500	550
La	µg/g	46.0	0.49	35.9	0.44	43.0	6.26	14.5	45.8	48.3	30.8	31	40	49
Ce	µg/g	81.9	2.11	56.0	1.73	75.3	13.8	18.3	79.2	89.2	52.7	63	50	96
Sm	µg/g	7.10	0.03	6.04	0.03	6.69	1.05	15.8	6.92	7.81	4.45	4.7	4.5	7
Eu	µg/g	1.34	0.13	1.21	0.13	1.35	0.25	18.9	1.29	1.79	0.95	1	1	1.2
Dy	µg/g	5.56	0.21	5.28	0.21	5.08	0.90	17.6	5.21	5.92	3.10	3.9	5	5.8
Yb	µg/g	1.63	0.12	2.45	0.15	2.32	0.56	24.0	2.49	3.02	1.35	2	3	3.9
Hf	µg/g	6.73	0.33	4.10	0.25	5.53	1.51	27.3	5.25	7.81	3.57	5.3	6	2.8
Ta	µg/g	1.28	0.15	1.14	0.14	0.86	0.73	85.5	1.21	1.78	0.00	0.9	2	2
W	µg/g	2.68	0.14	1.86	0.12	2.20	0.94	42.5	2.57	2.87	0.00	1.9	1.5	1.9
Th	µg/g	17.2	0.37	12.5	0.31	15.2	3.11	20.4	16.1	19.2	9.02	10.5	9	12
U	µg/g	2.78	0.10	1.97	0.08	2.57	0.75	29.4	2.62	3.88	1.32	2.7	2	3.7

[a] [2]; [b] [3].

7.8.2 EF of EA of GWC Samples of FGF

Base-line data selection is important to assess the EA of GWC samples (shale and sand) using different indices like I_{geo} and EF. In this work, the EA of UCC [7.2] has been nominated as the base-line data. Fe has been used in this work to calculate EF as Fe naturally has almost uniform concentrations and also displays alike to many trace elements' geochemistry [7.6-7.8].

To study the mobilization (due to weathering and depositional environmental condition at different stages) of EA with the crustal origin, EF for each EA in different GWC samples have been measured and are graphically presented in Fig. 7.22.

The EF values of the As ranges from 0.55 to 2.72 i.e. the enrichment of As are minor in GWC samples of this GF. Similar trend is obtained for Cs (EF range: 0.77 to 2.06) most of which are minorly enriched in GWC samples of GRW. Also rare earth lanthanide metals like La, Ce, Sm, Eu and Dy show enrichment.

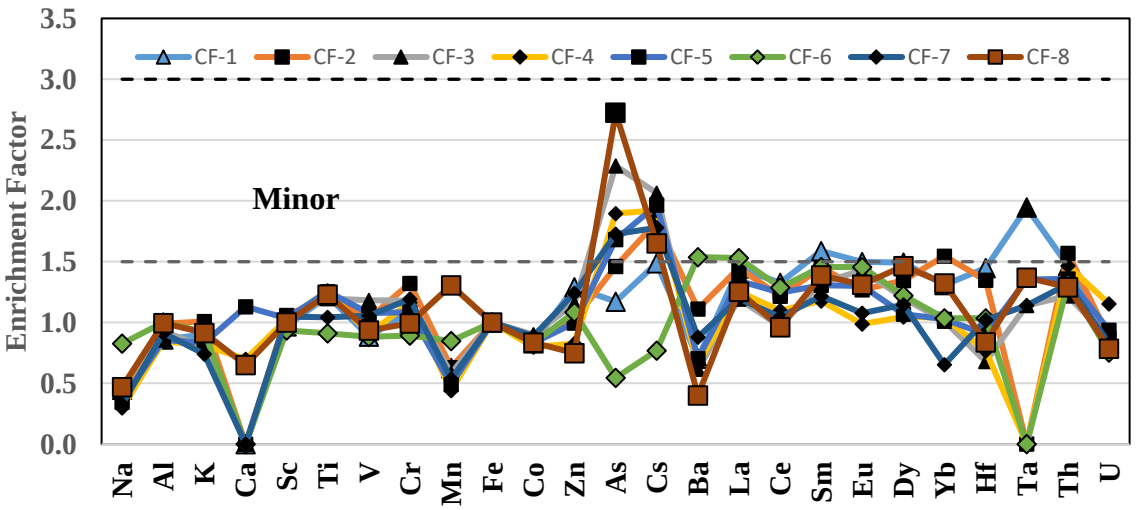

Figure 7.23: Plotted EF relative to UCC and Fe of the individual EA in the GWC samples of FGF.

7.8.3 I_{geo} of EA of GWC Samples of FGF

Depending on the choice of base-line data i.e. background levels, I_{geo} values exhibite huge variations. In this work, EA of UCC [7.2] have been nominated as the base-line data to calculate I_{geo}.

The graphical representation of I_{geo} of EA of FGF GWC samples have been shown in Fig. 7.24.

Based on [7.10] classification, graphical representation of I_{geo} shown in Fig. 7.24 revealed As and Cs are on the way to moderate geo-accumulation, I_{geo} in most of the GWC samples of FGF. In this GF ES, I_{geo} values present moderate to heavy geo-accumulation of As. So, there is a possibility of environmental S&S samples to be polluted more by As from GAA. The Max. I_{geo} value of Cs is 0.76 in GWC samples.

According to Fig. 8.3, comparatively lower values of almost all the elemental I_{geo} values are found in GWC sample ID: CF-6, where also RC levels of NR3 are found lower. In this GWC sample namely CF-6, elemental I_{geo} value of As is also found lowest in this sample relative to other GWC samples of FGF.

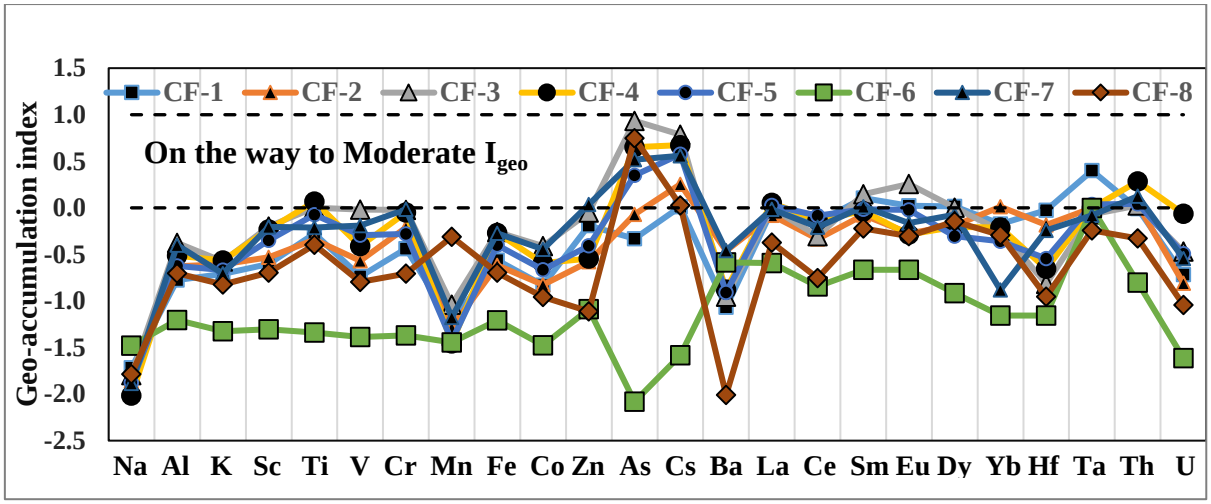

Figure 7.24: I_{geo} of EA of GWC samples of FGF.

7.8.4 EA Normalized to UCC of GWC Samples of FGF

The graphical representation of EA Normalized to UCC of GWC Samples of FGF have been shown in Fig. 7.25.

Graphical presentation of normalized data of GWC samples reveal moderate enrichment of the values of As and Cs relatived to UCC, where Max. values are 2.87 and 2.59 respectively. So, there is a possibility of environmental S&S samples to be polluted by As and Cs from GAA.

EA of most of the GWC samples are moderately enriched compare to UCC except Na, Ca, Mn, Ba and Ta.

According to Fig. 8.4, comparatively lower values of almost all the normalized elemental values are found in GWC sample ID: CF-6, where also RC levels of NR3 are found lower. In this GWC sample namely CF-6, elemental value of As normalized to UCC is also found lowest in this sample relative to other GWC samples of FGF.

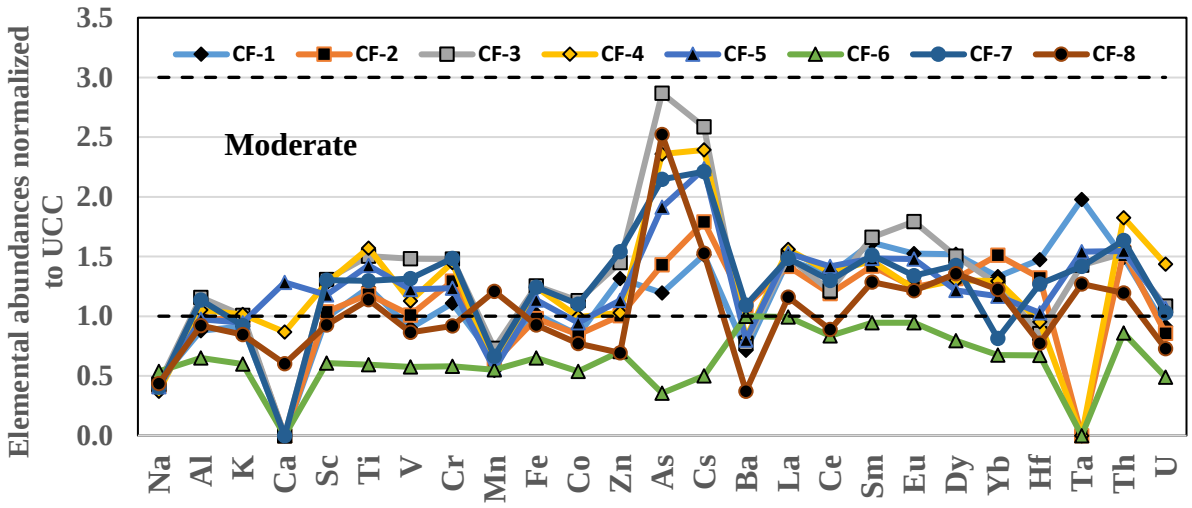

Figure 7.25: UCC normalized EA of GWC samples of FGF.

7.9.1 Inter-Comparison of EA of GWC Samples of the Three Gas Fields

Inter-Comparison of EA of GWC samples of GRW of the three GF namely Sbz GF**,** SGF and FGF of Bangladesh have been shown in Table 7.9. A total of 25 major, trace and REE elemental (Na, Al, K, Sc, Ti, V, Cr, Mn, Fe, Co, Zn, As, Rb, Cs, Ba, La, Ce, Sm, Eu, Dy, Yb, Hf, Ta, Th and U) abundances in GWC samples of these three GF have been presented with Max. values, Min. values, mean abundances (n=11), median value, relative standard deviations (RSD) and standard deviations (SD) along with the relative literature data of respective elements are also shown in Table 7.9.

Inter-comparison of EF, I_{geo} and UCC normalized EA in GWC samples of these three GF have been have been presented graphically in Fig. 7.26. Here SB

Sbz GF presents Shahbazpur gas field, SGF presents Saldanadi gas field and FGF presents Fenchuganj gas field respectively.

7.9.2 Inter-Comparison of (a) EF of EA in GWC Samples of Three Gas Fields (GF)

EF of all EA are comparable for these three GF. For three GF, As and Cs have comparatively higher enrichment than other EA in GWC samples. The EF values of the As ranges from 1.75 to 2.04 i.e. the enrichment of As are minor in GWC samples of these GF. The EF values of Cs from 1.68 to 1.94 which are minorly enriched GWC samples of these three GF. Also rare earth lanthanide metals like La, Ce, Sm, Eu, Dy and Yb show enrichment in these GF.

Table 7.9: Inter-comparison of EA in GWC samples of the three gas fields (GF), Bangladesh.

Element	Unit	**Shahbazpur**				**Saldanadi**				**Fenchuganj**				UCC[a]	World Soil Median[b]	Shale[b]
		Avg.	RSD (%)	Max.	Min.	Avg.	RSD (%)	Max.	Min.	Avg.	RSD (%)	Max.	Min.			
Na	[%]	1.15	1.14	1.39	0.97	1.06	1.03	1.21	0.98	1.05	11.4	1.31	0.90	2.43	0.5	0.6
Al	[%]	9.23	9.53	11.0	6.59	9.47	9.97	10.5	8.01	7.88	16.7	9.43	5.30	8.15	7.1	8.8
K	[%]	2.83	2.79	3.42	2.18	2.37	2.38	2.96	1.83	2.10	14.9	2.35	1.39	2.32	1.4	2.45
Sc	[µg/g]	15.6	16.2	20.7	9.40	14.0	14.1	17.2	11.4	15.1	22.3	18.3	8.51	14	7	13
Ti	[%]	0.48	0.49	0.62	0.38	0.48	0.46	0.62	0.41	0.47	24.5	0.60	0.23	0.38	0.5	0.46
V	[µg/g]	127	136	161	65.3	125	128	145	99.5	103	27.0	144	55.7	97	90	130
Cr	[µg/g]	103	100	137	56.4	99.5	98.8	115	79.0	110	26.5	136	53.4	92	70	90
Mn	[µg/g]	525	517	692	378	690	750	900	473	534	31.9	937	423	775	1000	850
Fe	[%]	4.52	4.70	5.61	3.11	4.25	4.03	4.71	3.86	4.14	19.8	4.91	2.55	3.92	4	4.8
Co	[µg/g]	19.5	19.6	27.2	12.4	18.1	16.2	25.9	15.0	15.5	21.4	19.5	9.32	17.3	8	19
Zn	[µg/g]	105	104	140	59.8	94.7	91.2	113	81.1	74.2	28.5	103	46.5	67	90	120
As	[µg/g]	11.6	9.67	20.7	0.00	10.6	9.30	24.1	5.26	8.87	44.2	13.8	1.70	4.8	6	13
Rb	[µg/g]	161	157	209	98.0	141	148	173	115	138	26.0	164	58.4	84	150	160
Cs	[µg/g]	11.0	10.6	18.4	4.75	8.94	9.04	12.5	5.73	9.04	36.4	12.7	2.45	4.9	4	5.5
Ba	[µg/g]	898	636	1847	393	431	429	483	372	519	28.4	681	232	624	500	550
La	[µg/g]	45.1	48.0	52.5	25.5	43.9	44.6	48.7	33.2	43.0	14.5	48.3	30.8	31	40	49
Ce	[µg/g]	84.3	88.6	98.8	51.4	85.6	88.8	96.6	63.5	75.3	18.3	89.2	52.7	63	50	96
Sm	[µg/g]	7.74	8.18	8.69	4.58	7.45	7.66	8.29	5.97	6.69	15.8	7.81	4.45	4.7	4.5	7
Eu	[µg/g]	1.66	1.73	1.91	1.15	1.62	1.65	1.80	1.38	1.35	18.9	1.79	0.95	1	1	1.2
Dy	[µg/g]	5.79	6.10	6.43	3.94	6.72	6.63	7.83	5.93	5.08	17.6	5.92	3.10	3.9	5	5.8
Yb	[µg/g]	2.80	2.70	3.33	2.16	3.00	3.01	3.80	2.25	2.32	24.0	3.02	1.35	2	3	3.9
Hf	[µg/g]	5.86	5.87	7.55	3.72	6.86	6.51	8.74	5.76	5.53	27.3	7.81	3.57	5.3	6	2.8
Ta	[µg/g]	1.38	1.44	1.74	0.72	1.29	1.36	1.47	0.88	0.86	85.5	1.78	0.00	0.9	2	2
Th	[µg/g]	18.9	20.6	22.2	11.6	18.1	18.4	20.2	13.0	15.2	20.4	19.2	9.02	10.5	9	12
U	[µg/g]	3.04	3.25	3.58	1.76	2.42	2.32	3.17	1.47	2.57	29.4	3.88	1.32	2.7	2	3.7

[a] [2]; [b] [3].

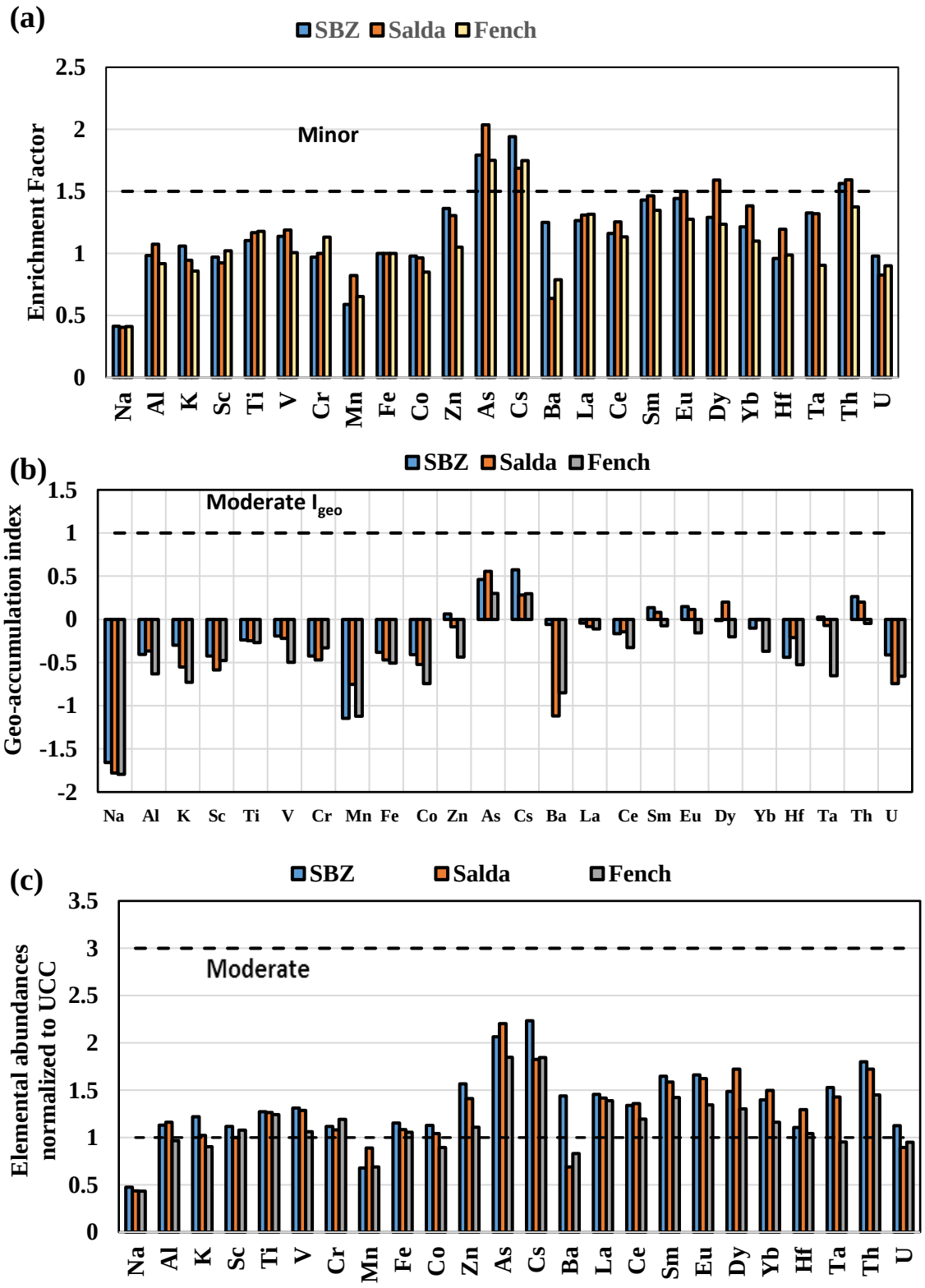

Figure 7.26: Inter-comparison of (a) EF, (b) I_{geo} and (c) UCC normalized data of EA in GWC samples of Sbz GF, SGF and FGF.

7.9.3 Inter-Comparison of (b) I_{geo} of EA in GWC Samples of Three Gas Fields (GF)

From graph (b) of Fig. 7.26, nearly similar trend is obtained for I_{geo} of Sbz GF, SGF and FGF where only As and Cs geo-accumulation are observed in these three GF. Slightly positive I_{geo} of Sm, Eu and Th are obserbed in two GF except FGF.

7.9.4 Inter-Comparison of (c) UCC Normalized EA in GWC Samples of Three GF

According to graph (c) of Fig. 7.26, comparatively lower values of almost all the normalized elemental values are found in core sample of FGF, where also RC levels of NR3 are found lower. In this GF core sample, Avg. elemental value normalized to UCC of As is also found lowest in this GF relative to other GWC samples of other two GF. EA of most of the GWC samples are moderately enriched compare to UCC except Na and Mn for the three GF namely Sbz GF, SGF and FGF of Bangladesh. Graphical presentation of normalized data of GWC samples reveal moderate enrichment of the values of As and Cs relative to UCC and comparatively higher than other elemental data for all three GF, where Max. values are 2.20 and 2.24 respectively. So, there is a possibility of environmental S&S samples to be polluted by As and Cs from GAA of these three GF.

7.10 The Major Constituent Minerals of Core Samples of Three Gas Fields by X-Ray diffraction (XRD) System

The XRD analytical technique is used for chemical composition information of all GWC samples along with some GWC samples have been analyzed using Energy Dispersive X-ray (EDX) examination to get an idea about the EA concentration, which are shown in table 7.10.1 and 7.10.3. According to table 7.10.2, XRD analysis of the GWC samples confirms the existence of quartz, muscovite, zircon, kyanite among the major constituent minerals.

Table 7.10.1: GWC sample (ID: CB-2.2) of Sbz gas field have been analyzed using EDX to get an idea about the EA concentration.

Element	Net Counts	Weight%	Atom%	Atom% Error
C	1329	11.44	21.17	± 0.62
O	5559	32.52	45.17	± 0.67
Na	215	0.79	0.76	± 0.09
Al	5564	11.93	9.83	± 0.19
Si	6302	13.94	11.03	± 0.18
K	751	2.00	1.14	± 0.05
Fe	3938	27.38	10.90	± 0.45
Total		100	100	

Table-7.10.2: Mineral identification of 22 GWC samples of gas wells of petroleum bearing zone from 3 different gas fields using XRD

SI. No	Name of Gas Field & Well No.	Core No.	Sample No	Depth (m)	Sample Type	Compound Name	Chemical Formula
1	Shahbazpur-2	C-1	CB-1.1	2591-91.8	Shale	Quartz	$Si\ O_2$
2	Shahbazpur-2	C-1	CB-1.2	2591.8-92	Shale	Quartz	$Si\ O_2$
3	Shahbazpur-2	C-1	CB-1.3	2592-93	Shale	Quartz	$Si\ O_2$
4	Shahbazpur-2	C-2	CB-1.4	3263-64	Shale	Quartz	$Si\ O_2$
5	Shahbazpur-4	C-1	CB-2.1	2929-30	Sand	Quartz	$Si\ O_2$
6	Shahbazpur-4	C-2	CB-2.2	3420-21	Sand	Quartz	$Si\ O_2$
7	Shahbazpur-4	C-3	CB-2.3	3698-99	Shale	Quartz, Zirconium Oxide	$Si\ O_2$, $Zr\ O_2$
8	Saldanadi-1	C-1	CS-1	1279-80	Shale	Quartz	$Si\ O_2$
9	Saldanadi-1	C-2	CS-2	1570-71	Shale	Quartz	$Si\ O_2$
10	Saldanadi-1	C-3	CS-3	1774-75	Shale	Quartz	$Si\ O_2$
11	Saldanadi-1	C-4	CS-4	2096-97	Shale	Quartz	$Si\ O_2$
12	Saldanadi-1	C-5	CS-5	2311-12	Fine Sand	Quartz, Graphite nitrate	$Si\ O_2$, C
13	Saldanadi-1	C-5	CS-7	2316-17	Shale	Quartz	$Si\ O_2$
14	Saldanadi-1	C-5	CS-6	2313-14	Fine Sand	Quartz	$Si\ O_2$
15	Fenchuganj-2	C-4	CF-1	2194-95	Shale	Quartz, Zirconium Oxide	$Si\ O_2$, $Zr\ O_2$
16	Fenchuganj-2	C-7	CF-2	3141-42	Shale	Quartz, Kyanite	$Si\ O_2$, $Al_2\ (\ Si\ O_4\ )\ O$
17	Fenchuganj-2	C-8	CF-3	3259-60	Shale	Quartz, Muscovite	$Si\ O_2$, $KAl_2(AlSi_3O_{10})(OH)_2$
18	Fenchuganj-2	C-8	CF-4	3263-64	Shale	Quartz, Muscovite	$Si\ O_2$, $KAl_2(AlSi_3O_{10})(OH)_2$
19	Fenchuganj-2	C-8	CF-5	3267-68	Shale	Quartz, Kyanite	$Si\ O_2$, $Al_2\ Si\ O_5$
20	Fenchuganj-2	C-10	CF-6	3624-25	Sand	Quartz Kyanite	$Si\ O_2$, $Al_2\ Si\ O_5$
21	Fenchuganj-2	C-11	CF-7	3770-71	Shale	Quartz, Kyanite	$Si\ O_2$, $Al_2\ Si\ O_5$
22	Fenchuganj-2	C-12	CF-8	4090-91	Shale	Quartz, Muscovite	$Si\ O_2$, $KAl_2(AlSi_3O_{10})(OH)_2$

Table 7.10.1: GWC sample (ID: CF-8) of FGF have been analyzed using EDX to get an idea about the EA concentration.

Element	Net Counts	Weight%	Atom%	Atom% Error
C	4997	1.38	3.23	± 0.05
O	167128	27.51	48.45	± 0.27
Na	4938	0.69	0.85	± 0.02
Al	109453	8.37	8.74	± 0.05
Si	178248	13.19	13.23	± 0.06
K	35575	3.02	2.18	± 0.03
Ca	9462	0.87	0.61	± 0.01
Mn	9633	2.00	1.03	± 0.05
Fe	194457	42.98	21.69	± 0.10
Total		100	100	

Chapter-8

Results and Discussion on Radiological Characterization

8 Radioactivity Concentrations (RC)

Table 5.1 presents the information of the gas field environmental (GFEv) samples and Table 5.2 shows the information of the gas well core (GWC) samples of the Sbz GF. In this way, Table 5.3 and Table 5.5 present the information of the GFEv samples and again Table 5.4 and Table 5.6 show the information of the GWC samples of the Saldanadi gas field (SGF) and Fenchuganj gas field (FGF) respectively. According to Table 6.3, the determined RC of ^{226}Ra, ^{232}Th and ^{40}K (NR3) in reference standard soil samples: IAEA-375 and IAEA-Soil-6 of this study have been in a decent agreement with the certified testified RC of the corresponding NR3.

8.1 RC of Shahbazpur (Sbz) Gas Field (GF)

8.1.1 Gas Well Core (GWC) Samples of GRW-2 & 4 of Sbz GF

The RC of NR3 of seven GWC samples from GRW-2 & 4 with deepness difference from 2591m to 3699m of Sbz GF of Bangladesh have been presented in Table 8.1. RC of ^{226}Ra in the GWC samples differ from 46.8±4.3 Bqkg^{-1} to 82.0±4.4 Bqkg^{-1}with an Avg. value of 60.2 Bqkg^{-1}, where Min. and Max. RC of ^{226}Ra are found in the GWC samples from same GRW (GRW-4) with changed GWC depth. The Min. ^{226}Ra RC-value 46.8±4.3 Bqkg^{-1} is found at 3420-3421m depth in sample CB-2.2 and the Max. value 82.0±4.4 Bqkg^{-1} is found at 2929-2930m depth in sample CB-2.1 i.e., greater radium RC is seen at lower depth of the similar GRW which is pointedly greater than the CWA value of 35 Bqkg^{-1} [8.1]. The Min. RC of ^{232}Th in the GWC samples is 75.3±3.9 Bqkg^{-1} at same GWC sample (CB-2.1) where ^{226}Ra value was also lowermost. Though, the Max. RC of ^{232}Th is 121.3±4.2 Bqkg^{-1} at different GRW (GRW-2, depth 2592-93m, CB-1.3), which is more than 4-times greater than the CWA value ([8.1]: 30 Bqkg^{-1}) for ^{232}Th. The Avg. value of ^{232}Th is 93.8±14.3 Bqkg^{-1}which is near about two times greater than the world Max. Avg. value of 50 Bqkg^{-1} for ^{232}Th. The Min. RC of ^{40}K is 1481±56 Bqkg^{-1} at same GWC sample where ^{226}Ra value is Max. (CB-2.1). The Max. RC of ^{40}K is 2756±85 Bqkg^{-1} which is found at depth 2592-93m in BoS (CB-1.3) of GWC-1 of GRW-2. The Avg. value of ^{40}K is 2194±392 Bqkg^{-1} which is more than five times greater than the CWA value of 400 Bqkg^{-1} for ^{40}K. Th/Ra ratio is comparable with each other of all GWC samples with an Avg. value 1.6 and is found slightly higher in GRW-2 than that of GRW- 4 of the Sbz GF. Low Th/U ratio shows favourable criteria for uranium mineralization and in this study lowest ratio is found 1.1 in sample CB-2.1 where Max. ^{226}Ra RC is found. Along with the existence of uranium (≈^{226}Ra) rich minerals (e.g., zircon), comparatively less oxic environment around the CB-2.1 empowerd the relatively higher ^{226}Ra abundance [8.3].

Table 8.1: RC in Bq kg^{-1} of NR3 of the gas well core (GWC) samples of Sbz GF.

Sample No.	^{226}Ra [Bqkg^{-1}]	^{232}Th [Bqkg^{-1}]	^{40}K [Bqkg^{-1}]	Th/Ra
CB-1.1	49 ± 4.0	89 ± 2.9	2136 ± 733	1.84
CB-1.2	60 ± 5.0	101 ± 3.7	2484 ± 69	1.69
CB-1.3	72 ± 5.1	121 ± 4.2	2756 ± 85	1.69
CB-1.4	50 ± 3.3	89 ± 2.4	2161 ± 45	1.78
CB-2.1	82 ± 4.4	92 ± 3.2	1481 ± 56	1.12
CB-2.2	47 ± 4.3	75 ± 3.9	2115 ± 60	1.61
CB-2.3	63 ± 4.4	88 ± 3.0	2228 ± 61	1.40
Average	60	94	2194	1.59
Min.	47	75	1481	1.12
Max.	82	121	2756	1.84
Word Avg.[a]	35	30	400	
UCC [b]	33	43	720	

[a][8.1],[b][8.2].

8.1.2: NORMs Distribution in S&S Samples of Sbz Gas Field (GF)

The RC values of the NR3 in the S&S samples with their corresponding SD are shown in Table 8.2. In the studied area, RC of ^{226}Ra varied from 26.3±3.6 to 55.0±4.8 Bqkg^{-1} with an Avg. value of 39.6±9.2 Bqkg^{-1}, where Min. and Max. RC of ^{226}Ra are obtained in the soil samples of same location at different depth (EB-4.1 and EB-4.2), which is 52m away from the RPSL and near the south side of the fresh water pond within the GFA. The Min. ^{226}Ra RC value of 26.3 ± 3.6 Bqkg^{-1} is obtained in 6″-8″ depth SubS sample from (EB-4.2) while the Max. value of 55.0 ± 4.8 Bqkg^{-1} is obtained at the (0 - 6″) SurS sample (EB-4.1) which is higher than the CWA value ([8.1]: 35 Bqkg^{-1}) for ^{226}Ra. Thus, higher radium activity is observed at SurS of same location may be due to the anthropogenic incorporation of ^{226}Ra from the GAA during rainy season. Overflowing of skimming pit and WDEvp pond during rainy season empowered the distribution of ^{226}Ra over a vast area IAGB. Moreover, wastes e.g., scale and sludge (Sc-Sl) from the GAA can also enrich the NORMs abundances in the ambient environment(AEv).

Table 8.2: Radioactivity concentration (RC) in Bq kg^{-1} of the naturally occurring radionuclides (NR3) in the GFEv S&S samples of Sbz gas field (GF)

Sample No.	^{226}Ra [Bqkg^{-1}]	^{232}Th [Bqkg^{-1}]	^{40}K [Bqkg^{-1}]	Th/Ra
EB-1	47 ± 5.21	78 ± 3.67	1005 ± 67	1.67
EB-2.1	45 ± 3.37	80 ± 2.66	798 ± 46	1.79
EB-2.2	34 ± 3.80	76 ± 3.85	788 ± 47	2.25
EB-3.1	53 ± 4.99	82 ± 3.51	1203 ± 62	1.55
EB-3.2	33 ± 5.41	75 ± 4.09	962 ± 70	2.26
EB-4.1	55 ± 4.77	76 ± 3.38	870 ± 86	1.39
EB-4.2	26 ± 3.61	71 ± 3.05	719 ± 56	2.68
EB-5	35 ± 3.83	73 ± 3.04	1029 ± 52	2.08
EB-6	30 ± 3.61	41 ± 2.56	610 ± 52	1.37
EB-7	38 ± 4.04	78 ± 4.38	650 ± 59	2.02
EB-8	40 ± 4.39	75 ± 3.28	970 ± 56	1.88
Average	40	73	873	1.90
Min.	26	41	610	1.37
Max.	55	82	1203	2.68
Literature data				
Word Avg.[a]	35	30	400	
UCC [b]	33	43	720	
SEB, Bangladesh [c]	18	46	321	
SB, Bangladesh[d]	42	81	833	
India[e]	37	69.6	396	

[a][8.1], [b][8.2], [c][8.4], [d][8.5], [e][8.6].

The Avg. RC of ^{232}Th is 73±11.1 Bqkg^{-1} and vary from 41.0±2.6 Bqkg^{-1} to 82±3.5 Bqkg^{-1}. The Min. RC of ^{232}Th is obtained in BoS sample (EB-6) from east side of WDEvp pond where chemical wastes are dumped. The Max. RC of ^{232}Th is obtained in SurS sample at the bank of the fresh water pond (EB-3.1), where many leafy vegetables grown at large scale and the location is near to many fruit trees. Along with, the Max. RC of ^{40}K (1203 ± 62 Bqkg^{-1}) is also obtained at the same SurS sample (EB-3.1). The Avg. value of RC of ^{40}K is 873±180 Bqkg^{-1} which vary from 610±52 Bqkg^{-1} to 1203±62 Bqkg^{-1}. Additionally, Avg. ^{226}Ra and ^{232}Th RC are about 1.5 times higher in GWC samples from GF compared to the samples from AEv, whereas Avg. ^{40}K RC is more than 2 times higher in GWC samples than the GFEv samples.

8.1.3 Redistributions of NORMs of Sbz Gas Field (GF)

Relatively lower RC of ^{40}K are found in EB-6 (610 ± 52 $Bqkg^{-1}$) and EB-7 (650 ± 59 $Bqkg^{-1}$). EB-7 is located in the vicinity of a local canal which is connected with the drainage system of the GF and is daily washed out by the coastal tide. Hence the sea-water is likely to be responsible in depleting the ^{40}K RC in EB-7. However, the SurS sample (near the local canal), EB-8 possesses higher ^{40}K RC compared to EB-6 and EB-7 which can be explained by the unavailability of tidal sea-water. Though the rain-water and over-flooded condition during rainy season may introduce anthropogenic NORMs to the local pedosphere.

It was predicted that comparatively higher RC would be found in the BoS samples of WDEvp pond, especially the eastern side where mud and brine (MB) chemicals are disposed (sample code: EB-6) and RC would be lower in soil samples from adjacent areas due to contamination from WDEvp pond. But after analysis the result has been found reversed i.e., lowest RC and values of all seven radiation hazard indices (RHI) found in sample EB-6 and highest values of all seven RHI found in sample EB-3.1. MB chemicals are dumped in north-east side of the WDEvp pond which seems to dilute the RM in those specific areas. Again, the location of sample EB-3.1 is near many fruit trees and at the bank of the fresh water pond. During maintenance work, the production equipment are used to clean by high-speed jet water, by which RM from Sc-Sl can be washed away and pass through the drain to nearby areas, skimming pit and WDEvp pond. These areas are generally over flooded during rainy season and results in the NORMs' spreading randomly in the areas where higher RC are found.

Furthermore, each and every SurS samples (0-6") have higher RC than SubS samples (6"-8"), which may be an evidence of radioactive contamination. Additionally, NORMs' concentrations in our studied area are comparatively higher than the previous literature works dealing with the similar geo-environmental samples in Bangladesh and India [8.1 - 8.2, 8.4 – 8.6] (Table 8.2), which is also invoking the NORMs' contamination. The ^{232}Th /^{226}Ra ratio for both the GFEv (1.90, Table 8.2) and GWC (1.59, Table 8.1) samples are significantly greater than one where the ^{232}Th /^{226}Ra ratio for GFEv samples are reletively higher compared to those of GWC samples. This enrichment of ^{232}Th (represented by ^{232}Th /^{226}Ra ratio >1) in the geological compartments can be explained by their geochemical provenance, e.g., dominance of felsic components, oxic depositional environment, tectonic setting, weathering etc [8.3, 8.7].

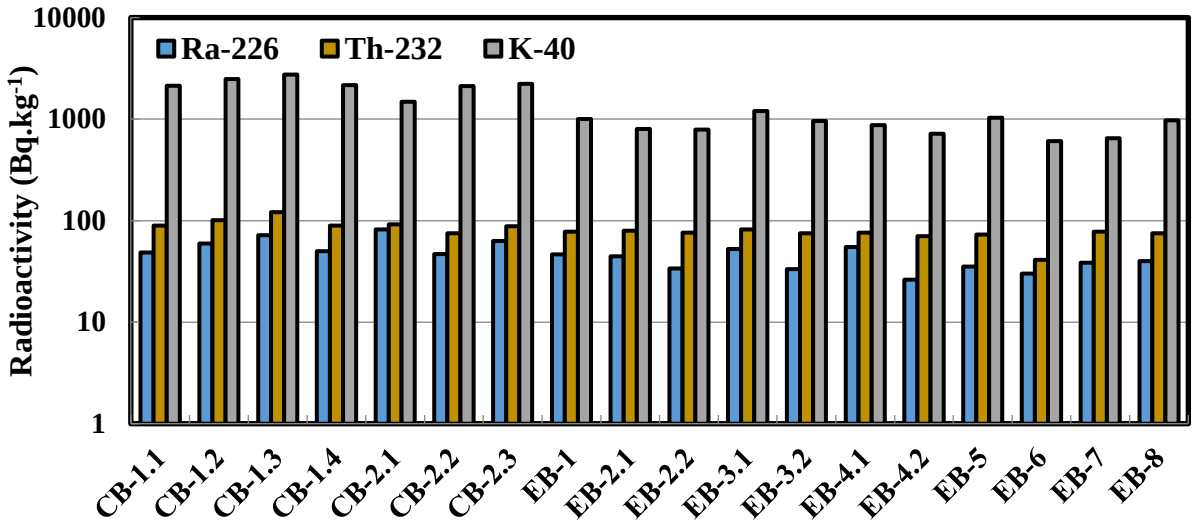

Figure 8.1: RC of NC-3 in the GFEv samples (EB-1 to EB-8) are compared with those of GWC samples (CB-1.1 to CB-2.3) of Sbz GF.

However, relatively higher ^{232}Th /^{226}Ra ratio for the GFEv samples are assumed to be governed by the geochemical mobility of ^{226}Ra through water leaching (due to higher solubility of ^{226}Ra in relatively higher oxic environment) [8.3]. Thus, relatively higher amounts of ^{232}Th and ^{226}Ra from GWC samples were introduced to the GFEv samples through GAA which were then lost it's (GFEv sample) incoming ^{226}Ra by water leaching.

8.1.4 **Radiological Risks Assessment of Sbz Gas Field**

Table 8.3 presents the values of seven RHI for GWC samples of the GF, whereas Table 8.4 show the RHI for S&S samples of Sbz GF. Additionally, Fig. 8.2 to Fig. 8.8 represents intercomparisons of RHI between the GWC samples and GFEv samples along with their corresponding recommended (CRec) values [8.1, 8.8 – 8.10].

8.1.4.1 Radium Equivalent Activity (Ra_{eq}) Assessment of Sbz Gas Field (GF).

The Ra_{eq} value for the GWC samples varied from 317 to 457 with a mean value (n=7) of 363±48.6 which is near to the CRec value 370. Only two GWC samples (CB-1.2 and CB-1.3) exceeded the CRec value. In both the well, deeper GWC samples likely to have higher Ra_{eq} value (Fig. 8.2). On the other hand, spatial variations of Ra_{eq} values are observed in the S&S samples of AEv (Avg. 211.5±32.5; range: 135.6-262.1) due to the anthropogenic and/or natural redistributions of NORMs. However, Ra_{eq} values for GFEv samples are significantly lower than those of GWC samples and CRec value.

Table 8.3 Radiation hazard indices (RHI) from the core (GWC) samples of well-2 & 4 of Sbz gas field and the corresponding recommended (CRec) values.

Sample No.	Ra_{eq}	H_{ex}	H_{in}	D	E_{ff}	I_{γ}	ELCR
	$[Bqkg^{-1}]$			$[\eta Gyh^{-1}]$	$[mSvy^{-1}]$		
CB-1.1	341	0.92	1.05	166	0.20	2.64	7.13×10^{-4}
CB-1.2	395	1.07	1.23	193	0.24	3.06	8.28×10^{-4}
CB-1.3	457	1.23	1.43	222	0.27	3.53	9.53×10^{-4}
CB-1.4	344	0.93	1.06	168	0.21	2.67	7.20×10^{-4}
CB-2.1	327	0.88	1.11	156	0.19	2.45	6.67×10^{-4}
CB-2.2	317	0.86	0.98	156	0.19	2.48	6.69×10^{-4}
CB-2.3	361	0.97	1.14	176	0.22	2.79	7.55×10^{-4}
Average	**363**	**0.98**	**1.14**	**177**	**0.22**	**2.80**	**7.58**$\times10^{-4}$
SD	49	0.10	0.10	24	0.00	0.40	1.02×10^{-4}
RSD	13	13.4	12.9	14	13.5	13.6	13.5
Median	344	0.90	1.10	168	0.20	2.70	7.20×10^{-4}
Max.	457	1.20	1.40	222	0.30	3.50	9.53×10^{-4}
Min.	317	0.90	1.00	156	0.20	2.50	6.67×10^{-4}
Recommended values [a]	370	<1	<1	55	0.46	1.00	2.90×10^{-4}

[a] [8.1, 8.8 – 8.10].

8.1.4.2. External and Internal Hazard Indices (H_{ex}) Assessment of Sbz Gas Field

According to Table 8.4, the mean value of H_{ex} is 0.57±0.10 with a range of 0.37 to 0.71, which are less than unity (i.e., under the criterion level) (Fig. 8.3). The values of the internal hazard index (H_{in}) ranged from 0.45 to 0.85 with a mean value of 0.68±0.10 (<1). Thus, in terms of H_{ex} and H_{in} indices, all S&S samples of Sbz GF are radiologically risk-less. On the other hand, the mean values of H_{ex} and H_{in} for the GWC samples are 0.98±0.10 (range: 0.9 to 1.2) and 1.14±0.10 (range: 1.0 to 1.4), respectively which invoke that GFEv samples, IAGB should be monitored routinely as the S&S samples can be contaminated by NORMs originated from GAA.

Table 8.4: Radiation hazard indices (RHI) of soil and sediment (S&S) samples of Sbz gas field environment and the corresponding recommended (CRec) values.

Sample No	Ra_{eq} [$Bqkg^{-1}$]	H_{ex}	H_{in}	D [ηGyh^{-1}]	E_{ff} [$mSvy^{-1}$]	I_γ	ELCR
EB-1	236	0.64	0.76	112	0.14	1.76	4.82×10^{-4}
EB-2.1	220	0.59	0.71	104	0.13	1.63	4.45×10^{-4}
EB-2.2	204	0.55	0.64	96	0.12	1.52	4.13×10^{-4}
EB-3.1	262	0.71	0.85	126	0.15	1.97	5.39×10^{-4}
EB-3.2	215	0.58	0.67	103	0.13	1.62	4.40×10^{-4}
EB-4.1	231	0.62	0.77	109	0.13	1.71	4.69×10^{-4}
EB-4.2	183	0.49	0.56	86	0.11	1.36	3.70×10^{-4}
EB-5	219	0.59	0.69	105	0.13	1.65	4.50×10^{-4}
EB-6	136	0.37	0.45	65	0.08	1.02	2.79×10^{-4}
EB-7	200	0.54	0.64	93	0.11	1.47	4.01×10^{-4}
EB-8	222	0.60	0.71	106	0.13	1.66	4.54×10^{-4}
Average	212	0.57	0.68	100	0.12	1.58	4.31×10^{-4}
Min.	136	0.37	0.45	65	0.08	1.02	2.79×10^{-4}
Max.	262	0.71	0.85	126	0.15	1.97	5.39×10^{-4}
Recommended values[a]	370.0	<1	<1	55	0.46	1.00	2.90×10^{-4}

[a] [8.1, 8.8-8.10].

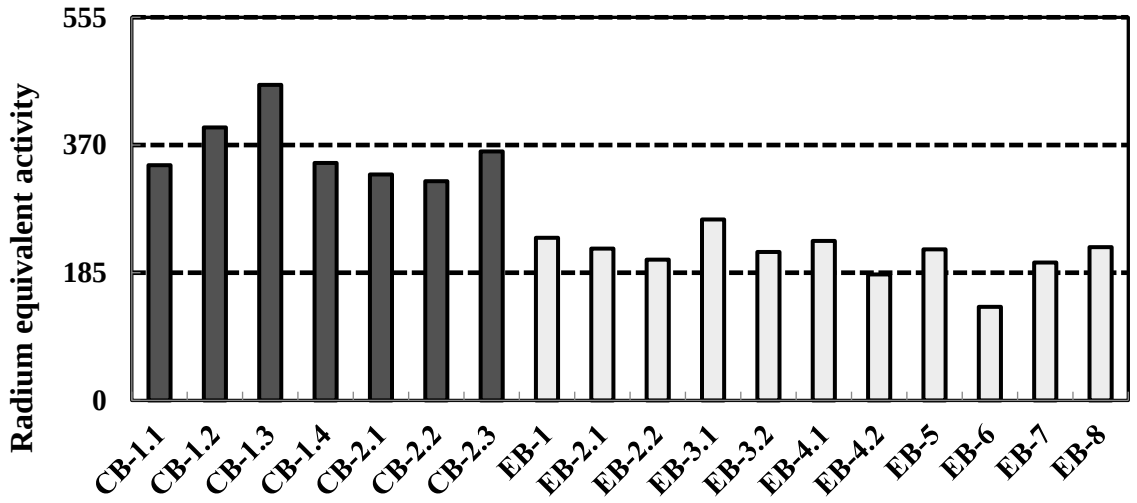

Figure 8.2: Variation of Ra_{eq} of AEv S&S samples are compared with the GWC shale & sand samples of GF.

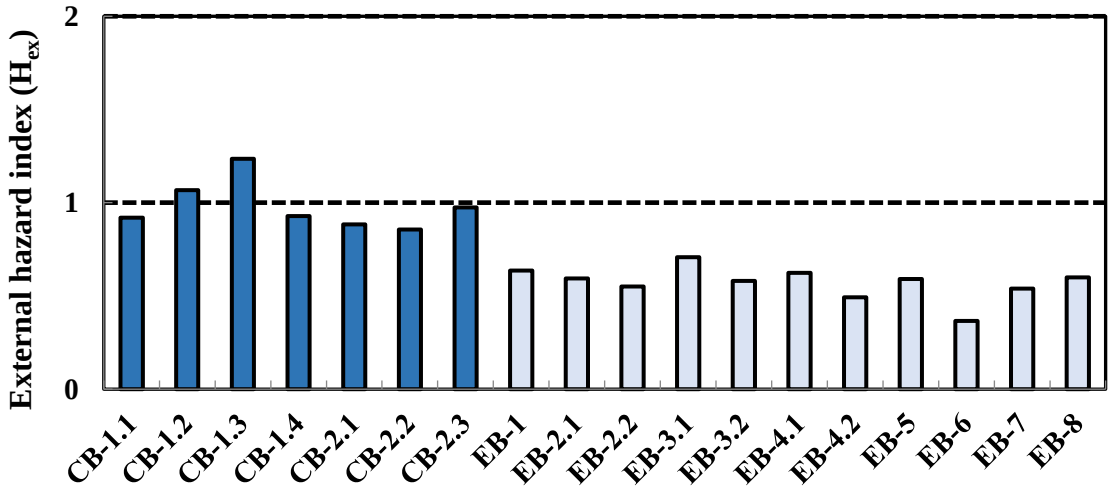

Figure 8.3: Variation of H_{ex} of AEv S&S samples are compared with the GWC shale & sand samples of GF.

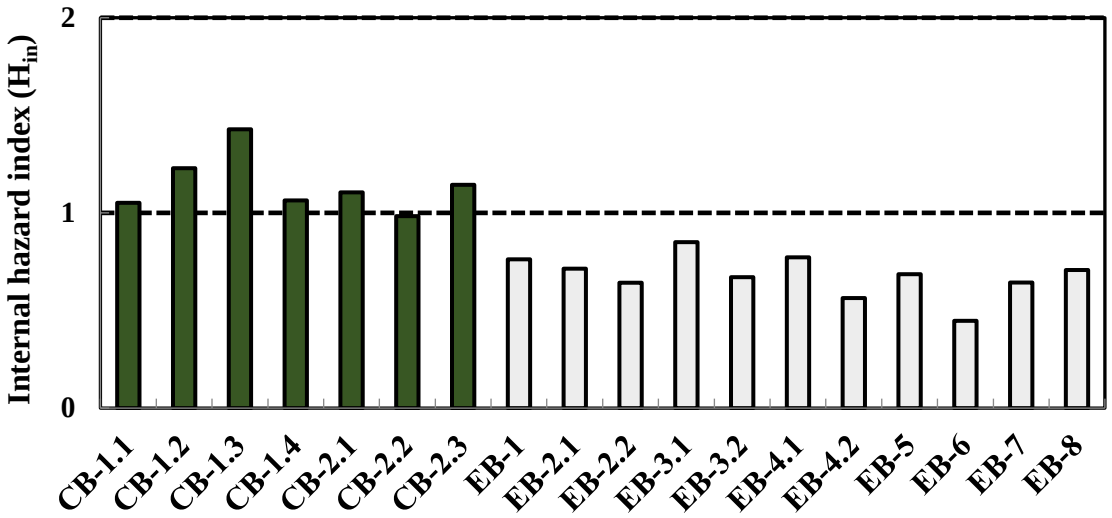

Figure 8.4: Variation of H_{in} of AEv S&S samples are compared with the GWC shale & sand samples of Sbz GF.

8.1.4.3. Absorbed Dose Rate (D) and Annual Effective Dose Rate (E_{ff}) Assessment of Sbz GF.

D for all the GWC samples are around three times higher from the CRec value 55 $nGyh^{-1}$ as shown in (Table 8.3, Fig. 8.5) which ranged from 157.1 to 224.2 $nGyh^{-1}$ with an Avg. of 178.2±24.0 $nGyh^{-1}$.

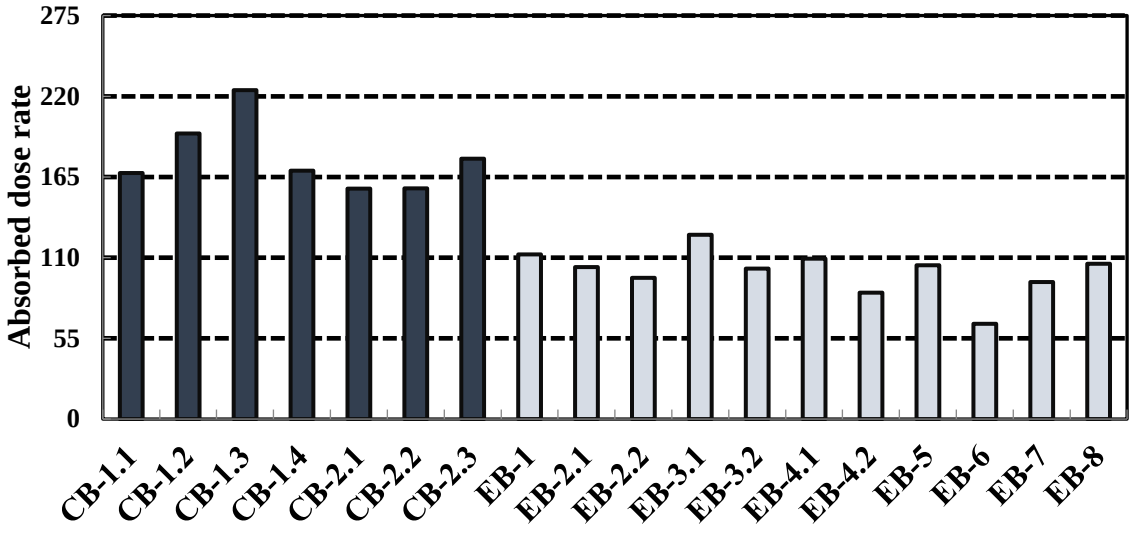

Figure 8.5: Variation of D in $nGyh^{-1}$ of the GFEv samples are compared with the GWC samples of Sbz GF, Bangladesh

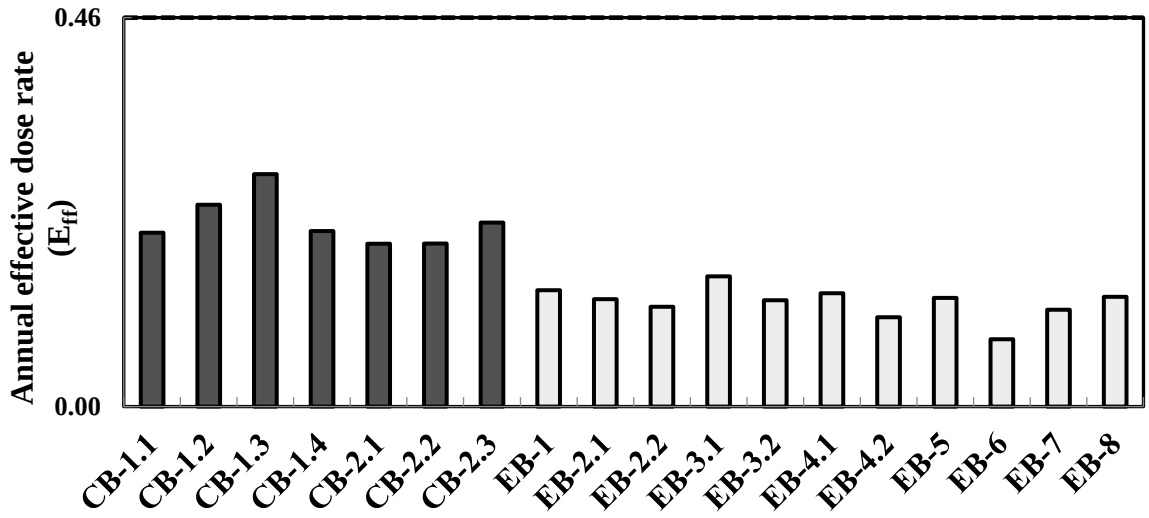

Figure 8.6: Variation of the E_{ff} in $mSv.y^{-1}$ of the GFEv samples are compared with the GWC samples of Sbz GF, Bangladesh.

However, D for samples both from BoS samples of WDEvp pond and soil samples far away from evaporation pond but linked through drainage system have nearly the same D which are around twice of the recommended value ($55nGyh^{-1}$). Following the NORMs distribution, SubS samples (EB-2.2, EB-3.2, EB-4.2) possess lower D compared to their corresponding SurS samples (EB-2.1, EB-3.1, EB-4.1). Avg. D-value for the samples is 99.2 ± 15.5 $nGyh^{-1}$ with a range of 64.2-124.2 $nGyh^{-1}$, where relatively lower values are observed for EB-6 and EB-7. On the other hand, the mean values of the E_{ff} are 0.22 $mSv.y^{-1}$ and 0.12 $mSv.y^{-1}$ for GWC samples and GFEv samples, respectively which are within the CRec value (0.46 $mSv.y^{-1}$).

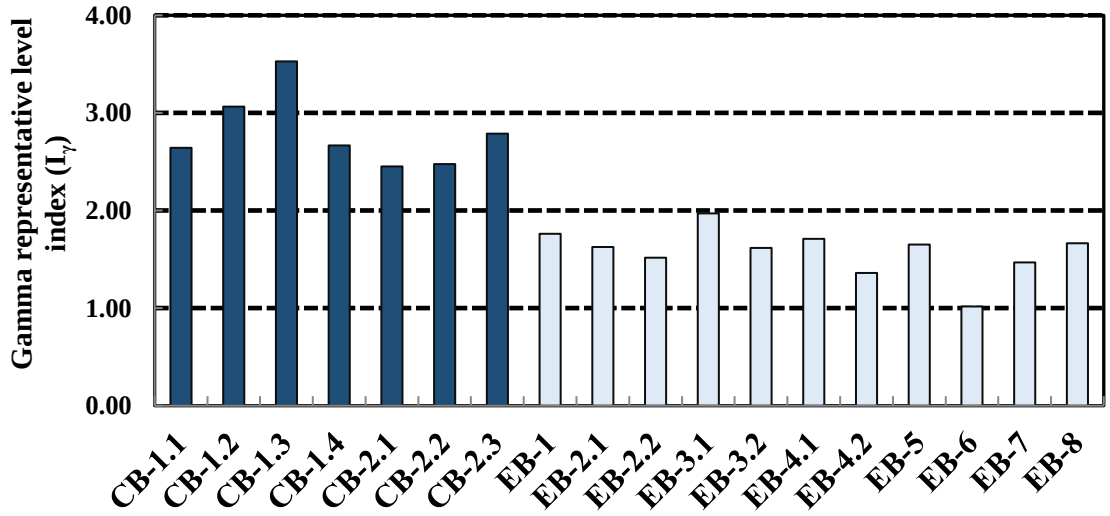

Figure 8.7: Variation of I_γ of the GFEv samples are compared with the GWC samples of Sbz GF, Bangladesh

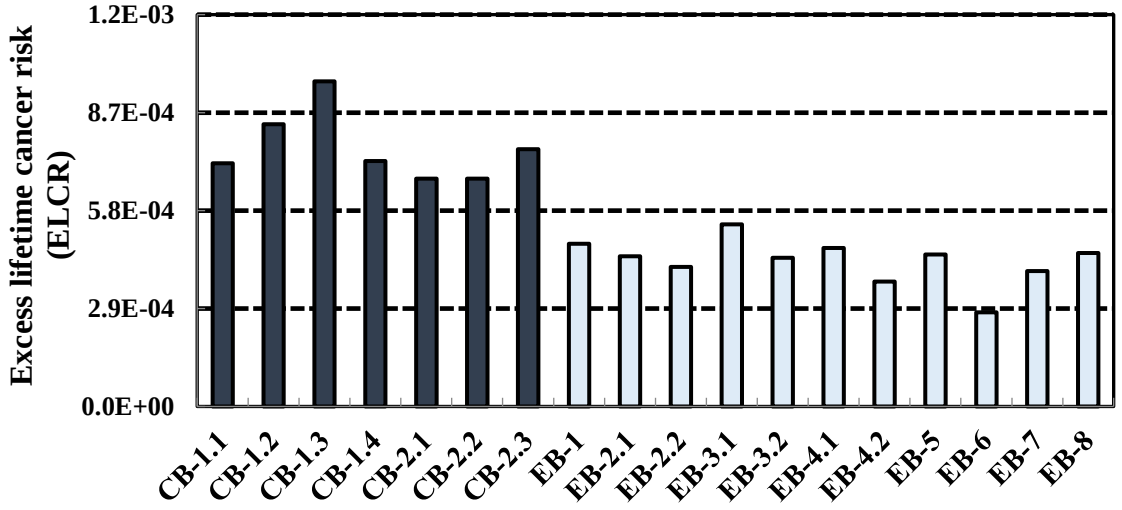

Figure 8.8: Variation of ELCR of the GFEv samples are compared with the GWC samples of Sbz GF, Bangladesh.

8.1.4.4 Gamma Representative Level Index (I_γ) Assessment of Sbz GF.

Concomitantly, for all GWC samples from well-2 & 4, values of I_γ are more than 2.5 to 3.5 times higher than that of CRec value (1.0) and are significantly higher than those in samples (Fig. 8.7). Although, GFEv S&S samples have I_γ value higher than CRec value.

8.1.4.5. Excess Lifetime Cancer Risk (ELCR) Assessment of Sbz gas field

ELCR in all samples (except for EB-6 and EB-7) are above the CRec value for ELCR with maximum value (in EB-3.1) nearly two times higher than CRec value (2.9×10^{-4} [8.6]) (Fig. 8.8). On the other hand, for all GWC samples of the GF from well-2 & 4, values of ELCR are more than 2 times higher of the CRec value (Table 8.3).

Day by day the waste increases in gas production field. The yearly PW deposition of Sbz GF is 27,53,244 liters along with producing more Sc-Sl. So, this is high time to be aware of preventing more contamination and taking necessary action against contamination from both R&C toxic elements. Due to the lack of knowledge and regular monitoring, industrial radioactive wastes (produced by G&O industries) are often disposed of as non-radioactive wastes which were beyond the IAEA (International Atomic Energy Agency) exemption limits [8.11]. Furthermore, there are many coconuts, date, mango trees and leafy vegetables with in the boundary of the GFA where comparatively higher RC levels along with excess values of three RHI (Fig. 8.5, 8.7 and 8.8) than CRec values have been found. Moreover, abundant grass grows in the areas of high RC, which are collected by the local inhabitants for their domestic animals. Thus, by consuming fruits,

vegetables, milk and meats, occupational workers and also public can indirectly be exposed to the radiation that may develop into cancer [8.12 – 8.13].

8.2 Radioactivity Concentration (RC) of Saldanadi Gas Field (SGF)

8.2.1. Gas Well Core (GWC) Samples of SGF

The RC of NR3 of seven GWC samples from well-1 with depth variation from 1279m to 2317m of SGF of Bangladesh have been presented in Table 8.5. RC of ^{226}Ra in the GWC samples ranged from 28.9 ± 3.5 Bqkg^{-1} to 76.7 ± 6.3 Bqkg^{-1}with an Avg. value of 55.3 Bqkg^{-1}, where Min and Max RC of ^{226}Ra are obtained in the same GWC samples of core-5 with only two meters depth variation. The Min ^{226}Ra RC value is obtained in fine sand sample at 2313-2314m depth in sample ID, CS-6 and the Max value is obtained in shale sample at 2316-2317m depth in sample CS-7, which is significantly higher than the CWA value of 35 Bqkg^{-1} [58]. The Min RC of ^{232}Th and ^{40}K in the studied GWC samples are 52.4 ± 2.7 Bqkg^{-1} and 824 ± 45 Bqkg^{-1} respectively at same GWC sample (CS-6) where ^{226}Ra value was also lowest. Again, the Max RC of ^{232}Th and ^{40}K with in these GWC samples are 119 ± 6.1 Bqkg^{-1} and 2864 ± 89 Bqkg^{-1} respectively at same GWC sample (CS-7) where ^{226}Ra value was also highest, which values are significantly higher than the CWA values [1] for ^{232}Th and ^{40}K respectively. The Avg. value of ^{232}Th is 91.7 Bqkg^{-1}which is more than three times higher than the CWA of 30 Bqkg^{-1} for ^{232}Th and the mean value of ^{40}K is 2039 Bqkg^{-1} which is more than five times higher than the CWA value of 400 Bqkg^{-1} for ^{40}K ([8.1]: 30 Bqkg^{-1} and 400 Bqkg^{-1} respectively). Th/Ra ratio is comparable with each other of all GWC samples of the SGF. According to lithological information, within seven GWC samples of SGF, only two are fine sand samples (ID: CS-5 and CS-6), where lowest RC of NR-3 have been found and all other samples are shale samples where comparatively higher RC of these all NR-3 have been found than fine sand samples.

Table 8.5 Radioactivity concentrations (in Bq kg^{-1}) of the naturally occurring radionuclides (NR-3) and Th/Ra ratio in the core (GWC) samples of Saldanadi gas field (SGF).

Sample No.	^{226}Ra	^{232}Th	^{40}K	Th/Ra
	[$Bqkg^{-1}$]	[$Bqkg^{-1}$]	[$Bqkg^{-1}$]	
CS-1	56.6 ± 4.3	96 ± 3.5	2248 ± 66	1.69
CS-2	56.5 ± 4.1	104 ± 3.2	2486 ± 58	1.84
CS-3	76.6 ± 5.6	119 ± 3.9	2612 ± 87	1.55
CS-4	53.8 ± 4.9	81 ± 4.8	2283 ± 84	1.51
CS-5	37.7 ± 3.9	71 ± 2.9	957 ± 47	1.90
CS-6	28.9 ± 3.5	52 ± 2.7	824 ± 45	1.81
CS-7	76.7 ± 6.3	119 ± 6.1	2864 ± 89	1.55
Average	55.3	92	2039	1.69
Min.	28.9	52	824	1.51
Max.	76.7	119	2864	1.90
Word Avg.[a]	35	30	400	
UCC [b]	33	43	720	

[a][8.1],[b][8.2].

8.2.2 NORMs Distribution in Surface Soil (SurS) Samples of Saldanadi Gas Field (SGF)

The RC of NR3 in the SurS samples of SGF with SD and the Th/Ra ratio are shown in Table 8.6. In the studied area, RC of ^{226}Ra varied from 18.6±3.5 to 42.1±4.6 $Bqkg^{-1}$ with a mean value of 29.6 $Bqkg^{-1}$ within the GFA. The Min ^{226}Ra RC value of 18.6±3.5 $Bqkg^{-1}$ is obtained in SurS sample of ID ES-1 while the Max value of 42.1±4.6 $Bqkg^{-1}$ is obtained at the SurS sample of ID ES-2 at north-east corner of WDEvp pond which is higher than the CWA value ([8.1]: 35 $Bqkg^{-1}$) for ^{226}Ra.

Table 8.6: Radioactivity concentration (Bq kg^{-1}) of the naturally occurring radionuclides and Th/Ra ratio in the environmental surface soil (SurS) samples of SGF.

Sample No.	^{226}Ra [Bqkg^{-1}]	^{232}Th [Bqkg^{-1}]	^{40}K [Bqkg^{-1}]	Th/Ra
ES-1	18.6 ± 3.5	51.5 ± 2.9	577 ± 51	2.77
ES-2	42.1 ± 4.6	80.2 ± 3.8	778 ± 65	1.90
ES-3	26.5 ± 4.2	58.0 ± 3.4	626 ± 59	2.18
ES-4	31.2 ± 3.9	83.4 ± 3.4	989 ± 58	2.67
Average	29.6	68.3	742	
Min.	18.6	51.5	577	
Max.	42.1	83.4	989	
Literature data				
Word Avg.[a]	35	30	400	
UCC [b]	33	43	720	
SEB, Bangladesh [c]	18	46	321	
SB, Bangladesh[d]	42	81	833	
India [e]	37	69.6	396	

[a][8.1], [b][8.2], [c][8.4], [d][8.5], [e][8.6].

The Avg RC of ^{232}Th is 68.3 Bqkg^{-1} and vary from 51.5±2.9 Bqkg^{-1} to 83.4±3.4 Bqkg^{-1}. The mean value of RC of ^{40}K is 742 Bqkg^{-1} which vary from 577±51 Bqkg^{-1} to 989±58 Bqkg^{-1}. Concomitantly, the Max RC of ^{40}K and ^{232}Th are found at the same SurS sample (ES-4) which location is far away from WDEvp pond. Additionally, Avg. ^{40}K and ^{232}Th RC are more than 1.5 times higher than the CWA values [8.1] for ^{40}K and ^{232}Th.

During rainy season, the rain-water and over-flooded condition may introduce anthropogenic NORMs to the local pedosphere of the GF.

Graphically the RC of NR3 in the ambient GFEv samples (ES-1 to ES-4) are compared with those of GWC samples (CS-1 to CS-7) of SGF have been presented in Fig. 8.9 for better understanding.

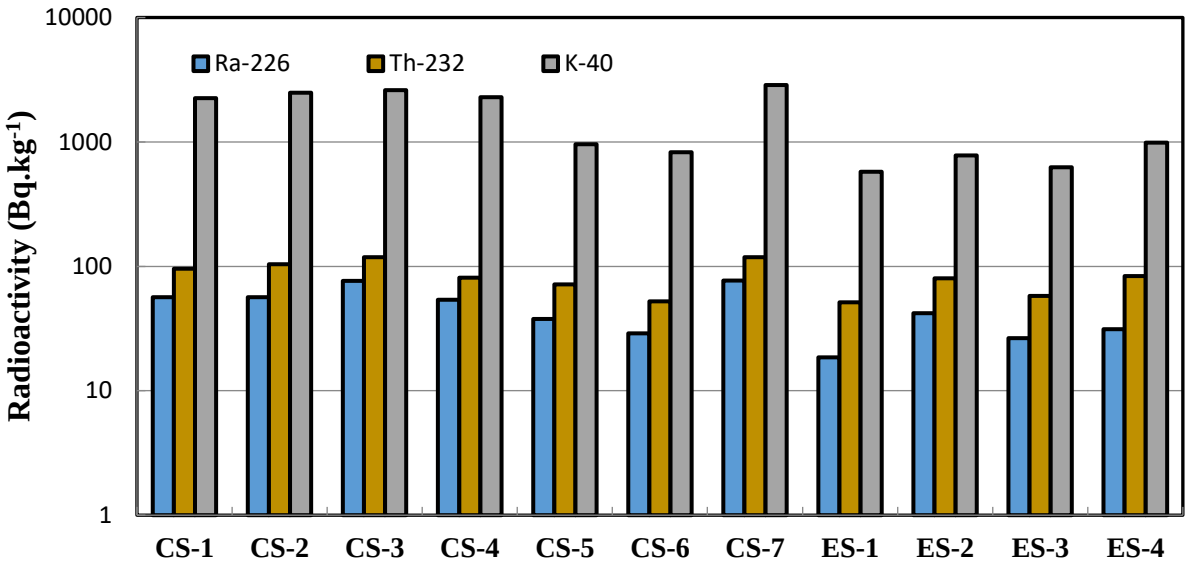

Figure 8.9: RC of ^{226}Ra, ^{232}Th and ^{40}K in the ambient ES (ES-1 to ES-4) are compared with those of GWC samples (CS-1 to CS-7) of SGF.

8.2.3 Radiological Risks Assessment of Saldanadi Gas Field (SGF)

Table 8.7 presents the values of seven RHI for GWC samples of the GF, whereas Table 8.8 show the RHI for soil samples of SGF. Additionally, Fig. 8.10 to Fig. 8.16 represent intercomparisons of RHI between the GWC samples and environmental (GFEv) samples along with their recommended values [8.1, 8.8 – 8.10].

Table 8.7: Radiation hazard indices (RHI) from the core (GWC) samples of Saldanadi gas field (SGF) and the corresponding recommended (CRec) values.

Sample No.	Ra_{eq}	H_{ex}	H_{in}	D	E_{ff}	I_{γ}	ELCR
	$[Bqkg^{-1}]$			$[\eta Gyh^{-1}]$	$[mSvy^{-1}]$		
CS-1	367	0.99	1.14	179	0.22	2.83	7.66×10^{-4}
CS-2	396	1.07	1.22	193	0.24	3.07	8.29×10^{-4}
CS-3	448	1.21	1.42	217	0.27	3.44	9.31×10^{-4}
CS-4	346	0.93	1.08	170	0.21	2.69	7.29×10^{-4}
CS-5	213	0.58	0.68	101	0.12	1.60	4.32×10^{-4}
CS-6	167	0.45	0.53	80	0.10	1.27	3.42×10^{-4}
CS-7	467	1.26	1.47	227	0.28	3.61	9.76×10^{-4}
Average	**343**	**0.93**	**1.08**	**167**	**0.20**	**2.64**	$\mathbf{7.15}\times10^{-4}$
SD	114	0.30	0.40	56	0.10	0.90	2.41×10^{-4}
RSD	33	33.1	32.9	34	33.8	33.7	33.8
Median	367	1.00	1.10	179	0.20	2.80	7.66×10^{-4}
Max.	467	1.26	1.47	227	0.28	3.61	9.76×10^{-4}
Min.	167	0.45	0.53	80	0.10	1.27	3.42×10^{-4}
Recommended values [a]	370	<1	<1	55	0.46	1.00	2.90×10^{-4}

[a] [8.1, 8.8 – 8.10].

Table 8.8: Radiation hazard indices (RHI) of SGF environmental (GFEv) soil samples and the CRec values.

Sample No	Ra_{eq} [$Bqkg^{-1}$]	H_{ex}	H_{in}	D [ηGyh^{-1}]	E_{ff} [$mSvy^{-1}$]	I_γ	ELCR
ES-1	137	0.37	0.42	65	0.08	1.02	2.78×10^{-4}
ES-2	217	0.59	0.70	102	0.13	1.60	4.38×10^{-4}
ES-3	158	0.43	0.50	75	0.09	1.17	3.20×10^{-4}
ES-4	227	0.61	0.70	108	0.13	1.70	4.63×10^{-4}
Average	**184**	**0.50**	**0.58**	**87**	**0.11**	**1.38**	$\mathbf{3.75}\times10^{-4}$
Min.	137	0.37	0.42	65	0.08	1.02	2.78×10^{-4}
Max.	227	0.61	0.70	108	0.13	1.70	4.63×10^{-4}
Recommended values [a]	370	<1	<1	55.0	0.46	1.00	2.90×10^{-4}

[a] [8.1, 8.8 – 8.10].

8.2.3.1 Radium Equivalent Activity (Ra_{eq}) Assessment of SGF

The Ra_{eq} value for the GWC samples varied from 167 $Bqkg^{-1}$ to 467 $Bqkg^{-1}$ with a mean value (n=7) of 343 $Bqkg^{-1}$ which is near to the CRec value of 370 $Bqkg^{-1}$. Only two GWC samples (CS-5 and CS-6) have significantly lower value than the CRec value but sample no. CS-5, CS-6 and CS-7 are from same GWC, where Max Ra_{eq} value found at CS-7. In different GWC samples likely to have comparable Ra_{eq} value rather than same GWC samples with small depth variation (Fig. 2.2). On the other hand, Ra_{eq} values in the AEv soil samples (Avg. 184 $Bqkg^{-1}$; range: 137 to 227 $Bqkg^{-1}$) are observed significantly lower than those of GWC samples and CRec value of 370 $Bqkg^{-1}$.

8.2.3.2. External and Internal Hazard Indices (H_{ex} & H_{in}) Assessment of SGF

For GWC samples of SGF, the mean value of H_{ex} is 0.93 with a range of 0.45-1.26 according to Table 8.7. The values of the H_{in} ranged from 0.53 to 1.47 with a mean value of 1.08. So, the mean values of H_{ex} and H_{in} for GWC samples which are around unity i.e., around the CRec level (Fig. 8.11, 8.12). On the other hand, the mean value of H_{ex} for the GFEv samples is 0.50 with range from 0.37 to 0.61 and for H_{in}, the mean value is 0.58 with range 0.42 to 0.70 respectively. Thus, in terms of H_{ex} and H_{in}, all soil samples of SGF are radiologically risk-less but invoke that GFEv samples IAGB should be monitored routinely as the S&S samples can be contaminated by NORMs originated from GAA.

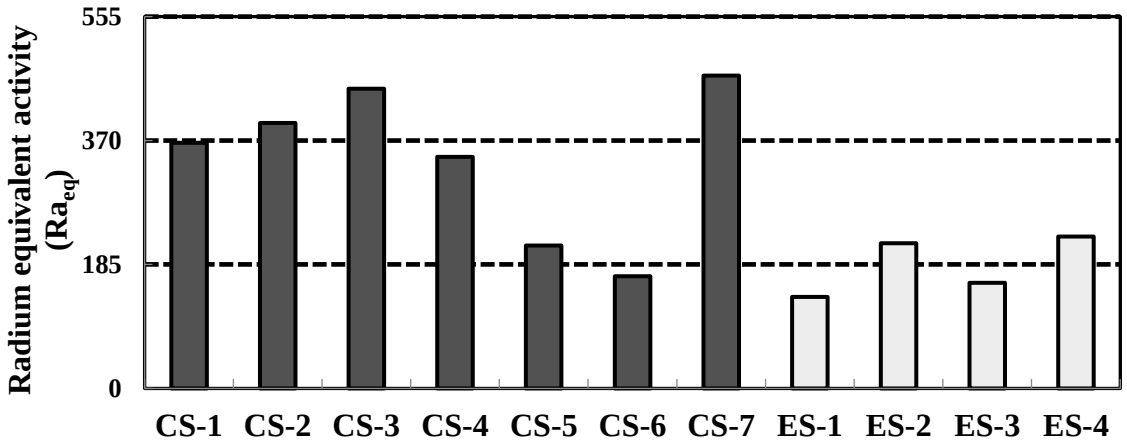

Figure 8.10: Variation of Ra_{eq} of GFEv soil samples are compared with the GWC samples of SGF.

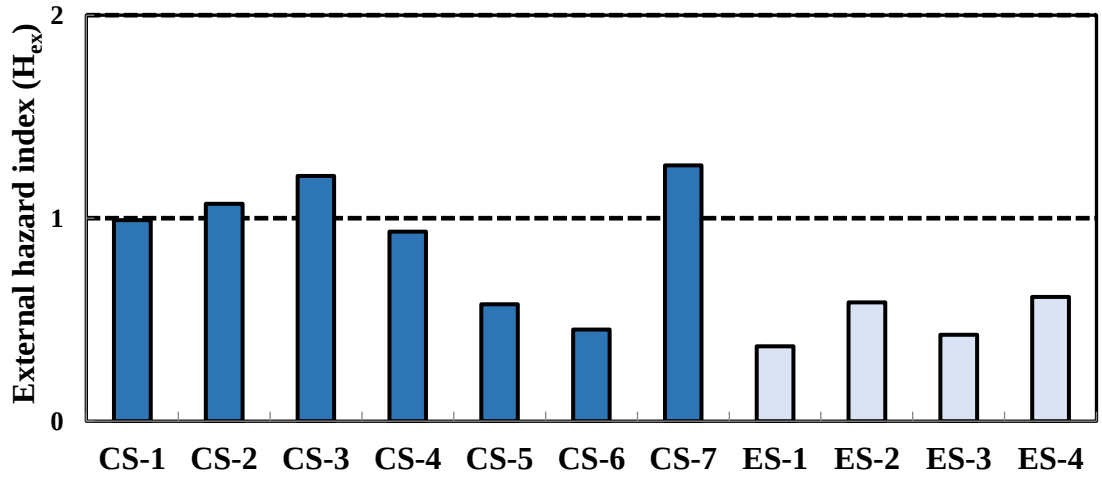

Figure 8.11: Variation of H_{ex} of GFEv soil samples are compared with the GWC samples of SGF.

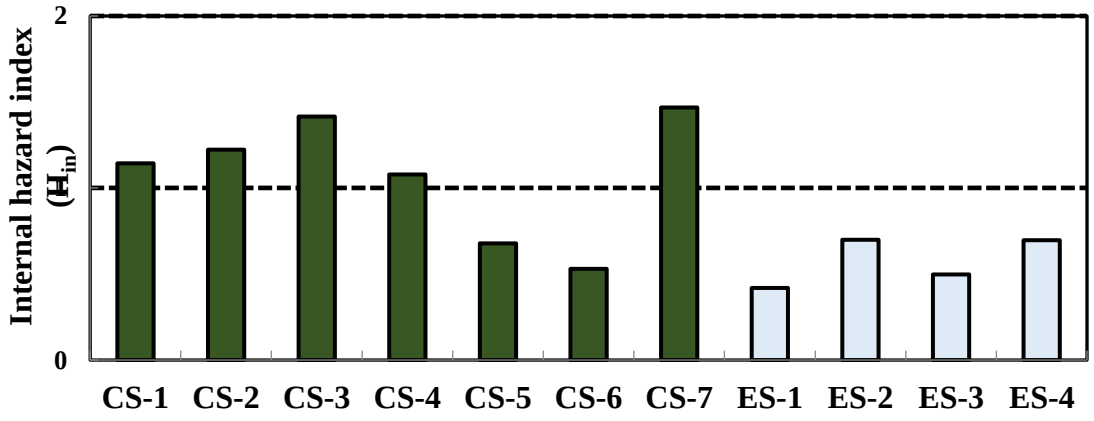

Figure 8.12: Variation of H_{in} of GFEv soil samples are compared with the GWC samples of SGF.

8.2.3.3. Absorbed Dose Rate (D) and Annual Effective Dose Rate (E_{ff}) Assessment of Saldanadi Gas Field

D for all the GWC samples are above the CRec value, 55 $nGyh^{-1}$ where most of them are more than three times higher from 55 $nGyh^{-1}$ as shown in (Table 8.7, Fig. 8.13) which ranged from 80 to 227 $nGyh^{-1}$ with an Avg of 167 $nGyh^{-1}$. Avg D-value for the surface samples is 87 $nGyh^{-1}$ with a range of 65 to 108 $nGyh^{-1}$. D for SurS samples are also above the CRec value of 55 $nGyh^{-1}$.

On the other hand, the mean values of the E_{ff} are 0.20 $mSv.y^{-1}$ and 0.11 $mSv.y^{-1}$ for GWC and surface samples, respectively which are within the CRec value i.e. 0.46 $mSv.y^{-1}$.

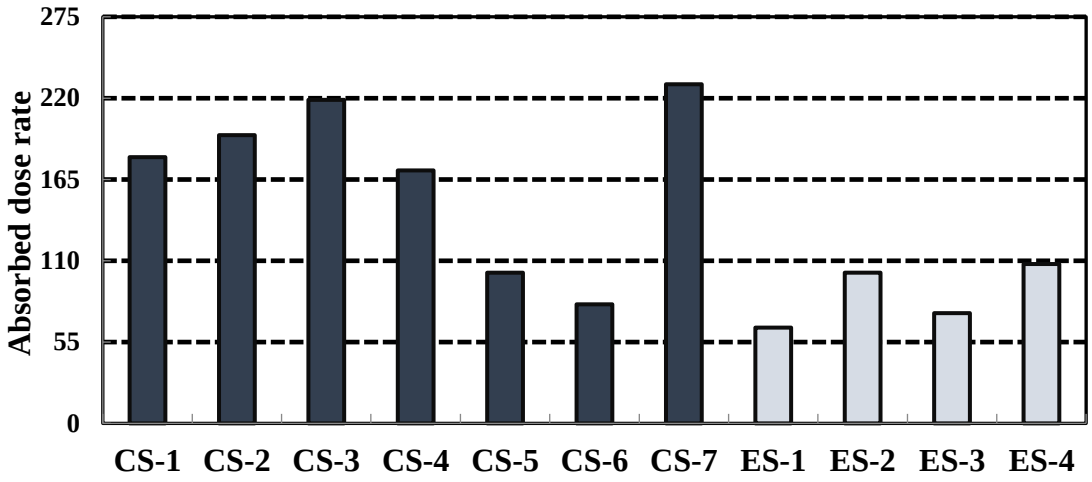

Figure 8.13: Variation of D in $nGyh^{-1}$ of the GFEv samples are compared with the GWC samples of SGF.

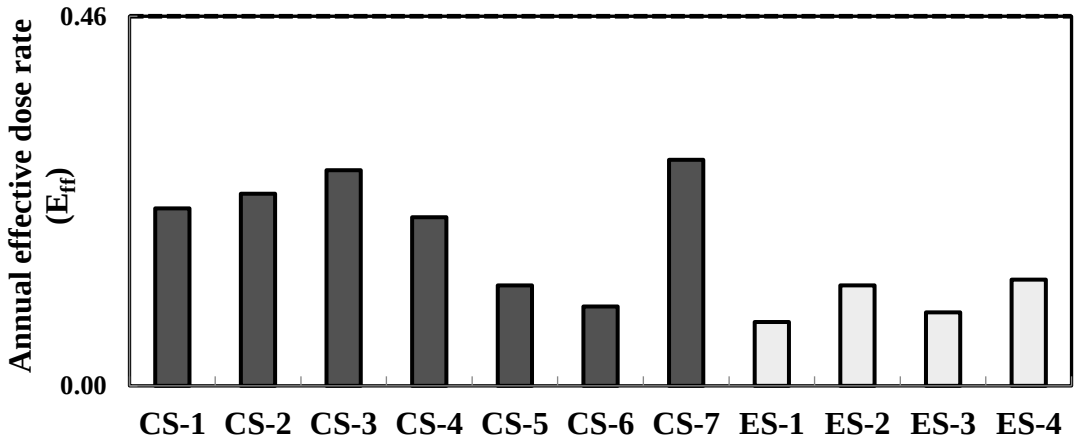

Figure 8.14: Variation of the E_{ff} in $mSv.y^{-1}$ of the GFEv samples are compared with the GWC samples of SGF, Bangladesh.

8.2.3.4 Gamma Representative Level Index (I_γ) Assessment of Saldanadi Gas Field

For all the samples both surface S&S and GWC, values of I_γ are above the CRec value of 1.0, where most of the GWC samples have around three times higher value than that of CRec value and are also significantly higher than those in SurS samples as shown in Fig. 8.15. I_γ values for core samples are ranged from 1.27 to 3.61 with an Avg. of 2.64. Avg I_γ-value for the surface samples is 1.38 with a range from 1.02 to 1.70.

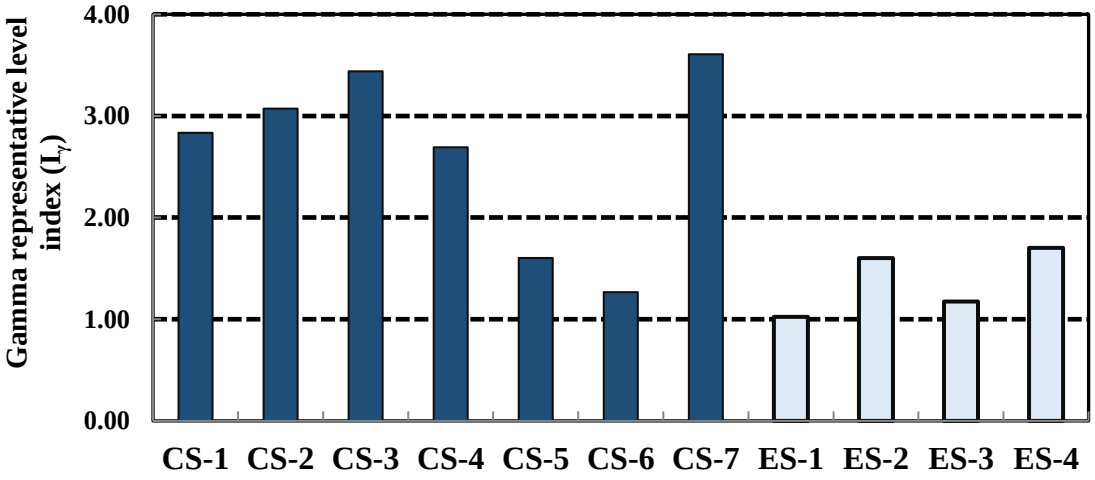

Figure 8.15: Variation of the I_γ of the GFEv samples are compared with the GWC samples of SGF.

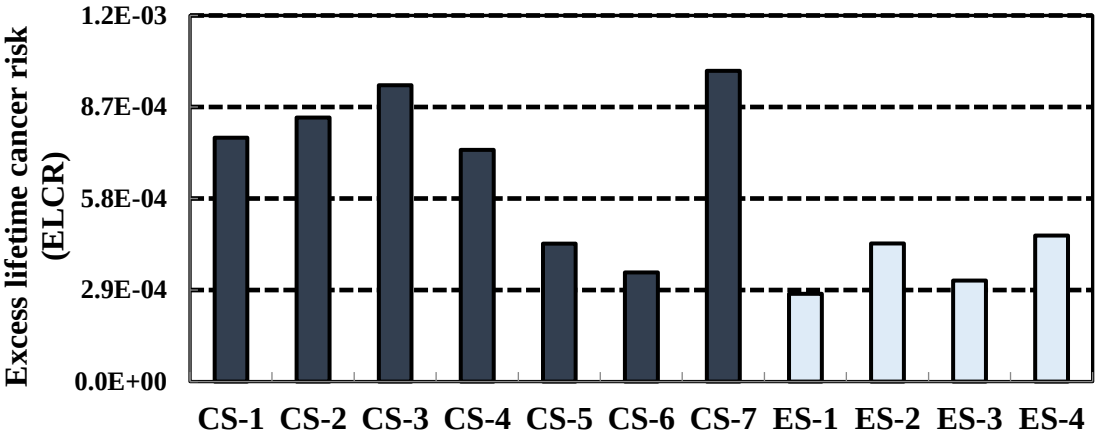

Figure 8.16: Variation of ELCR of the GFEv samples are compared with the GWC samples of SGF.

8.2.3.5. **Excess Lifetime Cancer Risk (ELCR) Assessment of SGF**

For most of the GWC samples of the gas field well of SGF, values of ELCR are around three times higher of the CRec value of 2.9×10^{-4} (Table 8.7). ELCR in all samples (except for ES-1, which is almost equal to the CRec value) are above the CRec value for ELCR. Here ELCR level index values for GWC samples are ranged from 3.42×10^{-4} to 9.76×10^{-4} with an Avg of 7.15×10^{-4}. Avg ELCR value for the surface samples is 3.75×10^{-4} with a range from 2.78×10^{-4} to 4.63×10^{-4}.

8.3 **Radioactivity Concentrations (RC) of Fenchuganj Gas Field (FGF)**

8.3.**1**. **Gas Well Core (GWC) Samples of of FGF**

The RC of NR3 of eight GWC samples from well-2 with depth variation from 2194m to 4091m of FGF of Bangladesh have been presented in Table 8.9. RC of ^{226}Ra in the drilling core samples ranged from 30.8±3.4 Bqkg^{-1} to 62.4±3.5 Bqkg^{-1}with a mean value of 47.5 Bqkg^{-1}, where Min RC of ^{226}Ra is obtained in the GWC sample of greater depth (4090-91m; ID: CF-8) than the depth (3770-71m; ID: CF-7) of Max ^{226}Ra RC. The Avg. value of ^{226}Ra is higher than the world Avg. value of ^{226}Ra (UNSCEAR, 2000 [8.1]: 35 Bqkg^{-1}).

RC of ^{232}Th in the drilling core samples ranged from 52.2±2.5 Bqkg^{-1} to 93.2±2.8 Bqkg^{-1}with a mean value of 74.9 Bqkg^{-1}. Here Min. RC of ^{232}Th is found in the core sample (sand sample) of greater depth (3624-25m; ID: CF-6) than the depth (3263-64m; ID: CF-4) of Max. ^{232}Th RC. The Avg. value of ^{232}Th is more than two times higher than the world Avg. value of ^{232}Th (UNSCEAR, 2000 [1]: 30 Bqkg^{-1}). RC of ^{40}K in the drilling core samples ranged from 1042±48 Bqkg^{-1} to 2218±58 Bqkg^{-1}with an Avg. value of 1805 Bqkg^{-1}, where Min RC of ^{40}K is also obtained in the core sample of greater depth (4090-91m; ID: CF-8) than the depth (3259-60m; ID: CF-3) of Max ^{40}K RC. The Avg. value of ^{40}K is more than four times higher than the world Avg. value of ^{40}K(UNSCEAR, 2000 [1]: 400 Bqkg^{-1}). Th/Ra ratio is comparable with each other of all core samples with an Avg value 1.6. Low Th/U ratio indicates favourable criteria for uranium mineralization and here lowest ratio is found 1.33 in sample CF-7 where ^{226}Ra activity is Max.

According to lithological information, within eight core samples of FGF, only one sample is sand sample (ID: CF-6), where lowest RC of ^{232}Th and comparatively lower values of ^{226}Ra and ^{40}K have been found and all other samples are shale samples.

Table 8.9: Radioactivity concentrations (in Bq kg^{-1}) of the naturally occurring radionuclides and Th/Ra ratio in the core samples of Fenchuganj gas field.

Sample No.	^{226}Ra [Bqkg^{-1}]	^{232}Th [Bqkg^{-1}]	^{40}K [Bqkg^{-1}]	Th/Ra
CF-1	58.4 ± 3.4	78.1 ± 2.7	1766 ± 50	1.34
CF-2	35.8 ± 2.9	71.8 ± 2.5	1792 ± 48	2.00
CF-3	49.5 ± 3.6	89.9 ± 3.0	2218 ± 58	1.82
CF-4	57.3 ± 3.3	93.2 ± 2.8	2136 ± 53	1.63
CF-5	46.9 ± 3.1	74.6 ± 2.6	1977 ± 51	1.59
CF-6	38.5 ± 3.3	52.2 ± 2.5	1484 ± 50	1.35
CF-7	62.4 ± 3.5	83.2 ± 2.8	2028 ± 54	1.33
CF-8	30.8 ± 3.4	56.4 ± 2.7	1042 ± 48.4	1.83
Average	47.5	74.9	1805	1.61
Min	30.8	52.2	1042	1.33
Max	62.4	93.2	2218	2.00
Word Avg.[a]	35	30	400	
UCC [b]	33	43	720	

[a][8.1],[b][8.2].

8.3.2 NORMs Distribution in Soil and Sediment Samples of FGF

The specific radioactivity values of the mentioned NR S&S samples of FGF with their respective standard deviations (SD) and the Th/Ra ratio are also presented in Table 8.10. In the studied area, RC of ^{226}Ra varied from 15.8 ± 2.9 to 31.6 ± 4.2 Bqkg^{-1} with an Avg value of 24 Bqkg^{-1}, where Min. and Max. RC of ^{226}Ra both are obtained in the soil samples of WDEvp Pond side area of sample ID, EF-4 and EF-3 respectively.

Table 8.10: Radioactivity concentration (Bq kg^{-1}) of the naturally occurring radionuclides and Th/Ra ratio in the environmental soil and sediment samples of Fenchuganj gas field.

Sample No.	^{226}Ra [Bqkg^{-1}]	^{232}Th [Bqkg^{-1}]	^{40}K [Bqkg^{-1}]	Th/Ra
EF-1	23.9 ± 3.0	41.2 ± 2.4	390 ± 42	1.72
EF-2	22.3 ± 3.7	40.4 ± 3.3	386 ± 48	1.81
EF-3	31.6 ± 4.2	67.3 ± 3.4	365 ± 54	2.13
EF-4	15.8 ± 2.9	18.4 ± 2.2	143 ± 39	1.16
EF-5	28.3 ± 3.9	78.4 ± 3.4	515 ± 54	2.77
Average	24.4	49.1	360	
Min.	15.8	18.4	143	
Max.	31.6	78.4	515	
Literature data				
Word Avg.[a]	35	30	400	
UCC [b]	33	43	720	
SEB, Bangladesh [c]	18	46	321	
SB, Bangladesh[d]	42	81	833	
India [e]	37	69.6	396	

[a][8.1], [b][8.2], [c][8.4], [d][8.5], [e][8.6].

The Avg. RC of ^{232}Th is 49 Bqkg^{-1} and vary from 18.4 ± 2.2 Bqkg^{-1} to 78.4 ± 3.4 Bqkg^{-1}. The mean value of RC of ^{40}K is 360 Bqkg^{-1} which vary from 143 ± 39 Bqkg^{-1} to 515 ± 54 Bqkg^{-1}. The Min RC of ^{232}Th and ^{40}K are also found in the same soil sample of sample ID EF-4 collected from WDEvp Pond side area where chemical wastes are dumped. The Max. RC of ^{232}Th and ^{40}K both are found in the same soil sample of sample ID EF-5 collected from out side of GF and plant area of FGF. The Avg. RC of ^{226}Ra and ^{40}K of FGF are less than the corresponding world Avg. values according to UNSCEAR, 2000 [8.1]. Only Avg. value of ^{232}Th FGF is higher than corresponding world Avg. value i.e. 30 Bqkg^{-1} [8.1].

These areas are generally over flooded during rainy season and results in the NORMs' spreading randomly in the areas where higher radioactivity levels are found.

For better understanding, the RC of ^{226}Ra, ^{232}Th and ^{40}K in the AEv samples (EF-1 to EF-5) are compared with those of core samples (CF-1 to CF-8) of FGF have been presented graphically in Fig. 8.17.

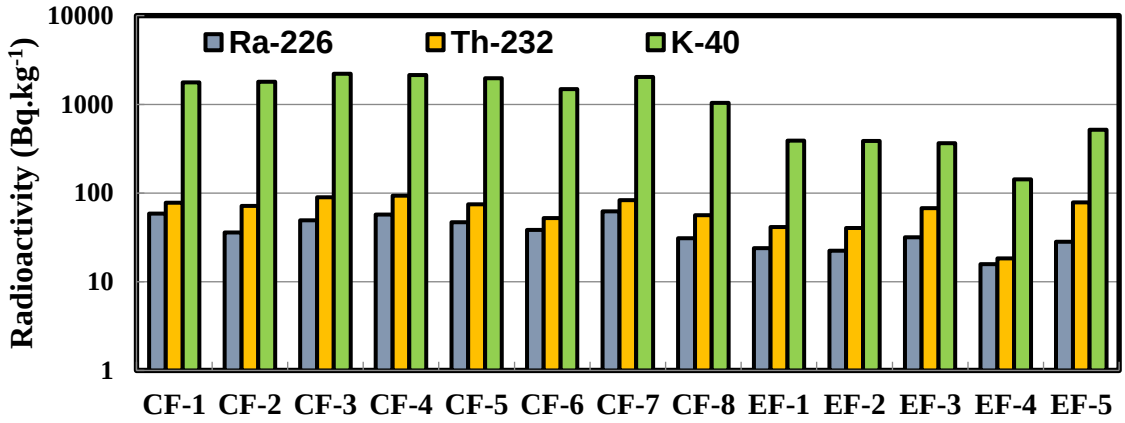

Figure 8.17: The RC of ^{226}Ra, ^{232}Th and ^{40}K in the GFEv samples (EF-1 to EF-5) are compared with those of GWC samples (CF-1 to CF-8) of FGF

8.3.3. **Radiological Risks Assessment of Fenchuganj Gas Field (FGF)**

Table 8.11 presents the values of seven RHI for core samples of the GF, whereas Table 8.12 shows the RHI for S&S samples of FGF. Additionally, Fig. 8.18 to Fig. 8.24 represents intercomparisons of radiological indices between the core samples and ES along with their recommended values [8.1, 8.8 – 8.10].

Table 8.11: Radiation hazard indices from the core samples of Fenchuganj gas field and the corresponding recommended values.

Sample No	Ra_{eq} [Bqkg^{-1}]	H_{ex}	H_{in}	D [ηGyh^{-1}]	E_{ff} [mSvy^{-1}]	I_γ	ELCR
CF-1	306	0.83	0.98	150	0.18	2.35	6.42×10^{-4}
CF-2	277	0.75	0.84	136	0.17	2.15	5.86×10^{-4}
CF-3	349	0.94	1.08	172	0.21	2.71	7.37×10^{-4}
CF-4	355	0.96	1.11	174	0.21	2.74	7.47×10^{-4}
CF-5	306	0.83	0.95	151	0.19	2.38	6.48×10^{-4}
CF-6	227	0.61	0.72	113	0.14	1.77	4.83×10^{-4}
CF-7	338	0.91	1.08	166	0.20	2.60	7.11×10^{-4}
CF-8	192	0.52	0.60	93	0.11	1.46	3.99×10^{-4}
Average	294	0.8	0.9	144	0.2	2.3	6.19×10^{-4}
Min	192	0.5	0.6	93	0.1	1.5	3.99×10^{-4}
Max	355	1.0	1.1	174	0.2	2.7	7.47×10^{-4}
Recommended values	370	<1	<1	55.0	0.46	1.00	2.90×10^{-4}

[1, 8-10]

Table 8.12: Radiation hazard indices of soil and sediment samples of Fenchuganj gas field environment and the corresponding recommended values.

Sample No	Ra_{eq} [$Bqkg^{-1}$]	H_{ex}	H_{in}	D [ηGyh^{-1}]	E_{ff} [$mSvy^{-1}$]	I_{γ}	ELCR
EF-1	113	0.30	0.37	53.0	0.07	0.83	2.28×10^{-4}
EF-2	110	0.30	0.36	51.6	0.06	0.81	2.22×10^{-4}
EF-3	156	0.42	0.51	71.8	0.09	1.13	3.08×10^{-4}
EF-4	53	0.14	0.19	24.7	0.03	0.38	1.06×10^{-4}
EF-5	180	0.49	0.56	83.4	0.10	1.32	3.58×10^{-4}
Average	**122**	**0.33**	**0.40**	**56.9**	**0.07**	**0.89**	**2.44**$\times10^{-4}$
Min.	53	0.14	0.19	24.7	0.03	0.38	1.06×10^{-4}
Max.	180	0.49	0.56	83.4	0.10	1.32	3.58×10^{-4}
Recommended values	370.0	<1	<1	55.0	0.46	1.00	2.90×10^{-4}

[1, 8-10]

8.3.3.1 Radium Equivalent Activity (Ra_{eq}) Assessment of FGF

The Ra_{eq} value for the core samples varied from 192 to 355 with a mean value (n=8) of 294 which is not near to the recommended value of 370. On the other hand, spatial variations of

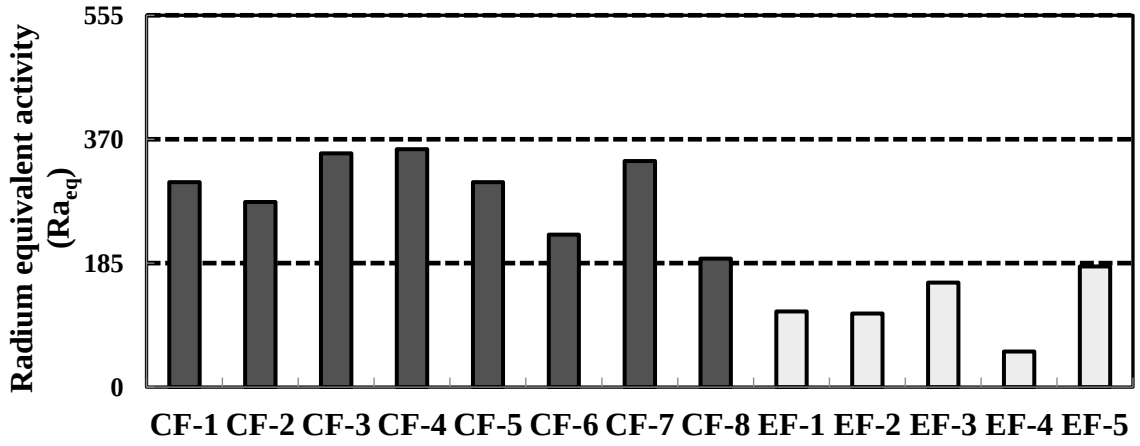

Figure 8.18: Variation of radium equivalent activity of GFEv samples (S&S) are compared with the GWC samples (shale & sand) of FGF.

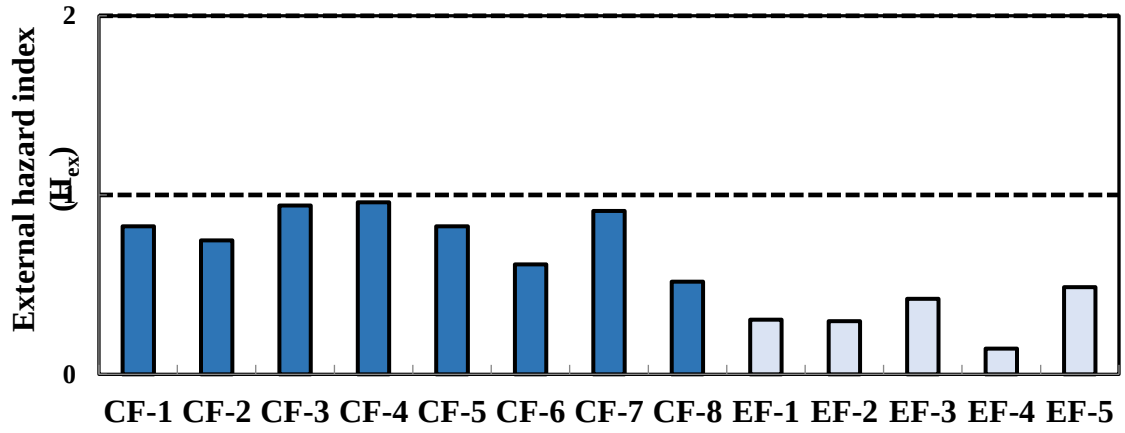

Figure 8.19: Variation of H_{ex} of GFEv S&S samples are compared with the GWC samples (shale & sand) of FGF.

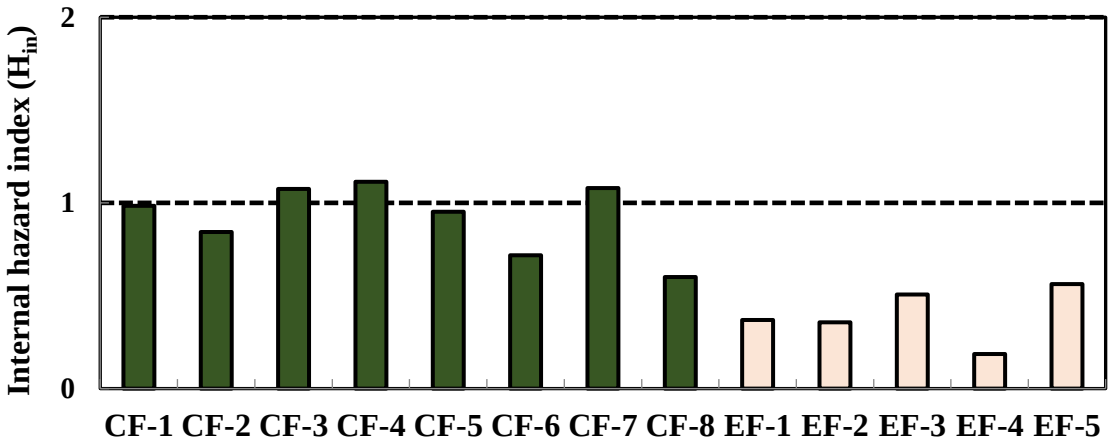

Figure 8.20: Variation of H_{in} of GFEv S&S samples are compared with the GWC samples (shale & sand) of FGF.

Ra_{eq} values are observed in the AEv samples (S&S) (Avg: 122; range: 53-180) due to the anthropogenic and/or natural redistributions of NORMs. However, Ra_{eq} values for ES are significantly lower than those of GWC samples and recommended value.

8.3.3.2. **External and Internal Hazard Indices Assessment of FGF**

For GWC samples of FGF, the mean value of H_{ex} is 0.79with a range of 0.52 to 0.96 according to Table 8.11. The values of the H_{in} ranged from 0.60 to 1.11with a mean value of 0.92. So, the values for GWC samples are near about and around unity for H_{ex} and H_{in} respectively (Fig. 8.19, 8.20). On the other hand, the mean value of H_{ex} for the ES is 0.33 with range from 0.14 to 0.49 and for H_{in}, the mean value is 0.40 with range 0.19 to 0.56 respectively. Thus, in terms of H_{ex} and H_{in}, all

soil samples of FGF are RR less but invoke that ES IAGB should be monitored routinely as the S&S samples can be contaminated by NORMs originated from gas-abstraction activities.

8.3.3.3. **Absorbed Dose Rate and Annual Effective Dose Rate Assessment of FGF**

Absorbed dose rate (D) for all the GWC samples are around or more than two times higher from the recommend value 55 $nGyh^{-1}$ as shown in (Table 8.11, Fig. 8.21) which ranged from 93 to 174 $nGyh^{-1}$ with an Avg. of 144 $nGyh^{-1}$. Avg. D-value for the surface samples is 57 $nGyh^{-1}$ with a range of 25 to 83 $nGyh^{-1}$, However, D for samples both from bottom sediment of WDEvp Pond and soil samples far away from WDEvp Pond have D around the recommended value of 55 $nGyh^{-1}$ except sampling location: chemical wastes of drilling dumped WDEvp Pond corner i.e. EF-4.

On the other hand, the mean values of the annual effective dose rate are 0.18 $mSv.y^{-1}$ and 0.07 $mSv.y^{-1}$ for GWC and surface samples, respectively which are within the recommended value i.e. 0.46 $mSv.y^{-1}$.

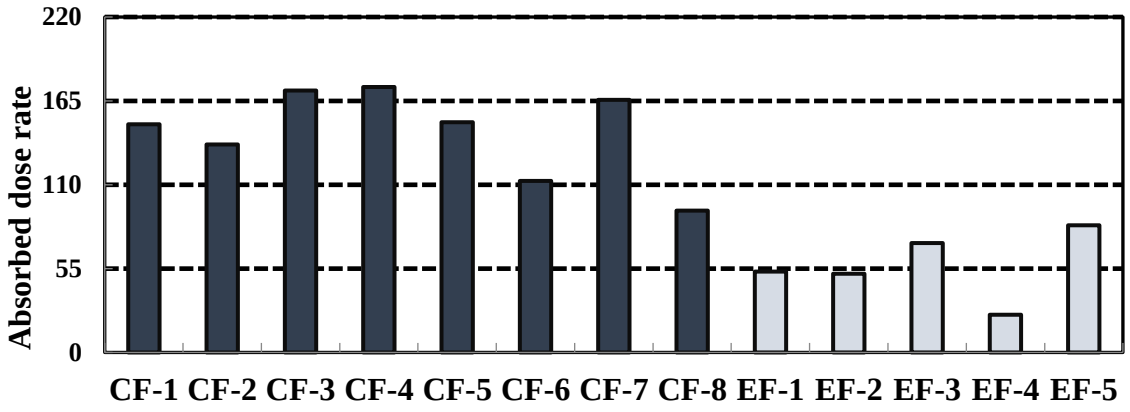

Figure 8.21: Variation of absorbed dose rate in $nGyh^{-1}$ of the GFEv samples are compared with the GWC samples of FGF.

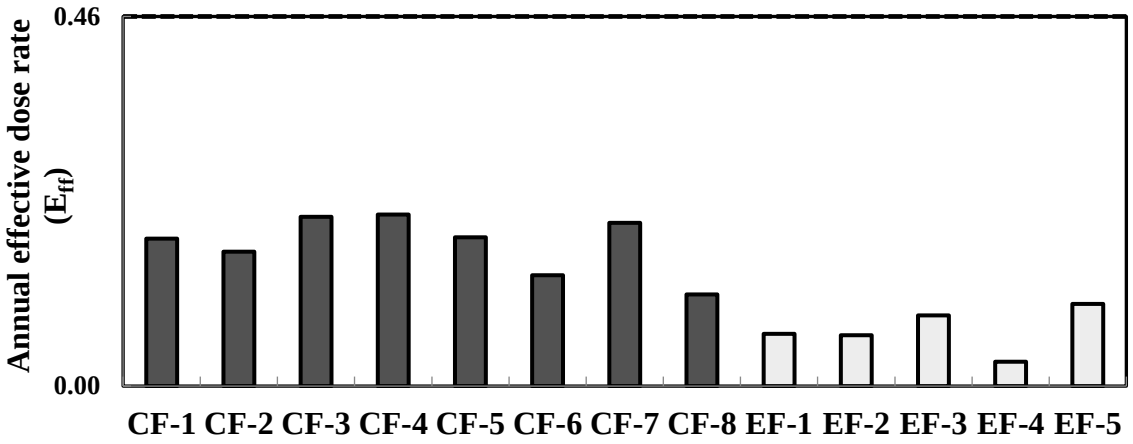

Figure 8.22: Variation of the annual effective dose rate in $mSv.y^{-1}$ of the GFEv samples are compared with the GWC samples of FGF, Bangladesh.

8.3.3.4 Gamma Representative Level Index Assessment of FGF

Gamma representative level index (I_γ) values of all the GWC samples are above the corresponding recommend value of 1.0, where most of the GWC samples have above two times higher value than that of corresponding recommended value and are also significantly higher than those in surface S&S samples as shown in Fig. 8.23. I_γ values for GWC samples are ranged from 1.46 to 2.74 with an Avg. of 2.27. Avg. I_γ-value for the surface samples is 0.89 with a range from 0.38 to 1.32.

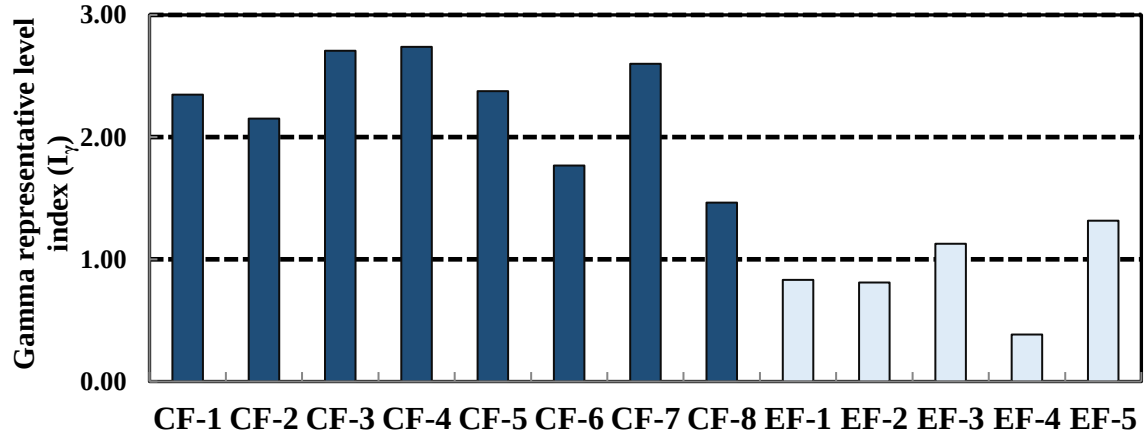

Figure 8.23: Variation of the gamma representative level index (Iγ) of the GFEv samples are compared with the GWC samples of FGF.

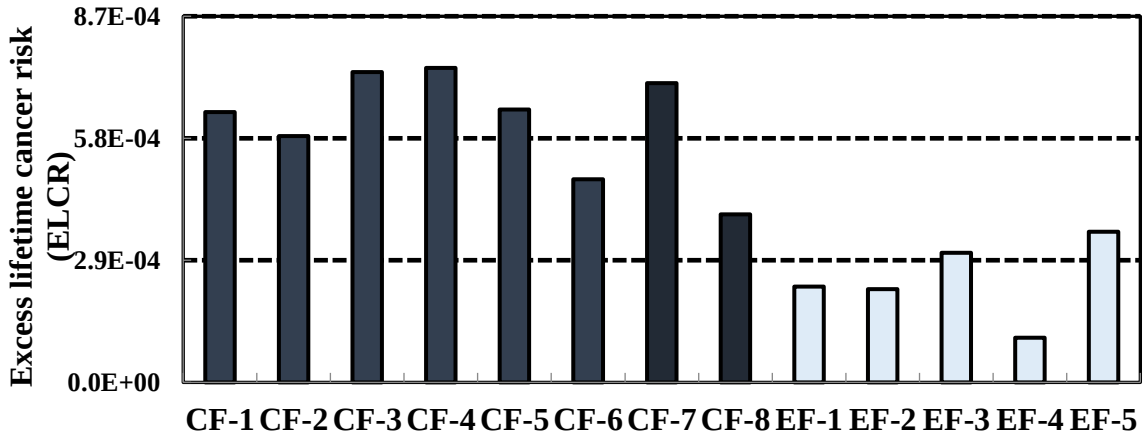

Figure 8.24: Variation of excess lifetime cancer risk (ELCR) of the GFEv samples are compared with the GWC samples of FGF.

8.3.3.**5**. **Excess Lifetime Cancer Risk Assessment of FGF**

All the GWC samples of well of FGF, values of excess life time cancer risk (ELCR) are above two times higher of the corresponding recommended value of 2.9×10^{-4} except two GWC samples of CF-6 and CF-8 (Table 8.11). ELCR value in two surface samples of ID EF-3 and EF-5 are above the corresponding recommended value. Here ELCR level index values for GWC samples are ranged from 3.99×10^{-4} to 7.47×10^{-4} with an Avg of 6.19×10^{-4}. Avg ELCR value for the surface samples is 2.44×10^{-4} with a range from 1.06×10^{-4} to 3.58×10^{-4}. So ES IAGB should be monitored routinely as the S&S samples can be more contaminated by NORMs originated from gas-abstraction activities.

8.4. Intercomparison of Three Gas Fields Namely Shahbazpur, Saldanadi and Fenchuganj Gas Fields for Both Their Gas Well Core Samples and Environmental Surface Samples

The concentrations ($Bqkg^{-1}$) of the TE-NORMs of this study are compared with those of soil samples of the G&O production facilities in different countries of the world which are presented in Table 8.13. The ^{226}Ra RC in our study are comparable with other countries of the world of the world for soil samples of the G&O production facilities. But Saudi Aribia, Iraq, Romania, Naigeria, Kuwait and Syria have higher activity for their Max value than our studied samples. Our ^{232}Th and ^{40}K RC range are significantly higher than other soil samples of the G&O production facilities in different countries of the world. Only Romania's Max values are comparable with our study. May be due to geological formation variation. According to the geo-chemical characteristics of the studied sediments implies that the Miocene sediments of Sbz structure were originated from felsic type (Himalayan) source rocks those have undergone moderate to severe chemical weathering which were deposited under oxic environmental condition [mahbuba].

Table 8.13: Concentrations (Bq kg^{-1}) of the TE-NORMs of this study are compared with those of soil samples of the G&O production facilities in different countries of the world.

Country	Concentration of the TENORM in soil samples					
	^{226}Ra		^{232}Th		^{40}K	
	[Bqkg^{-1}]		[Bqkg^{-1}]		[Bqkg^{-1}]	
	Range	Mean	Range	Mean	Range	Mean
This study: Shahbazpur Gas field, Bangladesh						
1. Environmental Sample	26 – 55	40	41 – 82	73	610- 1203	895
2. Core Sample	47 – 82	60	75 – 121	94	1481 – 2756	2194
This study: Fenchuganj Gas field, Bangladesh						
1. Environmental Sample	13 -27	21	17 - 71	44	143 - 515	360
2. Core Sample	31 - 62	48	52 - 93	75	1042 - 2218	1811
This study: Saldanadi Gas field, Bangladesh						
1. Environmental Sample	16 - 36	25	46 - 75	61	459 - 788	591
2. Core Sample	29 - 77	55	52 - 119	92	824 - 2864	2039
Literature data:						
Saudi Aribia [a]	8.68 – 156	23.2			108 – 446	278
Albania [b]	12 – 23	18.3			326 – 549	413.7
Iraq [c]	18.4 – 97.6		11.5 – 42.7		176.9 – 485.6	
Turkey [d]	24.79 – 70.48	46.47				
Romania [e]	60 – 330		8 – 87		53 – 960	
Ghana [f]			8.5 – 67.2	26.9	60.4 – 248.9	157
Nigeria [g]	19.2 – 94.2	41	17.7 – 47.5	29.7	107 – 712	412.5
Qatar [h]		20.05		16.43		216.69
Kuwait [i]	33.7 – 250.6	85	10.5 – 21.96	13	331 – 449.4	406
Syria [j]	18.90 – 210		16.8 – 55.9		44 – 213	
China [k]	16 – 82	57				
Oman [l]			5.7 – 9.1	7.1	93 – 293	151

[a][14], [b][15], [c][16], [d][17], [e][18], [f][19], [g][20], [h][21], [i][22], [j][23], [k][24], [l][12]

Also geo-chemical characteristics of most of the part of Bangladesh is originated from felsic type (Himalayan) source rocks. Again Miocene core sediments of Sbz gas wells are enriched with Ce, Th and Yb compare to Upper Continental Crust (UCC), which indicates the presence of heavy

minerals, e.g., rutile, apatite and monazite [mahbuba].and HM&M possess more radioactive materials.

Avg. RC of ^{226}Ra, ^{232}Th and ^{40}K of GWC samples of 1200m to 4000m depth gas reservoir zone for all three GF are significantly higher than the corresponding world Avg. values. On the other hand, environmental surface S&S samples in and around the GF have significantly lower radioactivity levels to those in GWC samples.

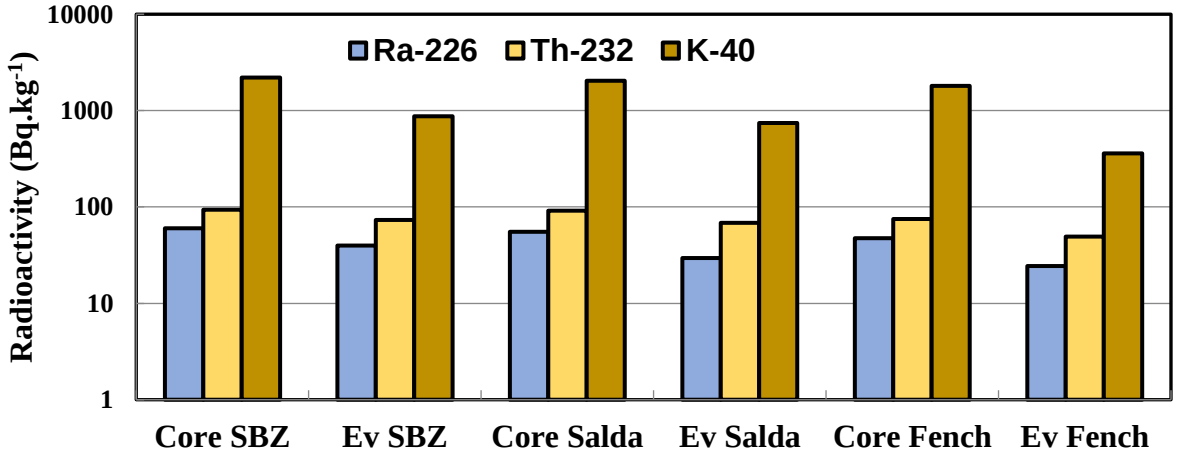

Figure 8.25: Intercomparison of RC of three GF namely Sbz, SGF and FGF for both their GWC samples and environmental surface samples.

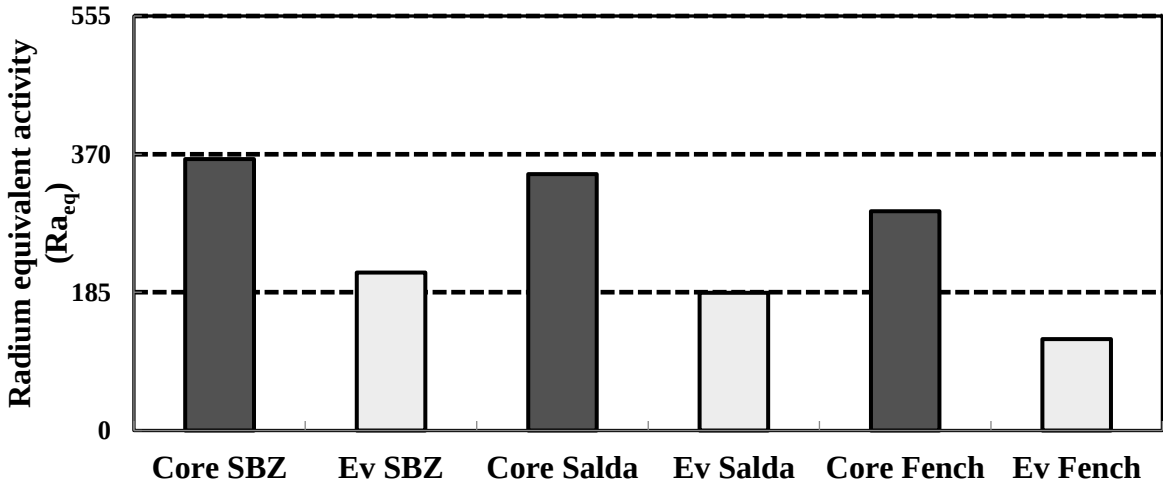

Figure 8.26: Intercomparison of Radium equivalent activity of three GF namely Sbz, SGF and FGF for both their GWC samples and environmental surface samples.

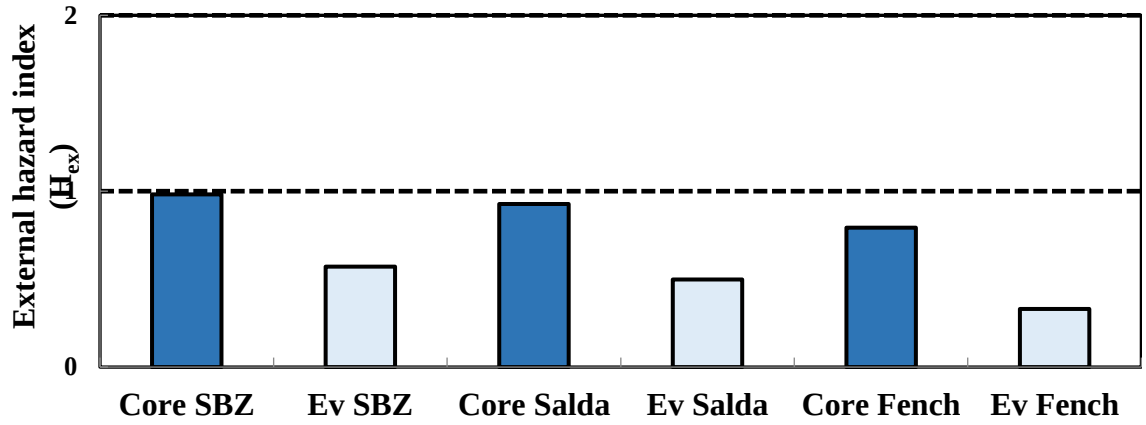

Figure 8.27: Intercomparison of H_{ex} of three GF namely Sbz, SGF and FGF for both their GWC samples and environmental surface samples.

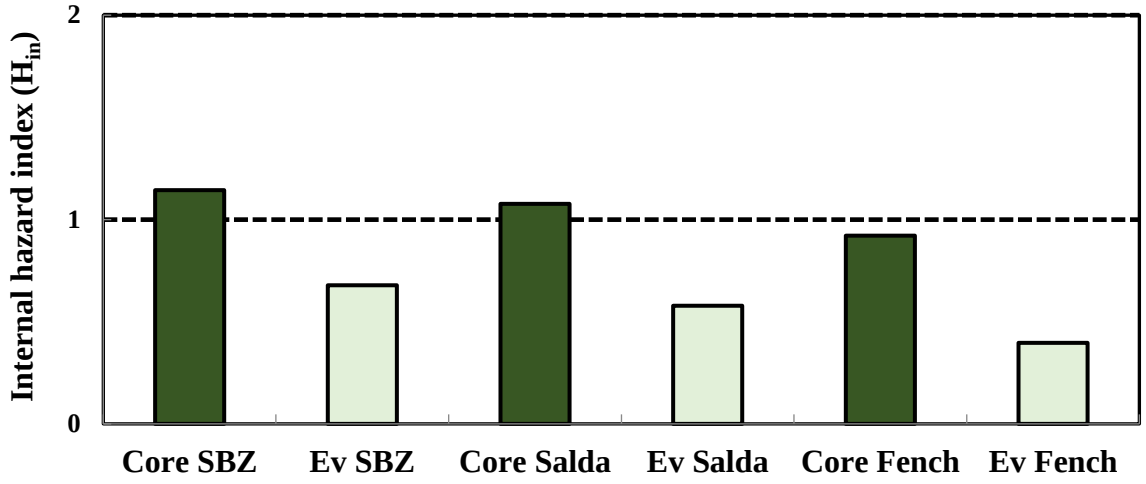

Figure 8.28: Intercomparison of H_{in} of three GF namely Sbz, SGF and FGF for both their GWC samples and environmental surface samples.

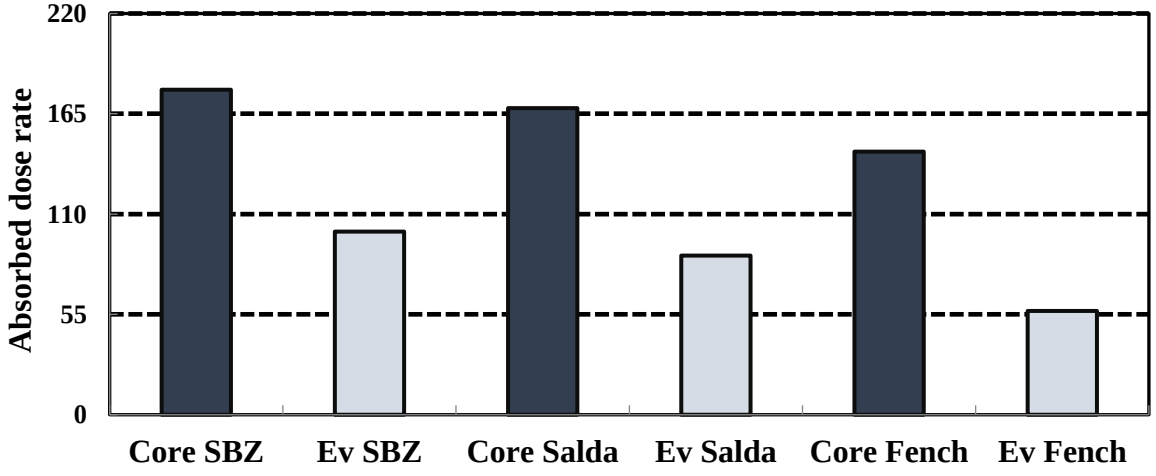

Figure 8.29: Intercomparison of absorbed dose rate of three GF namely Sbz, SGF and FGF for both their GWC samples and environmental surface samples.

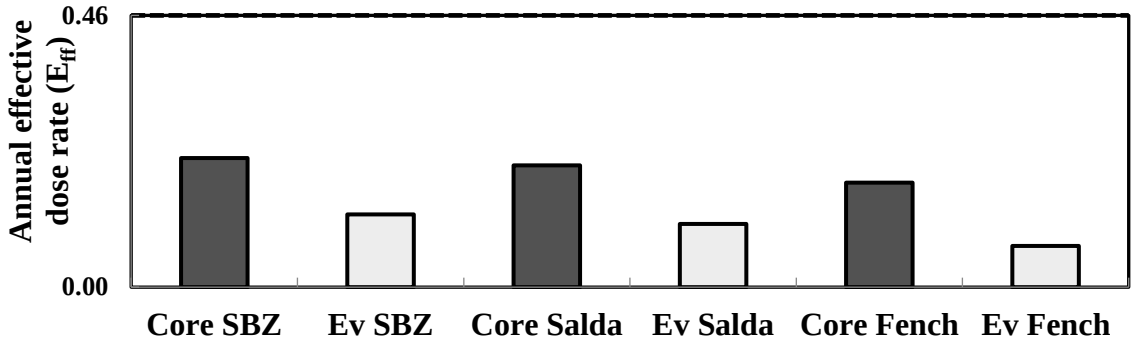

Figure 8.30: Intercomparison of annual effective dose rate of three GF namely Sbz, SGF and FGF for both their GWC samples and environmental surface samples.

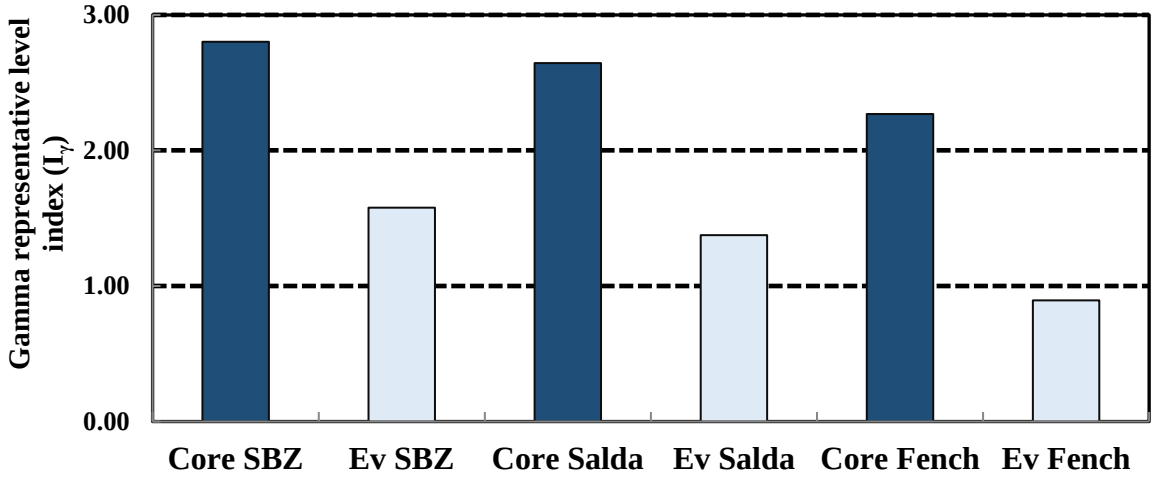

Figure 8.31: Intercomparison of gamma representative level index of three GF namely Sbz, SGF and FGF for both their GWC samples and environmental surface samples.

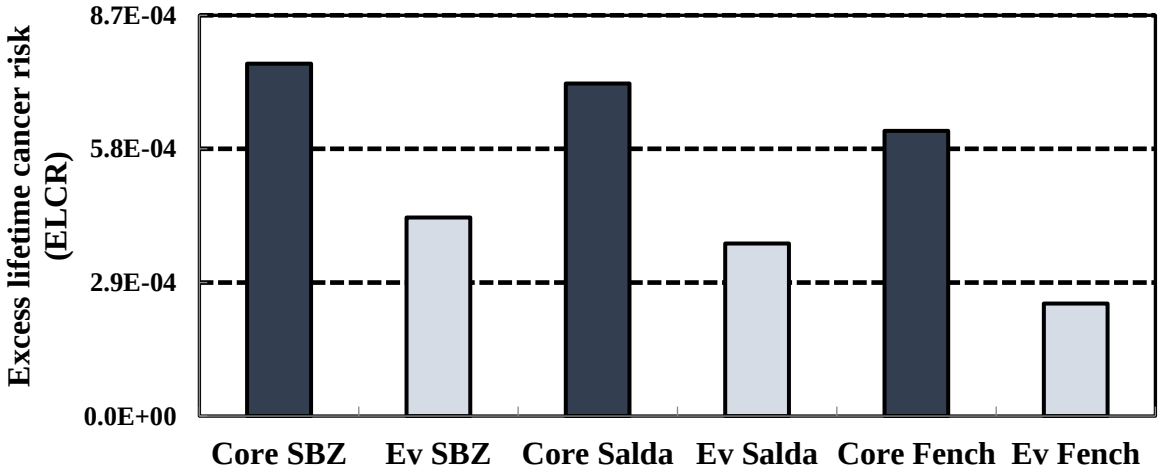

Figure 8.32: Intercomparison of excess lifetime cancer risk of three GF namely Sbz, SGF and FGF for both their GWC samples and environmental surface samples.

Intercomparison of three GF namely Sbz, SGF and FGF for both their GWC samples and environmental surface samples have been conducted. Fig. 8.26 to Fig. 8.32 represents seven RHI intercomparisons of these three GF for both their GWC samples and environmental SurS samples.

All seven RHI of core samples of 1200m to 4000m depth gas reservoir zone for all three GF are significantly higher than the corresponding recommended values. On the other hand, environmental SurS and sediment samples in and around the GF have significantly lower radioactivity levels to those in GWC samples of these three GF but values of most of the hazard indices of surface samples of these three GF are around the corresponding recommended values.

Evaluation of RHI suggests considerable risks and invoke that ES IAGB should be monitored routinely as the S&S samples can be contaminated more by NORMs originated from gas-abstraction activities.

Chapter-9

Conclusion

9.1 Conclusion

A total of 15 elemental (K, Ca, Ti, Cr, Mn, Fe, Ni, Cu, Zn, As, Rb, Sr, Y, Zr and Pb) abundances in gas field environmental (GFEv) soil and sediment (S&S) samples of Shahbazpur (Sbz) gas field (GF), Saldanadi gas field (SGF) and Fenchuganj gas field (FGF) of Bangladesh have been determined by EDXRF.

9.1.1 Elemental Identification of Shahbazpur (Sbz) Gas Field (GF)

In the Sbz GF environmental S&S samples, the concentration of Pb varies from 7.27 to 113 ppm with an Avg. value of 70.5 ppm, where the concentration of Pb of UCC (upper continental crust) and world soil median values are 17 ppm and 35 ppm respectively. Again, the Avg. concentration of As is 26.6 ppm and varies from 9.83 to 43.9 ppm in this study, where the concentration of As of UCC and world soil median values are 4.8 ppm and 6 ppm respectively. So, the Avg. concentration of both Pb and As in S&S samples of this GF are significantly higher than corresponding UCC and world soil median values.

In the Sbz GF environmental S&S samples:

(a) All three environmental indicators for assessing elemental contents are found comparatively higher values in two samples, one has been collected from the north-east side of WDEvp Pond where mud and brine (MB) chemicals are also disposed along with produced water and another sample from outside the GF boundary and beside a local canal which is connected through GF drainage system.

(b) Comparatively lower values of most of the elementals have been found in the sample locations, which are far away from produced water deposited and WDEvp Pond. Lowest values of most of the elementals, like Pb, As have been found in sample, which has been collected from outside the GF boundary and comparatively high land as base-line data.

The enrichment factor (EF) values in most of the samples of Sbz GF for Pb and As revealed that the S&S samples have been around severely enriched with these metals/metalloids. The geo-accumulation index (I_{geo}) revealed moderately contamination of Pb and moderate to heavy contamination of As in most of the S&S samples of this GF area. Again for As, contamination factor (CF) values are found high i.e. CF > 6 and for Pb, CF values are considerable in most of the samples. All these evidences reveal that these elements are from the anthropogenic origin.

9.1.2 Radiological Characterization of Shahbazpur (Sbz) Gas Field (GF)

(a) This research work discloses the potential rearrangements of NORMs from the gas abstraction activities (GAA) of Sbz GF. Radioactivity concentrations (RC) in gas-well core (GWC) samples

of 1200m to 4000m depth gas reservoir zone (Avg: ^{226}Ra: 60.2±13.1; ^{232}Th: 93.8±14.3; ^{40}K: 2194±392) are significantly higher than environmental samples (Avg: ^{226}Ra: 39.6±9.2; ^{232}Th: 73.2±11.1; ^{40}K: 873±180). RC in gas well core (GWC) samples from wells: 2 and 4 of this GF are about 2 to 5 times greater than the corresponding world average (CWA) values. On the other hand, GFEv S&S samples have significantly lower RC compared to those in GWC samples but are comparatively higher than the CWA values.

(b) In GFEv samples, RC in surface soil (SurS) samples are relatively higher than the corresponding sub-surface soil (SubS) samples which demand potential rearrangement of NORMs from the GWC to the ambient environment (AEv) owing to the hydrocarbon extraction activities (HEA).

(c) Potential RR (radiological risks) for both GWC and GFEv samples have been assessed in terms of RHI (radiological hazard indices) including Ra_{eq}, I_{γ}, D, E_{ff}, H_{ex}, H_{in}, and ELCR where, I_{γ}, D and ELCR for both GWC and GFEv samples exceeded the threshold limits, which demand health threats of radiation exposure.

9.2 Saldanadi Gas Field (SGF)

In the SGF environmental soil, the concentration of Pb varies from 85.5 to 1675 ppm with an Avg. value of 493 ppm. Again, the Avg. concentration of As is 33.8 ppm and varies from 29.2 to 37.6 ppm in this study. So, elemental abundances (EA) of both As and Pb in ES of this GF are very much higher than corresponding UCC and world soil median values. The highest concentration detected for the Pb in the sample is from north side of the WDEvp Pond corner where, used up batteries of car and other heavy vehicles of this GF have been dumped from which very high Pb and Sr concentration can be occurred compared to other environmental soil samples of this GF area. Again, in SGF, comparatively lower RC levels and values of all seven RHI found interestingly in this sample. EA of metals in chemically contaminated areas assume to dilute the RM (radioactive materials) in those demarcated areas.

9.3 Fenchuganj Gas Field (FGF)

In the FGF environmental S&S samples, the concentration of Pb varies from 101 to 114 ppm with an Avg. value of 107 ppm. Again, the Avg. concentration of As is 32.4 ppm with a Max. value of 42.6 ppm in this study. So, elemental abundances (EA) of both Pb and As in S&S samples of this GF are significantly higher than corresponding UCC and world soil median values. Lowest RC levels and values of all seven RHI found in sample, which is WDEvp Pond side area of FGF, where for Ca, Ti, Mn, As, Sr and Pb, EA have been found highest in that sample compared to other ES, i.e. interestingly the result has been found for metal/metalloid concentration exactly opposite from RC. In this way, Max. values of all RHI found in the sample, which location is selected as

base-line data from outside the GF and plant area of this GF, where lowest values of most of the EA have been found compared to other ES.

9.4 Inter-Comparison of Three Gas Fields (GF)

Excluding very high value of Pb in one soil sample of SGF, for all three environmental indicators, i.e. EF, I_{geo} and CF values of FGF are significantly higher compared to other two GF, where SGF (production started from 1998 but the number of gas reservoir wells of FGF are greater than SGF) is in second position and Sbz GF in last position. According to the duration of production of reserved gas, higher duration observed for FGF (production started from 2004) than the duration observed for Sbz GF (production started from 2009) which can be the evidences for environmental indicators variation, along with anthropogenic incorporation due to gas abstraction activities.

Again, similar trend is obtained for all three environmental indicators of EA Avg. values of the three GF samples with some exceptions of FGF samples.

According to all three environmental indicators of Avg. EA values of the three GF, ES are contaminated mostly by As, Pb and Ti which can be due to anthropogenic incorporation for gas abstruction activities.

I_{geo} of core samples analysis of FGF and Sbz GF by ED-XRF representation revealed moderate to heavy geo-accumulation of As and almost moderate to heavy geo-accumulation of Pb in all "gas reservoir well core samples" where, similar trend is obtained for both the GF core samples. For As and Pb values normalized to UCC are found high i.e. CF > 6 or almost high in all samples (except for As in one sample) of the two GF core samples. Almost all core samples show considerable enrichment of As and Pb, EA normalized to UCC which reveals that ES in and around gas-field boundary (IAGB) can be contaminated by As, Pb and other toxic metals/metalloids originated from gas-abstraction activities.

EA of GWC samples of FGF and some samples of Sbz GF have been conducted by two methods namely INAA and ED-XRF for inter-comparison. For large portion of samples, EA data are comparable for both methods with some errors, where INAA method is used as standard method. Owing to accuracy and precision, NAA method is used as adjudicator method when new methods are being established and also when other procedures produced unclear results.

Elemental Abundances (EA) of Gas-Well Core (GWC) Samples of the Three Gas Fields (GF):

EA in GWC samples of the three GF namely Shahbazpur (Sbz) gas field (GF), Saldanadi gas field (SGF) and Fenchuganj gas field (FGF) of Bangladesh have been conducted in this research work. A total of 25 major, trace and REE EA (Na, Al, K, Sc, Ti, V, Cr, Mn, Fe, Co, Zn, As, Rb, Cs, Ba, La, Ce, Sm, Eu, Dy, Yb, Hf, Ta, Th and U) in GWC samples of these three GF have been determined.

Inter-comparison of (a) EF (enrichment factor), (b) I_{geo} (geo-accumulation Index) and (c) normalized to UCC (upper continental crust) of EA in GWC samples of these three GF have been done.

Nearly similar trend is obtained for all three EC indicators of Sbz GF, SGF and FGF where only As and Cs geo-accumulation are observed in these three GF. Comparatively little bit lower values of almost all the normalized elemental values are found in core sample of FGF, where also RC of all NR3 (three natural radionuclides ^{226}Ra, ^{232}Th and ^{40}K) are found lower. Core samples data reveal moderate enrichment of the values of As and Cs relative to UCC and comparatively higher than other elemental data for all three GF. So, there is a possibility of environmental S&S samples to be polluted by As and Cs from GAA of these three GF.

The RC ($Bqkg^{-1}$) of the NORMs of this research work are compared with those of ES (environmental samples: soil) of the G&O PF in other countries. The ^{226}Ra RC in our study are comparable with other countries of the world of the world for ES (soil) of the G&O PF. But Saudi Aribia, Iraq, Romania, Naigeria, Kuwait and Syria have higher activity for their Max. value than our studied samples. Our ^{232}Th and ^{40}K RC range are significantly higher than other ES (soil) of the G&O PF in other countries due to geological formation variation. Only Romania's Max. values are comparable with our study.

Inter-comparison of three GF namely Sbz GF, SGF and FGF for both their GWC samples and ES have been conducted. All seven RHI of GWC samples of 1200m to 4000m depth gas reservoir zone for all three GF are significantly higher than the corresponding recommended values. Again, environmental surface S&S samples in and around the GF have significantly lower RC levels to those in GWC samples of these three GF but values of most of the RHI of surface ES of these three GF are around the CRec (corresponding recommended) values.

9.5 Cause of Gas Field Environmental (GFEv) Contamination

1. The largest portion of wastes of GF is 'produced water' which is deposited finally into the evaporation pond and all waste of production and drilling are also deposited into this pond, so the pond is the main deposit of toxic element wastes along with NORM waste. When this contaminated water, mostly in rainy season spread to the nearby environment, resulting soil contamination.
2. Wastes like Sc-Sl (scale and sludge) from the GAA can also enhance the contamination of metals/metalloids and NORMs in the ambient environment. At the time of maintenance work of gas production field, high-speed jet water is used to clean the equipment, by which contamination of metals/metalloids (M&M) and NORMs from Sc-Sl can be carried away to nearby regions through the drain on the way to WDEvp pond.
3. Technogenic migration of toxic elements and NORMs from the GRW (gas-reservoir well) to the AEv can make increasing load to the background environmental RC and M&M.

So environmental assessment is essential for the GF. Gradually the waste increases in gas PF. So, awareness of avoiding more EC (environmental contamination) and taking required deed against EC from both R&C (radiologically and chemically) toxic elements should be maintained. Moreover, there are many fruit trees and vegetables grown IAGB, where comparatively higher toxic elemental concentration and RC levels with additional values of three RHI like ELCR, than CRec (corresponding recommended) values have been found. Furthermore, plentiful grass grows in the GFA (Gas field area) with high RC and toxic EA (elemental abundance) and are collected for domestic animals by the local residents. Therefore, by consuming milk, meats, fruits and vegetables could be exposed indirectly to the radiation and toxic M&M, that may develop into cancer.

Evaluation of environmental indicators for assessing the EA and RHI suggest considerable risks and demand that ES in and around the GF should be supervised routinely as the S&S samples can be polluted more by toxic elements like, Pb, As etc. and NORM originated from GAA.

9.6 Recommendations

1. All environmental indicators for assessing the elemental contents suggest significant enrichment of As and Pb in all samples of three GF namely Sbz GF, SGF and FGF of Bangladesh and can be contaminated more through GAA. As mentioned earlier, Arsenic exposures have pointedly higher mortality rates for cancers of kidney, skin and liver and can disturbs almost all organs like cardiovascular, hepatobiliary, gastrointestinal, nervous, respiratory systems. Again, the highest percentage of lead is taken into the kidney of a human being, after that other soft tissues like liver, heart, brain and also skeleton being affected and lead can be moved to the developing fetus from the exposed pregnant mother. So, awareness and required actions for preventing more EC from both R&C hazardous elements should be maintained.

2. As mentioned earlier, newly developed integrated in-site hydrocarbon and uranium recovery technology is economically feasible with very low grades of uranium ore deposits as low as 0.002 % rather than dispose U, Th and many other valuable minerals as wastes directly into the environment which can cause severe EC and threat for public health and upcoming generations. It will be massive cost saving as exploration, abstraction, production procedure and other auxiliary G&O recovery systems are previously existing and those will be used for extracting U, Th, G&O and other precious mineral deposits, only separation facility to be attached. In this study, elemental identification of core samples of gas reservoir wells of different depth from 1279m to 4091m of three gas fields have been studied by NAA (Neutron Activation Analysis) method for representing high-quality EA data of GWC samples of gas reservoir zone for rare earth elements (REE) and trace elements more precisely to collect information about the concentration of EA of gas reservoir zone and also greater depth sedimentary formation zone and could be used as baseline data for mentioned technology in near future.

3. To implement essential regulations and take required actions against toxic elements and RR (radiological risks) from GAA and identical category of G&O industry globally, outcomes of this study could be able to support the policy-makers.

9.7 Future Studies

1. In future attempt, further research may be done to determine Plant Transfer Factor (PTF) both for HM&M and radionuclides of GF areas.
2. Assessment of EC from HM&M and radionuclides of water sample in fresh water pond or nearby local canal of GF regions.
3. Other GF of Bangladesh should be considered for further analysis both for drilling core and environmental samples.

Reference

Chapter-1

1.1 Ghanavati N, Nazarpour A, Watts MJ. Status, source, ecological and health risk assessment of toxic metals and polycyclic aromatic hydrocarbons (PAHs) in street dust of Abadan, Iran. Catena. 2019; 177:246–59.

1.2 Babaei H, Ghanavati N, Nazarpour A. Contamination level of mercury in the street dust of ahvaz city and its spatial distribution. JWSS-Isfahan University of Technology. 2018; 22(3):249–59.

1.3 Begum.M, Khan.R, Hossain.S.M, Mamun SMMA, Redistributions of NORMs in and around a gas-field (Shabazpur, Bangladesh): radiological risks assessment, 2021, Journal of Radioanalytical and Nuclear Chemistry, https://doi.org/10.1007/s10967-021-08107-x

1.4 Al Nabhani K, Khan F, Yang M (2015) Technologically enhanced naturally occurring radioactive materials in oil and gas production. A silent killer. Process Saf Environ Protect. https://doi.org/10.1016/j.psep.2015.09.014

1.5 Ahsan MA, Satter F, Siddique MAB, Akbor MA, Shamim A, Shajahan M, Khan R (2019) Chemical and physicochemical characterization of effluents from the tanning and textile industries in Bangladesh with multivariate statistical approach. Environ Monit Assess. https://doi.org/10.1007/s10661-019-7654-2

1.6 International Energy Agency (2019) Global Energy Demand Grew by 2.1% in 2017, and Carbon Emissions Rose for the First Time since 2014. Available from https://www.iea.org/newsroom/news/2018/march/global-energy-demand-grew-by-21-in-2017-andcarbon-emissions-rose-for-the-firs.html. (Accessed 21January 2019)

1.7 Shetol MH, Rahman MM, Sarder R, Hossain M, Riday I (2019) Present status of Bangladesh gas fields and future development. A review. J Nat Gas Geosci 4:347–354. https://doi.org/10.1016/j.jnggs.2019.10.005

1.8 IAEA (International Atomic Energy Agency) (2004) Radiation and waste safety in the oil and gas industry. IAEA-Safety Report No 34

1.9 API (American Petroleum Institute) (1992) Bulletin on management of naturally occurring radioactive materials (NORM) in oil and gas production, API Bulletin. E2, Washington, DC

1.10 NRPA (2004) Natural radioactivity in produced water from the norwegian oil and gas industry in 2003. Norwegian Radiation Protection Authority Report 005:2

1.11 A. Fakhru'l-Razi, A. Pendashteh, L. C. Abdullah, D. R. A. Biak, S. S. Madaeni, and Z. Z. Abidin, 2009, "Review of technologies for oil and gas produced water treatment," Journal of Hazardous Materials, vol. 170, no. 2-3, pp. 530–551.

1.12 Ray JP, Rainer Engelhardt F. Produced water: technological/environmental issues and solutions. Environ Sci Res 1992;46:1–5.

1.13 Jerry M. Neff, Kenneth Lee, Elisabeth M. DeBlois (2011). Produced Water: Overview of Composition, Fates, and Effects. Chapter · July 2011.

DOI: 10.1007/978-1-4614-0046-2_1

1.14 2021-22 fiscal year, Annual Report Production division, Bangladesh Petroleum Exploration and Production Company Ltd. (BAPEX).

1.15 OMAR, Salem A. S.,2013, *Characterisation and bioremediation of soil impacted by Libyan oilfield produced water*. Doctoral, Sheffield Hallam University (United Kingdom). http://shura.shu.ac.uk/20145/.

1.16 Ware, Katherine Daniels, 1993, Heavy metals and the petroleum industry, Calhoun: The NPS Institutional Archive, http://hdl.handle.net/10945/24175

1.17 T. I. R. Utvik, 2003, "Composition, characteristics of produced water

in the North Sea," in Proceedings of the Produced Water Workshop, Aberdeen, UK, March.

1.18 Nazarpour A, Ghanavati N, Babaenejad T. Evaluation of the level of pollution and potential ecological risk of some heavy metals in surface soils in the Ahvaz oil-field. Iranian Journal of Health and Environment. 2017; 10(3):391–400.

1.19 D. K. DeForest, K. V. Brix, and W. J. Adams, "Assessing metal bioaccumulation in aquatic environments: the inverse relationship between bioaccumulation factors, trophic transfer factors and exposure concentration," Aquatic Toxicology, vol. 84, no. 2, pp. 236–246, 2007

1.20 Paul B. Tchounwou, Clement G. Yedjou, Anita K. Patlolla and Dwayne J. Sutton, 2012. Heavy metal toxicity and the environment. Molecular, clinical and environmental toxicology, Springer. DOI 10.1007/978-3-7643-8340-4_6.

1.21 A. Wilk, E. Kalisinska, D. I. Kosik-Bogacka et al., "Cadmium, ´ lead and mercury concentrations in pathologically altered human kidneys," Environmental Geochemistry and Health, vol. 39, no. 4, pp. 889–899, 2017.

1.22 M. Ebrahimpour, M. Mosavisefat, and R. Mohabbati, "Acute toxicity bioassay of mercuric chloride: an alien fish from a river," Toxicological & Environmental Chemistry, vol. 92, no. 1, pp. 169–173, 2010.

1.23 Paul B. Tchounwou, Clement G. Yedjou, Anita K. Patlolla and Dwayne J. Sutton, 2012. Heavy metal toxicity and the environment. Molecular, clinical and environmental toxicology, Springer. DOI 10.1007/978-3-7643-8340-4_6.

1.24 Tchounwou PB, Wilson BA, Abdelgnani AA, Ishaque AB, Patlolla AK (2002) Differential cytotoxicity and gene expression in human liver carcinoma (HepG2) cells exposed to arsenic trioxide and monosodium acid methanearsonate (MSMA). Int J Mol Sci 3:1117–1132

1.25 Yedjou GC, Moore P, Tchounwou PB (2006) Dose and time dependent response of human leukemia (HL-60) cells to arsenic trioxide. Int J Environ Res Public Health 3:136–140

1.26 Flora SJS, Flora GJS, Saxena G (2006) Environmental occurrence, health effects and management of lead poisoning. In: Cascas SB, Sordo J (eds) Lead: chemistry, analytical aspects, environmental impacts and health effects. Elsevier, The Netherlands, pp 158–228

1.27 CDC (2001) Managing elevated blood lead levels among young children: recommendations from the advisory committee on childhood lead poisoning prevention. Centers for Disease Control and Prevention, Atlanta, GA

1.28 ATSDR (1999) Toxicological profile for Lead. Public Health Service, U.S. Department of Health and Human Services, Agency for Toxic Substances and Disease Registry, Atlanta, GA

1.29 CDC (1991) Preventing lead poisoning in young children: a statement by the centers for disease control. Centers for Disease Control and Prevention, Atlanta, GA

1.30 Pirkle JL, Brady DJ, Gunter EW, Kramer RA, Paschal DC, Flegal KM, Matte TD (1994) The decline in blood lead levels in the United States: The National Health and Nutrition Examination Surveys (NHANES). J Am Med Assoc 272:284–291

1.31 M. Begum, M. A. Hoque, S. F. Mahal, S. Yeasmin, M. S. Rahman, and all, 2019. Assessment of Background Radiation Level in Different Locations of Bangladesh. Journal of Nuclear Science and Application, Bangladesh Atomic Energy Commission.

1.32 UNSCEAR, Sources and effects of ionizing radiation, United Nations Scientific Committee on the Effects of Atomic Radiation, United Nations, New York (2000).

1.33 Bennett, B.G., Exposure to natural radiation worldwide, In: Proceedings of the Fourth International Conference on High Levels of Natural Radiation: Radiation Doses and Health Effects, 1996, Beijing, China, Elsevier, Tokyo, 15–23 (1997).

1.34 UNSCEAR, Sources and effects of ionizing radiation, United Nations Scientific Committee on the Effect of Atomic Radiation, United Nations, New York (1993).

1.35 Narayan K K, Krishna D K & Subbaramu M C, Population exposure to ionizing radiation in India, ISRP (K)-BR-3 (1991).

1.36 Malathi J., Selvasekarapandian S., Brahmanandhan G. M., Khanna D., Meenakshisundaram V. And Mathiyarsu R., Radiat. Prot. Dosim., 113, 415-420 (2005).

1.37 H. A. Al-Sulaiti, 2011. Determination of Natural Radioactivity

Levels in the State of Qatar Using HighResolution Gamma-ray Spectrometry. Faculty of Engineering and Physical Sciences, University of Surrey, UK.

1.38 Attallah MF, Awwad NS, Aly HF (2012) Environmental radioactivity of TE-NORM waste produced from petroleum industry in Egypt. Rev Charact Treat. https://doi.org/10.5772/CHAPTERDO

1.39 Habib MA, Khan R (2021) Environmental impacts of coal-mining and coal-fired power-plant activities in a developing country with global context. Springer Nature Switzerland AG Spatial modeling and assessment of environmental contaminants (Chapter 24). Environmental challenges and solutions. https://doi.org/10.1007/ 978-3-030-63422-3_24

1.40 Kumar S, Islam ARMT, Islam HMT, Hasanuzzaman M, Ongoma V, Khan R.,Mallick J (2021) Water resources pollution associated with risks of heavy metals from Vatukoula Goldmine, region, Fiji. J Environ Manag. https://doi.org/10.1016/j.jenvman.2021.112868

1.41 SMITH K.P.,1992, An Overview of Naturally Occurring Radioactive Materials (NORM) in Petroleum Industry, Argonne National Laboratory.

1.42 HILAL M.A., ATTALLAH M.F., MOHAMED G.Y., FAYEZ-HASSAN M., 2014, Evaluation of radiation hazard potential of TENORM waste from oil and natural gas production, Journal of Environmental Radioactivity, vol. 136, pp. 121-126.

1.43 A. Mykowska, A. Rogala, A. Kallas, J. Karczewski, J. Hupka, Radioactivity of drilling cuttings from shale resources of the Lower Paleozoic Baltic Basin. 51(2), 2015, 521−533

1.44 Begum M, Khan R, Roy DK, Habib MA, Rashid MB, Naher K, Islam MA, Tamim U, Das SC, Mamun SMMA, Hossain SM (2021) Geochemical characterization of Miocene core sediments from Shahbazpur gas-wells (Bangladesh) in terms of elemental abundances by Instrumental Neutron Activation Analysis. J Radioanal Nucl Chem. https://doi.org/10.1007/ s10967-021-07770-4

1.45 Omar M, Ali HM, Abu MP, Kontol KM, Ahmad Z, Ahmad SHSS, Sulaiman I, Hamzah R (2004) Distribution of radium in oil and gas Industry wastes from Malaysia. Appl Radiat Isot 60:779–782

1.46 El Afifi EM, Awwad NS (2005) Characterization of the TENORM waste associated with oil and natural gas production in Abu Rudeis, Egypt. J Environ Radioact 82:7–19

1.47 Gazineu MHP, de Arau´jo AA, Brand~ao YB, Hazin CA, GodoydeO. JM (2005) Radioactivity concentration in liquid and solid phases of scale and sludge generated in the petroleum industry. J Environ Radioact 81:47–54

1.48 Parmaksız A, Agus¸ Y, Bulgurlu F, Bulur E, Yıldız Ç, €Oncü T (2013) Activity concentrations of 224Ra, 226Ra, 228Ra and 40K radionuclides in refinery products and additional radiation dose originated from oil residues in Turkey. Radiat Prot Dosim 156:481–488

1.49 Kpeglo DO, Mantero J, Darko EO, Emi-Reynolds G, Faanu A, Manjon G, Vioque I, Akaho EHK, Garcia-Tenorio R (2016) Radiochemical characterization of produced water from two production offshore oilfields in Ghana. J Environ Radioact 152:35–45

1.50 Strand T, Lysebo I (1998) Proceedings of the 2nd international symposium on the treatment of NORM., Krefeld, Germany 10-13:137

1.51 Aoife Gallagher, Biological effects of Radiation. Department of Medical Physics & Bioengineering, St. James's Hospital

1.52 T. Shimura, I. Yamaguchi, H. Terada, O. Kengo, E. R. Svendsen and N. Kunugita. (2014), Radiation occupational health interventions offered to radiation workers in response to the complex catastrophic disaster at the Fukushima Daiichi Nuclear Power Plant, Journal of Radiation Research. · November 2014, pp 1–9. DOI: 10.1093/jrr/rru110

1.53 F. G. Spear, Radiation and living cells, P. John Wiley and sons, New York, 1953.

1.54 Kumar A, Karpe R, Rout S, Narayanan U, Ravi PM (2012) A comparative study of distribution coefficients (Kd) for naturally occurring uranium (U) and thorium (Th) in two different aquatic environments. INIS

1.55 Mao GZ, Liu CY, Zhang DD et al (2014) Effects of uranium on hydrocarbon generation of hydrocarbon source rocks with type-III kerogen. Sci China Earth Sci 57:1168–1179

1.56 Nabhani AK, Khan F (2020) Nuclear radioactive materials in the oil and gas industry. Elsevier. https://doi.org/10.1016/B978-0-12- 816825-7.00005-4

1.57 Hore-Lacy I (2016) Uranium for Nuclear power: resources, mining and transformation to fuel. Woodhead Publishing, pp 1–453

Chapter-2

2.1 Jonkers, G., Hartog, F. A., Knaepen, W. A. I. & Lancee, P. F. J. Characterization of NORM in the oil and gas production (E&P) industry. In proceedings of the International Symposium on Radiological Problems with Natural Radioactivity in the Non-nuclear Industry. Amsterdam. (1997).

2.2 Ebenezer T. Igunnu and George Z. Chen, Produced water treatment technologies, International Journal of Low-Carbon Technologies Advance Access published July 4, 2012

2.3 Ware, Katherine Daniels, 1993, Heavy metals and the petroleum industry, Calhoun: The NPS Institutional Archive, http://hdl.handle.net/10945/24175

2.4 Fakhru'l-Razi A, Pendashteh A, Abdullah LC, et al. Review of technologies for oil and gas produced water treatment. J Hazard Mater, 2009;170:530–51.

2.5 T. I. R. Utvik, "Composition, characteristics of produced water in the North Sea," in Proceedings of the Produced Water Workshop, Aberdeen, UK, March 2003.

2.6 Nazarpour A, Ghanavati N, Babaenejad T. Evaluation of the level of pollution and potential ecological risk of some heavy metals in surface soils in the Ahvaz oil-field. Iranian Journal of Health and Environment. 2017; 10(3):391–400.

2.7 H. Ali and E. Khan, "What are heavy metals? Long-standing controversy over the scientific use of the term' heavy metals'- proposal of a comprehensive definition," Toxicological & Environmental Chemistry, vol. 100, no. 1, pp. 6–19, 2018.

2.8 Kabata-Pendia A (2001) Trace elements in soils and plants, 3rd edn. CRC, Boca Raton, FL

2.9 Duffus JH (2002) Heavy metals – a meaningless term? Pure Appl Chem. , 74: 793-807.

2.10 Nazarpour A, Watts MJ, Madhani A, Elahi S. Source, spatial distribution and pollution assessment of Pb, Zn, Cu, and Pb, isotopes in urban soils of Ahvaz City, a semi-arid metropolis in southwest Iran. Scientific reports. 2019; 9(1):1–11. https://doi.org/10.1038/s41598-018-37186-2 PMID: 30626917

2.11 Ogunkunle CO, Fatoba PO. Pollution Loads and the Ecological Risk Assessment of Soil Heavy Metals around a Mega Cement Factory in Southwest Nigeria. Polish Journal of Environmental Studies. 2013; 22(2).

2.12 D. S. Malik and P. K. Maurya, “Heavy metal concentration in water, sediment, and tissues of fish species (Heteropneustis fossilis and Puntius ticto) from Kali River, India,” Toxicological & Environmental Chemistry, vol. 96, no. 8, pp. 1195–1206, 2014.

2.13 O. Chalkiadaki, M. Dassenakis, and N. Lydakis-Simantiris, “Bioconcentration of Cd and Ni in various tissues of two marine bivalves living in different habitats 18and exposed to heavily polluted seawater,” Chemistry and Ecology, vol. 30, no. 8, pp. 726–742, 2014.

2.14 S. Mahboob, H. F. Alkkahem Al-Balwai, F. Al-Misned, K. A. Al-Ghanim, and Z. Ahmad, “A study on the accumulation of nine heavy metals in some important fish species from a natural reservoir in Riyadh, Saudi Arabia,” Toxicological & Environmental Chemistry, vol. 96, no. 5, pp. 783– 798, 2014.

2.15 M. A. Barakat, “New trends in removing heavy metals from industrial wastewater,” Arabian Journal of Chemistry, vol. 4, no. 4, pp. 361–377, 2011.

2.16 P. C. Nagajyoti, K. D. Lee, and T. V. M. Sreekanth, “Heavy metals, occurrence and toxicity for plants: a review,” Environmental Chemistry Letters, vol. 8, no. 3, pp. 199–216, 2010

2.17 Goyer RA (2001) Toxic effects of metals. In: Klaassen CD (ed) Cassarett and Doull’s toxicology: the basic science of poisons. McGraw-Hill, New York, NY, pp 811–867

2.18 Arruti A, Ferna´ndez-Olmo I, Irabien A (2010) Evaluation of the contribution of local sources to trace metals levels in urban PM2.5 and PM10 in the Cantabria region (Northern Spain). J Environ Monit 12:1451–1458

2.19 Str€ater E, Westbeld A, Klemm O (2010) Pollution in coastal fog at Alto Patache, Northern Chile. Environ Sci Pollut Res Int 17:1563–1573

2.20 Garbarino JR, Hayes HC, Roth DA, Antweiler RC, Brinton TI, Taylor HE. Contaminants in the Mississippi River: Heavy metals in the Mississippi River. Reston, Virginia: U.S. GEOLOGICAL SURVEY CIRCULAR; 1995. pp. 1133

2.21 Hazrat Ali , Ezzat Khan and Ikram Ilahi, (2019), Environmental Chemistry and Ecotoxicology of Hazardous Heavy Metals: Environmental Persistence, Toxicity, and Bioaccumulation. Hindawi Journal of Chemistry, Volume 2019, Article ID 6730305, 14 pages

https://doi.org/10.1155/2019/6730305

2.22 Tchounwou PB, Patlolla AK, Centeno JA (2003) Carcinogenic and systemic health effects associated with arsenic exposure—a critical review. Toxicol Pathol 31:575–588

2.23 Tchounwou PB, Wilson BA, Abdelgnani AA, Ishaque AB, Patlolla AK (2002) Differential cytotoxicity and gene expression in human liver carcinoma (HepG2) cells exposed to arsenic trioxide and monosodium acid methanearsonate (MSMA). Int J Mol Sci 3:1117–1132

2.24 Yedjou GC, Moore P, Tchounwou PB (2006) Dose and time dependent response of human leukemia (HL-60) cells to arsenic trioxide. Int J Environ Res Public Health 3:136–140

2.25 Flora SJS, Flora GJS, Saxena G (2006) Environmental occurrence, health effects and management of lead poisoning. In: Cascas SB, Sordo J (eds) Lead: chemistry, analytical aspects, environmental impacts and health effects. Elsevier, The Netherlands, pp 158–228

2.26 CDC (2001) Managing elevated blood lead levels among young children: recommendations from the advisory committee on childhood lead poisoning prevention. Centers for Disease Control and Prevention, Atlanta, GA

2.27 ATSDR (1999) Toxicological profile for Lead. Public Health Service, U.S. Department of Health and Human Services, Agency for Toxic Substances and Disease Registry, Atlanta, GA

2.28 CDC (1991) Preventing lead poisoning in young children: a statement by the centers for disease control. Centers for Disease Control and Prevention, Atlanta, GA

2.29 ATSDR (1992) Case studies in environmental medicine—Lead toxicity. Public Health Service, U.S. Department of Health and Human Services, Agency for Toxic Substances and Disease Registry, Atlanta, GA

2.30 Pirkle JL, Brady DJ, Gunter EW, Kramer RA, Paschal DC, Flegal KM, Matte TD (1994) The decline in blood lead levels in the United States: The National Health and Nutrition Examination Surveys (NHANES). J Am Med Assoc 272:284–291

2.31 Pirkle JL, Kaufmann RB, Brody DJ, Hickman T, Gunter EW, Paschal DC (1998) Exposure of the U.S. population to lead: 1991–1994. Environ Health Perspect 106:745–750

2.32 U.S. EPA (2002) Lead compounds. Technology transfer network—air toxics website. Online available at http://www.epa.gov/cgi-bin/epaprintonly.cgi

2.33 Kaul B, Sandhu RS, Depratt C, Reyes F (1999) Follow-up screening of lead-poisoned children near an auto battery recycling plant, Haina, Dominican Republic. Environ Health Perspect 107:917–920

2.34 Smith, K.P., *An Overview of Naturally Occurring Radioactive Materials (NORM) in the Petroleum Industry*. 1992, ANL/EAIS-7, Argonne National Laboratory.

2.35 Anderson, B., *Dealing with Radioactive Scale in Offshore Oil Production.* Ocean Industry, 1990. **23-48**.

2.36 Veil, John A., Puder Markus G., Elcock Deborah, and Robert J. Redweik Jr., *A White paper Describing Produced Water from Production of Crude Oil, Natural Gas, and Coal Bed Methane*. 2004, Argonne National Laboratory.

2.37 Toxicity, mechanism and health effects of some heavy metals Monisha JAISHANKAR, Tenzin TSETEN, Naresh ANBALAGAN, Blessy B. MATHEW , Krishnamurthy N. BEEREGOWDA . Interdisciplinary Toxicology. 2014; Vol. 7(2): 60–72. doi: 10.2478/intox-2014-0009

2.38 M.R. Ghorbani, N. Ghanavati, T. Babaenejad, A. Nazarpour, K. Payandeh (2020), Assessment of the potential ecological and human health risks of heavy metals in Ahvaz oil field, Iran. PLOS ONE. https://doi.org/10.1371/journal.pone.0242703.

2.39 "raindrops on a dusty road", available from :http://www.pathologyoutlines.com/topic/bonemarrarsenic.html

2.40 Smith AH, Lingas EO, Rahman M. (2000). Contamination of drinking-water by arsenic in Bangladesh: a public health emergency. Bull World Health Organ 78(9): 1093–1103

2.41 An investigation on heavy metals in soils around oil field area A. R. Karbassi; S. Tajziehchi; S. Afshar. Global J. Environ. Sci. Manage., 1(4): 275-282, Autumn 2015. DOI: 10.7508/gjesm.2015.04.002

2.42 Impacts of Oil and Gas Production on Contaminant Levels in Sediments. 2020. Hossein D. Atoufi and David J. Lampert. Current Pollution Reports

https://doi.org/10.1007/s40726-020-00137-5

2.43 Distribution of heavy metals in agricultural soils near a petrochemical complex in Guangzhou, China. Junhui Li , Ying Lu, Wei Yin, Haihua Gan,Chao Zhang , Xianglian Deng . Jin Lian. Environmental Monitoring and Assessment (2009) 153:365–375 DOI 10.1007/s10661-008-0363-x

2.44 Characterisation of heavy metal pollutants of soils and sediments around a crude-oil production terminal using EDXRF. E.I. Obiajunwa, D.A. Pelemo, S.A. Owolabi, M.K. Fasasi, F.O. Johnson-Fatokun. Nuclear Instruments and Methods in Physics Research B 194 (2002) 61–64. PII: S01 6 8-5 8 3X(0 2)0 04 9 9- 8

2.45 Heavy Metal Toxicity and the Environment. Paul B. Tchounwou, Clement G. Yedjou, Anita K. Patlolla, and Dwayne J. Sutton, 2012. Molecular, Clinical and Environmental Toxicology, Springer. DOI 10.1007/978-3-7643-8340-4_6

2.46 Zimmerle, W., 1995. Petroleum Sedimentology. Kluwer, Dordrecht, p. 413.

2.47 Mao, G.Z., Liu, C.Y., Zhang, D.D., et al., 2014. Effects of uranium on hydrocarbon generation of hydrocarbon source rocks with type-III kerogen. Sci. China Earth Sci. 57, 1168–1179

2.48 Nabhani AK, Khan F (2020) Nuclear radioactive materials in the oil and gas industry. Elsevier. https://doi.org/10.1016/B978-0-12-816825-7.00005-4

2.49 El Afifi, E.M., Awwad, N.S., 2005. Characterization oftheTE-NORMwaste associatedwith oil and natural gas production in Abu Rudeis, Egypt. J. Environ. Radioact. 82, 7–19

2.50 Rood, A.D., White, G.J., Kendrick, D.T., 1998. Measurement of Rn-222 flux, Rn-222 emanation and R-226 Ra-228 concentration from injection well pipe scale. Health Phys. 75, 187–192

2.51 Gazineu, M.H.P., Araujo, A.A., Brandao, Y.B., Hazin, C.A., Godoy, J.M.D.O., 2005. Radioactivity concentration in liquid and solid phases of scale and sludge generated in the petroleum industry. J. Environ. Radioact. 81, 47–54

2.52 International Atomic Energy Agency (IAEA). *Extent of environmental contamination by naturally occuring radioactive materials (NORM) and technological options for migration*. (2003).

2.53 F.S. Al-Saleh, G. A. Al-Harshan (2008). Measurements of radiation level in petroleum products. Journal of Environmental Radioactivity, 99, 1026-1031.

2.54 Hajer Hrichi, Souad Baccouche, Jamel-Eddine Belgaied (2013). Evaluation of radiological impacts of tenorm in the Tunisian petroleum industry. Journal of Environmental Radioactivity, 115 , 107-113.

2.55 Accuracy of methods for reporting inorganic element concentrations and radioactivity in oil and gas wastewaters from the Appalachian Basin, U.S. based on an inter-laboratory comparison.T. L. Tasker, W. D. Burgos, M. A. Ajemigbitse, N. E. Lauer, A. V. Gusa, M. Kuatbek, D. May, J. D. Landis, D.

S. Alessi, A. M. Johnsen, J. M. Kaste, K. L. Headrick, F. D. H. Wilke, M. McNeal, M. Engle, A. M. Jubb, R. D. Vidic, A. Vengosh and N. R. Warner. Environmental Science Processes & Impacts. DOI: 10.1039/c8em00359a

2.56 Amin Taheri, Ali Taheri, Ali Asghar Fathivand, Nabiollah Mansouri (2019). Risk assessment of naturally occurring radioactive materials (NORM) in the hydrocarbon sludge extracted from the south pars gas field in Iran. Process Safety and Environmental Protection, 125, 102–120.

2.57 Assessment of naturally occurring radioactive material (NORM) in the oil drilling mud of Az Zubair oil field, Basra, Iraq. Sahar A. Amin. Environ Earth Sci (2016) 75:769. DOI 10.1007/s12665-016-5564-y

2.58 Maria Helena P. Gazineu, Andressa A. de Araújo, Yana B. Brandão and Clovis A. Hazin, "Radium-226 and Radium-228 in Scale and Sludge Generated in the Petroleum Industry", J. of Environmental Radioactivity, 72, 199-206, (2004).

2.59 g-Spectroscopy measurement of natural radioactivity and assessment of radiation hazard indices in soil samples from oil fields environment of Delta State, Nigeria E.O. Agbalagba , G.O. Avwiri , Y.E. Chad-Umoreh . Journal of Environmental Radioactivity 109 (2012) 64 – 70. doi:10.1016/j.jenvrad.2011.10.012

2.60 Radiochemical characterization of produced water from two production offshore oilfields in Ghana. D.O. Kpeglo , J. Mantero, E.O. Darko, G. Emi-Reynolds, A. Faanu, G. Manjon, I. Vioque, E.H.K. Akaho, R. Garcia-Tenorio. Journal of Environmental Radioactivity 152 (2016) 35-45. http://dx.doi.org/10.1016/j.jenvrad.2015.10.026

2.61 Canadian Association of Petroleum Producers (CAPP) Guide "Naturally Occurring Radioactive Material (NORM)" 2000.

2.62 Distribution of radium in oil and gas industry wastes from Malaysia. M. Omar, H.M. Ali, M.P. Abu, K.M. Kontol, Z. Ahmad, S.H.S.S. Ahmad, I. Sulaiman, R. Hamzah. Applied Radiation and Isotopes 60 (2004) 779–782. doi:10.1016/j.apradiso.2004.01.005

2.63 IAEA. "Radiation Protection and the Management of Radioactive Waste in the Oil and Gas Industry", IAEA Technical Report Series No. 34, Vienna (2003).

2.64 ICRP. International Commission on Radiological Protection. "Protection against radon-222 at home and at work". ICRP Publication 65. Ann. ICRP 23 (2), 1– 45 (1993).

Chapter-3

3.1 Susan J. Parry, Activation Spectrometry in Chemical Analysis, Volume 119 in Chemical Analysis, A Series of Monographs on Analytical Chemistry and Its Applications.

3.2 Hevesy, G., Levi, H., Math. Fys. Med. 34, p 145 1936.

3.3 M. S. Islam, M. M. Haque, M. A. Salam, M. M. Rahman, M. R. I. Khandokar, M. A. Sardar, P. K. Saha, A. Haque, M. A. Malek Sonar, M. M. Uddin, S. M. S. Hossain and M. A. Zulquarnain, 2004, Operation Experience with the 3 MW TRIGA Mark-II Research Reactor of

Bangladesh.Vienna University of Technology, Atomic Institute of the Austrian Universities (Austria); p. 47-52; 2. world TRIGA users conference; Vienna (Austria); 15-18 Sep 2004.

3.4 Barrett, C.S.J.V. Gilfrich, R. Jenkins, D.E. Leyden, J.C. Russ and P.K. Predecki, eds,1987, Advances in X-Ray Analysis, Vol, 30 (plenum press, New York)

3.5 K. Debertin, R.G. Helmer,1988, book name: Gamma and X-ray spectrometry with semiconductor detectors, published by: Physical Sciences & Engineering Division, Elsevier, ISBN: 0444871071.

3.6 Rudnick, R.L., Gao, S., 2014. Composition of the Continental Crust. Treatise on Geochemistry, 2nd ed.). pp. 1–64 Chapter 4.

3.7 Birch, G., 2003. Ascheme for assessing human impacts on coastal aquatic environments using sediments. In: In: Woodcoffe, C.D., Furness, R.A. (Eds.), Wollongong University Papers in Center for Maritime Policy 14 Coastal GIS, Australia.

3.8 Khan R, Das S, Kabir S, Habib MA, Naher K, Islam MA, Tamim U, Rahman AKMR, Deb AK, Hossain SM (2019) Evaluation of the elemental distribution in soil samples collected from shipbreaking areas and an adjacent island. J Environ Chem Eng 7(3):103189. https://doi.org/10.1016/j.jece.2019.103189

3.9 Ergin, M., Saydam, C., Basturk, O., Erdem, E., Yoruk, R., 1991. Heavy metal concentrations in surface sediments from the two coastal inlets (Golden Horn Estuary and Izmit Bay) of the northeastern sea of Marmara. Chem. Geol. 91, 269–285.

3.10 Bhuiyan, M.A.H., Parvez, L., Islam, M.A., Dampare, S.B., Suzuki, S., 2010. Heavy metal pollution of coal mine-affected agricultural soils in the northern part of Bangladesh. J. Hazard. Mater. 173, 384–392

3.11 Tamim, U., Khan, R., Jolly, Y.N., Fatema, K., Das, S., Naher, K., Islam, M.A., Islam, S.M.A., Hossain, S.M., 2016. Elemental distribution of metals in urban river sediments near an industrial effluent source. Chemospher 155, 509–518.

3.12 Brich, G.F., Olmos, M.A., 2008. Sediment-bound heavy metals as indicators of human influence and biological risk in coastal water bodies. ICES J. Mar. Sci. 65, 1407–1413.

3.13 Rubio, B., Nombela, M.A., Vilas, F., 2000. Geochemistry of major and trace elements in sediments of the Ria de Vigo (NW Spain): an assessment of metal pollution. Mar. Pollut. Bull. 40, 968–980.

3.14 Abrahim, G.M.S., Parker, R.J., 2008. Assessment of heavy metal enrichment factors and the degree of contamination in marine sediments from Tamaki Estuary, Auckland, New Zealand. Environ. Monit. Assess. 136, 227–238.

3.15 Ma, X., Zuo, H., Tian, M., Zhang, L., Meng, J., Zhou, X., Min, N., Chang, X., Liu, Y., 2016. Assessment of heavy metals contamination in sediments from three adjacent regions

3.16 Bhuiyan, M.A.H., Parvez, L., Islam, M.A., Dampare, S.B., Suzuki, S., 2010. Heavy metal pollution of coal mine-affected agricultural soils in the northern part of Bangladesh. J. Hazard. Mater. 173, 384–392

3.17 Hakanson, L., 1980. An ecological risk index for aquatic pollution control. A sedimentological approach. Water Res. 14, 975–1001.

3.18 Hakanson, L., 1980. An ecological risk index for aquatic pollution control. A sedimentological approach. Water Res. 14, 975–1001.

3.19 Zhao, S., Feng, C., Yang, Y., Niu, J., Shen, Z., 2012. Risk assessment of sedimentary elements in the Yangtze Estuary: new evidence of the relationships between two typical index methods. J. Hazard. Mater. 241–242, 164–172.

Chapter-4

4.1 Mollah N.I., Rahman M., Miah R.U., Basunia S. Hossain S.M.,1992. Technical Report, AERE, Ganakbari, Savar, Dhaka.

4.2 H.A. Enge, Introduction to Nuclear Physics, Addition-Wisely, P-192

4.3 Agbalagba EO, Avwiri GO, Chad-Umoreh YE (2012) γ-Spectroscopy measurement of natural adioactivity and assessment of radiation hazard indices in soil samples from oil felds environment of Delta State, Nigeria. J Environ Radioact 109:64– 70. https://doi.org/10.1016/j.jenvrad.2011.10.012

4.4 Beretka J, Mathew PJ (1985) Natural radioactivity in Australian building materials, industrial waste and by-product. Health Phys 48:87–95 57.

4.5 UNSCEAR (2000) Sources and efects of Ionizing Radiations, United Nations. Report to the General Assembly, with Scientifc Annexes, United Nations (A/55/46), New York.

4.6 ICRP (1990) Recommendations of the international commission on radiological protection. 21(1–3), 60.

Chapter-5

5.1 Begum.M, Khan.R, Hossain.S.M, Mamun SMMA, Redistributions of NORMs in and around a gas-field (Shabazpur, Bangladesh): radiological risks assessment, 2021, Journal of Radioanalytical and Nuclear Chemistry, https://doi.org/10.1007/s10967-021-08107-x

5.2 Begum M, Khan R, Roy DK, Habib MA, Rashid MB, Naher K, Islam MA, Tamim U, Das SC, Mamun SMMA, Hossain SM (2021) Geochemical characterization of Miocene core sediments from Shahbazpur gas-wells (Bangladesh) in terms of elemental abundances by Instrumental Neutron Activation Analysis. J Radioanal Nucl Chem. https://doi.org/10.1007/ s10967-021-07770-4

5.3 Well Completion Report of Fenchuganj well-2, BAPEX, 1988

5.4 Well Completion Report of Saldanadi well-1, BAPEX, 2002

5.5 Well Completion Report of Shahbazpur well-2, BAPEX, 2016

5.6 Well Completion Report of Shahbazpur well-4, BAPEX, 2014

5.7 Khan R, Islam MS, Tareq ARM, Naher K, Islam ARMT, Habib MA, Siddique MAB, Islam MA, Das S, Rashid MB, Ullah AKMA, Miah MMH, Masrura SU, Bodrud-Doza M, Sarker MR, Badruzzaman ABM (2020) Elemental and polycyclic aromatic hydrocarbons distributions in the sediments of an Urban river: infuence of anthropogenic runofs. Environ Nanotechnol, Monit Manag 14:100318. https://doi.org/10.1016/j.enmm.2020.100318

5.8 Hossain MK, Hossain SM, Azim R, Meaze AKMMH (2010) Assessment of radiological contamination of soils due to shipbreaking using HPGe digital gamma-ray spectrometry system. J Environ Prot 1:10–14. https://doi.org/10.4236/jep.2010.11002

Chapter-6

6.1 Syed Mohammod Hossain, Chief Scientific Officer of Bangladesh Atomic Energy Commission (BAEC), 21 April 2013, Power Point Presentation on "Theory and Application of NAA", BAEC Basic Nuclear Orientation Course.

6.2 Yeasmin Nahar Jolly, Ashraful Islam and Shawkat Akbar, 2013, Transfer of metals from soil to vegetables and possible health risk assessment, Journal SpringerPlus, 2:385. http://www.springerplus com/content/2/1/385

6.3 Refat Jahan Rakib, M. Belal Hossain, Yeasmin Nahar Jolly, Shirin Akther and Saiful Islam 2021, EDXRF Detection of Trace Elements in Salt Marsh Sediment of Bangladesh and Probabilistic Ecological Risk Assessment, Soil and Sediment Contamination: An International Journal. DOI: 10.1080/15320383.2021.1923644

Chapter-7

7.1 Bauluz B, Mayayo MJ, Fernandez-Nieto C, Lopez JMG (2000) Geochemistry of Precambrian and Paleozoic siliciclastic rocks from the Iberian Range (NE Spain): implications for source-area weathering, sorting, provenance and tectonic setting. Chem Geol 168(1–2):135–150

7.2 Rudnick, R.L., Gao, S., 2014. Composition of the Continental Crust. Treatise on Geochemistry, 2nd ed.). pp. 1–64 Chapter 4.

7.3 Bowen, H. J. M., 1979. Environmental Chemistry of the Elements New York: Academic Press

7.4 Birch, G., 2003. Ascheme for assessing human impacts on coastal aquatic environments using sediments. In: In: Woodcoffe, C.D., Furness, R.A. (Eds.), Wollongong University Papers in Center for Maritime Policy 14 Coastal GIS, Australia.

7.5 Khan R, Das S, Kabir S, Habib MA, Naher K, Islam MA, Tamim U, Rahman AKMR, Deb AK, Hossain SM (2019) Evaluation of the elemental distribution in soil samples collected from shipbreaking areas and an adjacent island. J Environ Chem Eng 7(3):103189. https://doi.org/10.1016/j.jece.2019.103189

7.6 Ergin, M., Saydam, C., Basturk, O., Erdem, E., Yoruk, R., 1991. Heavy metal concentrations in surface sediments from the two coastal inlets (Golden Horn Estuary and Izmit Bay) of the northeastern sea of Marmara. Chem. Geol. 91, 269–285.

7.7 Bhuiyan, M.A.H., Parvez, L., Islam, M.A., Dampare, S.B., Suzuki, S., 2010. Heavy metal pollution of coal mine-affected agricultural soils in the northern part of Bangladesh. J. Hazard. Mater. 173, 384–392

7.8 Tamim, U., Khan, R., Jolly, Y.N., Fatema, K., Das, S., Naher, K., Islam, M.A., Islam, S.M.A., Hossain, S.M., 2016. Elemental distribution of metals in urban river sediments near an industrial effluent source. Chemospher 155, 509–518.

7.9 Rubio, B., Nombela, M.A., Vilas, F., 2000. Geochemistry of major and trace elements in sediments of the Ria de Vigo (NW Spain): an assessment of metal pollution. Mar. Pollut. Bull. 40, 968–980.

7.10 Müller G, 1969. Index of geoaccumulation in sediments of the Rhine River. Geojournal, 2, 108–118.

7.11 Hakanson, L., 1980. An ecological risk index for aquatic pollution control. A sedimentological approach. Water Res. 14, 975–1001.

7.12 Zhao, S., Feng, C., Yang, Y., Niu, J., Shen, Z., 2012. Risk assessment of sedimentary elements in the Yangtze Estuary: new evidence of the relationships between two typical index methods. J. Hazard. Mater. 241–242, 164–172.

Chapter-8

8.1 UNSCEAR, 2000. Sources and effects of Ionizing Radiations, United Nations. Report to the General Assembly, with Scientific Annexes, United Nations (A/55/46), New York.

8.2 Rudnick RI, Gao S (2014) Composition of the continental crust. Treatise on geochemistry (2nd ed.), pp 1–64

8.3 Khan, R., Islam, H.M .T., Islam, A.R.M.T., 2021. Mechanism of elevated radioactivity in a freshwater basin :Radiochemical characterization, provenance and associated hazards. Chemosphere .https//:doi.org/10.1016/j.chemosphere.2020.128459

8.4 Rashed-Nizam, Q.M., Rahman, M.M., Kamal, M., Chowdhury, M.I., 2015 .Assessment of radionuclides in the soil of residential areas of the Chittagong metropolitan city, Bangladesh and evaluation of associated radiological risk .J Radial, Res 56 (1):22–29

8.5 Chowdhury, M.I., Kamal, M., Alam, M.N., Yeasmin, S., Mostafa, M.N., 2006 .Distribution of naturally occurring radionuclides in soils of the southern districts of Bangladesh .Radiat Prot Dosimetry 118 (1):126–130

8.6 Mishra, U.C.A., 2004 .Environmental impact of coal industry and thermal power plants in India .J .Environ Radioact 72 (1–2):35–40

8.7 Begum, M., Khan, R., Roy, D.K., Habib, M.A., Rashid, M.B., Naher, K., Islam, M.A., Tamim, U., Das, S.C., Mamun, S.M.M.A., Hossain, S.M., 2021 .Geochemical characterization of Miocene core sediments from Shahbazpur gas-wells (Bangladesh) in terms of elemental abundances by Instrumental Neutron Activation Analysis .J Radioanal Nucl Chem. https//:doi.org/10.1007/s10967-021-07770-4

8.8 OECD, 1979. Nuclear Energy Agency, Exposure to Radiation from natural radioactivity in building materials Reported by NEA group of Experts. OECD, Paris

8.9 UNSCEAR, 2008. Sources and effects of Ionizing Radiations, United Nations .Report to the General Assembly, with Scientific Annexes, United Nations

8.10 Darwish, D.A.E., Abul-Nasr, K.T.M., El-Khayatt, A.M., 2015. The assessment of natural radioactivity and it associated radiological hazards and dose parameters in granite samples from South Sinai, Egypt .J Radiat Res Appl Sc 8:17–25

8.11 ALNabhani, K., Khan, F., 2020 .Book :Nuclear Radioactive Materials in the Oil and Gas Industry .Elsevier .https//:doi.org/10.1016/B978-0-12-816825-7.00005-4

8.12 Sabbagh, S., Alhussen, S., 2012. Radioactive Pollutants in the Al-Amr Plants Soil from Petroleum Industry .Journal of Halab University Research 1(85):1–16.

8.13 Khandaker, M.U., Nasir, N.L.M., Asaduzzaman, K., Olatunji, A., Amin, Y.M., Kassim, H.A., Bradley, D.A., Jojo, P.J., Alrefaed, T., 2016. Evaluation of radionuclides transfer from soil-to-edible flora and estimation of radiological dose to the Malaysian populace. Chemosphere, 154, 528-536.

8.14 Alshahri, F., El-Taher, A., 2018 .Investigation of Natural Radioactivity Levels and Evaluation of Radiation Hazards in Residential-Area Soil Near a Ras Tanura Refinery, Saudi Arbia .Pol J Environ Stud., 28(1):25–34

8.15 Xhixha, G., et al., 2015 .Chemosphere A century of oil and gas exploration in Albania : assessment of Naturally Occurring Radioactive Materials (NORMs) .Chemosphere 139:30–39

8.16 Ali, H .A .H .K .K., Shafik, S .S ,.2017 .Radiological Assessment of NORM Resulting from Oil and Gas Production Processing in South Rumaila Oil Field, Southern Iraq .Iraqi J Sci., 58(2):1037–1050

8.17 Ozkok, Y. O., Parmaksız, A., A˘gus, Y., Bulgurlu, F., Bulur, E., Oncu, T., 2015. Measurement of enhanced radium isotopes ¨ in oil production wastes in Turkey .J Environ Radioact 141:82 . http//:dx.doi.org/10.1016/j.jenvrad.2014.12.011

8.18 Botezatu, E., Grecea, C., 2004. Radiological Impact Assessment on Behalf of Oil/Gas Industry . J Prev Med., 12(1–2):16–21

8.19 Galitskaya, P., Gumerova, R., Ratering, S., Schnell, S., Blagodatskaya, E., Selivanovskaya, S., 2015. Oily waste containing natural radionuclides :does it cause stimulation or inhibition of soil bacterial community .J Plant Nutr Soil Sci., 178(6).

8.20 Agbalagba, E.O., Avwiri, G.O., Chad-Umoreh, Y.E., 2012. γ-Spectroscopy measurement of natural radioactivity and assessment of radiation hazard indices in soil samples from oil fields environment of Delta State, Nigeria .Journal of Environmental Radioactivity 109:64–70 . https//:doi.org/10.1016/j.jenvrad.2011.10.012

8.21 Al-Kinani, A.T., Hushari, M., Alsadig, I.A., Al-Sulaiti, H., 2015 .NORM in soil and sludge samples in Dukhan oil Field, Qatar state .Donnish Journal of Research in Environmental Studies 2(4):37–43

8.22 Shams, H.M., Bradley, D.A., Regan, P.H., 2017. Determination of levels of naturally occurring radioactive materials in lagoon samples containing produced water from the Minagish oil field in the state of Kuwait .Radiat Phys Chem 137:193–197

8.23 Mohammad Ghafar, R.D., Marroshiah, F., 2017. Evaluation of Radioactivity and Potential Radiation Hazard of NORM waste due to Produced Water Draining in Crude Oil Tanks Area in Banyas, Tishreen Univ .J Res Sci Stud 39(3):195–210

8.24 Huang, T., Hao, Y., Pang, Z., Li, Z., Yang, S., 2017. Radioactivity of Soil, Rock and Water in a Shale Gas Exploitation Area, SW China .Water 9(5):299